

Green Chemistry

Cutting-edge research for a greener sustainable future

www.rsc.org/greenchem

Volume 9 | Number 9 | September 2007 | Pages 913–1028



ISSN 1463-9262

RSC Publishing

Green Solvents for Processes
Themed Issue

Wallis *et al.*
Improving the catalytic properties of
K-10 montmorillonite

Cantone *et al.*
Biocatalysis in non-conventional
media



1463-9262(2007)9:9;1-3



star service for authors

Organic & Biomolecular Chemistry ...

- easy online submission and manuscript tracking via ReSource
- free colour where scientifically justified
- short publication times, as low as 24 days from acceptance for papers, and 14 days for communications
- RSC Open Science, offering you the option of paying a fee in exchange for making your research paper available to all, via the web
- high exposure – top papers highlighted in the wider scientific press

There are many more reasons why you should choose OBC. In particular, we offer a first class professional publishing and independent peer review service as a society-based publisher. To get the best service, why not submit your work today?

... celebrating 5 years of publishing

RSC Publishing

www.rsc.org/obc

Registered Charity Number 207890

Green Chemistry

Cutting-edge research for a greener sustainable future

www.rsc.org/greenchem

RSC Publishing is a not-for-profit publisher and a division of the Royal Society of Chemistry. Any surplus made is used to support charitable activities aimed at advancing the chemical sciences. Full details are available from www.rsc.org

IN THIS ISSUE

ISSN 1463-9262 CODEN GRCHFJ 9(9) 913–1028 (2007)



Cover

The figure on the cover represents some of the effects of acid treatment on K-10 montmorillonite, set against a photo of Montmorillon, France: the type of locality for the mineral montmorillonite. Image reproduced with permission from Antonio F. Patti, *Green Chem.*, 9(9), 980.

CHEMICAL TECHNOLOGY

T65

Chemical Technology highlights the latest applications and technological aspects of research across the chemical sciences.

Chemical Technology

September 2007/Volume 4/Issue 9

www.rsc.org/chemicaltechnology

EDITORIAL

923

Green Solvents for Processes

Professor Walter Leitner, Scientific Editor for Green Chemistry, reflects on the role of alternative solvents in green chemistry.



EDITORIAL STAFF

Editor

Sarah Ruthven

Publishing assistant

Ruth Bircham

Team leader, serials production

Stephen Wilkes

Technical editor

Edward Morgan

Production Administration coordinator

Sonya Spring

Administration assistants

Clare Davies, Donna Fordham, Julie Thompson

Publisher

Emma Wilson

Green Chemistry (print: ISSN 1463-9262; electronic: ISSN 1463-9270) is published 12 times a year by the Royal Society of Chemistry, Thomas Graham House, Science Park, Milton Road, Cambridge, UK CB4 0WF.

All orders, with cheques made payable to the Royal Society of Chemistry, should be sent to RSC Distribution Services, c/o Portland Customer Services, Commerce Way, Colchester, Essex, UK CO2 8HP. Tel +44 (0) 1206 226050; E-mail sales@rscdistribution.org

2007 Annual (print + electronic) subscription price: £902; US\$1705. 2007 Annual (electronic) subscription price: £812; US\$1534. Customers in Canada will be subject to a surcharge to cover GST. Customers in the EU subscribing to the electronic version only will be charged VAT.

If you take an institutional subscription to any RSC journal you are entitled to free, site-wide web access to that journal. You can arrange access via Internet Protocol (IP) address at www.rsc.org/ip. Customers should make payments by cheque in sterling payable on a UK clearing bank or in US dollars payable on a US clearing bank. Periodicals postage paid at Rahway, NJ, USA and at additional mailing offices. Airfreight and mailing in the USA by Mercury Airfreight International Ltd., 365 Blair Road, Avenel, NJ 07001, USA.

US Postmaster: send address changes to Green Chemistry, c/o Mercury Airfreight International Ltd., 365 Blair Road, Avenel, NJ 07001. All despatches outside the UK by Consolidated Airfreight.

PRINTED IN THE UK

Advertisement sales: Tel +44 (0) 1223 432246; Fax +44 (0) 1223 426017; E-mail advertising@rsc.org

Green Chemistry

Cutting-edge research for a greener sustainable future

www.rsc.org/greenchem

Green Chemistry focuses on cutting-edge research that attempts to reduce the environmental impact of the chemical enterprise by developing a technology base that is inherently non-toxic to living things and the environment.

EDITORIAL BOARD

Chair

Professor Martyn Poliakoff
Nottingham, UK

Scientific Editor

Professor Walter Leitner
RWTH-Aachen, Germany

Associate Editors

Professor C. J. Li
McGill University, Canada
Professor Kyoko Nozaki
Kyoto University, Japan

Members

Professor Paul Anastas
Yale University, USA
Professor Joan Brennecke
University of Notre Dame, USA
Professor Mike Green
Sasol, South Africa
Professor Buxing Han
Chinese Academy of Sciences,
China
Professor Roshan Jachuck
Clarkson University, USA

Dr Alexei Lapkin
Bath University, UK
Dr Janet Scott
Unilever, UK
Professor Tom Welton
Imperial College, UK

ADVISORY BOARD

James Clark, York, UK
Avelino Corma, Universidad
Politécnica de Valencia, Spain
Mark Harmer, DuPont Central
R&D, USA
Herbert Hugl, Lanxess Fine
Chemicals, Germany
Makato Misono, nite,
Japan
Colin Raston,
University of Western Australia,
Australia

Robin D. Rogers, Centre for Green
Manufacturing, USA
Kenneth Seddon, Queen's
University, Belfast, UK
Roger Sheldon, Delft University of
Technology, The Netherlands
Gary Sheldrake, Queen's
University, Belfast, UK
Pietro Tundo, Università ca
Foscari di Venezia, Italy

INFORMATION FOR AUTHORS

Full details of how to submit material for publication in Green Chemistry are given in the Instructions for Authors (available from <http://www.rsc.org/authors>). Submissions should be sent via ReSource: <http://www.rsc.org/resource>.

Authors may reproduce/republish portions of their published contribution without seeking permission from the RSC, provided that any such republication is accompanied by an acknowledgement in the form: (Original citation) – Reproduced by permission of the Royal Society of Chemistry.

© The Royal Society of Chemistry 2007. Apart from fair dealing for the purposes of research or private study for non-commercial purposes, or criticism or review, as permitted under the Copyright, Designs and Patents Act 1988 and the Copyright and Related Rights Regulations 2003, this publication may only be reproduced, stored or transmitted, in any form or by any means, with the prior permission in writing of the Publishers or in the case of reprographic reproduction in accordance with the terms of licences issued by the Copyright Licensing Agency in the UK. US copyright law is applicable to users in the USA.

The Royal Society of Chemistry takes reasonable care in the preparation of this publication but does not accept liability for the consequences of any errors or omissions.

Ⓢ The paper used in this publication meets the requirements of ANSI/NISO Z39.48-1992 (Permanence of Paper).

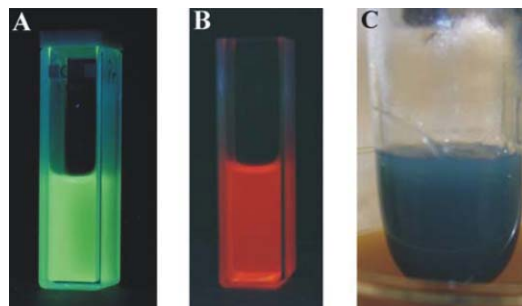
Royal Society of Chemistry: Registered Charity No. 207890

924

Ionic liquid-based approach to doped nanoscale oxides: $\text{LaPO}_4\text{:RE}$ (RE = Ce, Tb, Eu) and $\text{In}_2\text{O}_3\text{:Sn}$ (ITO)

Gunnar Bühler, Manola Stay and Claus Feldmann*

A microwave-assisted synthesis in ionic liquids is presented as a novel approach to functional nanomaterials. The performance of the examples $\text{LaPO}_4\text{:RE}$ (RE = Ce, Tb, Eu) and $\text{In}_2\text{O}_3\text{:Sn}$ (ITO) evidences the effectiveness of the synthesis.



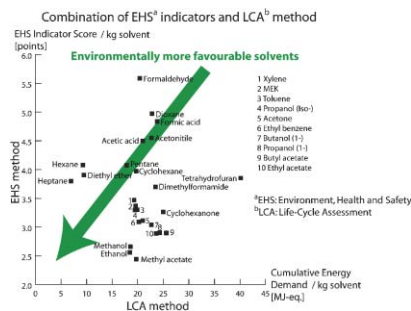
PAPERS

927

What is a green solvent? A comprehensive framework for the environmental assessment of solvents

Christian Capello, Ulrich Fischer* and Konrad Hungerbühler

This article addresses the question of how to measure how “green” a solvent is. We propose a framework that covers major aspects of the environmental performance of solvents over the full life-cycle, and also includes health and safety issues.

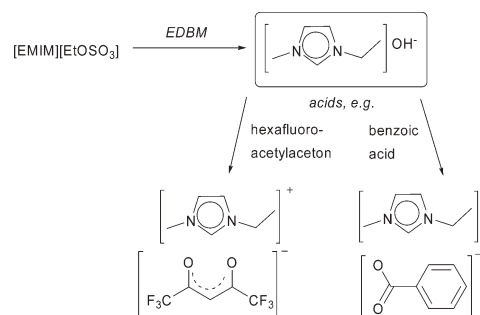


935

Synthesis of $[\text{EMIM}]\text{OH}$ via bipolar membrane electrodialysis – precursor production for the combinatorial synthesis of $[\text{EMIM}]$ -based ionic liquids

S. Himmler, A. König and P. Wasserscheid*

A new environmentally benign process for the production of aqueous solutions of $[\text{EMIM}]\text{OH}$ is reported. Electrodialysis with bipolar membranes (EDBM) was implemented for the first time to produce $[\text{EMIM}]\text{OH}$ from the ionic liquid $[\text{EMIM}][\text{EtOSO}_3]$ at the kg-scale.

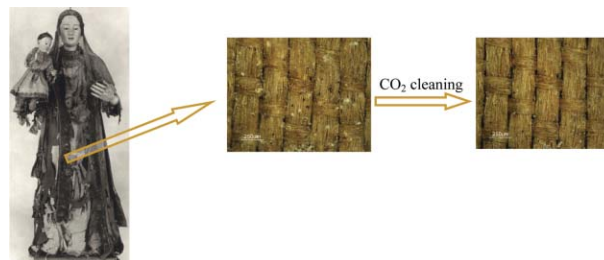


943

The art of CO_2 for art conservation: a green approach to antique textile cleaning

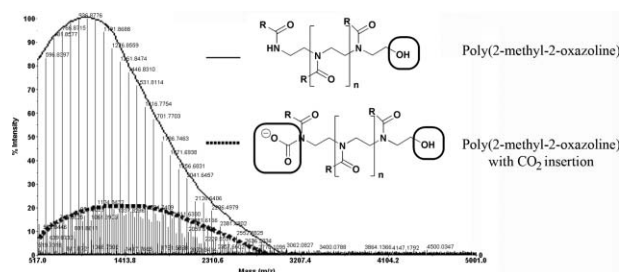
Micaela Sousa, Maria João Melo,* Teresa Casimiro and Ana Aguiar-Ricardo*

The CO_2 cleaning represents an enormous advantage for the cleaning of textiles of historic or artistic value, and allows the preservation of textile cultural heritage within the limits of disintegration.



PAPERS

948



Boron trifluoride catalyzed polymerisation of 2-substituted-2-oxazolines in supercritical carbon dioxide

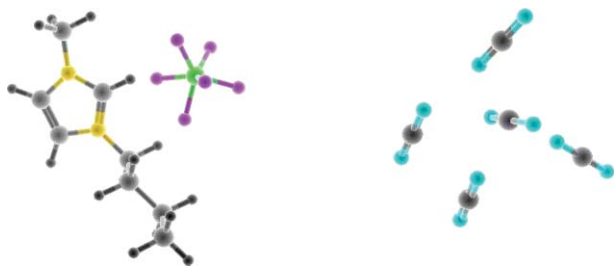
Carlota Veiga de Macedo, Mara Soares da Silva, Teresa Casimiro, Eurico J. Cabrita and Ana Aguiar-Ricardo*

In this work boron trifluoride was used as initiator for the polymerisation of three substituted 2-oxazolines in supercritical carbon dioxide. In each polymerisation, there was an unexpected CO₂ insertion in 10–25% of the overall polymer.

REGULAR RESEARCH ARTICLES

CRITICAL REVIEW

954



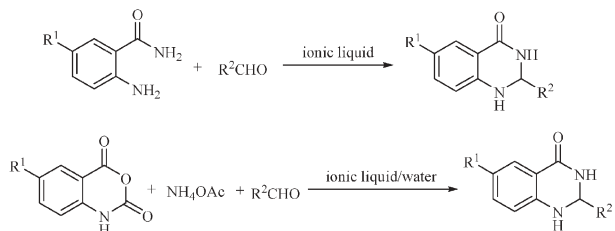
Biocatalysis in non-conventional media—ionic liquids, supercritical fluids and the gas phase

Sara Cantone, Ulf Hanefeld and Alessandra Basso*

The introduction of ILs, sc-fluids and solid–gas interphase reactions has definitely opened new perspectives in applied biocatalysis.

COMMUNICATIONS

972

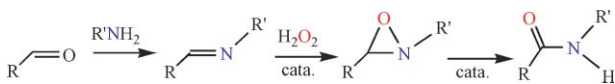


Eco-friendly synthesis of 2,3-dihydroquinazolin-4(1H)-ones in ionic liquids or ionic liquid–water without additional catalyst

Jiuxi Chen, Weike Su,* Huayue Wu,* Miao Chang Liu and Can Jin

2,3-Dihydroquinazolin-4(1H)-ones have been synthesized in high to excellent yields through direct cyclocondensation in ionic liquids (ILs) or one-pot three-component cyclocondensation in an ionic liquid–water solvent system without the use of any additional catalyst.

976



Atom economic synthesis of amides *via* transition metal catalyzed rearrangement of oxaziridines

Chin Hin Leung, Adelina M. Voutchkova, Robert H. Crabtree,* David Balcells and Odile Eisenstein*

A mild synthetic route to amides involves imine oxidation to an oxaziridine followed by a transition-metal catalyzed rearrangement to the amide.

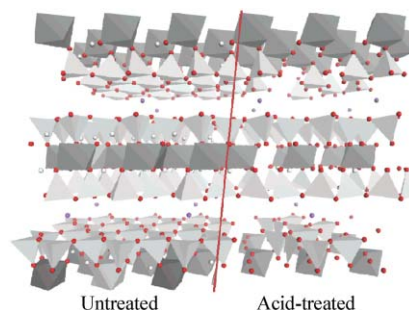
PAPERS

980

Assessing and improving the catalytic activity of K-10 montmorillonite

Philip J. Wallis, Will P. Gates, Antonio F. Patti,*
Janet L. Scott and Euneace Teoh

Procedures for assessing the catalytic activity of K-10 montmorillonite utilising physical and synthetic techniques are described. Significant and reproducible enhancements in K-10 reactivity can be obtained by acid treatment of the clay.

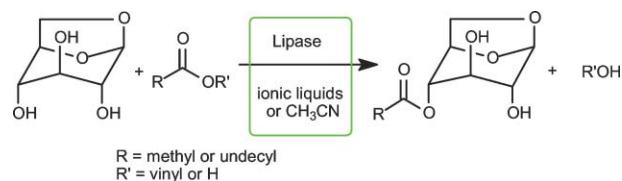


987

Enzymatic acylation of levoglucosan in acetonitrile and ionic liquids

Paola Galletti,* Fabio Moretti, Chiara Samori and
Emilio Tagliavini

Levoglucosan has been acylated in good yields using both vinyl esters and carboxylic acids in CH_3CN and ionic liquids.

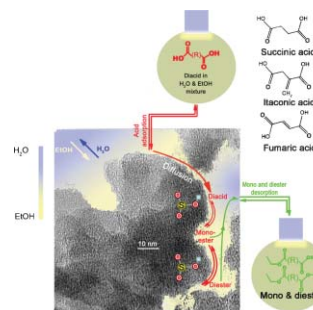


992

Tunable mesoporous materials optimised for aqueous phase esterifications

Vitaly L. Budarin, James H. Clark,* Rafael Luque,
Duncan J. Macquarrie, Apostolis Koutinas and
Colin Webb

Starbon[®] acids are tunable, mesoporous carbonaceous materials that can be optimised to carry out transformations of organic acids in aqueous solution.

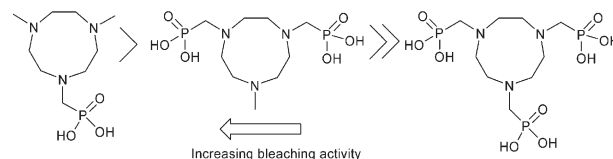


996

Investigations into the efficacy of methylphosphonic acid functionalised 1,4,7-triazacyclononane ligands in bleaching catalysis

Kirtida Shastri, Eileen W. C. Cheng, Majid Motevalli,
John Schofield, Jennifer S. Wilkinson and
Michael Watkinson*

In an attempt to reduce the dye and fabric damage caused by manganese complexes previously employed as low temperature bleaching catalysts in domestic laundry formulations, a novel series of analogues with aminophosphonic acid pendant arms has been prepared.



1008

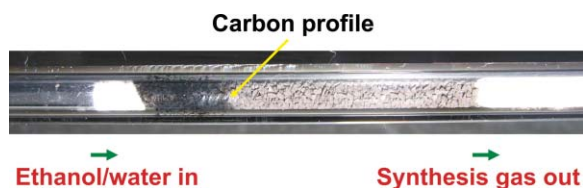


Renewable plant-based soybean oil methyl esters as alternatives to organic solvents

Scott K. Spear,* Scott T. Griffin, Kimberly S. Granger, Jonathan G. Huddleston and Robin D. Rogers*

Advancing the physico-chemical understanding of soybean oil methyl esters through studies into the free energy of transfer of a methylene group and Abraham's generalized solvation equation by partitioning more than 20 solutes is reported.

1016

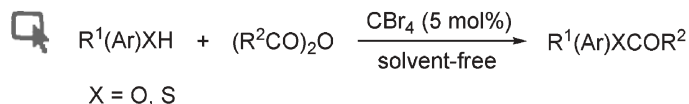


Renewable hydrogen: carbon formation on Ni and Ru catalysts during ethanol steam-reforming

Jeppe Rass-Hansen, Claus Hviid Christensen,* Jens Sehested, Stig Helveg, Jens R. Rostrup-Nielsen and Søren Dahl*

The catalytic steam-reforming of ethanol for the production of hydrogen is investigated with Ni and Ru catalysts; and quantitative and qualitative determinations of the carbon formation on these catalysts by TPO and TEM experiments provide new insight into this key challenge.

1022



Metal- and solvent-free conditions for the acylation reaction catalyzed by carbon tetrabromide (CBr₄)

Liang Zhang, Yong Luo, Renhua Fan* and Jie Wu*

Carbon tetrabromide was discovered to be highly effective for the acylation reaction under solvent-free conditions.

AUTHOR INDEX

- | | | | |
|--------------------------------|-------------------------------|--------------------------------|-----------------------------|
| Aguiar-Ricardo, Ana, 943, 948 | Eisenstein, Odile, 976 | Liu, Miaochang, 972 | Spear, Scott K., 1008 |
| Balcells, David, 976 | Fan, Renhua, 1022 | Luo, Yong, 1022 | Stay, Manola, 924 |
| Basso, Alessandra, 954 | Feldmann, Claus, 924 | Luque, Rafael, 992 | Su, Weike, 972 |
| Budarin, Vitaly L., 992 | Fischer, Ulrich, 927 | Macquarrie, Duncan J., 992 | Tagliavini, Emilio, 987 |
| Bühler, Gunnar, 924 | Galletti, Paola, 987 | Melo, Maria João, 943 | Teoh, Euneace, 980 |
| Cabrita, Eurico J., 948 | Gates, Will P., 980 | Moretti, Fabio, 987 | Voutchkova, Adelina M., 976 |
| Cantone, Sara, 954 | Granger, Kimberly S., 1008 | Motevalli, Majid, 996 | Wallis, Philip J., 980 |
| Capello, Christian, 927 | Griffin, Scott T., 1008 | Patti, Antonio F., 980 | Wasserscheid, P., 935 |
| Casimiro, Teresa, 943, 948 | Hanefeld, Ulf, 954 | Rass-Hansen, Jeppe, 1016 | Watkinson, Michael, 996 |
| Chen, Jiuxi, 972 | Helveg, Stig, 1016 | Rogers, Robin D., 1008 | Webb, Colin, 992 |
| Cheng, Eileen W. C., 996 | Himmler, S., 935 | Rostrup-Nielsen, Jens R., 1016 | Wilkinson, Jennifer S., 996 |
| Christensen, Claus Hviid, 1016 | Huddleston, Jonathan G., 1008 | Samori, Chiara, 987 | Wu, Huayue, 972 |
| Clark, James H., 992 | Hungerbühler, Konrad, 927 | Schofield, John, 996 | Wu, Jie, 1022 |
| Crabtree, Robert H., 976 | Jin, Can, 972 | Scott, Janet L., 980 | Zhang, Liang, 1022 |
| Dahl, Søren, 1016 | König, A., 935 | Sehested, Jens, 1016 | |
| da Silva, Mara Soares, 948 | Koutinas, Apostolis, 992 | Shastri, Kirtida, 996 | |
| de Macedo, Carlota Veiga, 948 | Leung, Chin Hin, 976 | Sousa, Micaela, 943 | |

FREE E-MAIL ALERTS AND RSS FEEDS

Contents lists in advance of publication are available on the web *via* www.rsc.org/greenchem - or take advantage of our free e-mail alerting service (www.rsc.org/ej_alert) to receive notification each time a new list becomes available.



Try our RSS feeds for up-to-the-minute news of the latest research. By setting up RSS feeds, preferably using feed reader software, you can be alerted to the latest Advance Articles published on the RSC web site. Visit www.rsc.org/publishing/technology/rss.asp for details.

ADVANCE ARTICLES AND ELECTRONIC JOURNAL

Free site-wide access to Advance Articles and the electronic form of this journal is provided with a full-rate institutional subscription. See www.rsc.org/ejs for more information.

* Indicates the author for correspondence: see article for details.



Electronic supplementary information (ESI) is available *via* the online article (see <http://www.rsc.org/esi> for general information about ESI).

Specialised
searching

requires
specialised
tools

Registered charity Number 207890

The graphical abstracting services at the RSC
are an indispensable tool to help you search
the literature.

Catalysts and Catalysed Reactions focuses on key primary journals covering: chiral catalysts, polymerisation catalysts, enzymatic catalysts and clean catalytic methods.

The online database has excellent functionality. Search by: authors, products, reactants and catalysts, catalyst type and reaction type.

With Catalysts and Catalysed Reactions you can find exactly what you need. Search results include diagrams of reaction schemes. Also available as a print bulletin.

For more information visit

RSCPublishing

www.rsc.org/databases

03/07/063

Better, faster communication

Look no further than the *Journal of Environmental Monitoring* for urgent publication of your cutting-edge research on all aspects of environmental science in the natural and anthropogenic environment.

Journal of Environmental Monitoring communications report high impact, preliminary results of current and immediate interest. Communications are fast-tracked through the publication process, given a high profile in the journal and widely promoted.

Featured on the cover is a recent communication on the rapid detection of contaminants in potable water.

Adrian J. Charlton *et al.*, *J. Environ. Monit.*, 2006, **8**, 1106



Submit your communication today!

RSC Publishing

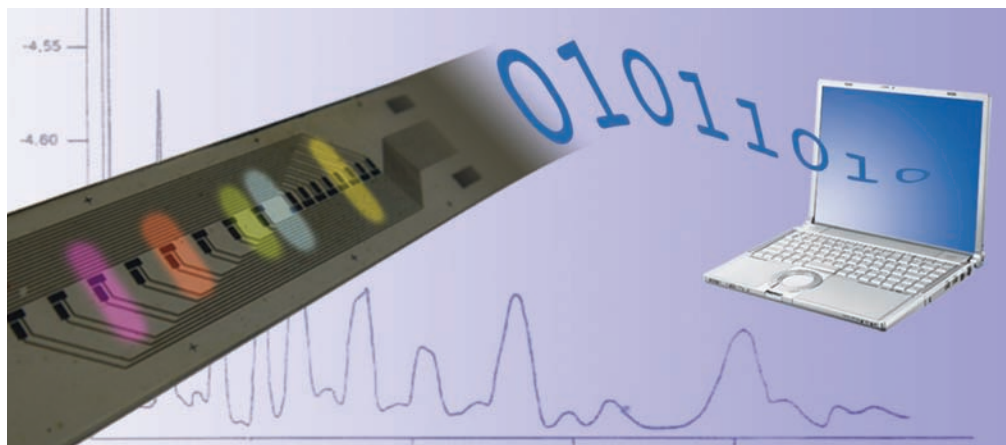
www.rsc.org/jem/communications

Registered Charity Number 207890

Chemical Technology

Photosensor array allows quality and quantity of mixture to be measured

Smart TLC



Italian researchers have developed a thin layer chromatography (TLC) plate that allows them to identify not only the presence of different components in a mixture, but also how much of each component is present.

Chromatography is a versatile and powerful technique that separates mixtures into individual components according to their different binding affinities to a

mobile and a stationary phase. Augusto Nascetti and colleagues at the University of Rome put the stationary phase of a TLC plate and amorphous silicon photodiodes on the same glass substrate to make the plate 'active' and allow real-time monitoring of the separation process.

In their technique, the team irradiate the plate with ultraviolet radiation while the separation

The intensity of the fluorescent signal is used to calculate the quantities present

is taking place. This excites the fluorescence of the different components of the mixture being analysed. The intensity of the fluorescence signal is proportional to the peak height detected and this can be used to determine the quantity of each component in the mixture.

According to Nascetti the preliminary results 'suggest that the proposed system can effectively add value to conventional TLC technology'. The technique operates on a small scale and requires only small amounts of eluents, which reduces both the cost and any risks associated with the use of harmful solvents. Advantageously, the plate can also be easily incorporated into a portable field device. Potential applications include uses in food quality control such as early detection of toxins in wine.

Kathryn Lees

Reference

D Caputo *et al*, *Lab Chip*, 2007, **7**, 978 (DOI: 10.1039/b709145a)

In this issue

China's pollution headache

Coal is the culprit in a year-long study of Chinese cities

Mars rocks

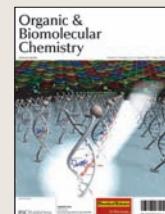
Laser-induced breakdown spectroscopy improved for mission

Instant insight: The shape of things to come

Paul Midgley and colleagues discuss using nanotomography to take a 3D glimpse of the nanoworld

Interview

Jim Heath talks about the discovery of C₆₀ and his more recent adventures



The latest applications and technological aspects of research across the chemical sciences

Application highlights

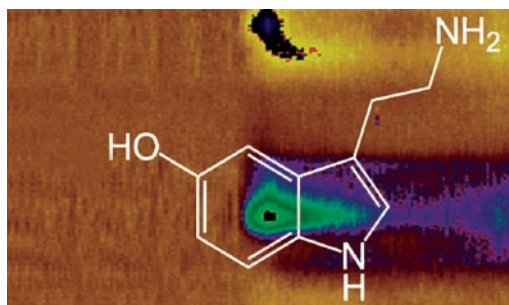
Important neurotransmitters can be studied simultaneously

Dual detection

Scientists in the US have developed a sensor that can detect dopamine and serotonin simultaneously *in vivo* for the first time.

Dopamine and serotonin are important neurotransmitters. Serotonin is known to regulate sleep and is a common target for depression medication. Dopamine has been linked to locomotion, reward and motivation, and is a common target for illicit drugs. The death of dopamine receptors is the cause of Parkinson's disease. However, the two are inherently linked; cocaine is known to act on both dopamine and serotonin transporters, for example. Consequently, the simultaneous, rapid, *in vivo* detection of these compounds is a requirement if their interactions in the brain are to be understood.

However, using electrochemistry to detect both compounds simultaneously has proven difficult, due to the compounds' similar oxidation potentials. Detecting dopamine causes fouling by serotonin, while methods to avoid serotonin fouling prevent dopamine



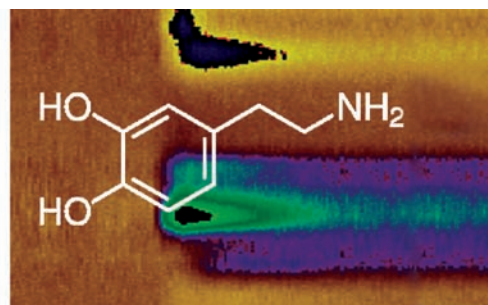
Serotonin (left) and dopamine (right) give different electrochemical signals at carbon nanotube electrodes

detection.

Now, Jill Venton and Kumara Swamy at the University of Virginia have developed carbon nanotube modified microelectrodes that can detect serotonin and dopamine at the same time.

'We showed that carbon nanotube sensors have increased sensitivity for dopamine and serotonin and are more resistant to fouling by oxidative products of serotonin,' explained Venton.

Mark Wightman, an expert in neurochemistry and electrochemistry at the University of North Carolina, Chapel Hill, US, appreciated the significance of their new technique. '*In vivo*



voltammetry at carbon-fibre microelectrodes provides the only way to follow the release and uptake of neurotransmitters in the brain as they control rapid behaviours on a second-to-second time scale,' he said. 'This new approach by Venton ... has several advantages.'

Although it is still unclear how the carbon nanotubes increase resistance to fouling Venton hopes the microelectrodes will allow further studies of dopamine and serotonin in the brain.

'The next challenge,' she said, 'is to create even smaller, nanotube-based electrodes to more closely approach the small size of synapses.' Edward Morgan

Reference

B E K Swamy and B J Venton, *Analyst*, 2007, DOI: 10.1039/b705552h

Polymer replaces oxide material in display cathode

Flexible electrodes

New bendy LEDs don't crack under the strain.

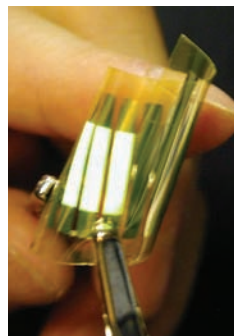
Electrodes made from conducting polymers make LEDs more flexible, according to a team from Imperial College London, UK.

Polymer LEDs consist of layers of light-emitting polymer sandwiched between two electrodes. Although various studies have tried to build polymer LEDs on flexible substrates, the electrode materials cannot always cope with being bent. One of the most commonly used cathode materials, indium tin oxide (ITO), is quite brittle, and tends to crack when the LED is flexed. ITO films are usually made by evaporation at high temperatures, but when working with plastic substrates the temperature has

to be kept much lower to avoid melting the plastic, and ITO films made at these lower temperatures tend to be of low quality.

The Imperial team replaced the ITO cathode with a conducting polymer layer, made from poly(3,4-ethylenedioxythiophene) and polystyrenesulfonate. They built their LEDs on overhead projector transparencies, and succeeded in making bright yellow LEDs which work even when tightly rolled up into a tube.

'The main challenge now is to drive up the conductivity of the polymer anode to the point where it actually starts to compete with ITO. This won't be easy but we have a few ideas up our sleeves,' said John deMello, who led the research.



Bendy LEDs have a future in biomedical devices

Reference

J Huang et al, *J. Mater. Chem.*, 2007, DOI: 10.1039/b705918n

'The other issue is LED lifetime. The organic layers are extremely air-sensitive so finding an effective way of protecting the devices inside flexible, transparent packaging is going to be absolutely crucial.'

Commercial applications are already on their way for these LEDs, added deMello. 'The technology has recently been licensed to a start-up company called Molecular Vision, who are using it to develop a new line of disposable diagnostic devices for health care testing. They're combining the LEDs with flexible photo-detectors (also developed at Imperial) to create ultra-miniaturised low cost sensors for the analysis of blood and urine.' Clare Boothby

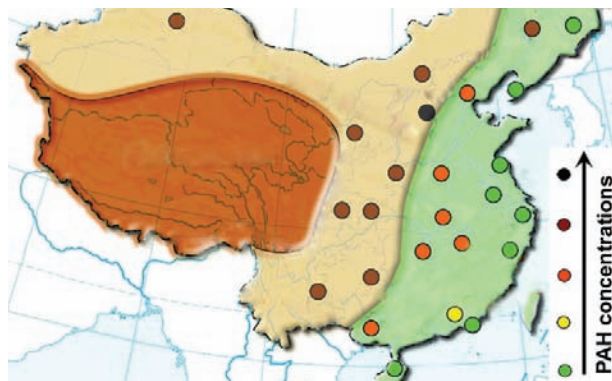
A year-long study of pollution in cities finds coal is the culprit

China's pollution headache

Chinese scientists have found concentrations of polycyclic aromatic hydrocarbons (PAHs) in some Chinese cities to be among the highest in the world, exceeding proposed EU air-quality standards in many cases.

PAHs are formed from the incomplete burning of fossil fuels and the International Agency for Research in Cancer has classified some of them as probable human carcinogens.

As China is the world's most populated country and largest consumer of coal, and its number of vehicles is growing along with its economy, Gan Zhang and co-workers set out to conduct a large-scale study of PAH levels across the whole of China, comparing 36 cities (and three rural locations) across all four seasons of 2005. The team, based mainly at Guangzhou



Institute of Geochemistry, found that levels were greatest in cities on higher ground (in north and north-west China), which had colder winters and burnt more coal.

Kevin Jones, of Lancaster University, UK, worked on the study and described this negative correlation between the average

Pollution levels were greatest in areas with colder winters

annual PAH concentrations and annual average temperature as 'significant' and explained that, although several factors acting in combination influenced air concentrations, 'winter time PAH concentrations correlated with estimated coal consumption'.

Ian Colbeck, director of the Centre for Environment and Society at the University of Essex, UK, said Zhang's study was 'another example of the adverse impact on the environment as a result of China's drive to increase industrial output'.

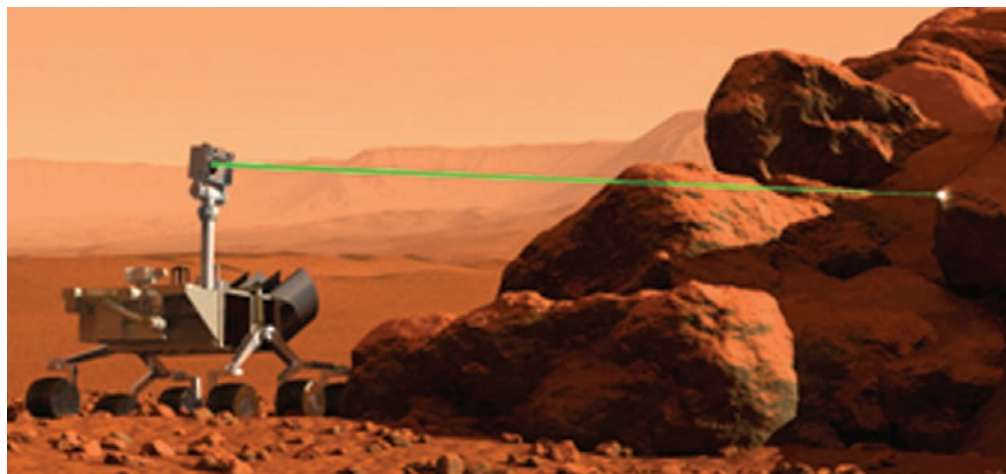
'The health implications of the high concentrations of PAHs in the densely populated Chinese cities are very significant,' added Colbeck. *Ian Gray*

Reference

X Liu *et al*, *J. Environ. Monit.*, 2007, DOI: 10.1039/b707977j

Laser-induced breakdown spectroscopy improved for mission

Mars rocks



The way in which the Mars Science Laboratory rover will identify Martian rocks has been tested by French scientists.

The Mars Science Laboratory rover is due to be launched in 2009. Its overall mission is to determine whether Mars is (or ever was) able to support microbial life. It

will carry an instrument called ChemCam, which will use laser-induced breakdown spectroscopy (LIBS) to remotely identify Martian rocks.

Jean-Baptiste Sirven, of the CEA Saclay, and colleagues tested chemometric methods for analysing LIBS spectra. A laser is used to

The Mars Science Laboratory rover will use a laser to vaporise the outer layer of Martian rocks

vaporise the dust-covered rock to get to the non-weathered layers below. The elements in the rock are excited by the laser and emit light at characteristic wavelengths. These spectra are then compared to spectra of known samples to classify the rock samples.

Sirven tried three different ways of statistically analysing the spectra. He found that a combination of methods would give the best results. At the start, a method that is able to differentiate between rocks of very similar composition would be used. Then, as the number of Martian spectra collected increases, a laboratory-calibrated model would become more accurate, as it became more representative of the planet geology. According to Sirven, the combined method correctly identifies over 99 per cent of samples.

Susan Batten

Reference

J-B Sirven *et al*, *J. Anal. Atomic Spectrosc.*, 2007, DOI: 10.1039/b704868h

Cancer markers monitored in real-time with a biocompatible device

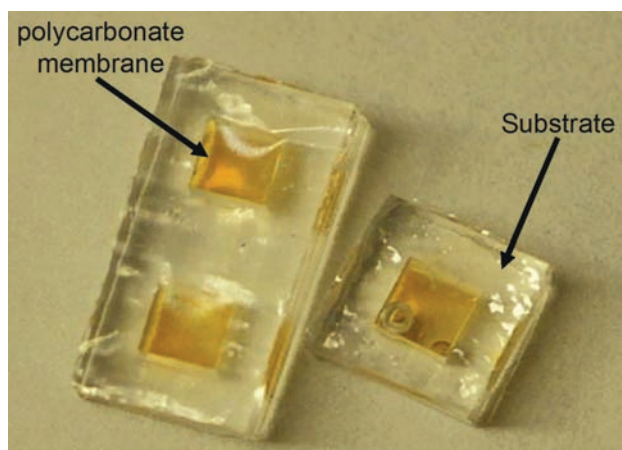
The only way is in

An implantable cancer sensor that uses a membrane to isolate cancer-detecting nanoparticles should help speed up diagnoses, according to researchers from the US.

Early diagnosis and choosing the right treatment are two of the most important factors in the fight against cancer. One of the best ways to monitor cancer is to look for so-called cancer markers – compounds which are produced by cancerous cells, but until now this has been done by performing blood tests or biopsies.

Michael Cima and colleagues from MIT and Harvard have come up with a way of testing for cancer markers in real-time which could make initial diagnosis quicker, and potentially give an indication of whether a particular treatment is effective.

Nanoparticles whose magnetic properties change in the presence of certain analytes (in this case the cancer markers) have been reported previously, but they have not been



Only the cancer markers can pass through the membrane – not the toxic nanoparticles

used in the body because of their stability and toxicity.

Cima's team solved this by encasing them in a polymer reservoir and semi-isolating them from the environment by using a membrane which only allows small molecules to pass. This allows the cancer markers in (and out) but the nanoparticles remain within the

device and are stable. 'We would hope to implant a device at the same time as performing a needle biopsy,' said Cima.

Hsian-Rong Tseng from the University of California, Los Angeles, US, said 'The components of the device are already known to be biocompatible, so this can easily be utilised as an implantable sensor. The multiple wells mean that the measurements can easily be repeated improving the quality of the data obtained.'

Martin Leach from the Institute of Cancer Research, London, UK, said 'This is indeed an interesting advance, at present the diffusion across the membrane is slow, but if this can be improved, one could envisage truly real-time experiments where it will be possible to observe where and how chemotherapeutics work.'

Cima and his team continue to work closely with clinicians in developing this technology. *Stephen Davey*

Reference

K D Daniel *et al*, *Lab Chip*, 2007, DOI: 10.1039/b705143c

Single nucleotide polymorphs found quickly and easily

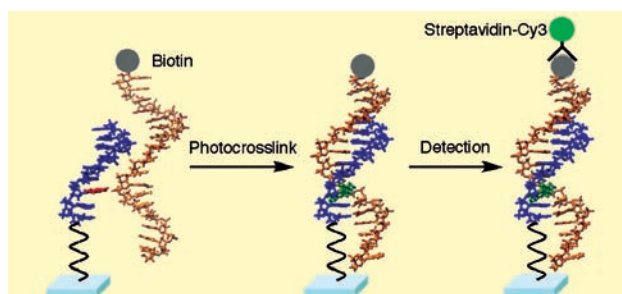
DNA chips detect disease

A DNA chip that can identify genetic mutations has been synthesised by Japanese scientists.

The most common form of genetic variation between individuals is caused by single-nucleotide differences in our DNA code. These are called single nucleotide polymorphisms (SNPs). SNPs can be used to identify disease genes and can highlight when a person is likely to develop a disease.

Kenzo Fujimoto and colleagues at the Japan Advanced Institute of Science and Technology have developed a simple and rapid method for identifying SNPs. They hope it could be the basis for automated diagnosis.

The method uses a short strand of DNA, known as an oligodeoxynucleotide probe, attached to a glass chip. The probe



contains DNA bases complementary to those in the DNA strand containing the SNP of interest, except that one base is replaced by a vinyl-containing nucleoside known as cvP. When Fujimoto placed the target DNA onto the chip and shone ultraviolet light on it, the cvP reacted with an adenine base on the target DNA, in a reaction known as photocrosslinking. Fujimoto

The blue DNA probe is crosslinked to the orange target strand

detected the photocrosslinked product using fluorescence imaging.

Photocrosslinking only occurs when all the bases on the probe are complementary to those on the target DNA, so if there is a mismatch in the strands the chip does not fluoresce.

'This method is an efficient reaction and proceeds with high sequence specificity,' said Fujimoto. 'Photochemical DNA manipulation is a highly original research theme.'

Hans-Achim Wagenknecht, of the University of Regensburg, Germany, said the work is a significant improvement for SNP detection. 'Such cheap, sensitive and reliable screening tools are needed to clinically diagnose genetic variations, infectious diseases and pharmacology,' he said. *Joanne Thomson*

Reference

T Ami *et al*, *Org. Biomol. Chem.*, 2007, DOI: 10.1039/b708264a

Instant insight

The shape of things to come

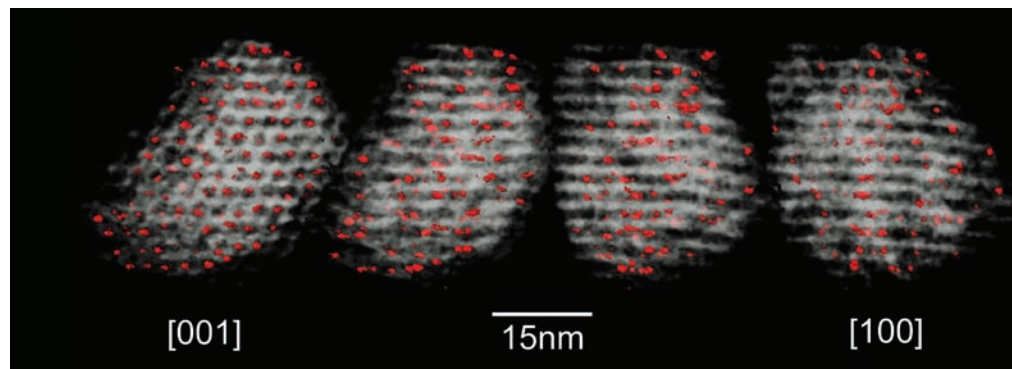
Paul Midgley, Edmund Ward, Ana Hungria and John Meurig Thomas discuss using nanotomography to take a 3D glimpse at the nanoworld

There is little doubt that medicine has benefited greatly from the ability to visualise the internal organs of the human body using a variety of radiation including X-rays, positrons, ultrasound and nuclear magnetic resonance. The invention of the 'cat-scan', or CT-scan, in the 1960s enabled such views to be further improved by allowing a full three-dimensional reconstruction of the internal architecture of the body. The basis behind the reconstruction is the technique of tomography, from the Greek word 'tomos' meaning 'slice' or 'section', in which a series of images, or projections, is used to create a three-dimensional view by back-projecting these images into a 3D space in a computer.

In the chemical sciences, relatively little advantage has been taken of tomographic techniques even though it has long been clear that the spatial resolution ultimately attainable by the use of X-rays and electron beams far exceed those associated with CT scans and NMR imaging of the human body.

Just as the morphology and size of organs is of key importance in the human anatomy, in nanoscience and nanotechnology the size and shape of an object may play a key role in determining its electronic and chemical behaviour. There are many examples where the physical and chemical properties of nanocrystals and clusters deviate significantly from their bulk crystalline phase. Gold in its bulk state displays no catalytic activity and yet in nanoparticle form it is an extremely good catalyst for selective oxidation of hydrocarbons and the complete combustion of carbon monoxide in air. The shape or crystal morphology can be equally important, such as in ceria nanoparticles for automotive catalysis.

The shape, size and distribution of nanoparticles and nano-structures are all key to their function and the



need for tomographic methods applicable to chemical systems (ranging from the physical to the biological) is therefore pressing, just as it is in the engineering and earth sciences.

In our Critical Review¹ we investigate nanotomographic methods that are open to the materials-oriented chemist and present a range of illustrative examples taken from nanoscale chemistry, along with contiguous sub-disciplines encompassing parts of biology and medicine.

We focus mainly on electron tomography (of which there are several variants), and its life sciences application, such as the study of cellular organelles, magnetotactic bacteria and the nuclear pore complex, and in the physical sciences, including supported catalysts, nanoalloys and binary II–VI compounds and polymers. Three-dimensional spatial resolution of 1 nm³ is now possible and efforts are afoot worldwide to reach atomic resolution in three dimensions using electron tomography. In anticipation of future developments, we also outline the rudiments of tomography via transmission X-ray microscopy, a technique that will undoubtedly be of tremendous importance, especially with greater access to next-generation synchrotron X-ray

A montage of projections of a scanning transmission electron tomogram. It shows a selective hydrogenation Ru₁₀Pt₂ nano-catalyst in which the distribution of nanoparticles (red) is revealed within a mesoporous silica support (white). A mean particle size of 100 atoms indicates the zeptogram (10⁻²¹ g) sensitivity of this 3D imaging technique

sources, such as the new Diamond Light Source in the UK. Other nanotomographic techniques highlighted in the review include atom probe field-ion microscopy (APFIM), a destructive technique applicable to conducting and semi-conducting samples. It uses time-of-flight mass spectrometry to identify single ions combined with position sensitive detection to produce a sensor capable of determining three-dimensional information with excellent resolution in both location and chemical identity. Serial sectioning, in which a three-dimensional model may be constructed from a series of slices, is possible with techniques such as atomic force microscopy and scanning electron microscopy (SEM), coupled with a focussed ion beam (FIB) workstation.

The need for three-dimensional visualisation and analysis at high spatial resolution is likely to increase as nanoscience and nanotechnology become increasingly important – nanotomography will play a key role in understanding structure, composition and physico-chemical properties at the nanoscale.

Read the full Critical Review 'Nanotomography in the chemical, biological and materials sciences' in issue 9 of Chemical Society Reviews.

Reference
1 P A Midgley et al, *Chem. Soc. Rev.*, 2007, **36**, 1477 (DOI: 10.1039/b701569k)

Easier and more efficient than traditional LLE

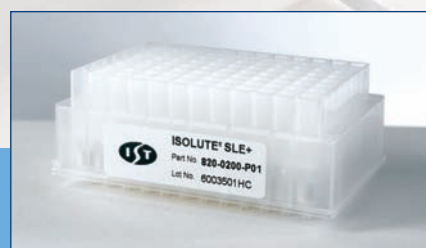
... SLE+ Supported Liquid Extraction Plates

Supported Liquid Extraction (SLE) provides an easier to automate alternative to liquid-liquid extraction (LLE), with no off-line steps (e.g. mixing or centrifuging) required. Problems including emulsion formation, and separation of liquid layers are eliminated.

ISOLUTE® SLE+ Supported Liquid Extraction Plates are optimized for simultaneous processing of 96 samples (extract up to 200 µL of plasma or urine per well), using a generic methodology for extraction of neutral, acidic and basic compounds.

ISOLUTE® SLE+ is available in the industry standard 2 mL fixed well 'SPE' plate format and is compatible with all commercially available automated liquid handling systems.

For more information or to request a free sample visit www.biotage.com.



NEW! ISOLUTE SLE+ Plates

Improve productivity and maximize analyte recovery with this new more efficient alternative to traditional liquid-liquid extraction.

- No emulsion formation
- Easy to automate
- Rapidly transfer methods from traditional LLE to ISOLUTE SLE+
- Excellent flow characteristics improve reproducibility


Biotage
www.biotage.com

Interview

Technology in a bottle

Jim Heath talks to Alison Stoddart about the discovery of C_{60} and his more recent adventures



Jim Heath

Jim Heath is Elizabeth W Gilloon professor of chemistry at California Institute of Technology, US, and director of the NanoSystems Biology Cancer Center. His current research spans many areas including nanotechnology, molecular electronics and cancer diagnosis. During his graduate studies with Richard Smalley, Jim was the principal student involved in the discovery of C_{60} .

What prompted you to study nanotechnology?

When I started it wasn't a field. As a graduate student, I was the guy who discovered C_{60} . That became one of the poster children of nanotechnology. Then, almost by accident I moved into the area. I worked at IBM for a while – synthesising silicon nanoparticles. I guess I fell in love with nanotechnology.

Can you describe the experiment where you saw C_{60} for the first time?

We were trying to emulate the surface of a carbon star. This was Harry Kroto's idea. We vaporised carbon with a laser in an environment that contained some of the small molecules that surround a carbon star, and then expelled it into a vacuum so we froze the chemistry very quickly. The first time I put carbon in the machine, I saw C_{60} . We had seen interesting clusters of systems before, but this looked unusual. So, even though we were focusing on small clusters, we decided to always monitor C_{60} . As Harry and I worked on the machine, we realised that C_{60} was a special molecule. I came to the conclusion that it was a closed ball. We had a long debate one day about its structure, we checked out books by Buckminster Fuller and Richard Smalley came up with the structure that night.

It took a while for the scientific community to accept the structure of C_{60} , why was this?

Our experiment was exotic but I thought we had an airtight case. It explained beautifully C_{60} , C_{70} , why we only saw even numbered carbon clusters and why the clusters weren't stable below a certain size. But chemists like to see X-ray crystal structures and NMR spectra and we didn't have these. We only had about 1000 molecules at any given time. But science works by people doubting what you do and pushing you forward.

Were you surprised that C_{60} became so popular?

C_{60} was a curiosity until 1991. Then Huffman and Krätschmer made solid-state C_{60} in gram-sized amounts. In fact, the surprise with C_{60} was how easy it was to make. Suddenly hundreds of groups worldwide were involved with C_{60} . This explosion was the power of having something interesting plus having something in a bottle. This made me realise that I didn't want to do gas phase chemical physics but I wanted to do something in a bottle.

What are your current research interests?

We work in the area of molecular electronics – making perfect electronic circuits that are macromolecular in dimension. In addition, we can make superconductors and thermoelectrics. A thermoelectric converts a temperature difference into a voltage – like an engine with no moving parts or it does the reverse and acts as a coolant. It turns out that solid-state thermoelectrics have limited uses because they aren't very efficient. If you could make them efficient then the rewards are amazing. We have made materials from oxygen and silicon that are close to the world record for thermoelectrics. These could be used in energy recovery systems in computer chips so wasted energy could be recycled.

I also work with cancer. Our goal is to translate molecular network models of cancer that describe how the disease evolves into tools that can be used in the clinic. We want to be able to do 1000 measurements from a finger prick of blood and at a fraction of a penny per measurement. We have made devices that are used by clinicians but it will be a similar advance as for computer chips. Right now, we can take a finger prick of blood and in a few minutes we do about 20 measurements and we ought to be able to do 40 next year. Our devices have no moving parts, they are made of just glass and plastic, because we want them to be practically free.

These two projects aim to tackle at least pieces of major global problems – energy and world healthcare.

What is your ultimate goal in the cancer project?

Take diabetes – it's a disease which has been transformed by technology over the last few years because you can monitor your glucose levels and take control of the disease. I would be interested to know if you could do this for cancer. It may be possible to detect cancer early on, before clinical signs, and you can always cure it at that point.

What is the secret of being a successful scientist?

It is important to be a good experimentalist, pick the right problems, look across different fields and collaborate with other scientists. When picking a problem, the pathway must be richer than the problem itself – so you have a chance of discovering something interesting along the way. It also helps to recognise when you are lucky.

Essential elements

Five fast and first-rate years

As celebrations for the fifth year of publishing for *Organic & Biomolecular Chemistry* (OBC) continue, RSC Publishing staff have been reflecting on the activities and successes.

Launched in 2003, OBC was built on the foundations laid by its predecessors *Perkin Transactions 1* and *2*. The intention was to ensure a strong international presence in the organic community – which has already been fulfilled. Not only does OBC have a competitive impact factor of 2.874, it also boasts quicker publication times than any of its competitors.

'The achievements over the first five years have been tremendous,' commented OBC editor Vikki Allen, 'and with the continued help of our authors, referees and readers we anticipate a first-rate future.'



As part of the celebrations for five successful years of publishing, the journal has featured a series of 'Top 5 articles' from a variety of geographic areas, plus members of the Editorial Board have selected their favourite five articles published in the journal

since launch.

Benjamin List, the winner of the 2007 OBC Lecture Award, spoke about the challenges for chemists during his lecture on organocatalysis at the 20th International Symposium: Synthesis in Organic Chemistry in July. Whatever the future

challenges across the broad organic spectrum of synthetic, physical and biomolecular chemistry, articles published in OBC are sure to be at the forefront.

Read more at www.rsc.org/obc

Packed with energy

One of the major challenges for the twenty-first century is the development of cleaner, sustainable sources of energy. The chemical sciences will play a critical role in successfully overcoming such issues, and the RSC is devoted to addressing them and working toward a better, cleaner future.

For more news on energy related research from RSC Publishing, please visit www.rsc.org/energy

Issue 30 of *Journal of Materials Chemistry* hosts a theme issue dedicated to New Energy Materials. Guest edited by M. Saiful Islam (University of Bath, UK) and including contributions from a range of internationally acclaimed authors, the issue highlights some of the latest developments in energy conversion and storage technologies making it a must-have for all scientists interested in energy research.

With the fastest publication rates in the industry and a soaring impact factor of 4.287 (a staggering increase of 58% over the past 2 years), *Journal of Materials Chemistry* has a well deserved reputation for excellence in the field.

Materials chemistry will play a critical role in developing



energy-related applications and therefore it is particularly timely to publish a focused set of articles covering this. The issue contains more than 20 articles on a range of topics, including: fuel cells, lithium-ion batteries, solar cells and hydrogen storage, and additionally hosts several feature, application and highlight articles.

Further information can be found at www.rsc.org/materials

Chemical Technology (ISSN: 1744-1560) is published monthly by the Royal Society of Chemistry, Thomas Graham House, Science Park, Milton Road, Cambridge UK CB4 0WF. It is distributed free with *Chemical Communications*, *Journal of Materials Chemistry*, *The Analyst*, *Lab on a Chip*, *Journal of Environmental Monitoring*, *Green Chemistry*, *CrystEngComm*, *Physical Chemistry Chemical Physics* and *Analytical Abstracts*. *Chemical Technology* can also be purchased separately. 2007 annual subscription rate: £199; US \$376. All orders accompanied by payment should be sent to Sales and Customer Services, RSC (address above). Tel +44 (0) 1223 432360, Fax +44 (0) 1223 426017 Email: sales@rsc.org

Editor: Neil Withers

Associate editors: Nicola Nugent, Celia Clarke

Interviews editor: Joanne Thomson

Essential Elements: Valerie Simpson and Ricky Warren

Publishing assistant: Jackie Cockrill

Publisher: Graham McCann

Apart from fair dealing for the purposes of research or private study for non-commercial purposes, or criticism or review, as permitted under the Copyright, Designs and Patents Act 1988 and the copyright and Related Rights Regulations 2003, this publication may only be reproduced, stored or transmitted, in any form or by any means, with the prior permission of the Publisher or in the case of reprographic reproduction in accordance with the terms of licences issued by the Copyright Licensing Agency in the UK. US copyright law is applicable to users in the USA.

The Royal Society of Chemistry takes reasonable care in the preparation of this publication but does not accept liability for the consequences of any errors or omissions.

Royal Society of Chemistry: Registered Charity No. 207890.

RSC Publishing

Green Solvents for Processes

DOI: 10.1039/b712156n

The colour of solvents

The use of organic solvents contributes strongly to the waste stream and is a major source of VOC emission in the chemical industry and related economic sectors. The search for alternative solutions continues to be an important area of green chemistry as reflected over the years by many contributions to this journal, including a series of papers based on contributions from the 2006 edition of the conference series on "Green Solvents for Processes" in this issue. Considerable progress has been made in science and application in this field, but it has also been pointed out that concentrating on a single aspect such as the solvent is often not sufficient for the "greening" of chemical processes (D. G. Blackmond, A. Armstrong, V. Coombe and A. Wells, *Angew. Chem., Int. Ed.*, 2007, **46**, 3798–3800; R. van Noorden, *Chemistry World*, 2007, **4**(6), 14–15). It may be useful to distinguish between two types of green solvents in the course of this important discussion.

The first class, which one may refer to as 1st generation, consists of organic liquid materials which provide the desired properties for a given process but have a significantly reduced ecological footprint than many solvents used traditionally in process development. A reliable data set is available and continues to emerge for a growing list of substances that fall into this category. Ideally, such solvents can be applied as drop-in solutions to an existing process. Provided that the alternative is economically

feasible, this will lead immediately to an improvement in the sustainability analysis as the remaining parameters remain largely unaffected. There is an enormous potential for this approach in many areas of chemical industry, and real world applications of green chemistry principles can be developed in a relatively short period of time on this basis.

Under the 2nd generation, one may summarize reaction media and concepts for solution phase applications that are not merely solvent replacements in the above sense, but possess physico-chemical properties that are significantly different from traditional organic solvents. This offers the molecular basis for the design of new process alternatives and engineering solutions with the potential to contribute to the development of more sustainable technical processes in a longer term strategy. In an early stage of development, it is much more difficult to assess this potential in quantitative terms and *a priori* analyses may be hampered by a lack of reliable criteria for a conclusive comparison. Clearly, there is no such thing as an "inherently green solvent" in this area. Progress will rely on the creativity to devise generic approaches and on research to evaluate their scope and limitations. The wide range of possibilities is narrowed down to promising opportunities in the course of this progress with a growing knowledge and understanding of the individual approaches. At the same time, new applications may emerge in areas that were not even considered in the original concept.

Similar considerations apply to other areas of green chemistry. The utilization of a renewable feedstock, for example, does not automatically lead to sustainable process. A full life cycle analysis of the *status quo* may well reveal that a petrochemical pathway is superior for a given product, if no green production process is available for the utilization of the preferred feedstock. The ongoing debate on alternative ways for the production of bio-fuels (for example, see: J. Johnson, *Chem. Eng. News*, 2007, 19–21; L. D. Schmidt and P. J. Dauenhauer, *Nature*, 2007, **447**, 914–915) provides an illustrative example that there is no golden path to sustainability.

Like in any other field of science, this non-linear development of research needs a forum for the presentation of success stories as much as for the critical discussion of ongoing trends and emerging areas. A scientific journal such as Green Chemistry provides an ideal platform for this open process based on its peer review system and on the broad readership that ultimately evaluates and determines the significance of the reported results. With an impact factor of 4.192 in 2007, it seems that the journal is on a good path to fulfil this challenging role.



Walter Leitner

Ionic liquid-based approach to doped nanoscale oxides: $\text{LaPO}_4\text{:RE}$ ($\text{RE} = \text{Ce, Tb, Eu}$) and $\text{In}_2\text{O}_3\text{:Sn}$ (ITO)^{†‡}

Gunnar Bühler, Manola Stay and Claus Feldmann*

Received 22nd November 2006, Accepted 30th January 2007

First published as an Advance Article on the web 9th February 2007

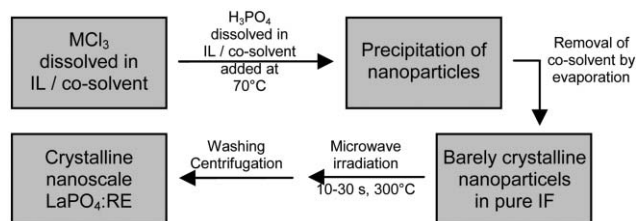
DOI: 10.1039/b617107a

A microwave-assisted synthesis in ionic liquids is presented as a novel approach to functional nanomaterials. $\text{LaPO}_4\text{:RE}$ ($\text{RE} = \text{Ce, Tb, Eu}$) and $\text{In}_2\text{O}_3\text{:Sn}$ (ITO) have been selected as examples to prove the effectiveness of the synthesis.

Ionic liquids (ILs) have attracted considerable interest in recent years due to their exceptional features, such as wide liquid range, excellent thermal stability, wide electrochemical window, and low vapor pressure.¹ In between, ILs have had a significant impact on organic synthesis.² Aiming at nanoscale materials and advanced nanostructures, exploration towards a beneficial use of ILs has just begun.³ First examples include the synthesis of elemental metals,⁴ oxides,⁵ and fluorides.⁶

This investigation addresses the relevance of ionic liquids with concern to the synthesis of nanoscale functional materials. Its focus is especially on the relevant material properties. To this purpose, two well-known functional materials have been selected: $\text{LaPO}_4\text{:RE}$ ($\text{RE} = \text{Ce, Tb, Eu}$) as a phosphor as well as $\text{In}_2\text{O}_3\text{:Sn}$ (ITO: indium tin oxide) as a transparent conductive oxide (TCO). Both materials are of major industrial importance.⁷ The emerging interest in high-quality materials on the nanoscale is currently hampered by several drawbacks. First, thermal post-treatments ($>400^\circ\text{C}$) are most often needed to remove all (OH)-contents and to crystallize the material.⁸ Second, coordinating, often harmful, surface-active solvents or stabilizers are required to control particle size and size distribution.⁹ Moreover, surface-active agents or advanced core-shell structures are prerequisite to reduce surface-allocated lattice defects.¹⁰ With all these measures, materials synthesis is complicated and time-consuming, often resulting in aggregate formation and often limiting the quality of the luminescent or conductive properties.

As a facile approach to nanoscale functional materials, here preparation is performed by a microwave-assisted synthesis in ionic liquids. The synthesis comprises four steps (Scheme 1): 1. Nucleation of nanoparticles in a mixture of an IL (e.g. $[\text{N}(\text{CH}_3)(n\text{-C}_4\text{H}_9)_3][\text{N}(\text{SO}_2\text{CF}_3)_2]$) and a co-solvent (e.g., ethanol, dimethylformide) at moderate temperatures (e.g. 70°C); 2. Removal of the co-solvent by evaporation; 3. Crystallization of nuclei by microwave irradiation in the pure IL at 300°C ; 4. Addition of a co-solvent (e.g., ethanol) and centrifugation. The



Scheme 1 Sequence of synthesis with concern to $\text{LaPO}_4\text{:RE}$ with $\text{M} = \text{La, Ce, Tb, Eu}$; $\text{RE} = \text{Ce, Tb, Eu}$; $\text{IL} = [\text{N}(t\text{-Bu})_3(\text{Me})][\text{N}(\text{SO}_2\text{CF}_3)_2]$, and ethanol or dimethylformamide as co-solvent.

application of microwaves is well-known for immediate and fast heating.¹¹ This attempt turned out to be very useful here, too.

Subsequent to the sequence of reaction, the nanoparticles are yielded as colourless ($\text{LaPO}_4\text{:RE}$) or deep blue ($\text{In}_2\text{O}_3\text{:Sn}$) powders. The nanocrystalline powders can easily be redispersed in, for instance, ethanol. Such ethanolic dispersions turned out to be colloiddally stable for weeks (Fig. 1). Dynamic light scattering (DLS) determined an average particle diameter of 18 nm ($\text{LaPO}_4\text{:RE}$) and 26 nm ($\text{In}_2\text{O}_3\text{:Sn}$), and excluded a significant aggregate formation (Fig. 2). SEM and TEM micrographs visualized the size and shape of as-prepared $\text{LaPO}_4\text{:RE}$ and $\text{In}_2\text{O}_3\text{:Sn}$ (ITO) nanocrystals (Fig. 3). Herein, $\text{LaPO}_4\text{:RE}$ has a slightly ellipsoidal shape, 10–15 nm in size. $\text{In}_2\text{O}_3\text{:Sn}$ particles exhibit a spherical to cubic shape, 25–30 nm in size. High resolution TEM images and X-ray diffraction patterns confirmed the crystallinity of individual particles as well as of the powdered material. As expected, $\text{LaPO}_4\text{:RE}$ crystallizes with the monazite type of structure, and $\text{In}_2\text{O}_3\text{:Sn}$ with a CaF_2 -type superstructure.

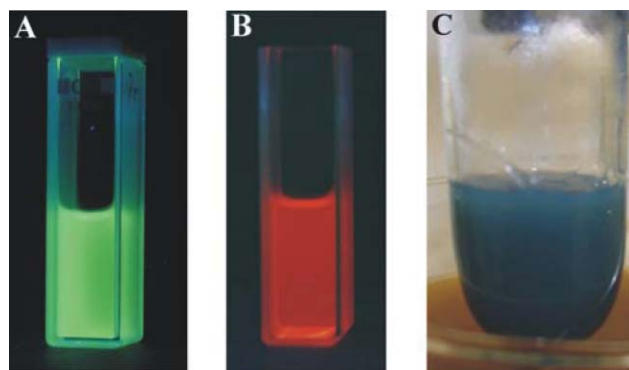


Fig. 1 Luminescence of (A) $\text{LaPO}_4\text{:Ce,Tb}$ (45 mol%, 15 mol%) and (B) $\text{LaPO}_4\text{:Eu}$ (5 mol%) redispersed in ethanol (excitation with 254 nm, 2.0 wt% each), and (C) as-prepared deep blue $\text{In}_2\text{O}_3\text{:Sn}$ (ITO, 7 mol%) in IF/ethanol mixture (1 : 1).

Institute of Inorganic Chemistry, University of Karlsruhe (TH), Engesserstrasse 15, D-76131, Karlsruhe, Germany.
E-mail: feldmann@aoe1.uni-karlsruhe.de; Fax: +49-721-6084892;
Tel: +49-721-6082855

[†] This paper was published as part of the special issue on Green Solvents for Processes.

[‡] Electronic supplementary information (ESI) available: Analytical characterisation and layer formation. See DOI: 10.1039/b617107a

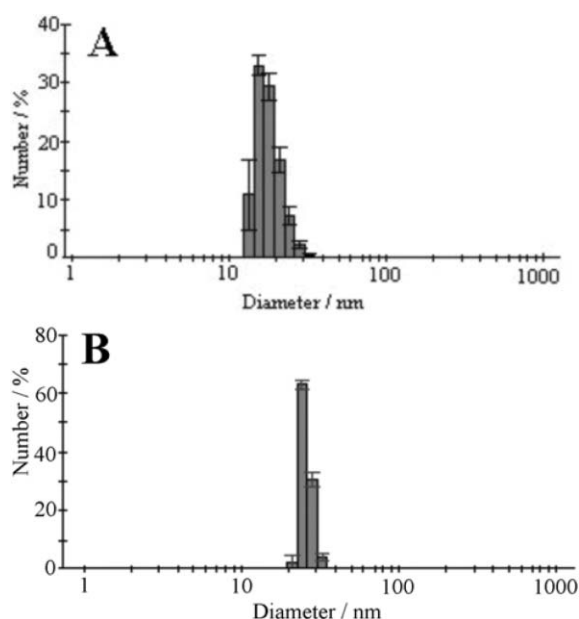


Fig. 2 DLS analysis of (A) $\text{LaPO}_4\text{:RE}$ and (B) $\text{In}_2\text{O}_3\text{:Sn}$ (ITO) nanocrystals redispersed in ethanol.

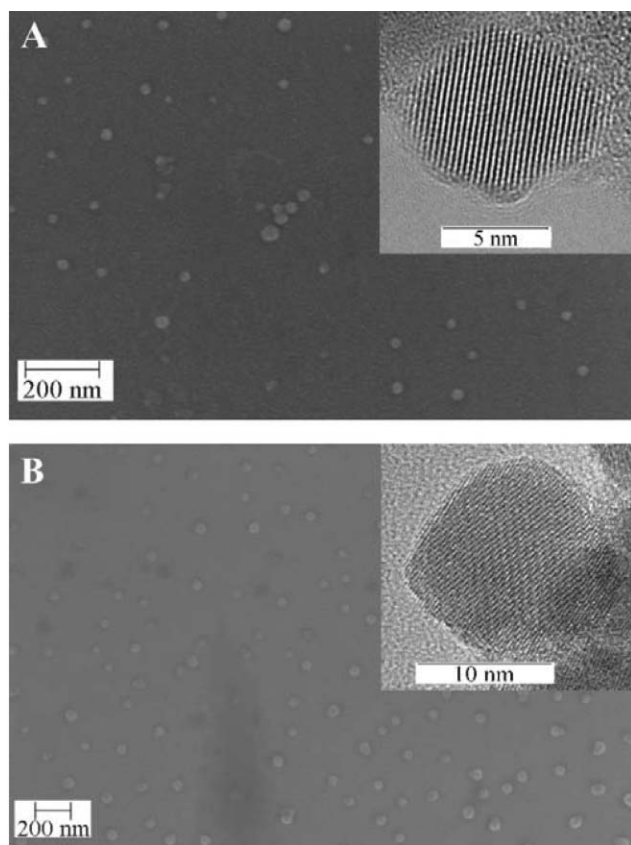


Fig. 3 SEM/TEM micrographs of as-prepared (A) $\text{LaPO}_4\text{:RE}$ and (B) $\text{In}_2\text{O}_3\text{:Sn}$ (ITO).

While exploring the material properties of as-prepared nanocrystals, excitation and emission spectra of $\text{LaPO}_4\text{:Ce,Tb}$ (45 mol%, 15 mol%) and $\text{LaPO}_4\text{:Eu}$ (5 mol%) match with the expectation.^{7a} Even dispersions in ethanol show a bright



Fig. 4 Ink-jet printed and densified $\text{In}_2\text{O}_3\text{:Sn}$ (ITO) layer with a thickness of 500 nm on paper. The letters 'ITO' printed on white paper illustrate the transparency of the $\text{In}_2\text{O}_3\text{:Sn}$ layer.

luminescence (Fig. 1). Moreover, the quantum yield of $\text{LaPO}_4\text{:Ce,Tb}$ turned out to be surprisingly high; here, 70% considering Tb^{3+} -related green emission, and 90% taking also a certain UV-emission due to Ce^{3+} into account were determined.¹² These values are one of the highest reported till now. In contrast to literature methods, neither strongly coordinating solvents, stabilizers nor advanced core-shell structures such as $\text{LaPO}_4\text{:Ce,Tb}$ or ZnS@CdSe are required to protect the surface of the luminescent nanocrystals.¹⁰ Continued studies have already shown that the IL constituents can be easily removed by washing with aqueous NaCl or exchanged by selected surface-active agents.^{12,13} In case of $\text{LaPO}_4\text{:Eu}$, due to the underlying luminescence mechanism, comparably high quantum yields are not to be expected.^{7a} For $\text{In}_2\text{O}_3\text{:Sn}$ (7 mol%), as-prepared dispersions in ethanol were ink-jet printed and densified by pressing in order to initiate a close contact of particles (Fig. 4). Four-point-probe measurements of the resulting transparent layers with a thickness of 500 nm exhibit a specific resistivity of $6.8 \times 10^{-2} \Omega \text{ cm}$. Based on a liquid-phase type of synthesis, an ITO layer exhibiting a considerable conductivity without performing any thermal or chemical post-treatment (*e.g.*, to remove all hydroxyl contents, to burn out organic residues, to reduce lattice defects, and to establish a sufficient carrier concentration) has not been realized till now.^{7b,8} The quality of the liquid phase approach is impressively elucidated by comparing to state-of-the-art magnetron sputtered ITO exhibiting the lowest resistivity values ($1.0\text{--}1.5 \times 10^{-4} \Omega \text{ cm}$).^{7b,14}

In summary, the experimental approach evidences a substantial advantage of ILs with respect to materials science. Both functional nanomaterials produced—luminescent $\text{LaPO}_4\text{:RE}$ (RE = Ce, Tb, Eu), as well as transparent conductive $\text{In}_2\text{O}_3\text{:Sn}$ (ITO)—exceed the properties of comparable materials realized by alternative liquid-phase methods. To this end, the high boiling point and the polar, but aprotic properties can be denoted as the advantageous features of the IL. As a consequence, highly crystalline and anhydrous oxide materials with a low defect concentration are accessible. Due to microwave irradiation, heating is extremely fast (10–30 s at 300 °C), resulting in an almost instantaneous crystallisation of particles. The underlying concept of a microwave-assisted synthesis in ILs is easy to perform, applying less harmful liquids and

precursors throughout. Based on the facile dispersibility, low-cost printing techniques seem to be suited to realize transparent and structured layers on glass, plastics, metal or paper, exhibiting intense luminescence or sufficient conductivity. §

Acknowledgements

The authors are grateful to W. Send and Prof. Dr D. Gerthsen for performing TEM analysis, and to Dr S. Lebedkin and Prof. Dr M. M. Kappes for performing photoluminescence. We also thank the DFG Center for Functional Nanostructures (CFN) at the University of Karlsruhe for financial support. Finally, we acknowledge the Degussa AG, Marl: projects of the Science-to-Business Center Nanotronics are co-financed by the European Union and are financially supported by the state of North-Rhine-Westphalia in Germany.

Notes and references

§ All procedures were performed using standard Schlenk-equipment. All chemicals were used as received from the supplier. $[\text{MeBu}_3\text{N}][(\text{SO}_2\text{CF}_3)_2\text{N}]$ as ionic liquid was synthesized according to a method described elsewhere.¹²

$\text{LaPO}_4\text{:Ce,Tb}$ (45 mol%, 15 mol%): 124 mg (0.334 mmol) $\text{LaCl}_3\cdot 6\text{H}_2\text{O}$, 140 mg (0.367 mmol) $\text{CeCl}_3\cdot 7\text{H}_2\text{O}$ and 47 mg (0.126 mmol) $\text{TbCl}_3\cdot 6\text{H}_2\text{O}$ were dissolved in 5 ml ethanol (EtOH) and 10 ml ionic liquid (IL). A solution of 163 mg (1.66 mmol) crystalline H_3PO_4 in 2 ml EtOH and 5 ml IL was added dropwise over a period of 30 minutes under vigorous stirring at a temperature of 70 °C. Thereafter, the transparent dispersion was maintained under reduced pressure while the temperature was raised to 100 °C until the gas evolution stopped. The vessel was kept under reduced pressure and placed in a standard laboratory microwave oven (MLS rotaprep). Here, the mixture was heated to 300 °C (pyrometric control) by irradiating with 800 W for about 10 s. The transparent dispersion was left to cool down, diluted with 20 ml of EtOH and placed in an ultrasound bath. The nanocrystals were washed and collected by centrifugation and redispersion in EtOH, which is performed thrice. After drying under reduced pressure, colourless solids were obtained in yields of 86–92%. For further analytical characterisation nanocrystals were applied as-prepared or after redispersing in EtOH.

$\text{LaPO}_4\text{:Eu}$ (5 mol%): 353 mg (0.95 mmol) $\text{LaCl}_3\cdot 6\text{H}_2\text{O}$ and 18 mg (0.05 mmol) $\text{EuCl}_3\cdot 6\text{H}_2\text{O}$ were dissolved in 5 ml ethanol (EtOH) and 10 ml ionic liquid (IL). A solution of 196 mg (2.00 mmol) crystalline H_3PO_4 in 2 ml EtOH and 5 ml IL was added dropwise over a period of 30 minutes under vigorous stirring at a temperature of 70 °C. Thereafter, the synthesis follows the procedure as given in case of $\text{LaPO}_4\text{:Ce,Tb}$. $\text{LaPO}_4\text{:Eu}$ was obtained with yields of 85–90%.

$\text{In}_2\text{O}_3\text{:Sn}$ (7 mol%): 21 mg (0.081 mmol) of SnCl_4 and 295 mg (1.008 mmol) of $\text{InCl}_3\cdot 4\text{H}_2\text{O}$ were dissolved in 15 ml of $[\text{N}(\text{CH}_3)(\text{C}_4\text{H}_9)_3][\text{N}(\text{SO}_2\text{CF}_3)_2]$ as ionic liquid (IL) and 2 ml of DMF

(solution A). In addition, $[\text{N}(\text{CH}_3)_4]\text{OH}$ was dissolved in 5 ml of IL and 2 ml of EtOH (solution B). Thereafter, solution A was added drop-wise to solution B under vigorous stirring at a temperature of 70 °C. Subsequently, all volatiles were removed under reduced pressure while raising the bath temperature to 160 °C. After the gas evolution stopped, the reaction vessel was maintained under reduced pressure of 3×10^{-3} mbar and placed in a microwave oven and heated to 300 °C within 15 seconds. The pressure was reduced immediately to 3×10^{-3} mbar to remove water stemming from preceding condensation. Finally, the dispersion was diluted with ethanol, and the blue particles were collected by centrifugation. Redispersion of the particles in ethanol, applying ultrasonic treatment, and centrifugation were repeated three times with the particles finally redispersed in ethanol.

- 1 *Ionic Liquids in Synthesis*, ed., P. Wasserscheid and T. Welton, Wiley-VCH, Weinheim, 2002.
- 2 J. Dupont, R. F. de Souza and P. A. Z. Suarez, *Chem. Rev.*, 2002, **102**, 3667.
- 3 M. Antonietti, D. Kuang, B. Smarsly and Y. Zhou, *Angew. Chem., Int. Ed.*, 2004, **43**, 4989.
- 4 R. Tatum and H. J. Fujihara, *Chem. Commun.*, 2005, 83; Y. Wang and H. J. Yang, *J. Am. Chem. Soc.*, 2005, **127**, 5316; C. C. Cassol, A. P. Umpierre, G. Machado, S. I. Wolke and J. Dupont, *J. Am. Chem. Soc.*, 2005, **127**, 3298.
- 5 Y. Zhou and M. Antonietti, *J. Am. Chem. Soc.*, 2003, **125**, 14960; H. Itoh, K. Naka and Y. Chujo, *J. Am. Chem. Soc.*, 2004, **126**, 3026; T. Nakashima and N. Kimizuka, *J. Am. Chem. Soc.*, 2003, **125**, 6386.
- 6 D. S. Jacob, L. Bitton, J. Grinblat, I. Felner, Y. Koltypin and A. Gedanken, *Chem. Mater.*, 2006, **18**, 3162.
- 7 *Phosphor Handbook*, ed. S. Shionoya and W. M. Yen, CRC Press, Boca Raton 1999; T. Minami, *Semicond. Sci. Technol.*, 2005, **20**, 35; M. Hall, E. Mast, C. Bonham and W. B. Sullivan, *Displays*, 2001, **22**, 65.
- 8 Q. Liu, W. Lu, A. Ma, J. Tang, J. Lin and J. Fang, *J. Am. Chem. Soc.*, 2005, **127**, 5276; J. Ederth, A. Hultåker, G. A. Niklasson, P. Heszler, A. R. van Doorn, M. J. Jongerius, D. Burgard and C. G. Granqvist, *Appl. Phys. A*, 2005, **81**, 1363; J. Ederth, P. Johansson, G. A. Niklasson, A. Hoel, A. Hultåker, P. Heszler, C. G. Granqvist, A. R. van Doorn, M. J. Jongerius and D. Burgard, *Phys. Rev. B*, 2003, **68**, 155410.
- 9 B. L. Cushing, V. L. Kolesnichenko and C. O'Connor, *J. Chem. Rev.*, 2004, **104**, 3893; *Nanoscale Materials in Chemistry*, ed. K. J. Klabunde, Wiley, New York, 2001.
- 10 S. Kumar and T. Nann, *Small*, 2006, **2**, 316; J. S. Steckel, J. P. Zimmer, S. Coe-Sullivan, N. E. Scott, V. Bulovic and M. G. Bawendi, *Angew. Chem., Int. Ed.*, 2004, **43**, 2154; K. Kömpe, H. Borchert, J. Storz, A. Lobo, S. Adam, T. Möller and M. Haase, *Angew. Chem., Int. Ed.*, 2003, **42**, 5513.
- 11 B. Ondruschka and W. Bonrath, *Chimica*, 2006, 326; J. A. Gerbec, D. Magana, A. Washington and G. F. Strousse, *J. Am. Chem. Soc.*, 2005, **127**, 15791; C. O. Kappe, *Angew. Chem., Int. Ed.*, 2004, **43**, 6250.
- 12 G. Bühler and C. Feldmann, *Angew. Chem., Int. Ed.*, 2006, **45**, 4864.
- 13 A. Zharkouskaya and C. Feldmann, unpublished results.
- 14 R. X. Wang, A. B. Djuricic, C. D. Beling and S. Fung, *Trends Semicond. Res.*, 2005, 137; P. Conhola, N. Martins, L. Raniero, S. Pereira, E. Fortunato, I. Ferreira and R. Martins, *Thin Solid Films*, 2005, **487**, 271; D. S. Ginley and C. Bright, *MRS Bull.*, 2000, **25**, 15.

What is a green solvent? A comprehensive framework for the environmental assessment of solvents

Christian Capello, Ulrich Fischer* and Konrad Hungerbühler

Received 1st December 2006, Accepted 22nd February 2007

First published as an Advance Article on the web 9th March 2007

DOI: 10.1039/b617536h

Solvents define a major part of the environmental performance of processes in chemical industry and also impact on cost, safety and health issues. The idea of “green” solvents expresses the goal to minimize the environmental impact resulting from the use of solvents in chemical production. Here the question is raised of how to measure how “green” a solvent is. We propose a comprehensive framework for the environmental assessment of solvents that covers major aspects of the environmental performance of solvents in chemical production, as well as important health and safety issues. The framework combines the assessment of substance-specific hazards with the quantification of emissions and resource use over the full life-cycle of a solvent. The proposed framework is demonstrated on 26 organic solvents. Results show that simple alcohols (methanol, ethanol) or alkanes (heptane, hexane) are environmentally preferable solvents, whereas the use of dioxane, acetonitrile, acids, formaldehyde, and tetrahydrofuran is not recommendable from an environmental perspective. Additionally, a case study is presented in which the framework is applied for the assessment of various alcohol–water or pure alcohol mixtures used for solvolysis of *p*-methoxybenzoyl chloride. The results of this case study indicate that methanol–water or ethanol–water mixtures are environmentally favourable compared to pure alcohol or propanol–water mixtures. The two applications demonstrate that the presented framework is a useful instrument to select green solvents or environmentally sound solvent mixtures for processes in chemical industry. The same framework can also be used for a comprehensive assessment of new solvent technologies as soon as the present lack of data can be overcome.

Introduction

Today, in the chemical industry, solvents are used in large quantities. In particular, in fine-chemical and pharmaceutical production, large amounts are used per mass of final products. Therefore, solvents define a major part of the environmental performance of a process and also impact on cost, safety and health issues. The idea of “green” solvents expresses the goal to minimize the environmental impact resulting from the use of solvents in chemical production. Recently, four directions towards green solvents have been developed: (i) substitution of hazardous solvents with ones that show better EHS (environmental, health and safety) properties, such as increased biodegradability or reduced ozone depletion potential (*e.g.* ref. 1–3); (ii) use of “bio-solvents”, *i.e.* solvents produced with renewable resources such as ethanol produced by fermentation of sugar-containing feeds, starchy feed materials or lignocellulosic materials⁴ (this substitution of petrochemically fabricated solvents leads to an avoidance of fossil resource use and fossil fuel CO₂ emissions to the environment); (iii) substitution of organic solvents either with supercritical fluids that are environmentally harmless (*e.g.* the use of supercritical CO₂ in polymer processing^{5–8} avoids the use of

chlorofluorocarbons, and thus reduces ozone depletion); or (iv) with ionic liquids that show low vapour pressure, and thus less emission to air (*e.g.* ref. 9, 10). Environmental improvements are achieved with all alternatives in different ways. Therefore, the question is raised of how to measure how green a solvent is. To this end, comprehensive evaluations of the pros and cons of these alternatives and their environmental performance have to be conducted and compared.

In this paper, we propose a framework for the environmental assessment of solvents that covers major aspects of the environmental performance of solvents in chemical production and also includes health and safety issues. This framework comprises the application of two environmental assessment methods with different scopes. The first method, the EHS assessment method,¹¹ is a screening method that aims to identify potential hazards of chemicals. The second method, the life-cycle assessment (LCA) method,¹² can be used for a detailed assessment of emissions to the environment as well as resource use over the full life-cycle of a solvent, including the production, the use, potential recycling, and the disposal. For the selection of the environmentally best performing solvent or solvent mixture, the results of the two assessment methods are combined.

The proposed framework is demonstrated on 26 pure organic solvents that are commonly used in the chemical industry, as well as on a case study in which various alcohol–water mixtures are presented for solvolysis of *p*-methoxybenzoyl chloride.¹³ With our framework, possible solvent

ETH Zurich, Institute for Chemical and Bioengineering, Wolfgang-Pauli-Strasse 10, 8093 Zurich, Switzerland.
E-mail: ufischer@chem.ethz.ch; Fax: +41-44-632-1189;
Tel: +41-44-632-5668

mixtures for the solvolysis are assessed in order to determine the most environmentally friendly option. The same framework can also be used for a comprehensive assessment of new solvent technologies (ionic liquids, supercritical fluids) as soon as the present lack of data regarding industrial production, recycling, and disposal processes as well as EHS characteristics is overcome.

Methods

The EHS method: identification of potential substance hazards

The use of solvents in the chemical industry is related to a number of hazards inherent to the solvent properties: organic solvents may well be flammable and explosive, they may well be toxic and persistent. The EHS assessment method is a screening method that identifies possible hazards of chemical substances in early phases of the chemical process design.¹¹ The EHS method relies heavily on the availability of data on physical and chemical properties, toxicity, environmental and safety aspects of the substances to be assessed. In an earlier complex software tool, these data were automatically collected from various databases by the EHS tool with the help of an interface between the tool and the databases. Results obtained from property estimation methods, such as quantitative structure–activity relationships (QSARs) are also considered for filling data gaps.

Recently, a simplified Excel tool¹⁴ has been created that only considers selected aspects and parameters for the different effect categories (see below). The data which are used as a basis for the assessment of chemical substances are selected manually from the most reliable sources. Until now, about 100 substances—mainly organic solvents—have been included into the new EHS assessment tool.

In the simplified EHS method,¹⁴ substances are assessed in nine effect categories: release potential, fire/explosion and reaction/decomposition (representing safety hazards), acute toxicity, irritation and chronic toxicity (representing health hazards), persistency, air hazard and water hazard (representing environmental hazards). For each effect category, an index between zero and one is calculated, resulting in an overall score between zero and nine for each chemical.

The life-cycle assessment (LCA) method: quantification of emissions and resource use over the whole life-cycle of a solvent

The use of solvents in chemical industry is associated with a variety of indirect environmental impacts. For example, non-renewable resource depletion as a consequence of petrochemical solvent production, air emissions due to solvent incineration or high energy investment for solvent recycling processes. In order to quantify environmental impacts that are also indirectly attributable to the use of solvents, the life-cycle assessment method¹² was used.

The life-cycle of organic solvents that we considered in this work is comprised of the petrochemical production, the use as reaction media in a chemical production process, and the subsequent waste-solvent treatment (Fig. 1). In the waste-solvent treatment, solvents are either recycled using distillation processes or they are treated in a hazardous

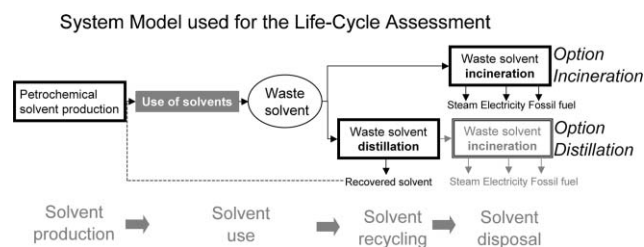


Fig. 1 System model of the solvent assessment using the life-cycle assessment method.

waste incineration plant. We defined one functional unit—that is the reference to which the inputs and outputs are related¹²—as the use of 1 kg of solvent as reaction media in a chemical production process.

To calculate the environmental impact for a specific solvent or solvent mixture, the Ecosolvent software tool (Ecosolvent-Tool)¹⁵ was used. This tool combines life-cycle inventories of the petrochemical production of 45 organic solvents (data were based on values presented in the ecoinvent database)¹⁶ and its treatment either using distillation processes or in a hazardous waste incineration plant.¹⁷ These technologies are represented by so called life-cycle inventory (LCI)¹⁸ models that are all based on industry data. With these models, solvent-specific environmental impacts were calculated, such as emission flows, ancillary uses, and the generation of products.

The incineration model of the Ecosolvent-Tool calculates inventory data of solvent combustion as a function of the elemental solvent composition and technology used. Causal relationships between the consumption of ancillaries and energies, the generation of co-products and the emissions of pollutants, and their causing components within the waste solvent were modelled with the help of consumption and emission factors and transfer coefficients. The resulting multi-input allocation model allows for the calculation of LCI data for specific waste solvents. This model is based on data of an incineration plant located within a large chemical production site in Switzerland with a capacity of about 35 000 t per year.¹⁹ Co-products of this incineration plant are steam and electricity. Environmental credits are granted for the energy production. These credits are based on the assumption that the produced energy is used in the chemical production site, and therefore the incineration of solvents prevents environmental impacts for the production of the same amounts of energy with an average mix of fossil fuels.

The model of distillation processes is based on empirical relationships that are used as an approximation if precise information (measured values) is missing. Such empirical relationships have been established by collecting and analyzing LCI data of 150 industrial waste-solvent distillation processes in collaboration with the Swiss chemical industry. The LCI data contain values for the demand of steam, electricity, cooling water, inert gas (nitrogen), and ancillary products, as well as for the amount of recovered solvent, residues, wastewater, and outlet air.²⁰ For the recovery of solvents, environmental credits are granted because it was assumed that the use of recovered solvent prevents the environmental impact of the petrochemical production of fresh solvents.

Table 1 Specification of solvent treatment processes used in this work. These assumptions reflect general conditions in the Swiss chemical industry according to the opinion of an expert panel²¹

Parameter	Assumptions	Comment
Incineration technology	Hazardous waste incinerator	Model description see ref. 19
Distillation technology	Batch distillation	Detailed description see ref. 20
Use of energy and ancillaries	Average use batch distillation	According to statistical analysis ²⁰
Production of energy and ancillaries	Average European production	Data were taken from ref. 16
Solvent recovery	Average solvent recovery of 90%	According to the opinion of an expert panel ²¹
Residue treatment	Incineration	Most commonly used technology for organic solvents ²²

The assumptions on which the assessment of the solvent treatment processes was made represent general conditions in the Swiss chemical industry²¹ (Table 1).

A life-cycle impact assessment method,²³ the cumulative energy demand (CED),²⁴ was used. The CED is a suitable screening indicator for the assessment of the production of solvents,²⁵ as well as for the solvent recycling and treatment in hazardous waste incineration plants²⁶ because it highly correlates with other, more complex, indicators such as eco-indicator 99.²⁷

Framework for the environmental assessment of solvents: combination of the EHS method and the LCA method

The assessment of how green a solvent is requires the consideration of various aspects. Such a multi-criteria evaluation can be achieved by combining the EHS method with the LCA method. The framework proposed in this work consists of the following steps:

Step (1) Assessment of the solvent or solvent mixture using the EHS-Tool.¹⁴

Step (2) Assessment of the solvent or solvent mixture using the Ecosolvent-Tool.¹⁵

Step (3) Combining the two environmental scores in order to evaluate the potential hazard with the life-cycle perspective.

Results and discussion

Application of the framework to 26 organic solvents

The 26 organic solvents that were investigated using the proposed framework and their CAS numbers are given in Table 2. These solvents cover a wide range of compounds that are common in the chemical industry (*e.g.* ref. 28).

Step (1): application of the EHS method. The EHS assessment results for the 26 pure organic solvents are given in Fig. 2. Overall high scores result for formaldehyde, dioxane, formic acid, acetonitrile and acetic acid. While formaldehyde shows a relatively low score for fire/explosion hazards, it has high scores in acute and chronic toxicity, irritation and air hazards. Dioxane has a high persistency, while acetic and formic acid both show high scores for irritation. Low overall scores were found for methyl acetate, ethanol and methanol, which inherit particularly low environmental hazards and relatively low health hazards. These examples demonstrate

Table 2 Results of the life-cycle assessment of the 26 organic solvents. The total CED of a treatment option is calculated based on these results: CED (Option Distillation) = CED (Solvent Production) + CED (Solvent Distillation); CED (Option Incineration) = CED (Solvent Production) + CED (Solvent Incineration)

Solvent	CAS-No.	Solvent production CED per kg solvent/MJ-eq.	Solvent distillation CED per kg solvent/MJ-eq.	Solvent incineration CED per kg solvent/MJ-eq.
Acetic acid	64-19-7	55.9	-34.9	-15.5
Acetone	67-64-1	74.6	-53.6	-33.9
Acetonitrile	75-05-8	88.5	-79.6	-29.7
Butanol (1-)	71-36-3	97.3	-74.6	-39.9
Butyl acetate	123-86-4	121.6	-95.9	-34.1
Cyclohexane	110-82-7	83.2	-63.4	-53.5
Cyclohexanone	108-94-1	124.7	-99.7	-40.4
Diethyl ether	60-29-7	49.8	-31.9	-40.2
Dioxane	123-91-1	86.6	-63.8	-27.6
Dimethylformamide	68-12-2	91.1	-67.6	-25.9
Ethanol	64-17-5	50.1	-31.2	-31.7
Ethyl acetate	141-78-6	95.6	-72.0	-27.6
Ethyl benzene	100-41-4	85.1	-64.9	-49.8
Formaldehyde	50-00-0	49.3	-28.8	-15.9
Formic acid	64-18-6	73.9	-50.1	-4.7
Heptane	142-82-5	61.5	-43.7	-54.5
Hexane	110-54-3	64.4	-46.7	-55.2
Methyl ethyl ketone	108-10-1	64.2	-44.6	-37.6
Methanol	67-56-1	40.7	-21.7	-22.2
Methyl acetate	79-20-9	49.0	-29.2	-22.8
Pentane	109-66-0	73.2	-54.5	-55.3
Propyl alcohol (<i>n</i> -)	71-23-8	111.7	-87.3	-36.5
Propyl alcohol (<i>iso</i> -)	67-63-0	65.6	-46.1	-36.5
Tetrahydrofuran	109-99-9	270.8	-230.7	-37.5
Toluene	108-88-3	80.0	-60.0	-49.3
Xylene	1330-20-7	72.5	-53.1	-49.9

EHS assessment of organic solvents

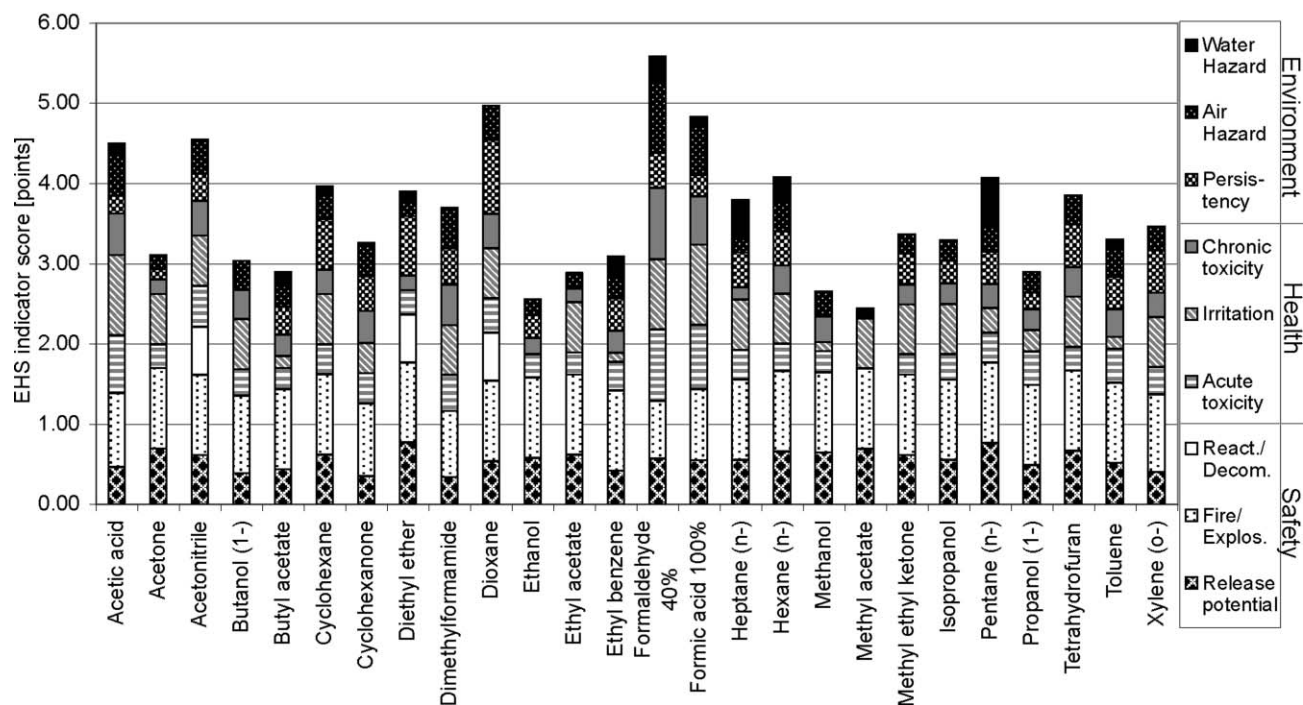


Fig. 2 Results of the EHS method for the 26 pure organic solvents (step (1) in the framework for the assessment of green solvents). The EHS result score is composed of environmental indicators (water and air hazard, persistence), as well as indicators for health (chronic and acute toxicity and irritation) and safety (reaction/decomposition, fire/explosion, release potential) hazards. The results were calculated using the EHS-Tool.¹⁴

how the EHS method not only provides a total score for the overall hazards associated with certain solvents, but also indicates the detailed aspects of each compound that are critical and that have to be considered with respect to the installation of precautionary technical measures when a certain solvent is used in a chemical process.

Step (2): application of the LCA method. The results of the life-cycle assessment of the 26 organic solvents are presented for the solvent production, the solvent recycling (distillation, including the residue treatment) and the solvent disposal (incineration) (Table 2). The CED of the petrochemical solvent production is in the range of 40 to 270 MJ-eq. per kg solvent. The production of solvents close to the petrochemical basic products (e.g. natural gas, naphtha) only require a few process steps (e.g. methanol from natural gas or hexane/heptane from naphtha) and therefore cause little environmental impact compared to highly elaborate solvents (e.g. tetrahydrofuran, cyclohexanone). The variability in the environmental impact of solvent production is also reflected in the environmental credits of solvent distillation because a solvent recovery of 90% was assumed (Table 2). The environmental credits of the solvent incineration (energy recovery) result in a CED between 15 and 55 MJ-eq. per kg solvent and they are directly related to the net calorific value. Thus, the higher the carbon fraction of a solvent is, the higher are the environmental credits of the solvent incineration.²⁹

The assessment of the full life-cycle is either composed of solvent production and solvent distillation (option distillation)

or solvent production and solvent incineration (option incineration). The results of both options is presented in Fig. 3.

The results of the incineration and distillation options correlate linearly (Fig. 3) because the results of both options are dominated by two environmental impacts: (1) the petrochemical solvent production that also determines the environmental credits for solvent recovery in distillation and (2) the

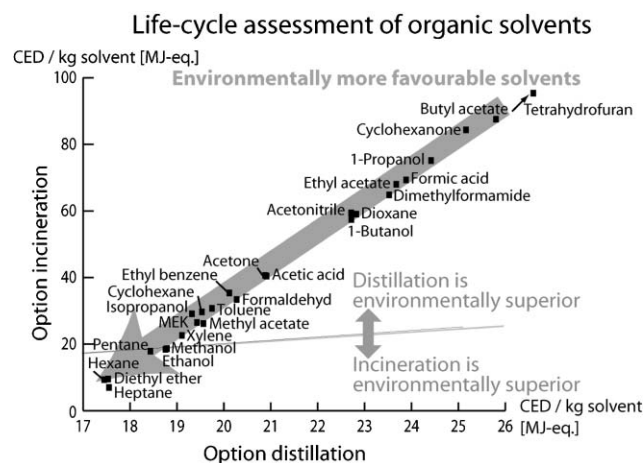


Fig. 3 Life-cycle assessment of the treatment options, incineration and distillation, for the 26 solvents (step (2) in the framework for the assessment of green solvents). Tetrahydrofuran is out of range (CED of 40.1 (distillation) and 233.4 (incineration) MJ-eq.). The results were calculated using the Ecosolvent-Tool.¹⁵

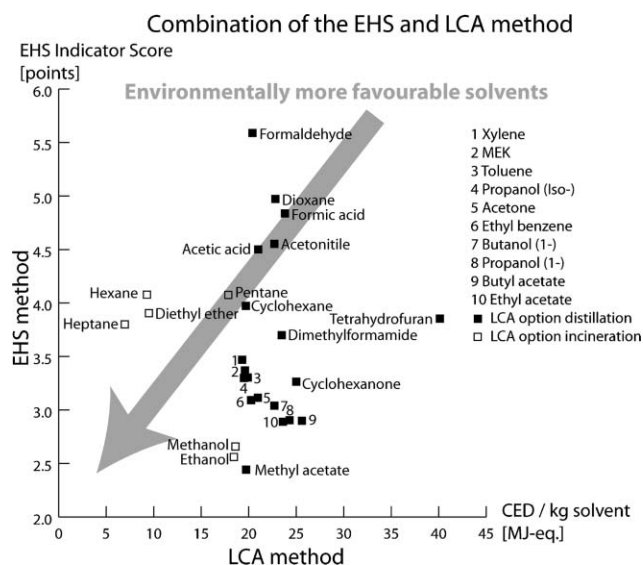


Fig. 4 Environmental assessment of the 26 organic solvents: combination of the EHS method with the LCA method (step (3) of the framework for the assessment of green solvents).

energy recovery of the incineration that also influences the distillation residue treatment (see Table 2).

As revealed by Fig. 3, the use of tetrahydrofuran, butyl acetate, cyclohexanone, and 1-propanol is not recommendable from a life-cycle perspective. These solvents cause high environmental impacts during petrochemical production (see Table 2). Also, formic acid, ethyl acetate, acetonitrile, dioxane, 1-butanol, and dimethylformamide are solvents of significantly higher environmental impact. This result is attributable to the fact that these solvents have a low net calorific value, and therefore low environmental credits for the incineration and residue treatment, combined with a relatively high environmental impact of the production (see Table 2).

At the other end, hexane, heptane, and diethyl ether are environmentally favourable solvents. With regard to the alkanes, high environmental credits for energy recovery (very high net calorific value) in combination with relatively low environmental impacts of their production are the reason for these results (see Table 2). Considering diethyl ether, the low environmental impact of the production and the relatively high credits for energy recovery are the deciding factors.

Step (3): combination of the EHS and the LCA method. In the last step of the framework for the assessment of green solvents, the results of the EHS method are combined with the results of the LCA method (Fig. 4). With regard to the LCA results, we used the environmentally best performing treatment option for each solvent (incineration or distillation, see Fig. 3).

The combination of the two assessment methods leads to a Pareto situation: on the one hand, methanol, ethanol or methyl acetate are preferred from the EHS perspective (see Fig. 2) and on the other hand, the life-cycle assessment method indicates that hexane, heptane or diethyl ether are the environmentally favourable solvents (see Fig. 3).

As can be seen in Fig. 4, dioxane, acetonitrile, acids, formaldehyde, and tetrahydrofuran are not recommendable solvents from an environmental point of view. In particular, the latter two solvents are outliers: the tetrahydrofuran stands out because the complex petrochemical production route requires several production steps (see Fig. 3) and the formaldehyde shows high scores in acute and chronic toxicity, irritation and air hazards (see Fig. 2). Additionally, pentane, cyclohexane, dimethylformamide, and cyclohexanone also show a significantly higher environmental impact compared to other solvents. Between these solvent groups a cluster of 10 solvents (numbered solvents in Fig. 4) show similar environmental impact.

Application of the framework to the case study

Case study description. In the case study, we applied the presented framework for the assessment of green solvents to 5 binary solvent mixtures that can be used for solvolysis of *p*-methoxybenzoyl chloride, in order to determine the most environmentally friendly option. Potential solvent mixtures have been reported by Bentley *et al.*¹³ for varying shares of the components and are summarized in Table 3. The corresponding product selectivities indicate the ratio of ester product to acid product, adjusted for changes in bulk solvent composition; thus, high selectivities (>1) denote a high yield on the ester product whereas low selectivities (<1) represent a high yield of the acid product. The reported selectivities depend only slightly on the solvent composition, except with regards to the methanol–water and the *n*-propyl alcohol–water mixtures, where the selectivity increases for more aqueous mixtures. This finding indicates that preferential

Table 3 The 5 binary solvent mixtures and their varying compositions investigated in the case study. Data were taken from Bentley *et al.*¹³

Mixture name (% v/v) main component/secondary component	Solvent composition/kg	Product selectivities at 25 °C (dominating product) as reported in Bentley <i>et al.</i>
Option 1: methanol–water		
MeOH–H ₂ O (90%)	methanol (0.71), water (0.29)	1.36–1.39 (ester product)
MeOH–H ₂ O (10%)	methanol (0.08), water (0.92)	1.28–1.40 (ester product)
Option 2: ethanol–water		
EtOH–H ₂ O (90%)	ethanol (0.71), water (0.29)	0.55–0.71 (acid product)
EtOH–H ₂ O (10%)	ethanol (0.08), water (0.92)	0.78–0.80 (acid product)
Option 3: methanol–ethanol		
MeOH–EtOH (80%)	methanol (0.63), ethanol (0.37)	1.54 (ester product)
MeOH–EtOH (20%)	methanol (0.16), ethanol (0.84)	1.51 (ester product)
Option 4: <i>n</i>-propyl alcohol–water		
<i>n</i> -PrOH–H ₂ O (90%)	<i>n</i> -propyl alcohol (0.72), water (0.28)	0.32–0.61 (acid product)
<i>n</i> -PrOH–H ₂ O (10%)	<i>n</i> -propyl alcohol (0.08), water (0.92)	0.78–0.82 (acid product)

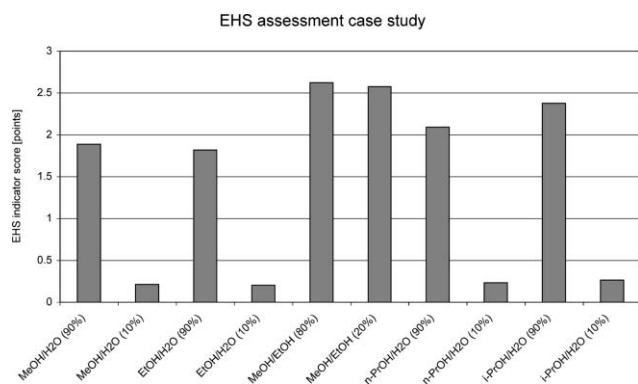


Fig. 5 EHS assessment of the 5 solvent mixtures of the case study at different shares of main and secondary component (step (1) in the framework for the assessment of green solvents). The results were calculated using the EHS-Tool.¹⁴

solvation may occur but it is not a major factor influencing the reactivity.¹³

Step (1): application of the EHS method. Fig. 5 shows the EHS assessment results obtained for the investigated solvent mixtures. These results were calculated as weight-based averages of the single substance assessment scores. The corresponding weight fractions of the different solvent mixtures are given in Table 3. In this analysis an overall EHS score of zero was postulated for water. As a consequence, all mixtures with a high mass fraction of water show low overall EHS scores as compared to the mixtures with high mass fraction of organic solvent. For the two ethanol–methanol mixtures almost identical scores resulted because the two pure substances have similar EHS scores (compare Fig. 2). For the mixtures, as for the pure substances, the most problematic EHS aspects could be identified (not shown here) in order to take corresponding measures during process development.

Step (2): application of the LCA method. In the second step, the environmental impacts of the life-cycle of the 5 solvent mixtures were assessed. The results of the treatment options, incineration and distillation, are presented in Fig. 6. Solvent mixtures with high water content show low environmental impacts. Although no or only low environmental credits for incineration and distillation are given for these mixtures, the cumulative energy demand for the production of water is about three orders of magnitude lower than for organic solvents.¹⁶ Therefore, the solvent mixtures with water as a component are superior to the methanol–ethanol mixture. If these solvent mixtures contain high shares of the organic component, similar results compared to the assessment of the pure solvents (Fig. 3) are obtained. The results of the methanol–ethanol mixture are different. With regard to the option incineration, the share of the components almost does not affect the result because both solvents have similar environmental impact of production and net calorific values (see Table 2). For the assessment of the option distillation, we assumed methanol to be the main component that is recovered, and with a decreasing share of methanol, the environmental credits for solvent recovery decrease. Generally, incineration is

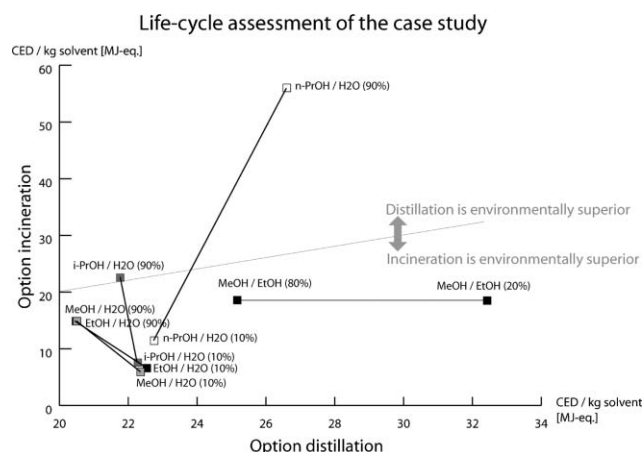


Fig. 6 Life-cycle assessment of the treatment options, incineration and distillation, for 5 solvent mixtures (step (2) in the framework for the assessment of green solvents). The values were calculated using the Ecosolvent-Tool.¹⁵

the environmentally superior treatment option for these solvent mixtures, in particular with high shares of water. Only with regard to the *n*-propyl alcohol–water mixture is distillation the superior treatment option for high concentrations of *n*-propyl alcohol because of its high environmental impact in the petrochemical production (see Table 2).

Step (3): combination of the EHS and the LCA method. In the last step of the framework for the assessment of green solvents the results of the EHS method are combined with the results of the LCA method (Fig. 7). With regard to the LCA score, the incineration option was used.

If high selectivities are desired in the solvolysis of *p*-methoxybenzoyl chloride, and thus a high yield of the ester product (see Table 3), either the methanol–water or the methanol–ethanol mixture has to be selected. The results of the environmental assessment reveal that in this relative

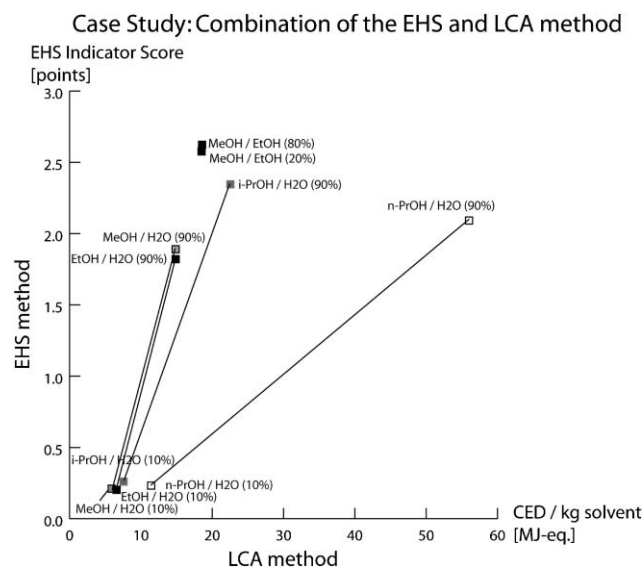


Fig. 7 Environmental assessment of the 5 binary solvent mixtures with various shares of the components.

comparison, the methanol–ethanol mixture is not recommendable from an environmental perspective. The methanol–water mixture is environmentally superior with regard to all ratios of methanol and water. However, the higher the water proportion, the more decreased its environmental impact is, due to the postulated EHS score of zero for water and low CED for the production of water.

In the case where the acid is the desired product of the solvolysis, a low selectivity is needed (see Table 3). The ethanol–water mixture turned out to be the environmentally preferable solvent mixture. However, the reported selectivities in the range of 0.55 to 0.80 (Table 3) are substantially higher than those for the isopropyl alcohol–water mixture (0.33–0.36). The selection of the optimal solvent mixture for the acid product represents, therefore, a trade-off between environment (ethanol–water mixture) and selectivity for the acid product (isopropyl alcohol–water mixture). The *n*-propyl alcohol–water mixture is not recommendable either from an environmental perspective or regarding the selectivity for the acid product.

Application of the framework to new solvent technologies

New solvent technologies show environmental advantages compared to conventional solvents (*e.g.* low vapour pressure (ionic liquids), CO₂-neutrality (supercritical CO₂)). However, in order to assess how green these solvent technologies are, more aspects have to be considered, such as environmental impacts arising from the industrial production, recycling and disposal processes, as well as EHS characteristics. For such a comprehensive environmental assessment, results from a life-cycle assessment can be combined with EHS indicators in the same way as presented in our framework. The presented tools (EHS-Tool, Ecosolvent-Tool) used for the quantification of the environmental impact focus, so far, on organic solvents (*i.e.* solvent treatment technologies, such as distillation or hazardous waste incineration). Regarding new solvent technologies there is presently a lack of data. But, for example, first results on the investigation of ionic liquids show that the production of an alkylimidazolium is very energy-intensive, at least on a laboratory scale (approx. 1000 MJ-eq. per kg of 1-alkyl-3-methylimidazolium chloride).³⁰ Additionally, it has been found that imidazolium type ionic liquids undergo poor levels of biodegradation¹⁰ and additional toxicological data are required, since almost no information about carcinogenicity, genotoxicity or teratological effects is available.³¹ These first results indicate that a comprehensive environmental assessment of new solvent technologies is needed for reliable conclusions on how green they are.

Conclusions

In the chemical industry, solvents belong to the most important group of chemicals due to the large amounts that are used annually (almost 4×10^6 t in Europe (2004)).²⁸ Therefore, solvents define a major part of the environmental performance of a process and also impact on safety and health issues. In the chemical industry, however, the selection of solvents for chemical processes and the subsequent waste-solvent management are mostly based on economic, safety, and logistical considerations.²² Environmental concerns are often of minor

importance for decision-makers, also due to the lack of comprehensive instruments or tools. In this paper, we present an easy applicable framework that can be used for a comprehensive environmental assessment of solvent use covering the environmental performance of solvents in chemical production as well as health and safety issues. The application of this framework facilitates the decision-making in the solvent and waste-solvent management with an environmental dimension.

The assessment of how green a solvent is requires the consideration of various aspects, such as environmental impacts arising from the industrial production, recycling and disposal processes, as well as EHS characteristics. New solvent technologies should also undergo such a comprehensive assessment to show their green potential. Such a multi-criteria evaluation can be achieved by combining the EHS method with the LCA method because these assessment methods complement one another: the EHS method focuses on the inherent hazards of solvents, whereas the LCA method quantifies a generic energy use (including attributable resource use and emissions) that is related to the solvent production and waste-solvent treatment. Therefore, the framework proposed in this work allows for a comprehensive environmental assessment independent of the actual use of a solvent (desired functionality, use in a specific technology). Context-specific factors such as recycling rates and losses, leading to more or less environmental impacts and risks, however, have to be investigated for each case study individually. Also, advantages of new solvent technologies regarding physical and chemical properties, compared to organic solvents, have to be analyzed on the basis of specific case studies. The proposed framework signifies an important building block in obtaining an overall assessment of solvents in which, obviously, also the technical aspects, such as solubility or selectivity, are to be considered together with economic factors.

In contrast to already published assessment methods for solvents (*e.g.* ref. 1, 3), the framework proposed in this paper is based on two automated software tools with different scope that are available at no cost.^{14,15} Both tools have been developed in close collaboration with chemical industry and therefore provide results of practical relevance.

So far, the presented framework is restricted to the assessment of organic solvents. Further research is needed to extend the already existing tools to new solvent technologies, such as ionic liquids or supercritical fluids. This also implies the investigation of alternative solvent production processes as well as new waste-solvent treatment technologies.

Acknowledgements

We gratefully acknowledge the Swiss Federal Office of Energy (project no. 100970) and the Swiss Federal Office for the Environment's funding of this project (project no. 810.3189.004).

References

- 1 A. Curzons, C. C. Constable and V. L. Cunningham, Solvent Selection Guide: A Guide to the Integration of Environmental, Health and Safety Criteria into the Selection of Solvents, *Clean Prod. Process.*, 1999, **1**, 82–90.

- 2 P. Curran, J. Maul, P. Ostrowski, G. Ublacker and B. Linclau, Benzotrifluoride and Derivatives: Useful Solvents for Organic Synthesis and Fluorous Synthesis in *Topics in Current Chemistry*, Springer-Verlag, Berlin, Heidelberg, 1999, vol. 206, pp. 79–106.
- 3 R. Gani, C. Jiménez-Gonzalez, A. Kate, P. A. Crafts, M. Jones, L. Powell, J. H. Atherton and J. L. Cordiner, A Modern Approach to Solvent Selection, *Chem. Eng.*, 2006, **1**, 30–41.
- 4 B. Savaiko, A Promising Future for Ethanol, *World Ethanol and Biofuels Report*, 2004, **2**(17), 20–22.
- 5 R. Noyori, Supercritical Fluids: Introduction, *Chem. Rev.*, 1999, **99**, 353–354.
- 6 S. Nalawade, F. Picchioni and L. Janssen, Supercritical Carbon Dioxide as a Green Solvent for Processing Polymer Melts: Processing Aspects and Applications, *Prog. Polym. Sci.*, 2006, **31**, 19–43.
- 7 J. Behles and J. DeSimone, Developments in CO₂ Research, *Pure Appl. Chem.*, 2001, **73**, 1281–1285.
- 8 D. Tomasko, H. Li, D. Liu, X. Han, M. Wingert, J. Lee and K. Koelling, A Review of CO₂ Applications in the Processing of Polymers, *Ind. Eng. Chem. Res.*, 2003, **42**, 6431–6456.
- 9 J. Leveque and G. Cravotto, Microwaves Power Ultrasound, and Ionic Liquids. A New Synergy in Green Organic Synthesis, *Chimia*, 2006, **60**, 313–320.
- 10 P. Scammells, J. Scott and R. Singer, Ionic Liquids: The Neglected Issues, *Aust. J. Chem.*, 2005, **58**, 155–169.
- 11 G. Koller, U. Fischer and K. Hungerbühler, Assessing Safety, Health, and Environmental Impact during Process Development, *Ind. Eng. Chem. Res.*, 2000, **39**, 960–972.
- 12 *Environmental management - Life cycle assessment - Principles and framework*, EN ISO 14040, European Committee for Standardisation, Brussels, Belgium, 1997.
- 13 T. W. Bentley, D. N. Ebdon, E. Kim and I. Koo, Solvent Polarity and Organic Reactivity in Mixed Solvents: Evidence Using a Reactive Molecular Probe to Assess the Role of Preferential Solvation in Aqueous Alcohols, *J. Org. Chem.*, 2005, **70**, 1647–1653.
- 14 H. Sugiyama, U. Fischer and K. Hungerbühler, *The EHS Tool*, ETH Zurich, Safety & Environmental Technology Group, Zurich, 2006, <http://www.sust-chem.ethz.ch/tools/EHS>.
- 15 C. Capello, S. Hellweg and K. Hungerbühler, *The Ecosolvent Tool*, ETH Zurich, Safety & Environmental Technology Group, Zurich, 2006, <http://www.sust-chem.ethz.ch/tools/ecosolvent>.
- 16 ecoinvent Centre, *ecoinvent data v1.1, Final Reports ecoinvent 2000 No. 1–15*, CD-ROM, Swiss Centre for Life Cycle Inventories, Dübendorf, 2004.
- 17 C. Capello, S. Hellweg, B. Badertscher, H. Betschart and K. Hungerbühler, Environmental Assessment of Waste-Solvent Treatment in the Pharmaceutical and Specialty Chemicals Industry. Part 1. The ECOSOLVENT Tool, *J. Ind. Ecol.*, 2007, in press.
- 18 *Environmental management - Life cycle assessment - Goal and scope definition and life cycle inventory analysis*, EN ISO 14041, European Committee for Standardisation, Brussels, Belgium, 1998.
- 19 C. Seyler, T. B. Hofstetter and K. Hungerbühler, Life Cycle Inventory for Thermal Treatment of Waste Solvent from Chemical Industry: A Multi-Input Allocation Model, *J. Cleaner Prod.*, 2005, **13**, 1211–1224.
- 20 C. Capello, S. Hellweg, B. Badertscher and K. Hungerbühler, Life-Cycle Inventory of Waste Solvent Distillation: Statistical Analysis of Empirical Data, *Environ. Sci. Technol.*, 2005, **39**, 5885–5892.
- 21 Expert panel of the project *Waste Solvent Management in Chemical Industry* consisting of Ciba Speciality Chemicals AG, Ems-Dottikon AG, Lonza Group Ltd., Novartis Pharma AG, Hoffmann-La Roche AG, Siegfried Ltd. and Valorec Services AG. 2003–2005.
- 22 C. Seyler, C. Capello, S. Hellweg, B. Bruder, D. Bayne, A. Huwiler and K. Hungerbühler, Waste-Solvent Management as an Element of Green Chemistry: A Comprehensive Study on the Swiss Chemical Industry, *Ind. Eng. Chem. Res.*, 2006, **45**, 7700–7709.
- 23 *Environmental management - Life cycle assessment - Life cycle impact assessment*, EN ISO 14042, European Committee for Standardisation, Brussels, Belgium, 1998.
- 24 Cumulative Energy Demand - Terms, Definitions, Methods of Calculation, in *VDI-Richtlinien 4600*, Verein Deutscher Ingenieure, Düsseldorf, 1997.
- 25 M. A. J. Huijbregts, L. Rombouts, S. Hellweg, R. Frischknecht, A. Hendriks, D. van de Meent, A. M. J. Ragas, L. Reijnders and J. Struijs, Is Cumulative Fossil Energy Demand a Useful Indicator for the Environmental Performance of Products? *Environ. Sci. Technol.*, 2006, **40**, 641–648.
- 26 C. Capello, S. Hellweg and K. Hungerbühler, Environmental Assessment of Waste-Solvent Treatment in the Pharmaceutical and Specialty Chemicals Industry. Part 2. General Rules of Thumb and Specific Recommendations., *J. Ind. Ecol.*, 2007, in press.
- 27 M. Goedkoop and R. Spriensma, *The Eco-Indicator 99: A Damage Orientated Method for Life-Cycle Impact Assessment*, Methodology report 2000a, pre consultants, 2000.
- 28 *Directory of Solvents*, ed. B. P. Whim and P. G. Johnson, Blackie Academic & Professional, London, 1996.
- 29 G. Wypych, *Handbook of Solvents*, ChemTec Publishing, Toronto, 2001.
- 30 D. Kralisch, A. Stark, S. Körsten, G. Kreisel and B. Ondruschka, Energetic, environmental and economic balances: Spice up your ionic liquid research efficiency, *Green Chem.*, 2005, **7**, 301–309.
- 31 B. Jastorff, K. Mölter, P. Behrend, U. Bottin-Weber, J. Filser, A. Heimers, B. Ondruschka, J. Ranke, M. Schaefer, H. Schröder, A. Stark, P. Stepnowski, F. Stock, R. Störmann, S. Stolte, U. Welz-Biermann, S. Ziegert and J. Thöming, Progress in evaluation of risk potential of ionic liquids—basis for an eco-design of sustainable products, *Green Chem.*, 2005, **7**, 362–372.

Synthesis of [EMIM]OH *via* bipolar membrane electrodialysis – precursor production for the combinatorial synthesis of [EMIM]-based ionic liquids†

S. Himmler,^a A. König^b and P. Wasserscheid^{*a}

Received 30th November 2006, Accepted 26th January 2007

First published as an Advance Article on the web 2nd March 2007

DOI: 10.1039/b617498a

A new environmentally benign process for the production of aqueous solutions of [EMIM]OH is reported. Electrodialysis with bipolar membranes (EDBM) was implemented for the first time to produce this hydroxide-based precursor in 5% concentration in water from the non-toxic bulk ionic liquid [EMIM][EtOSO₃] at the kg-scale. The results are discussed with regard to ease of operation, productivity and obtained product quality. Moreover, several structurally new ionic liquids were synthesized by reaction of the aqueous precursor solution with different acids, such as, *e.g.*, H₂SiF₆ or hexafluoroacetylacetone. But also the synthesis of well-established ionic liquids, such as, *e.g.*, [EMIM][BF₄] has been carried out using the hydroxide intermediate and the full procedure is compared to well-established ion metathesis protocols.

Introduction

Ionic liquids (ILs) are more and more applied as solvent substitutes in academic research and industry. These innovative liquids are, for example, used as lubricants,¹ heat transfer agents,^{2,3} performance additives in paints,⁴ process fluids for separation processes^{5,6} and in analytical devices.⁷ Up to now ionic liquids are prepared in many different ways. One of the simplest methods for the synthesis of such materials is the protonation of amines or phosphines with different acids. Already in 1914, a room temperature liquid salt of this type, namely ethylammonium nitrate, was reported.⁸ However, as decomposition through deprotonation may occur – at least in the presence of any base – the practical use of these salts is somehow limited.⁹ More stable ionic liquids are known to be obtained by the quaternization of an amine or phosphine with a suitable alkylation agent to form phosphonium, imidazolium, pyridinium or ammonium salts. In this case the nature of the alkylating agent determines the anion that is first obtained in the ionic liquid. Commonly used quaternization reagents are haloalkanes, trialkylphosphates, alkyltriflates and dialkylsulfates. If the desired anion cannot be obtained by direct alkylation, anion metathesis is frequently carried out using either silver salts in water¹⁰ or sodium salts in dry acetone¹¹ or CH₂Cl₂.¹² While the first method is hampered by the high price and redox instability of silver salts, the second is affected by the low solubility of most alkali salts in organic solvents, by the hygroscopicity of the NaCl precipitate and by the often necessary tedious filtration procedures. In contrast, anion metathesis is much easier if water-immiscible ionic liquids like

[PF₆]¹³ and [(CF₃SO₂)₂N]¹⁴ melts are formed and very pure ionic liquids can be obtained after several washing steps.⁹ A first method to synthesize different ionic liquids based on the bulk ionic liquid [EMIM][EtOSO₃] as an intermediate has recently been presented. It was demonstrated that this ionic liquid can be transformed by transesterification of the anion with different alcohols, *e.g.* 1-butanol or ethoxyethanol, into a range of halogen-free alkylsulfate ionic liquids.¹⁵

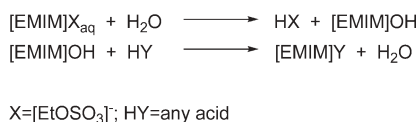
For obvious reasons it is very attractive to prepare 1,3-dialkylimidazolium ionic liquids by acid–base reactions from a suitable precursor compound and an acid. As there are many commercially available acids whose anions have not been investigated as components in ionic liquids yet, this method offers great potential for the discovery of new ionic liquids. A first method of this kind has already been presented in 2001 by Seddon and Earle. They described the preparation and distillation of imidazolium carbenes and their reaction with suitable alcohols and acids to form new ILs.¹⁶ Another very attractive precursor is 1,3-dialkylimidazolium hydroxide that is unstable in its pure form but relatively stable in aqueous solutions at low concentrations. So far, Ohno's group has reported the synthesis of ionic liquids *via* hydroxide precursors produced by classical ion exchange over a column. These authors carried out reactions between [EMIM]OH and triazole/tetrazole to form new ionic liquids carrying azole-based anions, and, furthermore, used amino acids as reaction agents.^{17,18} These publications demonstrate impressively the synthetic potential of hydroxide-based precursors for innovative ionic liquid syntheses.

In this paper we describe a completely different approach to produce aqueous solutions of 1,3-dialkylimidazolium hydroxide, specifically with the use of electrodialysis with bipolar membranes (EDBM).¹⁹ Despite the fact that a patent exists disclosing the possibility of the production of ionic liquids in 'electrochemical cells'²⁰ that comprise anode and cathode and are charged with solutions, so far no detailed information about the mode of operation, the efficiency and the technical potential of such a process has been reported either in the patent literature or in any other publication. Our goal was to

^aLehrstuhl für Chemische Reaktionstechnik der Friedrich-Alexander-Universität Erlangen-Nürnberg, Egerlandstrasse 3, Erlangen, D-91058, Germany. E-mail: wasserscheid@crt.cbi.uni-erlangen.de; Fax: +499131-8527421; Tel: +499131-8527420

^bLehrstuhl für Thermische Verfahrenstechnik der Friedrich-Alexander-Universität Erlangen-Nürnberg, Egerlandstrasse 3, Erlangen, D-91058, Germany

† This paper was published as part of the special issue on Green Solvents for Processes.



Scheme 1 Ionic liquid synthesis via a hydroxide precursor exemplified for $[\text{EMIM}][\text{EtOSO}_3]$.

prove the versatility of the EDBM process for a large-scale production of hydroxide ionic liquid precursors. Hereby, hydroxide precursors should be produced from a readily accessible precursor ionic liquid and water followed by acid addition to obtain the desired ionic liquid (see Scheme 1, exemplified for $[\text{EMIM}][\text{EtOSO}_3]$ being the feedstock ionic liquid).

In this study we focussed on the synthesis of $[\text{EMIM}]\text{OH}$ via EDBM since ionic liquids based on this cation seem to have the most suitable properties for most practical applications (e.g. concerning melting point and viscosity). In this contribution we describe on the one hand the production of $[\text{EMIM}]\text{OH}$ via EDBM, and on the other hand we further demonstrate the potential of this hydroxide precursor for the synthesis of different new and known ionic liquid structures.

Electrodialysis with bipolar membranes – introduction and theory

Electrodialysis (ED) is a membrane separation process in which ions are separated, concentrated and purified from mostly aqueous feed solutions under the influence of the driving force of an applied electrical potential gradient. The process is based on the property of ion permeable membranes to selectively transport ions. Applying a voltage between two electrodes generates the potential field that is required for the transport of these ions having positive or negative charge. ED is used to remove salts from food, from dairy products and from waste water streams, and is also used to concentrate salts, acids or bases.^{21,22} The ion permeable membranes that are used in ED are fabricated from ion exchange polymers and contain other polymers to improve mechanical strength and flexibility. The potential of the ED process has been extended by the invention of bipolar membranes (BMs). Fig. 1 illustrates the structure and function of a BM. Bipolar membranes that have been investigated in our work are made

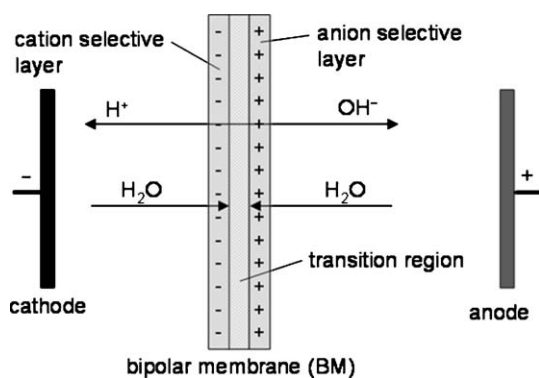
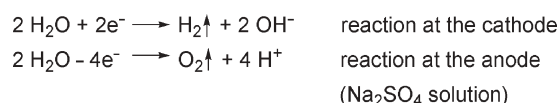


Fig. 1 Function and structure of a bipolar membrane.



Scheme 2 Electrode reactions during the EDBM process.

up of a cation selective layer and an anion selective layer that are fixed together.

Water can be split by these membranes into hydroxide and protons when a potential field is applied and the cation-exchange side faces the anode while the anion-exchange side faces the cathode. When bipolar membranes are combined with other cation- and anion-exchange membranes and placed between a pair of electrodes, acids and bases can be produced at either surface of the BM from a neutral salt.²³ In our case $[\text{EMIM}]\text{OH}$ and EtOSO_3H were produced from the 'salt' $[\text{EMIM}][\text{EtOSO}_3]$. The change of charge carriers from electrons to ions takes place at the electrodes in the form of chemical reactions: hydrogen is formed at the cathode whereas oxygen is produced at the anode when an aqueous Na_2SO_4 solution is used (see Scheme 2). For removing the gases from the electrodes the electrode chambers were flushed with the Na_2SO_4 solution.

In the electrodialytic system the flux of electrolytes dn_i/dt directly depends on the current flow I , valency of the ion z_i and the Faraday constant $F = 96\,500 \text{ (A s) mol}^{-1}$.

$$\frac{dn_i}{dt} = \frac{I}{z_i F} \quad (1)$$

The transported amount of equivalents Δn_i can be calculated at constant current flow I from current efficiency ζ , number of cells N and the time Δt the current was applied:

$$\Delta n_i = \frac{I \zeta N}{z_i F} \Delta t \quad (2)$$

With regard to electro-neutrality, eqn (2) also describes the formation of protons and hydroxide ions during the ED with bipolar membranes. Thus, the amount of hydroxide formed can also be calculated using eqn (2). The current density $J \text{ (A m}^{-2}\text{)}$ is defined by current flow per area and should be limited to a maximum of 70% from the limiting current density J_{lim} .²²

$$J = \frac{I}{A} \quad (3)$$

Now, the amount of hydroxide produced by EDBM can be calculated:

$$\Delta n_i = \frac{J A \zeta N}{z_i F} \Delta t \quad (4)$$

Eqn (4) shows which technical parameters influence the amount of equivalents produced. As the current density J is limited to approximately 1000 A m^{-2} , the amount of equivalents Δn_i can be controlled easily by the time Δt , the effective membrane area A and the number of cells N used. For the electrodialytic system used in this work, an amount of 0.078 equivalents produced per hour results when a current efficiency of $\zeta = 1$ is assumed (with $A = 64 \times 10^{-4} \text{ m}^2$,

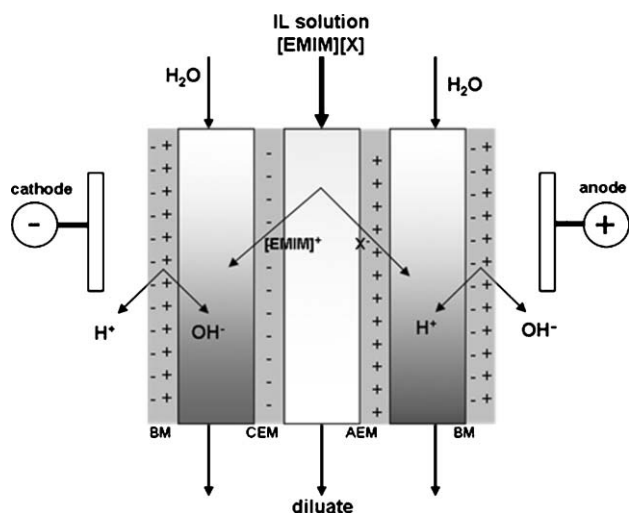


Fig. 2 Principle of the EDBM process.

$I = 2.1 \text{ A}$; $N = 1$; $z_i = 1$; $\zeta = 1$; $\Delta t = 3600 \text{ s}$. As every membrane has a specific permselectivity, only a certain part of the current I can be utilized for the flux of electrolytes.

Results and discussion

The production of hydroxide-based precursors for the synthesis of novel and well-established ILs by EDBM was investigated. The feed ionic liquid of choice was $[\text{EMIM}][\text{EtOSO}_3]$ as this is rather cheaply available in large scale and is easy to

handle due to its non-toxic nature.²⁴ Special exchange membranes from FuMA-Tech GmbH were selected according to the organic nature of our feed solution. The first electrodialysis cell set-up included one stack of membranes (see Experimental section) and was operated batch-wise. A rather diluted solution of the feed ionic liquid was chosen as, on one hand, the product $[\text{EMIM}]\text{OH}$ is unstable in concentrations higher than 20 wt% in water and, on the other hand, the selectivity of the process is improved in diluted systems. After the first run we could prove the principle and we successfully converted the feed stream $[\text{EMIM}][\text{EtOSO}_3]$ into the base $[\text{EMIM}]\text{OH}$ and the acid EtOSO_3H by application of a current (2.1 A) across the membranes. Even with this single stack set-up, *i.e.* 2 BMs, 1 AEM (anion-exchange membrane) and 1 CEM (cation-exchange membrane) were implemented in the cell (compare Fig. 2), the overall current efficiency was about 76%. About 1 mmol min^{-1} $[\text{EMIM}]\text{OH}$ could be produced with this lab-scale cell arrangement. Owing to the fact that membranes in general have certain limits in selectivity (permselectivity), contamination with foreign ions occurs as it is impossible to hold back every unwanted ion.²² In our case the main contaminants were sodium and sulfate ions from the electrode rinse solution that limited the overall purity of the $[\text{EMIM}]\text{OH}$ solution to $<95\%$. However, the more stacks of membranes are used in one cell the lower is the contamination with unwanted electrolytes from the rinse solution. For proving this fact, we implemented another set of membranes and carried out several experiments with the double stack set-up shown in Fig. 3. Another measure to reduce contamination of the

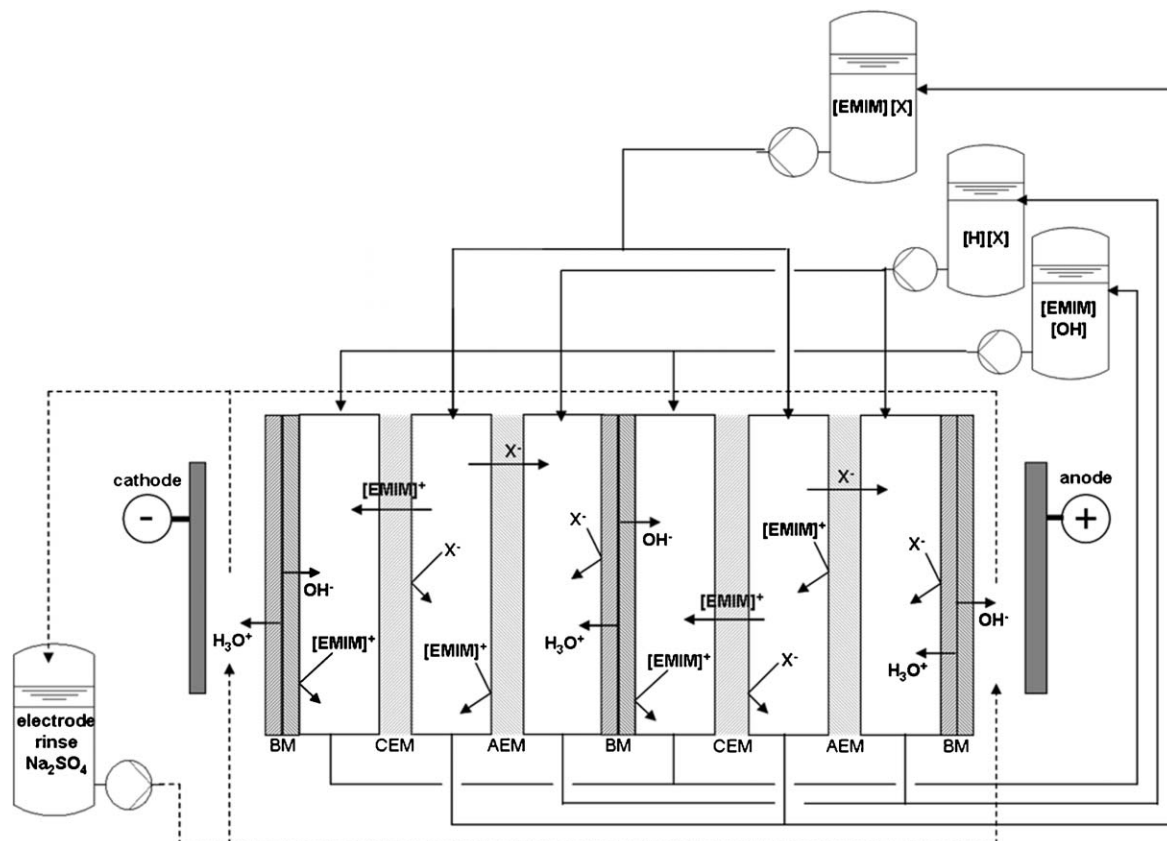


Fig. 3 Double stack set-up.

product cycles with foreign ions from the flushing solution that is under investigation now is the implementation of an independent flushing cycle between the two outer BMs and the electrodes.

Batch configuration

For our lab-scale experiments, we chose a batch configuration as the process remains very flexible to changes and the required exchange area can be kept at small dimensions. Up-scaling can simply be carried out by increasing the amount of feed solution in the process. Running in batch mode means that certain volume units of the different solutions (acid, base, feed solution) are circulated through the membrane stack and undergo repeatedly the separation process until the desired product concentration (here the concentration of [EMIM]OH in the base compartment) is reached. As we recorded the operating voltage U and the current I for each experiment (see Fig. 4) this mode of operation also gave us the possibility of directly controlling the exchange by interpreting the voltage curve.

The fall and rise of voltage over the cell directly depends on the total current applied and the overall resistance of the cell,

$$U_{\text{cell}} = I_{\text{total}} R_{\text{cell}} \quad (5)$$

where I_{total} = total current applied, constant in all experiments, and U_{cell} = total voltage over the cell.

The overall resistance of the cell includes the individual resistances of the membranes and those of the solutions in the compartments,

$$R_{\text{cell}} = R_{\text{BM}} + R_{\text{bc}} + R_{\text{CEM}} + R_{\text{fc}} + R_{\text{AEM}} + R_{\text{ac}} \quad (6)$$

where R_{cell} = total resistance of the stack, R_{BM} , R_{CEM} , R_{AEM} = resistances of the membranes, respectively, and R_{bc} , R_{fc} , R_{ac} = resistances of base compartment, feed compartment and acid compartment, respectively.

The resistances R_{bc} , R_{fc} , R_{ac} depend directly upon the concentration of the electrolytes in the solutions, which means

that low concentrations lead to high resistances and high concentrations of ions result in low resistances, respectively. At the beginning of each batch mode experiment the ion concentration in the feed compartment is high whereas the concentrations of ions in the acid and base compartments are low, *i.e.* the resistances R_{bc} and R_{ac} are high and so is the total resistance R_{cell} . A high voltage is needed to ensure a constant current flow (here 2.1 A). The more ions are exchanged over time, the lower become the resistances of the acid and base solutions and the total resistance and voltage. However, when the concentration of ions in the feed solution decreases over time, the resistance in the feed solution R_{fc} increases and so does R_{cell} and the voltage U_{cell} . Complete exchange is indicated when the voltage finally reaches its starting value and the current drops to a low value. By plotting the voltage over the time we were able to control the experiments until the exchange was completed.

Kinetics of the exchange

For the kinetic investigation of the electrodialysis process we took samples at defined times and analysed them by ion chromatography. As expected, the ion exchange proceeds in a linear way according to the current applied. Fig. 5 illustrates the decrease of [EMIM] ions in the feed compartment over the operation time and the accumulation of this cation species in the base compartment. In addition, the negligible increase of [EMIM]⁺ in the acid compartment, depending on the permselectivity of the membranes, is shown. As we carried out the experiments in batch mode the alteration of [EMIM]⁺ concentration was not exactly linear at the beginning and the end of the experiments as a sufficient electrolyte concentration had to be built up in every compartment for allowing a constant current flow. Comparing the gradient $\Delta n_{[\text{EMIM}]^+}/\Delta t$ in the feed compartment and in the base compartment according to eqn (1) it shows the same absolute value of $2.0 \times 10^{-5} \text{ mol s}^{-1}$, *i.e.* the concentration of [EMIM]⁺ changes at the same rate in both compartments. At constant current flow, the time needed for the exchange of a certain amount of equivalents can then be calculated exactly.

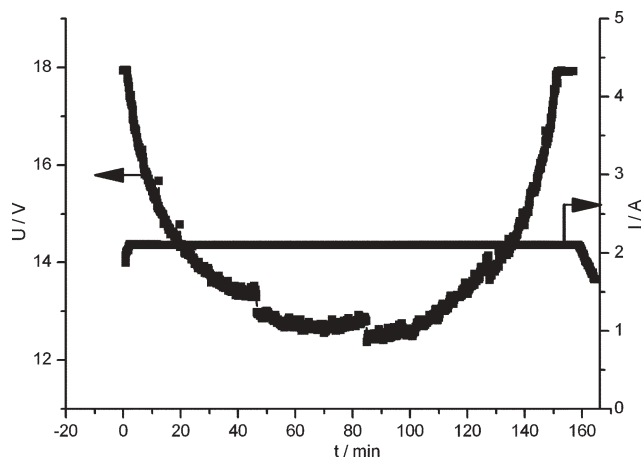


Fig. 4 Typical plot of voltage and current *versus* time for an EDBM experiment.

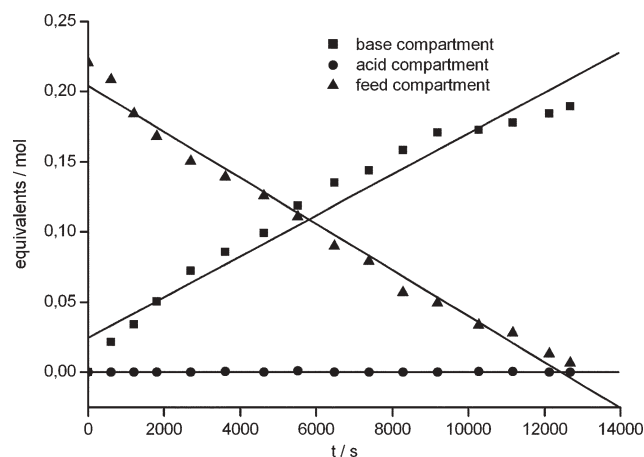


Fig. 5 Concentration–time profiles for the exchange of [EMIM]⁺ in the different compartments of the EDBM cell.

Table 1 Comparison of different dimensions of EDBM processes²⁶

		Lab-scale EDBM	Pilot plant EDBM	Production plant EDBM
Membrane area installed/m ²		6.4×10^{-3}	3.8	40.3
Production quantity ^{a,b}	kmol d ⁻¹	1.41×10^{-3}	0.83	8.97
	kg d ⁻¹	0.18	110.0	1166.5

^a Calculated for $\zeta = 75\%$, $N = 1$, $z_i = 1$, $I = 2.1$ A, $F = 96\,500$ (A s) mol⁻¹. ^b Based on lab-scale experiments.

Double stack set-up

After implementing the double stack set-up (shown in detail in Fig. 3), we found that the contamination with ions from the outer cycle was immediately reduced by more than half of the amount that was found in the solutions after the first experiments using the single stack set-up. Sodium and sulfate concentrations in the product solution were altogether lower than 0.8 wt%. The concentration of ethylsulfate ions, coming from the feed solution, was in most cases lower than 1 wt%. Furthermore, the mass balance of the whole process could be closed. These results in the double stack set-up proved that the contamination with unwanted electrolytes from the rinse solution is dramatically decreased by increasing the number of stacks since fewer ions from the outer flushing cycle reach the inner compartments.

Up-scaling

For our lab-scale set-up, we implemented a batch configuration as explained above. For scaling up the batch mode process, different possibilities can be envisaged. On the one hand we could use more stacks for running the EDBM (numbering up) resulting in shorter exchange times for comparable amounts of solution. On the other hand more salt solution could be used for the exchange. However, for large-scale applications, batch-mode operation comes to its limit because with increasing amounts of feed solution large storage tanks, compared to the size of the plant, have to be installed. Therefore, we work on a different possibility for up-scaling by changing the mode of operation from batch to feed-and-bleed mode. This means that the solutions (acid, base and feed solution) are circulated through the membrane stack but a part of each solution is continuously removed and replaced by fresh solution. One of the most important advantages of the feed-and-bleed mode is the lower energy costs than those for batch mode since the process is carried out at ideal conditions. Ideal process conditions are reached when the overall resistance of the cell can be kept small due to sufficient electrolyte concentrations in the different solutions throughout the whole process. The overall power consumption is then reduced compared with the batch-mode operation. Applied in microfiltration, ultrafiltration, nanofiltration, and reverse osmosis membranes, the feed-and-bleed mode design is also standard in larger industrial- and waste-treatment membrane systems for water treatment recovery and recycling, and for maximum concentration of contaminants with low final volumes of concentrate.²⁵ To get a better impression of which amounts of [EMIM]OH could be synthesized on the large scale using the EDBM process we extrapolated our results from the lab-scale batch EDBM experiments with the single and the double stack set-up to pilot plant scale and

production plant scale. With a typical commercially available pilot plant (e.g. FuMA-Tech) an amount of about 110 kg of [EMIM]OH could be produced per day and a production rate higher than 1100 kg d⁻¹ could be reached in a typical production plant.²⁶ Table 1 shows impressively that the multi-kg scale can be reached by implementing adequate techniques that are readily available.

Synthesis of ionic liquids from [EMIM]OH

The synthesis of ionic liquids *via* hydroxide-based precursors, illustrated in Scheme 3, is not only a simple acid–base titration but it also has various advantages. One point is that water is the only by-product formed during this neutralization reaction. Another advantage is that no organic solvents are needed, even if solid acids are used (e.g. benzoic acid) since the aqueous precursor solution itself serves as solvent. Furthermore, a great variety of different ILs can be synthesized due to the large amount of commercially available inorganic and organic acids. Even more interesting is the fact that defined mixtures of one cation with different anions can be readily synthesized and evaluated by adding defined mixtures of acids.

During our study we synthesized several new ionic liquid structures and studied their most important physical properties such as melting point, temperature of thermal decomposition and viscosity. The results are listed in Table 2. It became quite clear to us that ionic liquids with various technically interesting properties, such as low viscosity, low melting point, high density or high thermal stability can be produced using the [EMIM]OH precursor. Even well-established systems, such as [EMIM][BF₄], which are notoriously difficult to obtain in halide-free quality by the traditional anion metathesis routes are easily accessible by reacting one equivalent of [EMIM]OH with one equivalent of tetrafluoroboric acid. While [EMIM][BF₄] produced *via* the EDBM hydroxide

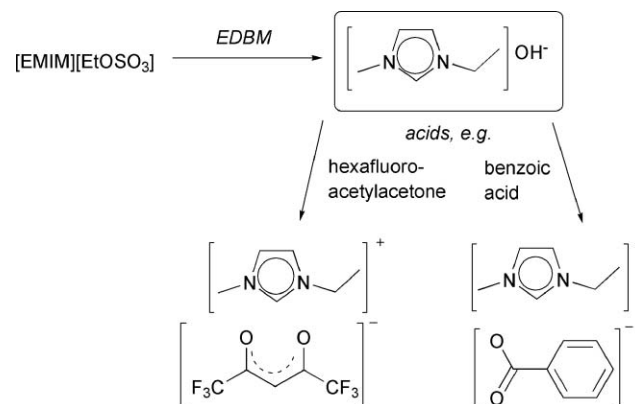
**Scheme 3** Synthesis of ILs using OH-based precursors.

Table 2 Ionic liquids synthesized from [EMIM]OH by acid–base reaction and their properties

Ionic liquids	Yield of acid–base reaction (%)	Purity of final product ^a (%)	Water content/ppm	Density/g mL ⁻¹	Viscosity ^b /mPa s	<i>T</i> _{decomp} ^c /°C	<i>T</i> /°C
[EMIM][MeSO ₃]	>99	>99	980	1.24	207	359	−14 ^d
[EMIM][Ph-SO ₃]	>99	>99	765	1.31	1200	345	−54 ^e
[EMIM][HSiF ₆]	99	98	680	1.38	—	338	<RT ^f
[EMIM][BF ₄]	99	>99	540	1.30	34	415	13–15 ^d
[EMIM][Ph-COO]	99	>99	1050	1.29	4990	231	−40 ^e
[EMIM][F ₆ acac]	>99	98	560	1.35	20 ^g	272	31 ^d

^a Major impurities determined by IC: SO₄^{2−}, EtOSO₃[−], Na⁺. ^b Viscosities measured at 25 °C. ^c *T*_{decomp}: temperature of thermal decomposition. ^d Melting point. ^e Glass transition temperature. ^f Mp could not be determined by DSC. ^g Viscosities measured at 40 °C.

process is naturally free of any halide impurities it does contain small amounts of ethylsulfate, sodium and sulfate. The purity of the final products ranged from 98 to >99% depending on the charge of [EMIM]OH used and was determined by ion chromatography.

Experimental

Commercially available ion-exchange membranes (FuMA-Tech GmbH, fumasep, FKB, FBM, FAB) were integrated into an electrodialysis cell (four-cell electrodialysis unit ED 64004, PCA) according to a three-cell set-up. The principle is shown in Fig. 2. The membrane dimension was 11 × 11 cm with an effective membrane area of 64 cm². The number of membrane pairs was 4 for the first experiments (2 BMs, 1 CEM, 1 AEM), that means one stack, and 7 for the latest experiments (3 BMs, 2 CEM, 2 AEM), two stacks. The membranes were separated by net spacers with a silicone frame. Before starting experiments the membranes were rinsed with de-ionised water. Salt solution was supplied to the plant by hose-pumps at room temperature and a velocity of 60 mL min^{−1}. The concentration of the feed solution was 7.5 wt% and 10 wt% [EMIM][EtOSO₃], respectively, in de-ionised water since the precursor [EMIM]OH is not stable in aqueous solutions with concentrations >20%. An electric current (2.1 A) was passed across the ion-exchange membranes through Pt/Ir-coated titanium electrodes. For the evaluation of the EDBM process, concentrations were measured before and after the experiments in all compartments (base, acid, feed and electrode rinse compartments). For rinsing the electrodes during the experiment a 5 wt% NaSO₄ solution was used. After all experiments the membranes were rinsed and stored in a 5 wt% NaSO₄ solution. All experiments were carried out in a batch-wise mode of operation for 2–7 h, depending on the amount of feed solution.

Determination of acid/base content

The content of [EMIM]OH in the product solutions was determined by titration with 0.1 M HCl solution. Bromothymol blue was used as the pH indicator. The content of EtOSO₃H was determined likewise with 0.1 M NaOH solution.

Ion chromatography

Cations and anions were analysed simultaneously by ion chromatography (Dionex Corp., CA, USA). A CS12 A plus guard column was used in an ICS-90 ion chromatography

system for analysis of the cations [EMIM]⁺ and Na⁺. For the analysis of [SO₄]^{2−} and [EtOSO₃][−] an AS50 ion chromatography compartment, an AS11-HC plus guard column, an EG50 eluent generator and an IC25 pump were used. More details concerning ion chromatography measurement are found in ref. 27.

Data logging

Voltage was applied using a power-supply DPS-4005PFC (Votcraft). Online data logging was possible for the most important operating parameters [operating voltage *U*, current *I*, temperature base compartment (*T*₁) and acid compartment (*T*₂)] using a digital multimeter DMM 2700 (Keithley Instruments) and the software LabView 7.0 for visualization.

Synthesis of ionic liquids

All acids (all grades >99%) were purchased from Aldrich, Fluka and Riedel de Haën. [EMIM][EtOSO₃] was provided from Solvent Innovation GmbH with commercial grades >98%.

For the precursor [EMIM]OH in aqueous solution, 1 equiv. was weighed into a Schlenk round-bottomed flask and 1 equiv. of an acid was added dropwise to the hydroxide solution. The reaction mixture was then stirred for several minutes at room temperature. The excess of water was removed using a rotary evaporator and afterwards a high vacuum (<1 mbar) at 70 °C was applied overnight to ensure water contents lower than 1000 ppm.

Determination of water content

The water content was determined by coulometric Karl-Fischer titration using a Metrohm 756 KF Coulometer with a Hydranal[®] Coulomat AG reagent.

Viscosity

The viscosities of the ionic liquids were measured under an argon atmosphere using an MCR 100 rheometer from Anton Paar, Graz. Temperature control was maintained by a Peltier element. Viscosity measurements were always carried out with samples of defined water content that was determined directly prior to the measurement by coulometric Karl-Fischer titration.

Density

Density was measured at room temperature in a BLAUBRAND pycnometer with a defined volume of 5.330 mL according to DIN ISO 3507.

Thermal stability

Thermogravimetric measurements were conducted on a Netzsch TG 209 with the samples placed in an open Al_2O_3 pan and heated from room temperature up to 500 °C at a heating rate of 10 K min⁻¹ under a protective gas atmosphere. The temperature of decomposition (T_{decomp}) was determined by using the TG-onset temperature, which is the intersection of the baseline below the decomposition temperature with the tangent to the mass loss *versus* temperature plots in the TGA experiment.

Determination of melting points

Differential scanning calorimetry (DSC) was carried out using a Netzsch DSC 205 Phoenix under an argon atmosphere with samples hermetically sealed in Al pans and cooled to -140 °C and then reheated at a cooling and heating rate of 10 K min⁻¹. The melting points were determined from the DSC thermograms during the programmed reheating steps.

NMR spectroscopy

NMR spectra were recorded on a JEOL ECX +400 spectrometer (¹H: 400 MHz). Deuterated DMSO was used as the internal standard. The chemical shifts are noted in parts per million (ppm), the coupling constants in Hz. The data are given in the following way:

¹H-NMR: chemical shift (multiplicity, number of protons, assignment, coupling constant).

[EMIM][MeSO₃] 1-ethyl-3-methylimidazolium methylsulphonate: ¹H-NMR (400 MHz, d₆-DMSO, [ppm]) δ 1.41 (t, 3H, NCH₂CH₃, $J = 7.25$), 2.32 (s, 3H, CH₃SO₃), 3.85 (s, 3H, NCH₃), 4.19 (q, 2H, NCH₂CH₃, $J = 7.24$), 7.70 (s, 1H, NCHCN), 7.79 (s, 1H, NCHCN), 9.21 (s, 1H, NCHN).

[EMIM][BF₄] 1-ethyl-3-methylimidazolium tetrafluoroborate: ¹H-NMR (400 MHz, d₆-DMSO, [ppm]) δ 1.40 (t, 3H, NCH₂CH₃, $J = 7.24$), 3.85 (s, 3H, NCH₃), 4.20 (q, 2H, NCH₂CH₃, $J = 7.24$), 7.69 (s, 1H, NCHCN), 7.77 (s, 1H, NCHCN), 9.20 (s, 1H, NCHN).

[EMIM][F₆AcAc] 1-ethyl-3-methylimidazolium hexafluoroacetylacetonate: ¹H-NMR (400 MHz, d₆-DMSO, [ppm]) δ 1.41 (t, 3H, NCH₂CH₃, $J = 7.25$), 3.85 (s, 3H, NCH₃), 4.19 (q, 2H, NCH₂CH₃, $J = 7.24$), 5.27 (s, 1H, CF₃COCHCOCF₃), 7.70 (s, 1H, NCHCN), 7.79 (s, 1H, NCHCN), 9.21 (s, 1H, NCHN).

[EMIM][HSiF₆] 1-ethyl-3-methylimidazolium hexafluorohydrogensilicate: ¹H-NMR (400 MHz, d₆-DMSO, [ppm]) δ 1.40 (t, 3H, NCH₂CH₃, $J = 7.24$), 3.85 (s, 3H, NCH₃), 4.20 (q, 2H, NCH₂CH₃, $J = 7.24$), 7.69 (s, 1H, NCHCN), 7.77 (s, 1H, NCHCN), 9.18 (s, 1H, NCHN).

[EMIM][Ph-COO] 1-ethyl-3-methylimidazolium benzoate: ¹H-NMR (400 MHz, d₆-DMSO, [ppm]) δ 1.38 (t, 3H, NCH₂CH₃, $J = 7.25$), 3.86 (s, 3H, NCH₃), 4.21 (q, 2H, NCH₂CH₃, $J = 7.24$), 7.27 (m, 2 × 1H, CHCHCHCHCOO⁻), 7.27 (m, 1H, CHCHCHCHCHCOO⁻), 7.76 (m, 2 × 1H, CHCHCOO⁻), 7.85 (s, 1H, NCHCN), 7.89 (s, 1H, NCHCN), 9.20 (s, 1H, NCHN).

[EMIM][Ph-SO₃] 1-ethyl-3-methylimidazolium benzyldisulfonate: ¹H-NMR (400 MHz, d₆-DMSO, [ppm]) δ 1.36 (t, 3H, NCH₂CH₃, $J = 7.25$), 3.83 (s, 3H, NCH₃), 4.17 (q, 2H, NCH₂CH₃, $J = 7.24$), 7.35 (m, 2 × 1H, CHCHCHCHCSO₃⁻), 7.35

(m, 1H, CHCHCHCHCHCHCSO₃⁻), 7.65 (m, 2 × 1H, CHCHCSO₃⁻), 7.77 (s, 1H, NCHCN), 7.78 (s, 1H, NCHCN), 9.18 (s, 1H, NCHN).

Conclusion

In this contribution we have presented a new and highly promising approach for the production of hydroxide-based precursors for the benign synthesis of ionic liquids. In contrast to conventional processes of ion exchange over resins or columns, the electrodialysis described here with bipolar membranes (EDBM) produces aqueous solutions of 1-ethyl-3-methylimidazolium hydroxide with much lower production of waste water from the commercially available and non-toxic [EMIM][EtOSO₃]. The whole process – including the simple conversion of OH-based precursors into the final ionic liquids by merely adding an acid of choice – has great potential for the development of novel and especially task-specific ionic liquids. One crucial point is the suitability of the EDBM process for inline-production. This means that the process is very flexible with respect to capacity and feed applied. Another important fact is that the rather simple process of numbering up is applicable for transferring the EDBM process to larger scales. In most cases, the operating conditions in a lab-scale EDBM can be reproduced on an industrial scale.²² The production quantities that can be reached with EDBM plants in dimensions of pilot plants and production plants have been calculated on the basis of our experiments and indicate impressively the technical applicability of the new process approach. By implementing a large membrane area the multi-kg level in the production of [EMIM]OH could easily be reached with the EDBM process. With our lab-scale double stack set-up we reached a daily production of approximately 28 kg d⁻¹ m⁻² [EMIM]OH (220 mol d⁻¹ m⁻²) in the form of a 5% aqueous solution with a product quality of >98%.

Interestingly, the EDBM process gives not only access to a simple and continuous mode of operation with greatly reduced waste water production, this membrane process also provides the possibility of selectively exchanging a specific anion species of a complex ionic liquid mixture containing more than one anion (in contrast to any ion exchange process *via* resins or columns). In the future, such a process could be of great technical interest with respect to the purification of ionic liquids after synthesis and to the regeneration of 'spent' ionic liquids (*e.g.* removal of undesirable anions).

Acknowledgements

The authors would like to thank Solvent Innovation GmbH for providing [EMIM][EtOSO₃] and the Deutsche Bundesstiftung Umwelt for the financial support of this project (grant number: AZ 24214).

References

- Q. Lu, H. Wang, C. Ye, W. Liu and Q. Xue, *Tribol. Int.*, 2004, **37**, 547.
- G. Olbert, T. Mattke, M. Fiene, O. Huttenlocher and U. Hammon, BASF AG, Germany, *Ger. Pat. Appl.*, DE 2003-10316418 10316418, 2004.

- 3 M. E. Van Valkenburg, R. L. Vaughn, M. Williams and J. S. Wilkes, *Proc. Electrochem. Soc.*, 2002, **19**, 112.
- 4 B. Weyershausen and K. Lehmann, *Green Chem.*, 2005, **7**, 15.
- 5 Y. A. Beste, H. Schoenmakers, W. Arlt, M. Seiler and C. Jork, BASF AG, Germany, *Ger. Pat. Appl.*, DE 2003-10336555 10336555, 2005.
- 6 C. Jork, M. Seiler, Y.-A. Beste and W. Arlt, *J. Chem. Eng. Data*, 2004, **49**, 852.
- 7 A. Bösmann and T. J. S. Schubert, Germany, *Br. Pat. Appl.*, GB 2005-107722414553, 2005.
- 8 P. Walden, *Bull. Acad. Imper. Sci. (St. Petersburg)*, 1914, 1800.
- 9 *Ionic liquids in synthesis*, ed. P. Wasserscheid and T. Welton, Wiley-VCH, Weinheim, 2003.
- 10 J. S. Wilkes and M. J. Zaworotko, *J. Chem. Soc., Chem. Commun.*, 1992, 965.
- 11 J. Fuller and R. T. Carlin, *Proc. Electrochem. Soc.*, 1999, **98**, 227.
- 12 L. Cammarata, S. Kazarian, P. Salter and T. Welton, *Phys. Chem. Chem. Phys.*, 2001, **3**, 5192.
- 13 C. M. Gordon, J. D. Holbrey, A. R. Kennedy and K. R. Seddon, *J. Mater. Chem.*, 1998, **8**, 2627.
- 14 P. Bonhôte, A.-P. Dias, N. Papageorgiou, K. Kalyanasundaram and M. Grätzel, *Inorg. Chem.*, 1996, **35**, 1168.
- 15 S. Himmler, S. Hörmann, R. van Hal, P. S. Schulz and P. Wasserscheid, *Green Chem.*, 2006, **8**, 887.
- 16 M. J. Earle and K. R. Seddon, Great Britain, *World Pat. Appl.*, WO 2001-GB1487 2001077081 20010405, 2001.
- 17 W. Ogihara, M. Yoshizawa and H. Ohno, *Chem. Lett.*, 2004, **33**(8), 1022.
- 18 K. Fukumoto, M. Yoshizawa and H. Ohno, *J. Am. Chem. Soc.*, 2005, **127**(8), 2398.
- 19 S. Himmler, M. Medved, A. König and P. Wasserscheid 'Bipolar Membrane Electrodialysis and Ion Exchange Technology – Precursor Production for the Synthesis of novel Ionic Liquids', Green Solvents for Processes (international conference), held 8–11 October 2006, Lake Constance, Friedrichshafen, Germany.
- 20 R. Moulton, *US Pat. Appl.*, US, 2003/0094380, 2003.
- 21 T. Melin and R. Rautenbach, *Membranverfahren*, Springer-Verlag, Berlin, Heidelberg, New York, 2004.
- 22 *Handbook on bipolar membrane technology*, ed. A. J. B. Kemperman, Twente University Press, Enschede, 2000.
- 23 W. Johnson, 'Properties and Applications of a Novel Bipolar Membrane', *Fourth Forum Proceedings*, published by The Electrosynthesis Company, Inc., Lancaster, NY, USA, 1990.
- 24 For example, from Solvent Innovation GmbH, Cologne (www.solvent-innovation.de) or BASF AG (www.basionics.de).
- 25 F. J. Brady, *Environ. Protection*, 2006, **17**, 6.
- 26 From FuMA-Tech GmbH, St. Ingbert (www.fumatech.com).
- 27 A. König, D. Weckesser and D. Jensen, *GIT Labor-Fachzeitschrift*, 2006, **50**(6), 546–549.

The art of CO₂ for art conservation: a green approach to antique textile cleaning†

Micaela Sousa,^a Maria João Melo,^{*ab} Teresa Casimiro^b and Ana Aguiar-Ricardo^{*b}

Received 1st December 2006, Accepted 10th April 2007

First published as an Advance Article on the web 8th May 2007

DOI: 10.1039/b617543k

The use of CO₂ as a dry-cleaning solvent for old silk textiles was investigated. The cleaning procedures under study were tested on the 18th century religious garments from Virgin and Child from Palácio das Necessidades, Lisbon. The effect of using different cleaning solvent streams, supercritical and liquid CO₂, CO₂ + isopropanol and CO₂ + isopropanol + water, was evaluated concerning the dirt particles extracted, weight loss and colour variation of the scapulary samples tested. Particularly, the use of liquid CO₂ and the addition of water as a co-solvent had a strong positive effect on removal of dirt particles. CO₂-assisted cleaning proved to be a very safe method for the cleaning of very deteriorated silk textiles. The fibres and the textile structure were not physically damaged and the method did not promote the loss of material, which is an enormous advantage for the cleaning of textiles of historic or artistic value.

Introduction

Conservators are committed to the development of safe techniques to clean textiles of historic or artistic value. Cleaning procedures must be designed to physically preserve the fibres and their structure and to avoid the shrinkage of materials, as happens during traditional wet cleaning. This is particularly important in severely damaged textiles, as in the case for the garments of the Virgin and Child (Fig. 1), an 18th century sculpture from Palácio das Necessidades in Lisbon, Portugal. The Virgin's garments are composed of several pieces that were heavily damaged; the fibres could easily suffer disintegration by simple handling. Our goal has been to develop new methods and procedures for cleaning the antique and fragile clothes of the Virgin and Child, since the previously performed wet cleaning tests damaged them unacceptably. The results of our preliminary studies were described by Sousa *et al.*¹ Our first "green" approach to antique textile cleaning investigated the harmfulness of the dry supercritical CO₂ (scCO₂) method in relation to colour variation due to solubilization of mordant ions, as well as loss of textile material, be it in weight or dimension, and efficacy by evaluating the amount of removal of external dirt particles. The comparison with the wet cleaning demonstrated that scCO₂ is a very safe solvent for cleaning very deteriorated silk textiles. As well as its safety as cleaning agent, CO₂ is considered a "green" solvent. Stricter regulation is pushing researchers to find modern environmental technologies and alternatives to perchloroethylene and other toxic organic

solvents generally used in dry cleaning, which is the only method that could also be applied to this case study. Studies have linked prolonged perchloroethylene exposure to liver or kidney damage, short-term contact can cause headaches, nausea, and irritation of the skin, eyes, nose and throat.²



Fig. 1 Virgin and Child, an 18th century sculpture from Palácio das Necessidades, Lisbon. Photo copyright: Portuguese Institute of Conservation and Restoration (IPCR), Department of Textiles Conservation.

^aDepartamento de Conservação e Restauro, Faculdade de Ciências e Tecnologia, Universidade Nova de Lisboa, 2829-516 Monte de Caparica, Portugal. E-mail: mjm@dq.fct.unl.pt

^bREQUIMTE/CQFB, Departamento de Química, Faculdade de Ciências e Tecnologia, Universidade Nova de Lisboa, 2829-516 Caparica, Portugal. E-mail: aar@dq.fct.unl.pt; Fax: +351 212 948 385; Tel: +351 21 2949648

† This paper was published as part of the special issue on Green Solvents for Processes.

Special concern must be taken to avoid the use of these hazardous substances by conservators and to minimize the emission of these compounds. ScCO₂ is considered a “green” alternative—CO₂ is non-flammable, relatively non-toxic and relatively inert—because after the extraction process it can be easily released as a gas simply by returning to atmospheric pressure and temperature conditions.³ Therefore, no toxic residues will be present in the extracted materials or in the extracted compounds. Furthermore, processes involving CO₂ as a solvent do not increase CO₂ emissions but reuse the waste CO₂ produced by other industries.

Supercritical CO₂ has already been tested and applied in conservation and restoration operations, such as cleaning, protection and consolidation. CO₂ has demonstrated a great potential in replacing current conventional processes used in the conservation and restoration of paper, wood, waterlogged, ethnographic materials, stone and textiles.^{4–8}

In this paper, we present the results obtained for the cleaning of scapulary samples from the 18th century religious garments from the Virgin and Child sculpture, with CO₂ at liquid and supercritical conditions with and without the use of co-solvents. Different sequences of cleaning extractions in continuous conditions were tested. The best cleaning procedure was established by analysis of loss of textile material, colour variation and dirt removal.

Experimental

Materials

The co-solvent isopropanol (IPA) was an analytical reagent puriss. P.A., purchased from Fluka Riedel-de-Haën. All reagents were used as received without further purification.

CO₂ was obtained from Air Liquide with 99.998% purity.

Characterization of textile samples

The silk textile samples from the sculpture Virgin and Child were collected from the scapulary of the Virgin (Fig. 2(a)). All the square samples used in the tests with co-solvents were cut in 1 cm² pieces from a bigger sample of the scapulary (7 cm × 5 cm, Fig. 2(b)). This bigger sample was separated from the scapulary just by simple handling, since the fibres are very weak and are at risk of disintegration.

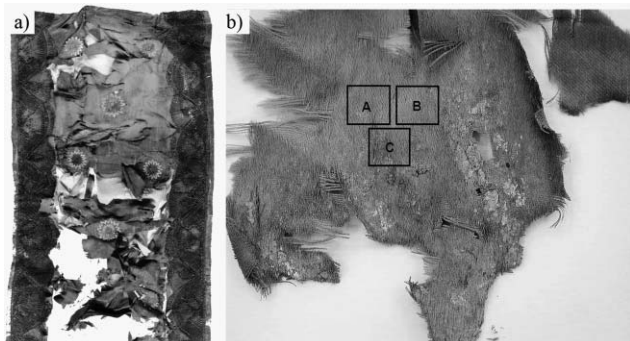


Fig. 2 (a) Detail of the Virgin and Child scapulary; (b) sample with 7 cm × 5 cm dimensions showing samples A, B and C of 1 cm².

The textile fibres were characterized through optical microscopy in longitudinal and cross sections and infrared spectroscopy as described in earlier work.¹ The scapulary samples were identified as silk *Bombyx mori*, and display a brownish colour with the following average colour coordinates: $L = 44.9 (\pm 1.43)$, $a^* = 4.9 (\pm 0.71)$ and $b^* = 13.8 (\pm 1.68)$.

In order to control physical losses, textile samples were weighed, before and after the dry-CO₂ cleaning procedures, in a Startorius Research balance with 0.00001 g accuracy.

Characterization of the dirt particles

The garments from the sculpture the Virgin and Child are an example of a silk textile heavily deteriorated and soiled. The silk fibres have lost their mechanical properties and are collapsing, with consequent loss of material. The presence of soil particles will catalyze the textile degradation, and therefore a cleaning operation will be the first step for a complete restoration of the garments. The dirt particles that were present in the fibres from the Virgin and Child were characterized by infrared spectroscopy whenever possible. The sampling of the soil particles was performed in 4 samples with *circa* 1 cm², and in a bigger sample of *circa* 7 × 10 cm; the particles were separated by colour and form. The results obtained were consistent and it was possible to conclude that the main exogenous compounds were calcium carbonate and calcium sulfate particles (see Fig. 3(a)), with dimensions between 10–20 μm. Other black particles, probably carbonaceous particles, of similar dimensions were present in lower amounts, but could not be analyzed as sampling was very difficult due to their loss of cohesion. Besides the above described particles, which are expected and common in air, large amounts of cellulose fibres, as small crusts, were also characterized since they could be removed physically. These crusts were most probably a result of contamination by the paper used for the storage protection of the sculpture, this was confirmed by comparing the infrared spectra of the crust and paper, which is shown in Fig. 3(b). Contrary to the airborne particles of gypsum and calcium carbonate, this soil was an unexpected contamination, which complicated the extraction of dirt particles with scCO₂.

CO₂-assisted cleaning experiments

The scapulary samples were cleaned in a laboratory scale apparatus shown schematically in Fig. 4, which is an improved version of the previous one described by Sousa *et al.*¹ The measurements were carried out in a visual 4.5 mL stainless steel cell equipped with two sapphire windows, which allows full visualization of the sample during the cleaning process. First the sample is carefully placed within a metallic support and introduced into the cell. The cell is then immersed in a thermostated water bath, and the system is pressurized with fresh CO₂ until the desired pressure is brought into the cell (approximately 20 MPa) using a Gilson liquid pump at a CO₂ flow rate of 0.98 g min^{−1}. Then a CO₂ (or a CO₂ + co-solvent stream) passes through the vessel with a flow rate of 1.5 mL min^{−1} for two hours. The co-solvent is introduced using a slave pump connected and controlled by the master pump. The solvent mass compositions used were:

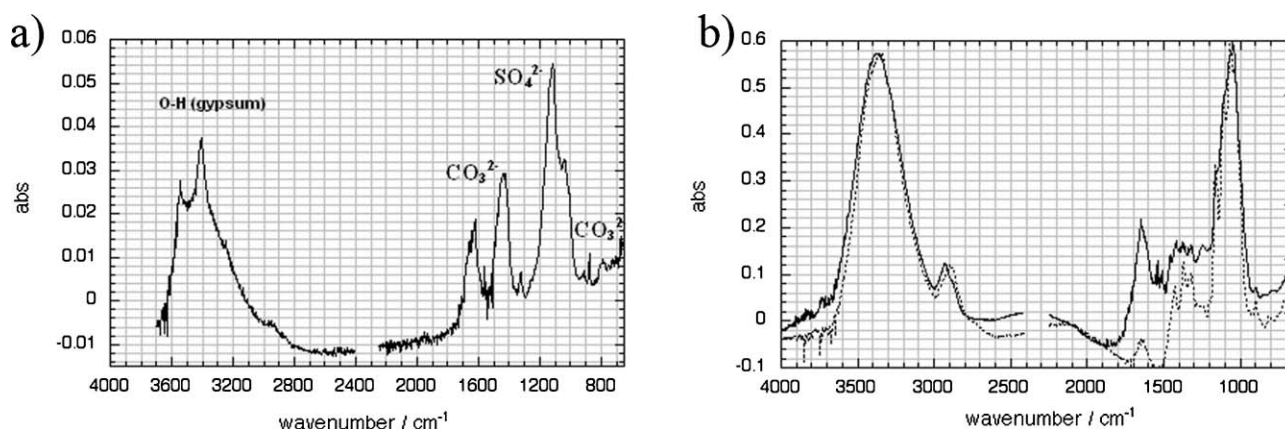


Fig. 3 (a) Infrared spectrum of soil particles where gypsum ($\text{CaSO}_4 \cdot 2\text{H}_2\text{O}$) and calcium carbonate are present; (b) representative infrared spectra for the whitish crust (full line) compares well with the spectra obtained for the paper used for storage protection (dotted line).

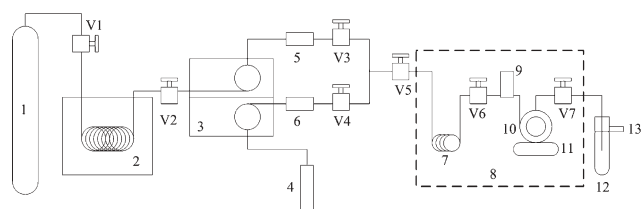


Fig. 4 Experimental cleaning apparatus: (1) CO_2 cylinder; (2) refrigeration unit; (3) high-pressure liquid pump, master and slave Gilson pumps; (4) co-solvent; (5) and (6) check-valves; (7) pre-heater; (8) thermostated bath; (9) pressure transducer; (10) high-pressure visual cell; (11) cell support; (12) trap; (13) vent; (V1) to (V7) high-pressure valves.

98.35% CO_2 + 1.65% isopropanol, 98.13% CO_2 + 1.64% isopropanol + 0.23% H_2O , and 97.83% CO_2 + 1.66% isopropanol + 0.51% H_2O . Experiments at supercritical conditions were conducted at 40 °C and 20 MPa, and 25 °C and 20 MPa when using liquid CO_2 . At the end of the experiment the samples were further cleaned with only CO_2 to remove traces of any co-solvent.

At the exit, the extract (co-solvents and residues) was collected by precipitation, due to the decompression, in a glass tube immersed in an ice bath.

Safety warning. These experiments involve high pressures and must only be carried out in an apparatus with the appropriate pressure rating at the dry-cleaning temperature. The technology involved needs to be operated by qualified high pressure engineers.

Optical microscopy

To ascertain the removal of the dirt particles, the samples were analyzed by Zeiss Axioplan Z Imaging optical microscopy with a Canon Power Shot G3 digital camera (Model PC1032), before and after the cleaning. The quantification of dirt particles extracted with the CO_2 cleaning was performed through digital image treatment using the program Paint Shop Pro. This program allows the measurement of the dirt particulate area before and after the cleaning in the photographs obtained with the optical microscope.

Micro Fourier transform infrared spectroscopy

Infrared spectra were acquired with a Nicolet Nexus spectrophotometer interfaced with a Continuum microscope, with a MCT-A detector cooled by liquid nitrogen. The spatial resolution is 30 μm . All the spectra presented were obtained in transmission mode, using a Thermo diamond anvil compression cell. The spectra were obtained in the range of 4000–650 cm^{-1} , with a resolution of 4 cm^{-1} and 128 scans. They are shown here as acquired, except for the removal of the CO_2 absorption at approx. 2300–2400 cm^{-1} .

Colourimeter

Colour determinations were made using a Datacolor International colourimeter. The optical system of the measuring head uses diffuse illumination from a pulsed Xenon lamp over a 8 mm diameter measuring area, with a 10° viewing angle geometry. The reference source was D65 and the calibration was performed with a bright white tile standard plate and with a black trap standard. With the aid of a positioning Melinex mask, the measuring head was positioned on the same area of each textile sample; for each determination of the L , a^* , b^* values, the mean value of six measurements was calculated.

Results and discussion

Table 1 summarizes the cleaning experiments undertaken with different solvent streams and includes the percentage of dirt extraction and corresponding weight loss of the three extensively soiled scapulary samples, shown in Fig. 2(b), named A, B and C.

The investigation of the best cleaning procedure with real sample tissue is always difficult, as a real sample can not be exactly duplicated. This is confirmed by the different extent of cleaning obtained with scCO_2 (entries 1 and 5, Table 1) for samples A and B.

In our previous work, scCO_2 was able to remove about 50–70% of usual dirt particles found in textiles. However, the tissue samples under study, A, B and C, were extensively dirty and the help of co-solvents was needed.

Table 1 Percentage of dirt particles extracted and loss in mass of the samples from the scapulary of Virgin and Child sculpture after cleaning with different streams

Entry	Sample	Cleaning stream composition ^a	Extracted dirt particles (%)	Δ weight (%)
1	A	scCO ₂	25	2
2	A	98.34% scCO ₂ + 1.66% IPA	–42	5
3	A	98.34% liquid CO ₂ + 1.66% IPA	10	2
4	A	98.13% liquid CO ₂ + 1.64% IPA + 0.23% H ₂ O	53	2
5	B	scCO ₂	35	2
6	B	Liquid CO ₂	53	3
7	C	97.83% liquid CO ₂ + 1.66% IPA + 0.51% H ₂ O	51	10

^a IPA = isopropanol

Sample A was first cleaned with scCO₂. This operation removed about 25% of the soiling without significant weight loss (entry 1, Table 1). The addition of isopropanol as a co-solvent to scCO₂ did not improve the efficiency of the cleaning of sample A, as can be seen from entry 2 of Table 1. In fact, it seems that the percentage of dirt increased. A possible explanation for this fact is the migration of dirt particles existing inside the fibres to the surface of the textile due to the high diffusivity of the scCO₂ + isopropanol stream. Sample B was also cleaned using scCO₂, which was able to remove 35% of dirt particles (entry 5, Table 1). This sample was then cleaned with liquid CO₂, this procedure had a significant impact on the cleaning, since more than 50% of dirt particles were extracted (entry 6, Table 1), as can be seen in Fig. 5(a) and (b). This can be explained by the higher density of the liquid CO₂ which allows a better removal of dirt particles at the textile surface.

Sample A was further treated with liquid CO₂ and isopropanol as a co-solvent (entry 3, Table 1). This cleaning stream was able to remove only 10% of the remaining dirt of the previous experiment. The addition of a small percentage of water as a co-solvent to the stream liquid CO₂ + isopropanol had a very positive influence on the removal of dirt particles of sample A (entry 4, Table 1). It was possible to remove more than 50% of remaining dirt particles that were strongly linked to the textile and were not extracted with the previous experiments (entries 1–3, Table 1), as can be seen in Fig. 6(a) and (b).

The variation in the water content, from 0.23% to 0.51%, in the solvent stream did not have an impact on the percentage of cleaning (entries 4 and 7, Table 1). However, the stream with the highest water content promoted the humidification of the textile to a considerable amount (entry 7, Table 1), and the physical losses increased to 10% instead of the usual 3%.

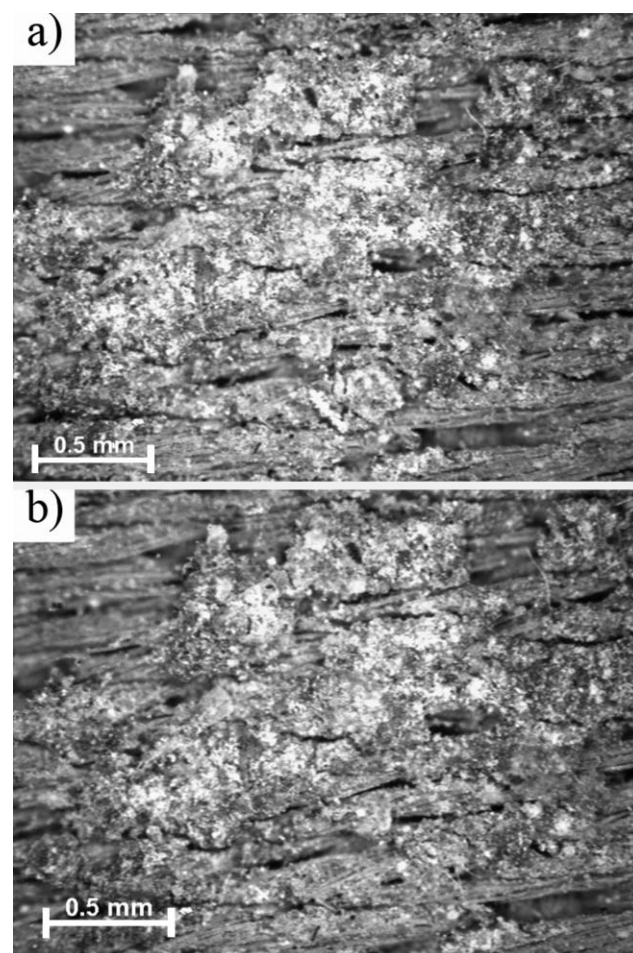
Only in the tests performed with liquid CO₂ + water + isopropanol as co-solvents did the luminosity of the textile samples decrease as a result of the extraction of white dirt particles. The other samples with cellulose crusts only showed colour variation within the experimental error. In all the tests performed, the hue did not significantly change, which means that the mordant were not extracted with the CO₂ cleaning and did not change the final colour of the textile.

Conclusions

The use of water as a co-solvent had a positive effect on the cleaning of the dirtier areas of the Virgin and Child's textiles.

The CO₂-assisted cleaning process did not physically damage the fibres nor their structure and did not promote the loss of material, which is an enormous advantage when cleaning textiles of historic or artistic value.

In this work, a two-step process was proposed to clean the textiles from the garments of the Virgin and Child. In the first step, the textile was cleaned with supercritical CO₂ which was able to remove about 50–70% of usual dirt particles found in textiles and 25–35% of dirt in the more extensively soiled areas. In the second extraction, the textile was cleaned with liquid CO₂, further removing approximately 50% of dirt particles from the more extensively soiled areas. The addition of

**Fig. 5** Image of textile sample B corresponding to entry 6 of Table 1: (a) before; (b) after cleaning.

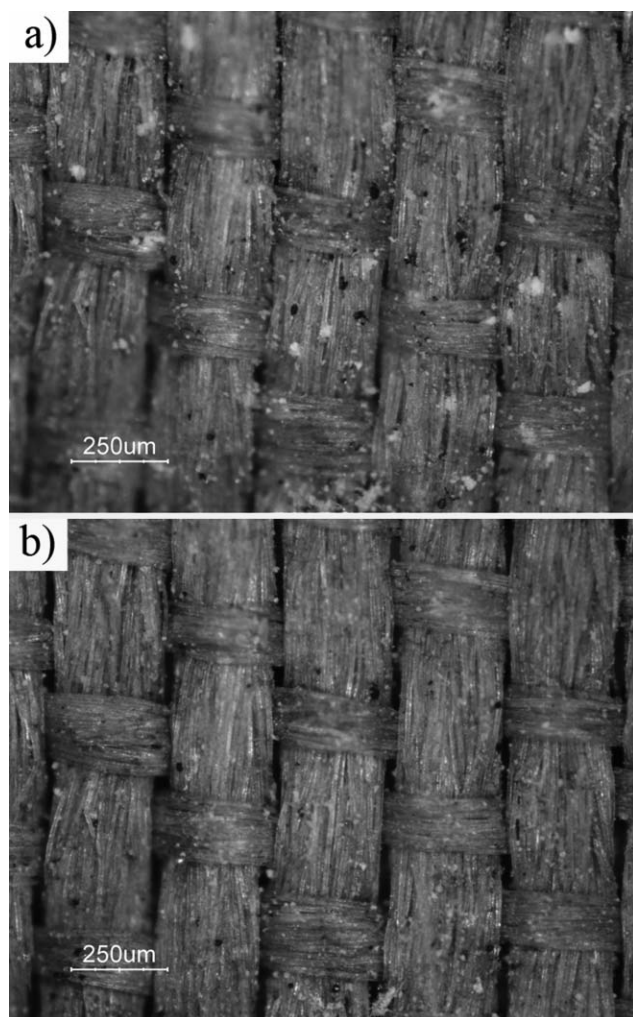


Fig. 6 Image of textile sample A corresponding to entry 4 of Table 1: (a) before; (b) after cleaning.

co-solvents (isopropanol and isopropanol + water) promoted the extraction of polar particles strongly attached to the textile,

such as carbonates and sulfates, removing another 20% of dirt. The addition of water was required for sufficient removal of dirt particles in areas of the textile where the amount of carbonaceous particles was probably higher.

It should be pointed out that other wet cleaning methods used in conservation and restoration of textiles cannot be applied to this case study because they can cause severe damage contrary to the CO₂ cleaning. The liquid and/or supercritical CO₂, either with or without the use of co-solvents, represents an enormous advantage for the cleaning of textiles of historic or artistic value, and allows the preservation of textile cultural heritage within the limits of disintegration. The technology involved needs experts and the cooperation between high pressure engineers and conservation scientists to make accessible further applications of supercritical technology on an appropriate scale.

Acknowledgements

We would like to thank the Portuguese Institute of Conservation and Restoration for the textile samples from the Virgin and Child sculpture.

References

- 1 M. Sousa, M. J. Melo, A. Aguiar-Ricardo and P. Cruz, A Green Approach to Antique Textile Cleaning, in *The 14th Triennial Meeting The Hague Preprints*, ed. A. B. Paterakis, ICOM Committee for Conservation, 2005, vol. 1, pp. 944–954.
- 2 Toxicological profile for tetrachloroethene, Agency for Toxic Substances and Disease Registry, United States Public Health Service, Atlanta, Georgia, January, 1990.
- 3 G. Brunner, *Gas Extraction. An Introduction to Fundamentals of Supercritical Fluids and their Application to Separation Processes*, Steinkopff Darmstadt, Springer, New York, 1994.
- 4 E. Selli, E. Lange, A. Mossa, G. Testa and A. Seves, *Macromol. Mater. Eng.*, 2000, **280**, 71.
- 5 B. Kaye, D. J. Cole-Hamilton and K. Morphet, *Stud. Conserv.*, 2000, **45**, 233.
- 6 F. E. Hénon, M. Camaiti, A. L. C. Burke, R. G. Carbonell, J. M. DeSimone and F. Piacenti, *J. Supercrit. Fluids*, 1999, **15**, 173.
- 7 A. Unger, *Focus Gas*, 2004, **22**, 20.
- 8 E. Jelen and A. Weber, *Pestic. Outlook*, 2003, **14**, 7.

Boron trifluoride catalyzed polymerisation of 2-substituted-2-oxazolines in supercritical carbon dioxide†‡

Carlota Veiga de Macedo, Mara Soares da Silva, Teresa Casimiro, Eurico J. Cabrita and Ana Aguiar-Ricardo*

Received 8th December 2006, Accepted 24th April 2007

First published as an Advance Article on the web 11th May 2007

DOI: 10.1039/b617940a

In the last few years there has been an intensive research on multifunctional polymers for therapeutical applications. Poly(2-substituted-2-oxazolines) are strong candidates for the development of new polymeric therapeutics. In this work, boron trifluoride etherate was used, for the first time, as initiator for the polymerisation of three substituted 2-oxazolines in supercritical carbon dioxide. The effect of temperature, pressure and initial monomer/initiator molar ratio on the yield, average molecular weight and polydispersity of the synthesized polymers was investigated. The products of the reaction were characterized by NMR, FT-IR and MALDI-TOF mass spectrometry. In all reactions, low molecular weight polymers were obtained in high yield with narrow molecular weight distribution. 2-Methyl- and 2-ethyl-2-oxazolines yielded water soluble products with degrees of polymerisation varying from 18 to 27 and 17 to 24, respectively, while poly(2-phenyl-2-oxazoline) was found to be insoluble in water and the degree of polymerisation varying from 10 to 12. In each polymerisation, there was an unexpected CO₂ insertion in 10–25% of the overall polymer. A possible explanation for this insertion is given.

Introduction

Carbon dioxide has been intensively investigated as a polymerisation reaction medium due to its environmentally benign characteristics, low cost, non-toxicity, non-flammability, density-dependent solvent strength, low critical temperature and moderate critical pressure.¹

The most studied polymerisations in supercritical CO₂ are those presenting a free-radical mechanism, which are, for example, the polymerisation of monomers, such as styrene and different methacrylates.^{2–5} Ionic polymerisations,⁶ such as ring opening polymerisations (ROP's),^{7–9} are less documented in the literature.

The 2-substituted-2-oxazolines are important monomers for the synthesis of polyethylenimine derivatives.¹⁰ A large range of macromolecular compounds can be synthesized (homopolymers, copolymers and functionalized polymers) due to the high versatility of the 2-substituted-2-oxazolines. The production of polymeric materials with a controlled architecture by the quenching of the living oxazolinium species with various nucleophiles has been extensively studied in the last few years.^{11–14} The name of “living” polymerisation was given by Szwarc because the polymeric chain ends remain active until a direct termination occurs.¹⁵

Oxazoline polymers have been widely used for a broad range of specific applications such as non-ionic polymer surfactants,

polymer networks, polymer composites, biorelated materials and optical-active polymers.¹⁶ 2-Alkyl-2-oxazolines, due to their low toxicity (LD50 > 4 g kg^{−1}) and high hydrophilicity, are also being used as controlled drug-delivery systems and in the hydrophilization of surfaces.¹⁷

The polymerisation chemistry of 2-oxazolines shows wide versatility depending on the nature of monomers, initiators, and terminating agents. These monomers can undergo facile ring-opening cationic polymerisation of a living nature¹⁶ or can participate in additional reactions with many electrophiles, such as in zwitterionic copolymerisations,¹⁸ and the coupling reactions of bis-oxazoline monomers.¹⁹ Well-defined degrees of polymerisation and low polydispersity are achieved with this living mechanism.¹⁷

The polymerisation of 2-phenyl-2-oxazoline in supercritical carbon dioxide using methyl trifluoromethanesulfonate as the initiator, has been previously reported.²⁰

In this work, boron trifluoride etherate (BF₃·OEt₂), a Lewis acid, is used for the first time as initiator in the polymerisation of three substituted 2-oxazolines in supercritical carbon dioxide. The effects of temperature, pressure and initial monomer/initiator ratio on the poly-2-substituted-2-oxazolines average molecular weight and polydispersity are studied.

Experimental

Materials and general methods

The monomers 2-ethyl-2-oxazoline (EtOx) and 2-phenyl-2-oxazoline (PhOx) as well as boron trifluoride etherate were purchased from Sigma–Aldrich. 2-Methyl-2-oxazoline (MeOx) was purchased from Fluka and carbon dioxide was supplied by Air Liquid with a purity of 99.998%. The monomers and the

REQUIMTE/CQFB, Departamento de Química, Faculdade de Ciências e Tecnologia, Universidade Nova de Lisboa, 2829-516, Caparica, Portugal. E-mail: aar@dq.fct.unl.pt; Fax: +351 212 948 385; Tel: +351 21 2949648

† This paper was published as part of the special issue on Green Solvents for Processes.

‡ Electronic supplementary information (ESI) available: Determination of molecular weight distributions. See DOI: 10.1039/b617940a

initiator ($\text{BF}_3 \cdot \text{OEt}_2$) were freshly distilled prior to use. All distillations were carried out under argon atmosphere.

The infrared spectra were obtained by microspectrophotometry in a FT-IR "Nicolet Nexus" equipment with a microscope "Continuum" with a diamond cell.

All NMR spectra reported were acquired in a Bruker ARX 400 spectrometer in methanol- d_4 .

The MALDI-TOF mass spectrometry was performed on a AUTOFLEX Bruker apparatus using dithranol (1,8,9-anthracenetriol) as the matrix for poly-2-phenyl-2-oxazoline (PPhOx) and DHB (2,5-dihydroxybenzoic acid) for 2-methyl and 2-ethyl-2-oxazoline polymers (PMeOx and PEtOx, respectively). The samples were prepared by mixing methanol solutions of the polymer (10^{-4} M) and matrix in a typical ratio 1 : 1 (v/v). All the polymer analyses were carried out at the Associated Laboratory of REQUIMTE.

Polymerisation reaction

A typical procedure for the polymerisation is as follows (example to prepare poly(2-ethyl-2-oxazoline)): polymerisation reactions are carried out in a 11 mL stainless-steel reactor equipped with two aligned sapphire windows (Fig. 1). EtOx (1.94 g, 19.6 mmol) is charged into the reactor, which is then placed inside a thermostatted bath. A water bath is used for temperatures up to 60 °C, while for higher temperatures an oil bath is used. After the required temperature is attained, freshly distilled $\text{BF}_3 \cdot \text{OEt}_2$ (200 μL , 1.58 mmol) is introduced in the reactor through a six port switching HPLC valve. Carbon dioxide is then introduced into the reactor until the desired pressure is achieved. After 24 h the pressure is slowly released and the reactor is cooled to room temperature. The crude product obtained, a yellow viscous foam, is then recovered from the cell and poured into methanol for termination of the living polymer. The final polymer is obtained upon recrystallization using methanol and diethyl ether and subsequently

dried in vacuum. Alternatively the termination of the living polymer can be carried out directly with water. A typical procedure is the following: at the end of the polymerisation reaction, the pressure is decreased to 4 MPa and an excess of water (a tenfold excess with relation to the amount of initiator) is added to the crude product using a high-pressure HPLC valve. The mixture was kept at 60 °C, under stirring, during the reaction time. After depressurization of the cell the crude product is recovered and purified, as stated previously.

The polymerisation reactions of 2-methyl and 2-ethyl-2-oxazolines yielded water soluble products while poly(2-phenyl-oxazoline) was found to be insoluble in water. The products of the polymerisation reaction were characterised using NMR, FT-IR and MALDI-TOF MS. These techniques were able to determine molecular weights, chain terminators and CO_2 insertion. In all reactions low molecular weight polymers were obtained. The degrees of polymerisation varied from $n = 18$ –27 for PMeOx, from $n = 17$ –24 for PEtOx and $n = 10$ –12 for PPhOx. The last two are probably best described as oligomers. The results concerning M_n and polydispersion index (PDI) are summarized in Tables 1–3.

Poly-2-methyl-2-oxazoline (PMeOx): $\nu_{\text{max}}/\text{cm}^{-1}$ 1745 (HO(C=O)N–), 1643 (Me(C=O)N–); $^1\text{H-NMR}$, ppm (400 MHz, CD_3OD) $\delta = 2.1$ (Me), 3.5 (CH_2).

Poly-2-ethyl-2-oxazoline (PEtOx): $\nu_{\text{max}}/\text{cm}^{-1}$ 1743 (HO(C=O)N–), 1639 (Me(C=O)N–); $^1\text{H-NMR}$, ppm (400 MHz, CD_3OD) $\delta = 1.1$ (Me), 2.4 ($\text{CH}_2\text{-CO}$), 3.5 (CH_2).

Poly-2-phenyl-2-oxazoline (PPhOx): $\nu_{\text{max}}/\text{cm}^{-1}$ 1725 (HO(C=O)N–), 1631 (Me(C=O)N–); $^1\text{H-NMR}$, ppm (400 MHz, MeOD) $\delta = 3.5$ (CH_2), 7.1–8.1 (Ph).

Results and discussion

The polymerisation of 2-substituted-2-oxazolines using $\text{BF}_3 \cdot \text{OEt}_2$ as initiator was successfully carried out in supercritical carbon dioxide. The reactions were carried out at pressures from 10 up to 21 MPa and at temperatures between 40 and 90 °C. A study of the effect of three experimental conditions, temperature, pressure and monomer/initiator ratio, upon the average molecular weight and polydispersity of the synthesized polymers was undertaken. Tables 1, 2 and 3 show the results obtained in the polymerisation of MeOx, EtOx and PhOx monomers respectively. High yields, over 80%, were obtained for all the experimental conditions, except at 40 °C where yields from 6–40% were obtained.

The polymers presented a yellowish colour at temperatures above 60 °C, possibly due to side reactions.²¹

One of the most unexpected results of this study was the fact that CO_2 insertion occurred in part of the oxazoline polymers. This CO_2 insertion was confirmed with the combination of FT-IR and MALDI-TOF MS techniques. Fig. 2 shows the FT-IR spectrum of a PEtOx sample corresponding to entry 15 of Table 2. In this spectrum, besides the amide carbonyl (1639 cm^{-1}) there is also an absorption peak at 1743 cm^{-1} which was assigned to the stretching vibration of the carbonyl (C=O) in a carbamic acid, which confirms the CO_2 insertion into the polymer. This absorption was found in the FT-IR spectra of all polymers. Fig. 3 shows the characteristic MALDI-TOF mass spectra of each type of synthesized

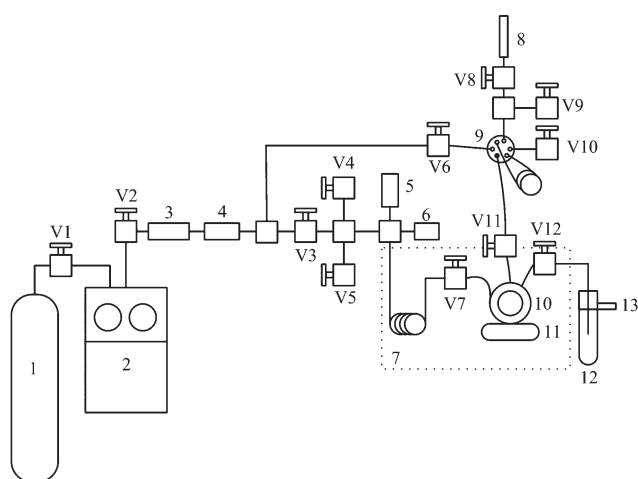


Fig. 1 Schematic representation of the experimental apparatus. 1– CO_2 cylinder; 2–high-pressure pump; 3–line filter; 4–check-valve; 5–high-pressure transducer; 6–rupture disc; 7–thermostatted bath; 8–syringe; 9–HPLC high-pressure valve; 10–high pressure visual cell; 11–immersible stirrer; 12–schlenk; 13–vent; V1 to V12–HIP high-pressure valves; V4 and V5–gas inlet (argon or nitrogen) or vacuum exit; V9–vacuum exit.

Table 1 Effect of temperature, pressure and monomer/initiator ratio in the polymerisation reaction of 2-methyl-2-oxazoline in scCO₂

Entry	Monomer ^a	T/°C	p/MPa	[M]/[I]	Yield (%) ^b	M _n ^c /Da	M _w /M _n ^c	CO ₂ ^d (%)	M _n ^e /Da	M _w /M _n ^e
1	MeOx	40	15	15	42	1500	1.3	26	1499	1.3
2	MeOx	50	15	15	39	1599	1.3	15	1793	1.4
3	MeOx	60	16	15	94	1823	1.4	23	1945	1.4
4	MeOx	70	16	15	93	1819	1.4	25	1857	1.3
5	MeOx	80	17	15	92	2309	1.4	22	2336	1.4
6	MeOx	90	17	15	99	2254	1.4	20	2348	1.4
7	MeOx	60	11	15	76	1816	1.5	27	1775	1.5
3	MeOx	60	16	15	94	1823	1.4	23	1945	1.4
8	MeOx	60	20	15	80	1568	1.3	18	1671	1.3
3	MeOx	60	16	15	94	1823	1.4	23	1945	1.4
9	MeOx	60	16	20	85	1991	1.4	19	2216	1.3
10	MeOx	60	17	30	81	1873	1.4	23	1957	1.3
11	MeOx	60	16	59	57	1841	1.4	23	1924	1.4

^a Reactions were carried out in an 11 mL cell. 23 mmol of monomer were used in all entries. ^b Determined after isolation and recrystallization.^c Molecular weight and polydispersity (M_w/M_n) of the polymer without CO₂ insertion as determined from the MALDI-TOF spectra;^d Percentage of polymer with insertion of CO₂ determined from the MALDI-TOF spectra; ^e Molecular weight and polydispersity (M_w/M_n) of the polymer with CO₂ insertion as determined from the MALDI-TOF spectra.**Table 2** Effect of temperature, pressure and monomer/initiator ratio in the polymerisation reaction of 2-ethyl-2-oxazoline in scCO₂

Entry	Monomer ^a	T/°C	p/MPa	[M]/[I]	Yield (%) ^b	M _n ^c /Da	M _w /M _n ^c	CO ₂ ^d (%)	M _n ^e /Da	M _w /M _n ^e
12	EtOx	40	16	12	11	1790	1.3	27	1729	1.2
13	EtOx	50	16	12	78	1886	1.4	23	1784	1.4
14	EtOx	60	16	12	90	1717	1.5	28	1531	1.5
15	EtOx	70	17	12	94	1911	1.4	25	1811	1.4
16	EtOx	80	16	12	84	1659	1.4	16	1753	1.4
17	EtOx	90	17	12	74	1830	1.3	27	1741	1.3
18	EtOx	70	11	12	63	2282	1.3	24	2371	1.2
15	EtOx	70	17	12	94	1911	1.4	25	1811	1.4
19	EtOx	70	21	12	97	2118	1.3	22	2222	1.2
15	EtOx	70	17	12	94	1911	1.4	25	1811	1.4
20	EtOx	70	17	17	78	2104	1.4	25	2113	1.3
21	EtOx	70	16	25	90	2369	1.4	22	2442	1.4
22	EtOx	70	16	50	94	2222	1.3	25	2249	1.3

^a Reactions were carried out in an 11 mL cell. 23 mmol of monomer were used in all entries. ^b Determined after isolation and recrystallization.^c Molecular weight and polydispersity (M_w/M_n) of the polymer without CO₂ insertion as determined from the MALDI-TOF spectra.^d Percentage of polymer with insertion of CO₂ determined from the MALDI-TOF spectra. ^e Molecular weight and polydispersity (M_w/M_n) of the polymer with CO₂ insertion as determined from the MALDI-TOF spectra.**Table 3** Effect of temperature, pressure and monomer/initiator ratio in the polymerisation reaction of 2-phenyl-2-oxazoline in scCO₂

Entry	Monomer ^a	T/°C	p/MPa	[M]/[I]	Yield (%) ^b	M _n ^c /Da	M _w /M _n ^c	CO ₂ ^d (%)	M _n ^e /Da	M _w /M _n ^e
23	PhOx	40	17	10	6	1400	1.5	10	1592	1.4
24	PhOx	50	16	10	73	1584	1.4	11	1675	1.4
25	PhOx	60	15	10	95	1528	1.3	12	1594	1.3
26	PhOx	70	16	10	99	1684	1.4	13	1702	1.4
27	PhOx	80	16	10	99	1697	1.4	13	1743	1.4
28	PhOx	90	16	10	87	1814	1.3	13	1812	1.3
29	PhOx	60	11	10	96	1418	1.4	14	1370	1.4
25	PhOx	60	15	10	95	1528	1.3	12	1594	1.3
30	PhOx	60	20	10	99	1527	1.3	5	1842	1.5
25	PhOx	60	16	10	95	1528	1.3	12	1594	1.3
31	PhOx	60	17	13	83	1498	1.4	14	1471	1.4
32	PhOx	60	16	19	99	1746	1.3	16	1696	1.3
33	PhOx	60	15	38	80	1691	1.4	19	1629	1.3

^a Reactions were carried out in an 11 mL cell. 23 mmol of monomer were used in all entries. ^b Determined after isolation and recrystallization.^c Molecular weight and polydispersity (M_w/M_n) of the polymer without CO₂ insertion as determined from the MALDI-TOF spectra.^d Percentage of polymer with insertion of CO₂ determined from the MALDI-TOF spectra. ^e Molecular weight and polydispersity (M_w/M_n) of the polymer with CO₂ insertion as determined from the MALDI-TOF spectra.

polymer. The produced polymers contain two fractions, which present similar average molecular weights and molecular weight distributions. Analysis of the MALDI-TOF mass spectra of the polymer mixtures revealed that one distribution is

associated with a water terminated polymer chain in which a single CO₂ molecule was incorporated. To the best of our knowledge, this is the first report of CO₂ insertion in the polymerisation reaction of 2-substituted-2-oxazoline monomers.

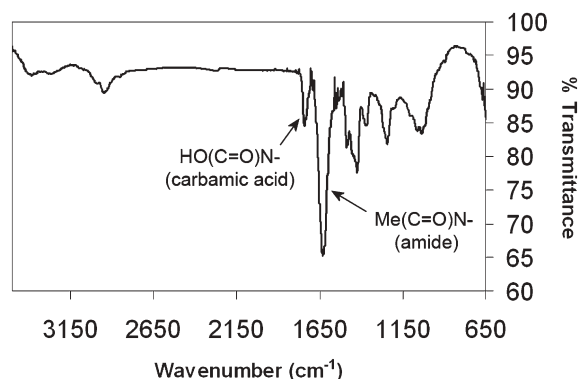


Fig. 2 FT-IR spectrum of poly(2-ethyl-2-oxazoline) at 70 °C and 16 MPa.

Polymerisation of substituted oxazolines is typically performed using polar solvents, such as acetonitrile, dichlorobenzene and nitrobenzene. The polymerisation is initiated by a strong electrophile (usually an alkyl, aryl halide or a tosylate), which is attacked by the endocyclic nitrogen of the oxazoline to form an oxazolinium ring. The C–O bond of the oxazolinium ring is weakened and the propagation occurs by the nucleophilic attack of the next monomer to this carbon atom. Two types of propagation routes have been identified based on ionic or covalent active species, depending upon reaction conditions and counterion structure. However, it was demonstrated that even though both ionic and covalent active species are present, the polymerisation depends almost exclusively on the cationic species.²²

When using a Lewis acid, such as $\text{BF}_3 \cdot \text{OEt}_2$, as initiator, there will be no covalent active species, and in principle the only active species in the propagation step are the cationic oxazolinium. In this work, this active species is terminated with the attack of water. Concerning the CO_2 insertion, a plausible mechanism would be the nucleophilic attack of the nitrogen atom to a CO_2 molecule at the beginning of the polymer chain, as is shown in Scheme 1. The available experimental data does not allow us to determine exactly in which stage of the reaction the CO_2 insertion occurs. However, we believe that this should happen right after the first propagation step, *i.e.* after the oxazoline ring activation by the BF_3 complexation (initiation) and after the attack of another oxazoline to the carbon atom of the activated ring. The exchange of complexed BF_3 by covalently bound CO_2 in the first propagation step may have a stabilizing effect of the oxazolinium due to an interaction between the oxazolinium ring of the living end and the carboxylate group (Scheme 1). This stabilizing effect should be more pronounced for oxazolines bearing substituents in position 2 which are less effective in the stabilization of the positive charge, like methyl or ethyl, and less important for the 2-phenyl substituted ring, since in this case there is an effective stabilization of the positive charge by the aromatic ring. This mechanism is compatible with different observable relative ratios of CO_2 incorporation for each monomer.

The results of the average molecular weight and polydispersity of the synthesized polymers, corresponding to the fractions with and without CO_2 insertion, are presented in

Tables 1, 2 and 3. It is possible to observe that all the synthesized polymers were obtained with low average molecular weights and narrow polydispersity. This result is not surprising considering the low molecular weight distributions obtained (average chain length of n units). In addition, it is evident that these polymer characteristics are not greatly influenced by the studied reaction conditions of temperature and pressure or the monomer/initiator ratio.

In spite of this general behaviour, an evident increase in the molecular weight of the polymers was observed by increasing temperature, as can be seen from entries 1 to 6 in Table 1, entries 12 to 17 in Table 2 and entries 23 to 28 in Table 3, respectively for PMeOx, PEtOx and PPhOx. This trend was expected, since by increasing the temperature more energy is brought to the system and consequently this should speed up the reaction, leading to higher molecular weights.

Increasing pressure from 10 up to 21 MPa had no influence upon the molecular weight of the synthesized polymers. The acceleration of the polymerisation reactions with increasing pressure is typically observed due to the negative volume activation. Usually this effect is only noticeable at very high pressures, above 100 MPa.²⁰

By lowering the monomer/initiator ratio, keeping the percentage of monomer in relation to carbon dioxide constant, there were no significant changes in the average molecular weight of the polymers. This result was unexpected since usually the molecular weight increases with increasing the monomer/initiator ratio. Only a full kinetic study can explain the observed dependence of the polymer average molecular weight and polydispersity with pressure, temperature and monomer/initiator ratio, which is related with the stability of the initiation group and the propagation kinetics.

Concerning the percentage of CO_2 insertion into the polymers, a significant difference between the phenyl and the alkyl-based polymers was obtained. While 10% of the polymers with the PhOx monomer present CO_2 insertion, the polymers synthesized with the alkyl monomers, MeOx and EtOx, present a much higher percentage, around 25%. This percentage is essentially the same for all the experimental conditions. This difference in the CO_2 initiated polymer fraction may be due to the different nature of the substituents in position 2 of the three monomers, as was suggested above. When the first cationic ring is attacked, the change of BF_3 by a CO_2 molecule will have a charge stabilizing effect in the oxazolinium (see Scheme 1). After the initiation step, the phenyl group will have a higher stabilizing effect of the cation active species than the alkyl groups, thus explaining the lower CO_2 insertion ratio in the PPhOx.

Conclusions

It was demonstrated that the polymerisation of 2-substituted-2-oxazoline can be successfully performed in supercritical CO_2 , as an alternative to conventional organic solvents, using BF_3 etherate as initiator. Low molecular weight polymers are obtained in high yield and low polydispersity. The characterization of the polymers by MALDI-TOF and FT-IR shows that in all reactions a fraction of the polymer chains had CO_2 insertion, giving rise to a polymer with a carboxylate end

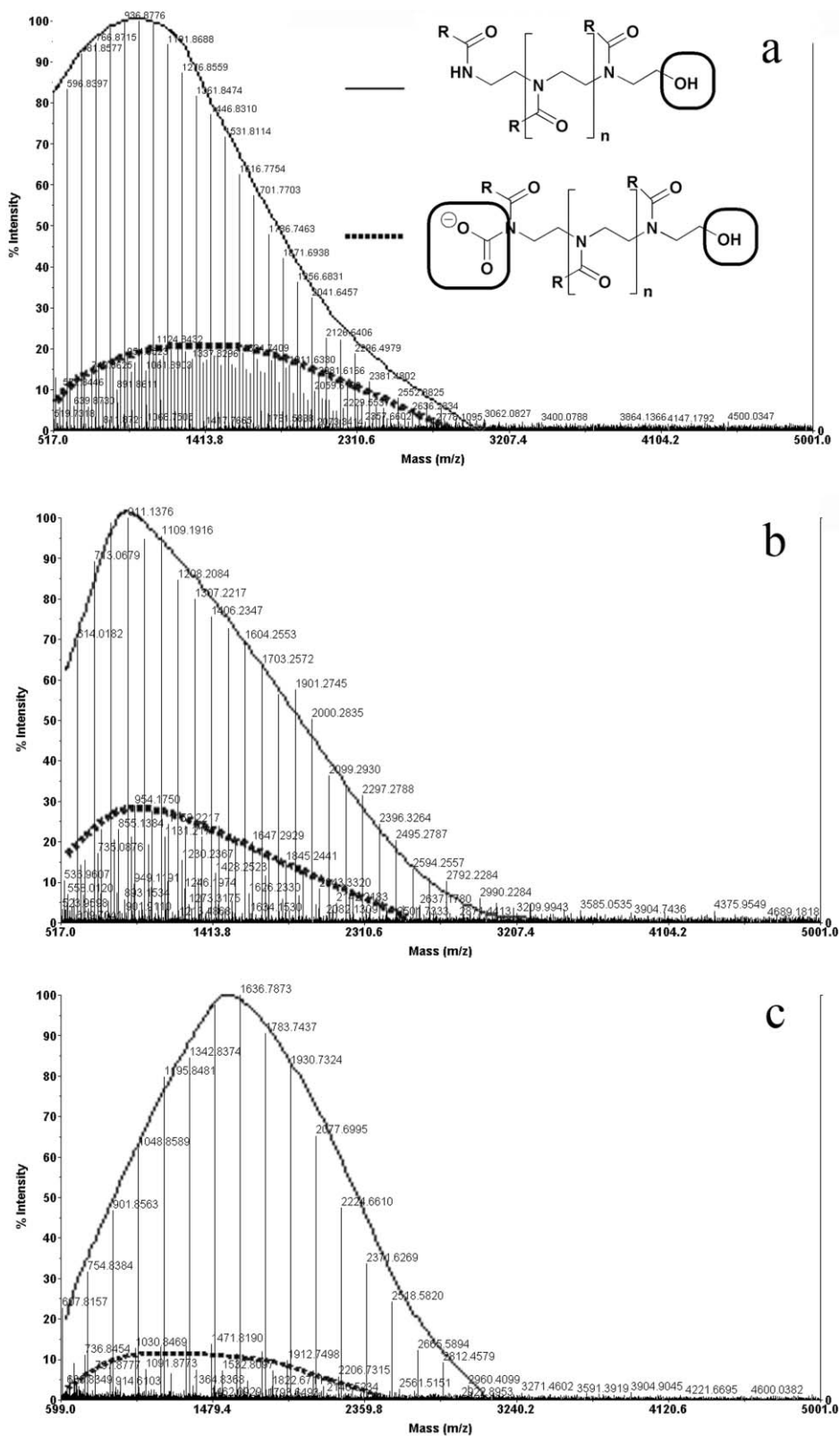
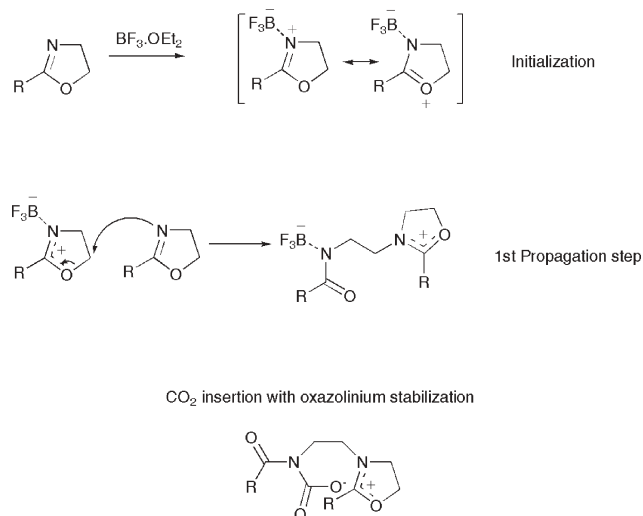


Fig. 3 MALDI-TOF mass spectra of (a) poly(2-methyl-2-oxazoline) (M_n : 1819), having degrees of polymerization of 18–27, acquired using DHB as the matrix; (b) poly(2-ethyl-2-oxazoline) (M_n : 1911), having degrees of polymerization of 17–24, acquired using DHB as the matrix; (c) poly(2-phenyl-2-oxazoline) (M_n : 1814), having degrees of polymerization of 10–12, acquired using dithranol as the matrix. Two different distributions are shown: (—) polymer chains without CO_2 insertion; (···) polymer chains with CO_2 insertion.



Scheme 1 Oxazolinium stabilization after CO₂ insertion.

group. The percentage of carboxylate ended polymer seems to be related to the structure of the monomer. Further kinetic studies are being performed in order to elucidate the mechanism of CO₂ insertion and the optimization of the experimental conditions in order to obtain a fully CO₂ inserted polymer.

Acknowledgements

The authors thank the financial support from Fundação para a Ciência e Tecnologia (FCT-Lisbon) through contract SFRH/BD/19055/2004, FEDER and FSE.

References

- 1 S. G. Kazarian, *Polym. Sci. Ser. C*, 2000, **42**(1), 78.
- 2 C. Lepilleur and E. J. Beckman, *Macromolecules*, 1997, **30**(4), 745.
- 3 D. A. Canelas, D. E. Betts and J. M. DeSimone, *Macromolecules*, 1996, **29**(8), 2818.
- 4 M. R. Giles, R. M. T. Griffiths, A. Aguiar-Ricardo, M. M. C. G. Silva and S. M. Howdle, *Macromolecules*, 2001, **34**(1), 20.
- 5 T. Casimiro, A. M. Banet-Osuna, A. M. Ramos, M. Nunes da Ponte and A. Aguiar-Ricardo, *Eur. Polym. J.*, 2005, **41**, 1947.
- 6 A. I. Cooper, *J. Mater. Chem.*, 2000, **10**, 207.
- 7 M. R. Clark and J. M. DeSimone, *Macromolecules*, 1995, **28**, 3002.
- 8 F. Stassin, O. Halleux and R. Jérôme, *Macromolecules*, 2001, **34**(4), 775.
- 9 D. D. Hile and M. V. Pishko, *Macromol. Rapid Commun.*, 1999, **20**, 511.
- 10 S. Kobayashi and H. Uyama, *Trends Macromol Res*, 1994, **1**, 121.
- 11 G. David, V. Alupeu and B. C. Simionescu, *Eur. Polym. J.*, 2001, **37**, 1353.
- 12 B. M. Culbertson, *J. Dentistry*, 2006, **34**(8), 556.
- 13 G. H. Hsiue, C. H. Wang, C. L. Lo, C. H. Wang, J. P. Li and J. L. Yang, *Int. J. Pharm.*, 2006, **317**(1), 69.
- 14 O. Nuyken, R. Weberskirch, M. Bortenschlager and D. Schonfelder, *Macromol. Symp.*, 2004, **215**, 215.
- 15 M. Szwarc, M. Levy and R. Milkovich, *J. Am. Chem. Soc.*, 1956, **78**, 2656.
- 16 K. Aoi and M. Okada, *Prog Polym Sci*, 1996, **21**, 151–208.
- 17 M. Einzmann and W. H. Binder, *J. Polym. Sci., Part A: Polym Chem.*, 2001, **39**, 2821.
- 18 R. Nomura, Y. Shintaku and T. Masuda, *Polym. J.*, 2000, **32**(10), 904.
- 19 Y. Chalamet and M. Taha, *J. Polym. Sci., Part A: Polym. Chem.*, 1997, **35**(17), 3697.
- 20 A. F. Mingotaud, F. Dargelas and F. Cansell, *Macromol. Symp.*, 2000, **153**, 77.
- 21 R. Hoogenboom, M. W. M. Fijten, C. Brändli, J. Schroer and U. S. Schubert, *Macromol. Rapid Commun.*, 2003, **24**, 98.
- 22 A. Dworak, *Macromol. Chem. Phys.*, 1998, **199**, 1843.

Biocatalysis in non-conventional media—ionic liquids, supercritical fluids and the gas phase†

Sara Cantone,^a Ulf Hanefeld^b and Alessandra Basso^{*a}

Received 2nd January 2007, Accepted 12th April 2007

First published as an Advance Article on the web 10th May 2007

DOI: 10.1039/b618893a

During the last decades much attention has been paid, by both academia and industry, to the development of new solvents. The introduction of ILs, sc-fluids and solid–gas interphase reactions has definitely opened new perspectives. ILs have been introduced into organic chemistry to meet the increasing demand for clean technologies in industrial processes. However, the toxicology of ILs remains unclear and further studies are necessary to assess their sustainability. Use of supercritical fluids is already a mature technique and their power lies less in their number but more in the variety of characteristics that one sc-fluid can have depending on the pressure. Enzyme-catalysed reactions at the solid–gas interphase have undergone a rapid development, and this will definitely find a place in the production of high value added compounds, such as fragrances.

1. Introduction

Enzymes are versatile catalysts that can accelerate a huge variety of reactions under a wide range of conditions. For a

long period it was thought that enzymes should be restricted to their natural environment: diluted aqueous reaction media at normal pressure and ambient temperatures. Indeed, industrially, enzymes were first employed only for hydrolytic processes. With an increase of the range of enzyme applications the aqueous medium became limiting. Several decades ago the application of enzymes in organic solvents was pioneered by Klibanov and today water and organic solvents are conventional media for enzymes.^{1–3} Temperature and pressure can be rather extreme (e.g. thermophilic enzymes from archeobacteria) and, what at the beginning sounded quite unexpected, enzymes can work under these

^aLaboratory of Applied and Computational Biocatalysis, Dipartimento di Scienze Farmaceutiche, Università degli Studi, Piazzale Europa 1, 34127 Trieste, Italy. E-mail: basso@units.it; Fax: (+39) 04052572; Tel: (+39) 0405583110

^bGebouw voor Scheikunde, Technische Universiteit Delft, Julianalaan 136, 2628 BL Delft, The Netherlands. E-mail: u.hanefeld@tudelft.nl; Fax: (+31)-(0)15-278-1415

† Dedicated to Prof. Paolo Linda, an inspiring scientist, on the occasion of his retirement.



Ulf Hanefeld

Ulf Hanefeld was born in 1966 in Köln, Germany, and grew up in then West-Berlin and London. In 1993 he received his PhD from the Georg-August-Universität zu Göttingen, Germany, having performed the research both in Göttingen (Prof. H. Laatsch) and Seattle, WA, USA (Prof. H. G. Floss). After many post-doctoral years with Prof. C. W. Rees at Imperial College London, UK, Prof. J. Staunton in Cambridge, UK and Prof. J. J. Heijnen and Dr A. J. J. Straathof in Delft, the

Netherlands, he received a research fellowship for five years from the Royal Netherlands Academy of Arts and Sciences (KNAW). He is an academic staff member of the Technische Universiteit Delft in the Netherlands. His research focuses on enzymes in organic synthesis and heterogeneous catalysis. In 2005 he enjoyed a sabbatical stay at the Dipartimento di Scienze Farmaceutiche, Università degli Studi Trieste. Stunning views of the Adriatic Sea and scientific discussions during the coffee breaks formed the stimulating environment in which the basis for this review was laid.



Alessandra Basso

Alessandra Basso was born in 1973, and in 1998 received her Laurea degree in Pharmaceutical Chemistry and Technology at the University of Trieste under the supervision of Professor Paolo Linda. In 2001 she received her PhD in Chemical Sciences at the University of Trieste. During her post-doc she was involved in a European Project on solid phase biocatalysis, and in 2003 she joined the group of Prof. S. Flitch for a post-doc

position. From 2004 she has been an associate researcher in the group of Prof. L. Gardossi at the University of Trieste. Her scientific interests are focused on biocatalysis in non-conventional media, on techniques of enzyme immobilisation and stabilisation and also on solid phase chemistry, with particular attention to the rational understanding of diffusion phenomena inside polymers.

“non-natural” conditions even better than under the “natural” conditions.⁴

Developments in genomics, directed evolution and the exploitation of biodiversity have led to improvements in the stability, economy, specificity and overall potential applicability of enzymes, and it is not surprising that the number of commercial applications for enzymes is increasing every year.^{5,6}

Biocatalysis in organic solvents has been a major area of research over the last two decades and is going to enjoy the same status for the next decades due to many advantages associated with it. The first examples of biocatalysis in organic solvents actually date back to the end of the nineteenth century, when the experiments were done in the presence of non-water miscible solvents, such as toluene, in order to prove the reversibility of the catalytic reaction.^{7,8}

In the 1930s, Ernest Alexander Sym published ground breaking work on the activity of pancreatic-lipase preparations in organic solvents, finding a correlation between the equilibrium position and the water concentration of the system.^{9,10} However, despite the rational and modern approach of his studies it is surprising that biocatalysis in organic solvent did not “take off” until the 1980s.¹¹

The biocatalysis community waited almost 50 years before it confirmed that the use of organic solvent is not only feasible, but also that in such seemingly hostile environments enzymes become more stable. In addition, this allowed improved solubility of water insoluble organic compounds, suppressed unwanted hydrolytic side reactions, eased product recovery and shifted the unfavoured thermodynamic equilibria of aqueous reaction media.¹²

An essential understanding of the behaviour of enzymes in organic solvents came from the studies of Halling on the water activity, a crucial parameter for determining the correct degree of hydration of enzymes in non-aqueous media.¹³ Lipases, proteases, hydrolases and many other enzymes work efficiently in organic solvents containing little or no water. To perform at its best, each enzyme requires an optimal degree of hydration that is guaranteed by working at controlled water activity (a_w).¹⁴ However, the control of a_w is not the only parameter

determining the activity of enzymes in organic solvents. Enzymes work well in water and in relatively non-polar organic solvents ($\log P > 2$), those that do not mix with water. These hydrophobic solvents do not strip the crucial water from the enzyme surface,^{15–17} while hydrophilic organic solvents ($\log P < 2$) remove this water leading to protein unfolding.¹⁸ Consequently the catalytic activity of enzymes in water miscible solvent systems is often much lower than activities in aqueous solutions.^{19–22}

This means that enzymes work well in relatively apolar solvents and in water, but not in polar and protic solvents. Consequently a large gap in the solubility for enzyme-catalysed reactions is left.

During the last decades much attention has been paid, by both academia and industry, to the development of new solvents that are environmentally friendly. Following a series of green principles,^{5,23} they should be environmentally benign, less hazardous and help to improve industrial processes. Two new classes of solvents seem to fulfil these criteria. These non-conventional solvents are ionic liquids (ILs) and supercritical fluids (sc-fluids). They would both exactly fill the gap in solubility for enzyme-catalysed reactions that is left open between conventional solvents and water.

ILs have been introduced into organic chemistry to meet the increasing demand for clean technologies in industrial processes.^{24–26} They can be considered as the ideal tailor-made solvents due to the possibility of modifying the anions or the cations that compose these liquid salts. Due to their virtually absent vapour pressure, ILs have been waved, in the last years, as the green solvents *par excellence* that, in the future, could substitute the toxic and flammable organic solvents.²⁷ Up to now, however, a quite innocent use of these “environmentally friendly” solvents can be observed. In the light of preliminary studies,^{28–30} the toxicology of ILs remains unclear, and further studies are necessary to assess their sustainability. With a green vision of the overall process it is essential to recycle ILs and to avoid the use of organic solvents to recover products from the IL at the end of it.

The combination of ILs with supercritical fluids can be a good strategy to circumvent the use of organic solvents to recover solutes.³¹ Thanks to the high solubility of sc-fluids in the ILs,^{32–35} the mass transfer of solutes is increased, and it is possible to couple (bio)transformations in ILs with extraction by sc-fluids.

2. Biocatalysis in ionic liquids

The first assays of biocatalysed reactions in these unusual media were remarkably successful, showing that enzymes not only tolerate these solvents, but, indeed, that they are also stable and the activity is comparable or even better than in organic solvents.³⁶ Starting from these preliminary studies the number of papers in this field has increased spectacularly and several reviews on the topic are now available.^{37–41} However, so far most studies are of an exploratory nature. The relationships between the structure of the IL and the activity or stability of the enzyme is not yet clearly understood. This is, however, a prerequisite for this methodology to be developed to the full.



Sara Cantone

Sara Cantone (1979) studied Pharmaceutical Chemistry and Technology at University of Trieste, where she graduated in November 2004 in the group of Prof. Paolo Linda under the supervision of Prof. C. Ebert. Her thesis was focused on the activity and stability of Penicillin G amidase in ionic liquids. Currently, she is in the last year of her PhD in the Laboratory of Applied and Computational Biocatalysis at the University of Trieste.

Her scientific interests are focused on biocatalysis in non-conventional media and solid phase synthesis.

With this aim, the research is moving now from the approach “works or doesn’t work” to the understanding of the intimate mechanisms that regulate the biocatalysts in these new and unusual solvents. Similarly to their behaviour in organic solvents, enzymes require a certain degree of hydration in ionic liquids. This should be guaranteed by controlling the water activity (a_w) of the system. It is particularly difficult in the case of the hygroscopic ionic liquids that can contain very different amounts of water, depending on the synthetic procedure, the drying process or the storage conditions.⁴²

2.1 Properties of ionic liquids

An ionic liquid usually consists of an organic cation, often containing a nitrogen heterocycle, and an inorganic anion. The 1-alkyl-3-methylimidazolium ionic liquids are the most widely used for biocatalysis,^{43–45} although 1,4-dialkylpyridinium ionic liquids have also been used for some biocatalytic processes.^{46,47} Anions can be fluorinated (PF_6^- or BF_4^-), alkylsulfates or alkylsulfonates (RSO_4^- or RSO_3^-) and triflates (Tf_2N^- ; see Table 1). Their characteristics can be tuned by modifying anion and cation properties. The hydrophilicity and lipophilicity are determined mainly by the anions

of an ionic liquid, *e.g.* [bmim][BF_4] is fully water miscible whereas [bmim][PF_6] can be considered immiscible. The lipophilicity of dialkylimidazolium salts is also influenced to some extent by the chain length of the alkyl group, *e.g.* water is less soluble in [bmim][PF_6] than [omim][PF_6] (11700 and 6700 ppm, respectively).⁴³

An important parameter that characterizes ILs is the polarity. A study from Seddon on the polarity of 1,3-dialkylimidazolium ILs was based on the determination of the wavelengths of maximum adsorption and molar transition energies for Nile Red dissolved in ILs.⁴⁸ For ILs with [bmim] as the cation, the polarity decreases through the series of nitrite, nitrate, tetrafluoroborate and hexafluorophosphate. This decrease in polarity correlates with increasing anion size, hence a reduction in the effective anion charge density, *i.e.* the negative charge is better delocalised and is therefore less available for interactions with solutes, in this case Nile Red. [Tf_2N] is larger than the above mentioned anions but it is more polar than the [PF_6] analogue. In this case it was evident that the negative charge is only partially delocalized within the anion.⁴⁹ In general, it can be stated that for 1-alkyl-3-methylimidazolium [$C_n\text{mim}$] ILs, the polarity is apparently determined by the anion when the 1-alkyl groups are short

Table 1 Nomenclature of the most commonly used ILs in biocatalysed processes (see also Table 2)

Ionic Liquid			
Cation	Anion	Common notation	Water miscibility
1-Butyl-3-methylimidazolium	Tetrafluoroborate	[bmim][BF_4]	Yes
	Hexafluorophosphate	[bmim][PF_6]	No
	Bis[(trifluoromethyl)sulfonyl] imide	[bmim][Tf_2N] ^b	— ^a
	Trifluoromethanesulfonate	[bmim][Tfms]	Yes
	Glycolate	[bmim][OHCH_2COO]	— ^a
1-Butyl-2,3-dimethylimidazolium	Octylsulfate	[bmim][OctSO_4]	Yes
	Tetrafluoroborate	[bdmim][BF_4]	Yes
	Hexafluorophosphate	[bdmim][PF_6]	No
	Trifluoromethanesulfonate	[bdmim][Tfms]	— ^a
1-Butyl-4-methylpyridinium	Tetrafluoroborate	[bmp][BF_4]	Yes
1-Ethyl-3-methylimidazolium	Tetrafluoroborate	[emim][BF_4]	Yes
	Bis[(trifluoromethyl)sulfonyl] imide	[emim][Tf_2N] ^b	No
	Trifluoromethanesulfonate	[emim][Tfms]	Yes
1-Ethylpyridinium	Tetrafluoroborate	[EtPy][BF_4]	— ^a
	Trifluoroacetate	[EtPy][CF_3COO]	— ^a
1-Butylpyridinium	Bis[(trifluoromethyl)sulfonyl] imide	[BuPy][Tf_2N] ^b	— ^a
1-Butyl-1-methylpyrrolidinium	Bis[(trifluoromethyl)sulfonyl] imide	[BmPy][Tf_2N] ^b	Part. miscible
1-Hexyl-2,3-dimethylimidazolium	Tetrafluoroborate	[hdmim][BF_4]	Part. miscible
1-Hexyl-3-methylimidazolium	Tetrafluoroborate	[hmim][BF_4]	Part. miscible
	Hexafluorophosphate	[hmim][PF_6]	No
1-(3-Hydroxypropyl)-3-methylimidazolium	Hexafluorophosphate	[hpmim][PF_6]	— ^a
	Glycolate	[hpmim][OHCH_2COO]	— ^a
	Chloride	[hpmim][Cl]	— ^a
1,3-Dimethylimidazolium	Methylsulfate	[mmim][MeSO_4]	Yes
3-Methyl-3-nonylimidazolium	Hexafluorophosphate	[mnim][PF_6]	No
1-Methoxyethyl-3-methylimidazolium	Tetrafluoroborate	[moemim][BF_4]	— ^a
	Hexafluorophosphate	[moemim][PF_6]	— ^a
1-Octyl-3-methylimidazolium	Tetrafluoroborate	[omim][BF_4]	Part. miscible
	Hexafluorophosphate	[omim][PF_6]	No
1-Octyl-3-nonylimidazolium	Hexafluorophosphate	[onim][PF_6]	No
	Bis[(trifluoromethyl)sulfonyl] imide	[mtoa][Tf_2N] ^b	No
Methyltriethylammonium	Bis[(trifluoromethyl)sulfonyl] imide	[btma][Tf_2N] ^b	No
3-Hydroxypropyl-trimethylammonium	Bis[(trifluoromethyl)sulfonyl] imide	[htma][Tf_2N] ^b	— ^a
3-Cyanopropyl-trimethylammonium	Bis[(trifluoromethyl)sulfonyl] imide	[cptma][Tf_2N] ^b	— ^a
Butyltrimethylammonium	Bis[(trifluoromethyl)sulfonyl] imide	[btma][Tf_2N] ^b	— ^a
5-Cyanopentyl-trimethylammonium	Bis[(trifluoromethyl)sulfonyl] imide	[cptma][Tf_2N] ^b	— ^a
Hexyltrimethylammonium	Bis[(trifluoromethyl)sulfonyl] imide	[htma][Tf_2N] ^b	— ^a

^a Not reported. ^b Anion also abbreviated as: (CF_3SO_2) 2N^- , N(Tf) $_2$, NTf $_2$.

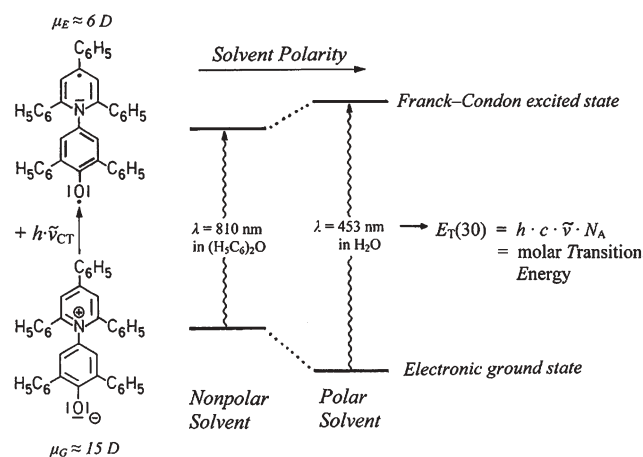


Fig. 1 Qualitative illustration of the influence of the solvent on the intramolecular charge-transfer visible absorption of the standard betaine dye. C. Reichardt, *Green Chem.*, 2005, 7, 339. Reproduced by permission of The Royal Society of Chemistry.⁵⁰

($C_n < 6$) and by the cation when the 1-alkyl groups are long ($C_n > 6$).

Studies from Reichardt have shown that the polarity of ILs can also be empirically determined by exploiting the extraordinary large negative solvatochromism of betaine dye (Fig. 1).⁵⁰

In general, the polarity of 1,3-dialkyl-imidazolium-based ionic liquids corresponds to that of short-chain primary and secondary alcohols or secondary amides such as *N*-methylformamide.

It is undoubted that the chemical structure of the ionic liquid affects their physical properties, but how is still poorly understood. The relative acidity or basicity of the ions forming the ILs has been little investigated.⁵¹ The common idea that many ions are inert is not always correct. Typical ILs anions (BF_4^- , PF_6^- , MeSO_3^- or Tf_2N^-) can be described as “neutral” or “very weakly basic” in the sense of the Lewis acid/base definition, and ILs formed from these ions are often used as inert solvents. Nonetheless, ILs cannot be considered completely inert. The widely used imidazolium based ILs in particular show weak acidity at the C2 proton of the ring.^{52,53} This could interact with acidic/basic solutes or with the protein, affecting the stability or activity of the enzymes.

The effect of ILs on the enzyme activity, however, is not only determined by the overall solvent properties, such as polarity or acidity/basicity, but it also depends on the contribution of individual ions. Once the ILs interact with the water present in the enzymatic system, they dissociate into independent cations and anions, that may affect the protein stability as described by Hofmeister,⁵⁴ and the same ion effect can also be found, in ILs, on enzyme stability,⁵⁵ specificity⁵⁶ and activity (Fig. 2).⁵⁷

These empirical rules, that are effective in the case of ILs but not extendable to dried or hydrophobic media, form a guideline in the design and choice of ILs for specific enzymatic applications. ILs are available from commercial sources (Sigma–Aldrich, Solvent Innovation, Merck, etc.) or can readily be prepared on laboratory scale (Fig. 3).

This is also the root of a general problem: related to the use of ILs is the variability of the reported data on their physical

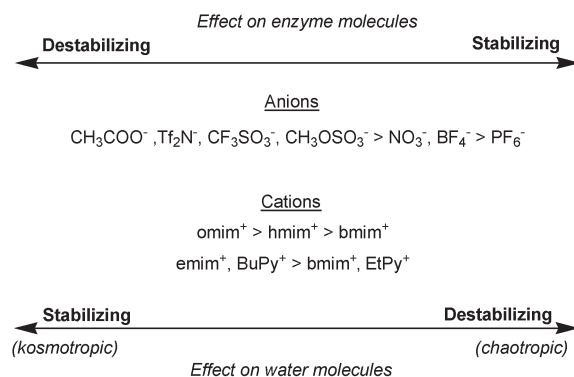


Fig. 2 Ion effect on water molecules and consequently on enzyme.⁵⁷

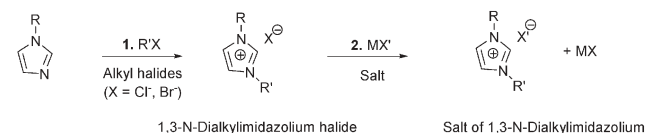


Fig. 3 Preparation of ILs. In the first step, 1,3-*N*-dialkylimidazolium halide is synthesized with alkyl halides. Anion exchange is made by metathesis of 1,3-*N*-dialkylimidazolium halide with the corresponding salt.⁸⁵

properties. As an example, melting points reported for $[\text{bmim}][\text{BF}_4]$ vary from 5.8 °C to 15 °C.⁵⁸ Another example is the variability in the reported viscosity of $[\text{bmim}][\text{PF}_6]$ that, at 1 bar and in a range 283–363 K, differs by 30% or more over most of that temperature range.⁴² This disagreement in viscosity, and other physical properties, seems primarily to be due to inconsistent sample purity. The presence of organic solvents, halides or water, has been shown to decrease the viscosity of ILs. Solvents and halides can be removed by extraction and evaporation, but water, due to the hygroscopic nature of many ILs, is rapidly adsorbed even by the “hydrophobic” ILs, so that it is difficult to control its content.

As mentioned above, the behaviour of enzymes in non-aqueous media is strictly related to the degree of hydration of biocatalysts. This parameter, the importance of which was demonstrated for organic solvents, is even more crucial in ILs, where the water content can vary from batch to batch. Thus, only by working in systems at similar a_w it is possible to reliably compare the behaviour of biocatalysts in different ILs and solvents. To complicate matters a good method to control a_w is not yet known.

2.2 Enzymes that work in ionic liquids

The majority of enzymes reported to be active in ILs are lipases, the “work horses” of biocatalysis. It is well known that polar organic solvents like methanol or DMF inactivate lipases. Although ILs have a polarity similar to these polar solvents, many ILs, mainly $[\text{C}_n\text{mim}][\text{BF}_4]$ and $[\text{C}_n\text{mim}][\text{PF}_6]$, do not deactivate lipases. They therefore close the polarity gap between water and organic solvents with $\log P > 2$. The advantages of performing reactions in polar media can thus be utilised (Table 2).

Table 2 Examples of biocatalysed reactions in ILs

Solvent	Enzyme	Form ^a	Source	Reaction	Comments	Ref.
[bmim][PF ₆]	Lipase	N, I	<i>Candida rugosa</i>	Transesterification and synthesis of polyesters	Higher stability than in organic solvent	92
			<i>Candida antarctica</i> (CaL-B)		Activity greater than in hexane	
[bmim][PF ₆] [bmim][BF ₄]		N, I	<i>Candida antarctica</i> (CaL-B)	Alcoholysis, ammoniolysis, perhydrolysis	Reaction rates comparable or better than in organic solvent	70
[bmim][PF ₆]		N	<i>Candida antarctica</i> (CaL-B)	Transesterification: kinetic resolution of chiral alcohols	Good activity and, in some cases, improved enantioselectivity	65
[bmim][Tfms] [bmim][Tf ₂ N] [bmp][BF ₄]			<i>Pseudomonas</i> sp. <i>Alcaligenes</i> sp. <i>Thermomyces lanuginosa</i> <i>Mucor miehei</i>			
[moemim][BF ₄]		N	<i>Pseudomonas cepacia</i> (PCL) <i>Candida antarctica</i> (CaL-B)	Acetylation of 1-phenylethanol, acetylation of glucose.	Reactions are fast than in organic solvents and more regioselective thanks to the better solubility of glucose in IL	59
[emim][BF ₄] [omim][BF ₄] [bmim][BF ₄] [hmim][BF ₄] [bdmim][BF ₄] [hdmim][BF ₄] [bmp][BF ₄] [hmim][PF ₆] [omim][PF ₆] [bmim][PF ₆] [emim][Tfms] [bdmim][Tfms]		I	<i>Candida antarctica</i> (CaL-B)	Amine synthesis	Enantioselective acylation of 1-phenylethylamine in [bdmim][Tfms]	69
[bmim][PF ₆] [bmim][BF ₄] [hmim][BF ₄]		N	<i>Candida rugosa</i>	Enantioselective hydrolysis	Addition of ionic liquid enhanced enantioselectivity and recyclability of lipase	68
[bmim][PF ₆] [nmim][PF ₆] [bmim][BF ₄] [hmim][BF ₄]		N	<i>Candida rugosa</i>	Esterification of 2-chloropropanoic acid with 1-butanol	Water removal applied to enhance the synthesis	62
[bmim][BF ₆] [onim][PF ₆]		N	<i>Candida rugosa</i>	Esterification of 2-substituted-propanoic acids and 1-butanol	Higher enantioselectivity than in n-hexane	93
[bmim][BF ₆] [moemim][BF ₆]		N	<i>Candida rugosa</i>	Acylation of glycosides	Higher reaction rates and selectivity than in conventional organic solvents	60
[bmim][BF ₆] [bmim][BF ₄]		N, I	<i>Pseudomonas cepacia</i>	Transesterification of 2-hydroxymethyl-1,4-benzodioxane	The enzyme-IL mixture could be recycled for several runs	63
[bmim][BF ₄] [bmim][PF ₆]		I	<i>Pseudomonas cepacia</i>	Hydrolysis and alcoholysis of 3,4,6-tri-O-acetyl-D-glucal	High regioselectivity	61
[emim][BF ₄] [emim][Tf ₂ N] [bmim][PF ₆] [bmim][BF ₄] [bmim][Tf ₂ N] [mtoa][Tf ₂ N] [bdmim][BF ₄]		I	<i>Candida antarctica</i> (CaL-B) α -chymotrypsin <i>Candida antarctica</i> (Novozym 435)	Transesterification reactions Transesterification using vinyl-acetate as acyl donor	All ILs improved the thermal stability of both enzymes	64
[bmim][Tf ₂ N] [bmim][BF ₄] [bmim][PF ₆]		I	<i>Candida antarctica</i> (Novozym 435)	Ring-opening polymerisation of ϵ -caprolactone or polycondensation of 1,4-butanediol with dimethyl adipate and dimethyl sebacate	Lipase reused for 10 times without losing enantioselectivity and reactivity Reactions proceed faster and to higher molecular weight; low volatility of ILs allows to perform reactions in open vessel	66 86
[bmim][BF ₄] [bmim][PF ₆] [Et ₃ MeN][MeSO ₄] [emim][EtSO ₄] [bmim][lactate] [EtNH ₃][NO ₃] [bmim][NO ₃]		N,I	<i>Candida antarctica</i> (Novozym 435)	Transesterification of ethyl butanoate with 1-butanol	When performed in [bmim][BF ₄] and [bmim][PF ₆] reaction rate comparable to that in organic solvent	99

Table 2 Examples of biocatalysed reactions in ILs (*Continued*)

Solvent	Enzyme	Form ^a	Source	Reaction	Comments	Ref.
[bmim][Tf ₂ N]	Esterase	N, I	<i>Bacillus subtilis</i>	Transesterification of 1-phenylethanol	Activity and enantioselectivity similar to organic solvent	67
[bmim][PF ₆]			<i>Bacillus stearothermophilus</i>		Higher stability than in organic solvent	
[bmim][BF ₄]					<i>a_w</i> controlled by means of saturated salt solutions	
[bmim][PF ₆]	Protease	N	Thermolysin	Synthesis of Z-aspartame	The dissolved enzyme is completely inactive; immobilized enzyme shows excellent stability and a competitive rate in comparison to that obtained in organic solvent	71
[bmim][PF ₆] [omim][PF ₆]		N	α -chymotrypsin	Transesterification of <i>N</i> -acetyl-L-phenylalanine ethyl ester with 1-propanol	Transesterification rates within an order of magnitude of those observed in organic solvents	72
[emim][BF ₄] [emim][Tf ₂ N] [bmim][PF ₆] [bmim][BF ₄] [bmim][Tf ₂ N] [mtoa][Tf ₂ N] [bmim][Tf ₂ N] [emim][Tf ₂ N]		I	α -chymotrypsin	Transesterification reactions	Improved the thermal stability (increased half-life); the relative stabilisation depends on the hydrophobicity of IL	59,73
[bmim][PF ₆] [bmim][BF ₄] [bmim][Tf ₂ N] [emim][Tf ₂ N]		N	α -chymotrypsin	Transesterification of <i>N</i> -acetyl-L-phenylalanine ethyl ester with 1-butanol	Good enzyme stability and high enantioselectivity	74
[EtPy][CF ₃ COO]		N	Novo alcalase (from <i>Bacillus licheniformis</i>)	Hydrolysis	Enhancement in enantioselectivity and activity; highly enantiomeric amino acid obtained	46
[emim][BF ₄] [EtPy][BF ₄] [bmim][BF ₄]		N	BL-alcalase (from <i>Bacillus licheniformis</i>)	Kinetic resolution of amino acid ester	High optical purity and high yield	47
		N	Papain	Asymmetric hydrolysis of D,L- <i>p</i> -Hydroxyphenylglycine methyl ester	Enhancement in stability	75,76
[bmim][PF ₆] [bmim][BF ₄] [bmim][Tf ₂ N]		N	Epoxide hydrolase (Recombinant)	Stereoselective hydrolysis of epoxides	Reaction rates generally comparable with those in buffer solution	77
[bmim][PF ₆] [bmim][BF ₄] [bmim][MeSO ₄] [omim][PF ₆] [omim][BF ₄] [omim][MeSO ₄] [bmim][Tf ₂ N]		I	Penicillin G amidase (PGA 450)	Synthesis of the amide of L-phenylglycine methyl ester with methyl phenylacetate	Similar activity than in organic solvent	85
	Dehydrogenase	N	Alcohol dehydrogenase (from <i>Lactobacillus brevis</i>)	Enantioselective reduction of 2-octanone	Highly enantioselective reduction of 2-octanone, faster than that obtained in buffer/methyl <i>tert</i> -butyl ether	78
[bmim][PF ₆] [bmim][OHCH ₂ COO] [bdmim][PF ₆] [hpmim][PF ₆] [hpmim][OHCH ₂ COO] [hpmim][Cl]		N	Morphine dehydrogenase (from <i>Pseudomonas putida</i>)	Oxydation of codeine to codeinone	Data about dependence of activity upon water content	79
[bmim][Tf ₂ N] [bmim][PF ₆] [omim][PF ₆] [bmim][PF ₆]	Peroxidase	N	Cytochrome c Microperoxidase-11 (MP-11)	Oxidation of guaiacol	Activity higher or comparable to that obtained in organic solvent	81
		N	Peroxidase (from <i>Coprinus cinereus</i>)	Oxidation of thioanisoles	Stereoselectivity similar to that obtained in water	83
[mmim][MeSO ₄] [bmim][OctSO ₄] [omim][PF ₆] [bmp][BF ₄] [bmim][PF ₆]	Mandelate racemase	N	<i>Pseudomonas putida</i>	Kinetic resolution of (<i>R,S</i>)-mandelic acid	Reaction rates are influenced by <i>a_w</i> , at <i>a_w</i> < 0.8 no activity.	80
	Laccase		Laccase C (from <i>Trametes</i> sp.)	Oxidation of anthracene	Yield increased	82

As an example, acetylation of 1-phenylethanol catalysed by lipase from *Pseudomonas cepacia* (PCL) was as fast and enantioselective in ILs as in toluene, and the acetylation of glucose, catalysed by CaL-B, was more regioselective in ionic liquids.⁵⁹ The increased solubility of glucose by up to one hundred times in ILs, favours the formation of the mono-acetylated product instead of mono- and diacetylated product mixtures, observed in organic solvents. The enhanced solubility of glycosides in ILs was also exploited in the acylation of monoprotected glycosides with vinyl acetate, and reactions in [bmim][PF₆] and [moemim][PF₆] took place more rapidly and more selectively than in conventional organic solvents.⁶⁰ A positive influence of [bmim][PF₆] on the rates and regioselectivity of lipase-catalysed hydrolysis and alcoholysis of 3,4,6-tri-*O*-acetyl-glucal has also been reported.⁶¹

Other examples of lipase-catalysed reactions in ionic liquids are direct esterifications⁶² and transesterifications,^{63,64} enantioselective transesterifications,^{65–67} enantioselective hydrolyses,⁶⁸ enantioselective acylation of amines⁶⁹ and ammoniolysis.⁷⁰

Although the majority of enzymes reported to be active in ILs are lipases, other biocatalysts have also been investigated. Many proteases have demonstrated their activity in ionic liquids. *Z*-aspartame was synthesised under thermodynamic control in a thermolysin-catalysed reaction of *Z*-L-aspartate and L-phenylalanine methyl ester hydrochloride in

[bmim][PF₆]. Next to an outstanding stability of the native enzyme in the IL, the observed initial rates were competitive with those of the enzymatic synthesis in acetonitrile.⁷¹ The activity of α -chymotrypsin in ILs was first reported in the kinetic transesterification of *N*-acetyl-L-phenylalanine ethyl ester with 1-propanol in [bmim][PF₆] and [omim][PF₆].⁷² Further studies of a kinetically controlled process with chymotrypsin have confirmed that the enzyme shows similar activity in ILs ([emim][BF₄], [bmim][BF₄], [bmim][PF₆], [emim][Tf₂N], [mtoa][Tf₂N]) as in organic solvents. Analogously to organic solvents, the enzyme requires a certain degree of hydration to be active.⁷³ However, it has to be noted that comparing the activity of enzymes in different media at similar water content is somewhat misleading. On the contrary, working at fixed values of a_w allows the separation of true solvent effects from other effects and only then the enzymatic activity in different solvents can be compared.¹³

The transesterification, catalysed by α -chymotrypsin, of *N*-acetyl-L-phenylalanine ethyl ester with 1-butanol was studied at controlled a_w in [bmim][Tf₂N] and [emim][Tf₂N]. The kinetics and the selectivity of the reaction, also concerning the competing hydrolysis, were similar to those in organic solvents.⁷⁴

The protease subtilisin (Novo alcalase), was assayed in [EtPy][CF₃COO] in the kinetic resolution of *N*-acetyl amino acids.⁴⁶ The IL seems to exert a detrimental effect on the

Table 2 Examples of biocatalysed reactions in ILs (Continued)

Solvent	Enzyme	Form ^a	Source	Reaction	Comments	Ref.
[mmim][MeSO ₄]	β -galactosidase	N	<i>Bacillus Circulans</i>	Transglycosilation, synthesis of <i>N</i> -acetylglucosamine	Better yields than in buffer; the enzyme tolerates only 25% v/v of IL; suppressed secondary hydrolysis	84
[bmim][PF ₆]		C	Baker's yeast	Enantioselective reduction of ketones	Possibility of distil the products directly from the ionic liquid; ionic liquid recycled after use	88
[bmim][PF ₆] [bmim][Tf ₂ N] [mtoa][Tf ₂ N]		C	<i>Lactobacillus kefir</i> (whole cells)	Asymmetric reduction of 4-chloroacetophenone to (<i>R</i>)-1-(4-chlorophenyl) ethanol	ILs alone do not damage the cell membrane; co-factor regeneration.	89
[bmim][BF ₄] [bmim][PF ₆]		C	<i>Saccharomyces cerevisiae</i> (immobilized cells)	Asymmetric reduction of acetyltrimethylsilane	ILs more biocompatible with <i>Saccharomyces cerevisiae</i> ; possibility of <i>in situ</i> coenzyme regeneration.	90
sc-CO ₂ /[bmim][Tf ₂ N]	Lipase	N, I	<i>Candida Antarctica</i> (Novozym 435)	Esterification and enantiomer separation	Excellent enantioselectivity and enantiomer separation; anion has a great influence on biocatalyst performances; high long-term stability of lipase	134
sc-CO ₂ /[bmim][Tf ₂ N]		I	<i>Candida Antarctica</i> (CaL-B)	Acylation of 1-octanol by vinyl acetate	High reaction yields, fully retained enzymatic activity after 24h process	133
[emim][Tf ₂ N] [bmim][Tf ₂ N] [mtoa][Tf ₂ N] [bmim][PF ₆] [htma][Tf ₂ N] [cptma][Tf ₂ N] [btma][Tf ₂ N] [cptma][Tf ₂ N] [htma][Tf ₂ N]		N, I	<i>Candida Antarctica</i> (CAL-A and CAL-B) <i>Mucor miehei</i> (MML)	Resolution of glycidol	Improved activity, the system permitted the kinetic resolution in continuous operation	132
[bmim][PF ₆] [htma][Tf ₂ N] [cptma][Tf ₂ N] [btma][Tf ₂ N] [cptma][Tf ₂ N] [htma][Tf ₂ N]		N	<i>Candida Antarctica</i> (Novozym 525L)	Resolution of <i>rac</i> -1-phenylethanol	All ILs were suitable media for kinetic resolution; very high enantioselectivity	136
sc-CO ₂ /[btma][Tf ₂ N] sc-CO ₂ /[mtoa][Tf ₂ N]		I	<i>Candida Antarctica</i> (Novozym 525L) on silica supports	Resolution of <i>rac</i> -1-phenylethanol	Synthetic activity in CO ₂ /ILs improved of up to six times with respect to organic solvent	137

^a I: immobilised, N: native, C: cells

enzyme activity when increasing the IL concentration. Again the comparison with organic solvents is not really informative since comparisons have been done at fixed amounts of water (15% ionic liquid or acetonitrile in water) but not at the same a_w . The reported improvement in the enantioselectivity, in the IL, nevertheless stipulates further investigations.

Papain was reported in the asymmetric hydrolysis of D,L-*p*-hydroxyphenylglycine methyl ester in a diluted aqueous solution of [bmim][BF₄] showing a slightly better stability and activity than those obtained in aqueous mixtures with polar solvents, such as acetonitrile or 2-propanol.^{75,76} Soluble epoxide hydrolase was shown to catalyze the hydrolysis of epoxides in [bmim][PF₆], [bmim][Tf₂N] and [bmim][BF₄].⁷⁷ Conversions obtained were comparable with those observed in buffer solutions, but interestingly the enantioselectivity improved (from 72% to 90% with [bmim][PF₆]) and the spontaneous hydrolysis of the starting materials in the buffer is suppressed in the IL.

Cofactor-dependent dehydrogenases have also been reported to be active in biphasic water/IL systems.^{78,79} The use of such classes of enzymes also involves the use of expensive cofactors such as NADPH or NADP⁺. In these biphasic systems, the enzyme and the cofactor, which are dissolved in the aqueous phase, are physically separated from the substrates and products, which are mainly in the IL phase.⁷⁸ Such a reaction system allows for ready recycling of co-factors, guarantees acceptable enzyme stability with an additional positive effect, due to the use of ionic liquids: higher reaction rates compared to traditional organic solvent (Fig. 4).

Kragl has also reported on the use of a mandelate racemase in different ionic liquids. The study focuses on the use of the enzyme in the highly hydrophilic [bmim][MeSO₄] and [bmim][OctSO₄]. To be active, the enzyme requires a_w values of over 0.7. To obtain these values in these hydrophilic ILs, large percentages of water need to be added (from a minimum of 20% to more than 40%); just like for polar solvents.⁸⁰ No effect of these concentrated salt solutions on the enzyme stability is mentioned, but a strong denaturing effect, similar to the effect of polar solvents, can reasonably be expected (Fig. 2).

Peroxidases (hemin, MP-11, and cyt-*c*) demonstrated their activity in [bmim][PF₆], [omim][PF₆] and [bmim][Tf₂N]. Hydrophobic, non-coordinating ILs provide an environment less disruptive than traditional solvents with similar polarity (methanol), and the nature of ILs accelerates the peroxidase reaction by stabilising the highly charged intermediates generated in the rate-determining step.⁸¹

Interestingly, a multi-copper oxidase, laccase, possessed catalytic activity in [bmp][BF₄] and [bmim][PF₆]. The enzyme tolerates moderate concentrations of the water miscible

[bmp][BF₄], and increasing concentrations of this IL resulted in a decrease of the laccase activity, causing enzyme precipitation (50%, v/v). A detailed analysis of kinetic data revealed that the decrease in the laccase activity was a result of a simultaneous decrease in V_{max} and increase in K_m passing from aqueous buffer to co-solvent mixture (20% v/v of tert-butanol buffer) to [bmp][BF₄] (25% v/v). This behaviour was rationalised in terms of co-solvent-induced denaturation of the enzyme.⁸²

Peroxidase and glucose oxidase catalysed the oxidation of thioanisoles in [bmim][PF₆] with a stereoselectivity similar to that obtained in water and with the advantage that all substrates and products were perfectly soluble in IL.⁸³

Also β -galactosidase was demonstrated to be active in [mmim][MeSO₄] and [bmim][MeSO₄] in the synthesis of *N*-acetyl lactosamine, with the advantage of a suppressed hydrolysis of products (from 30% yield in buffer to 58% in ILs). However, a decrease in the enzymatic activity was observed with increasing ionic liquid content, and the maximum amount tolerated by the enzyme was 25% (v/v).⁸⁴

In a recent paper, it was reported that the hydrolase penicillin G amidase has a similar activity in organic solvents and ionic liquids, when working at comparable a_w values.⁸⁵ However, the stability of the enzyme strongly depends on the cation/anion composition, due to a dual interaction effect of the IL either with the protein or with the water present in the system, causing a sort of "water stripping effect".

The enzymatic synthesis of polyesters in ILs has also been investigated.⁸⁶ Significant challenges could be overcome.⁸⁷ Polyester synthesis was assayed either by ring-opening polymerisation (ROP) of ϵ -caprolactone or by polycondensation of 1,4-butanediol with dimethyl adipate and dimethyl sebacate in different ILs catalysed by Novozym 435 (Fig. 5).⁸⁶

The polycondensation of butanediol with diesters in ILs has a clear advantage, due to the low volatility of ILs. The reactions can be performed at higher temperatures, leading to

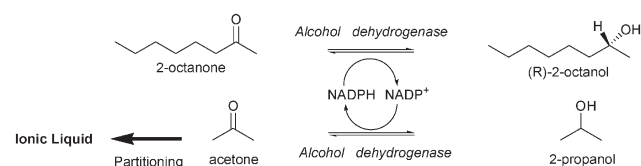
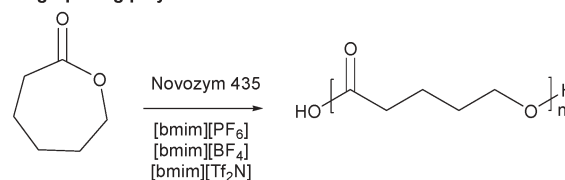


Fig. 4 Alcohol dehydrogenase production of *R*-2-octanol in biphasic water/IL system.⁷⁸

Ring-opening polymerisation



Polycondensation

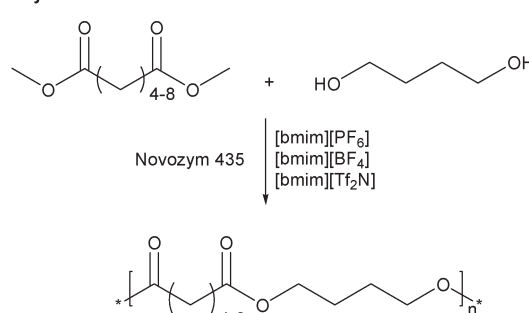


Fig. 5 Enzymatic synthesis of polyesters in ILs.⁸⁶

higher yields. In the case of the ROP of ϵ -caprolactone in [bmim][PF₆], [bmim][BF₄] or [bmim][Tf₂N], the tested ILs do not provide an advantage over toluene.

The reduction of ketones in [bmim][PF₆], catalysed by baker's yeast encapsulated in calcium alginate beads has been reported. As expected, results showed that the enantiomeric excesses obtained in IL were comparable to those obtained in other media, since the enzymes that catalyse this reaction remain within the cell, which is again protected by the alginate. An advantage of using an IL for this reaction is that under vacuum it is possible to distil the alcohols directly from [bmim][PF₆].⁸⁸ In another example, [bmim][Tf₂N] exhibits good solvent properties in the asymmetric reduction of *p*-chloroacetophenone to (*R*)-1-(4-chlorophenyl)ethanol with *Lactobacillus kefir*, acting as a substrate reservoir and in situ extracting agent.⁸⁹ Another enantioselective process was reported for immobilised *Saccharomyces cerevisiae* cells in [bmim][PF₆] and [bmim][BF₄] in the asymmetric reduction of acetyltrimethylsilane that leads to the formation of enantio-pure organosilyl alcohols.⁹⁰

In general, the high efficiency of whole cells in ILs can be attributed to:

- better biocompatibility of ILs than polar organic solvents;
- optimal distribution coefficients of substrates and products that reduces product enrichment inside the cells;
- a favourable ionic interaction with the charged groups of the membrane.⁹¹

2.3 Effect of ILs on enzyme activity and stability

Similarly to their behaviour in organic solvents, enzymes require an optimal degree of hydration to be active in ILs. Differently from an organic solvent that is constituted by one molecule, ILs dissociate into an anion and a cation. Whereas the cation is generally responsible for the hydrophobic character of the IL, the anion is the major factor in the interaction with water molecules.

In general, the behaviour of anions that interact strongly with water molecules (called kosmotropic, see Fig. 2)⁵⁷ is similar to the "water stripping" effect caused by polar organic solvents. Thus, anion-solvating water molecules are not available for the system—and consequently for the enzyme—and low water activities (a_w) are expected in such systems. This effect influences the hydration status of the enzyme and consequently its activity and stability.

Data reported in the literature confirm these speculations. As the examples discussed below demonstrate, enzyme activity and stability in ILs is, to a large extent, anion dependent.

The transesterification activity of free lipase (*Candida rugosa*) was higher in [bmim][PF₆] than in hexane, the initial rate is 1.5 times faster.⁹²

Esterase from *Bacillus stearothermophilus* showed increased stability in [bmim][PF₆] and [bmim][BF₄] compared to MTBE or hexane, with a half-life increased from 80 h (MTBE) to 220 h in ILs.⁶⁷

[PF₆] and [BF₄], which are chaotropic anions—do not interact so strongly with the water present in the system so that to the enzyme is guaranteed an optimal hydration status.

In the esterification of 2-substituted propanoic acids with 1-butanol in [bmim][PF₆] and [onim][PF₆], *Candida rugosa* lipase could be recycled five times, maintaining its activity and enantioselectivity.⁹³ On the other hand, the same enzyme was inactive in [bmim][CH₃COO], [bmim][NO₃], [bmim][CF₃COO], [bmim][MeSO₃] and [bmim][CF₃COO], and hydration of the enzyme failed to improve activity.⁹² These anions are more nucleophilic than [PF₆] and may coordinate more strongly to positively charged sites in the enzyme structure, causing conformational changes in the lipase.⁹⁴ In the same work, stability studies have shown that porcine pancreatic lipase suspended in [bmim][PF₆] at 50 °C retained 94% of its original activity after 48 h (61% retained activity in THF). In comparison, Novozym 435, when suspended for 24 h at 30 °C in ILs with [NO₃] as anion, lost its activity completely.

Immobilised penicillin G amidase (PGA)⁸⁵ is highly stable in [bmim][PF₆] and [bmim][BF₄], whereas it was deactivated within a few hours when suspended in [bmim][MeSO₄]. Detrimental effects of alkylsulfates were reported also for *Candida antarctica* lipase B,⁹⁹ for mandelate racemase,⁸⁰ and for β -galactosidase.⁸⁴ In fact, when β -galactosidase was suspended in [bmim][MeSO₄], the enzyme retained only 71% of its initial activity after 12 h of incubation.⁸⁴ This deactivation can be explained by considering that [MeSO₄] is a kosmotrope anion, thus also explaining the low a_w values measured in ILs containing this anion.⁸⁵

Contrary to the above described, when native lipase from *Candida antarctica* was used in the kinetic resolution of 1-phenylethanol, it showed good thermal stability up to 100 °C in MTBE as well as in [bmim][Tf₂N]. The enzyme in its suspended form in the IL could be reused three times with less than 10% loss of activity, after removal of products by distillation under reduced pressure.⁶⁵

Erbeldinger *et al.* have reported a similar effect with thermolysin. The lyophilised thermolysin needed to be in suspension in order to maintain its activity in the [bmim][PF₆]. When the enzyme was used dissolved in the IL (at concentrations lower than 3 mg mL⁻¹) it was completely inactive.⁷¹

In both cases, the suspended enzymes were active, while the dissolved thermolysin was inactive. This deactivation can reasonably be explained by considering the counter-ion effect caused by IL anions and cations that show strong electrostatic interactions with the charged sites of the dissolved enzyme.

2.4 Spectroscopic techniques for analysis of the enzyme structure in ILs

To exploit the full potential that ILs offer to enzyme catalysis it is important to understand the causes of deactivation. Commonly this activity loss is induced by conformational changes. These can be followed by spectroscopic techniques such as fluorescence, CD, or FTIR.

By exploiting fluorescence and CD spectroscopic techniques, it was possible to explain the much higher synthetic activity and stability exhibited by CaL-B in ILs than that observed in hexane.⁹⁵ CD spectroscopy allows the analysis of conformational modifications in the secondary structure of proteins. The far-UV region (190–240 nm) corresponds to the peptide

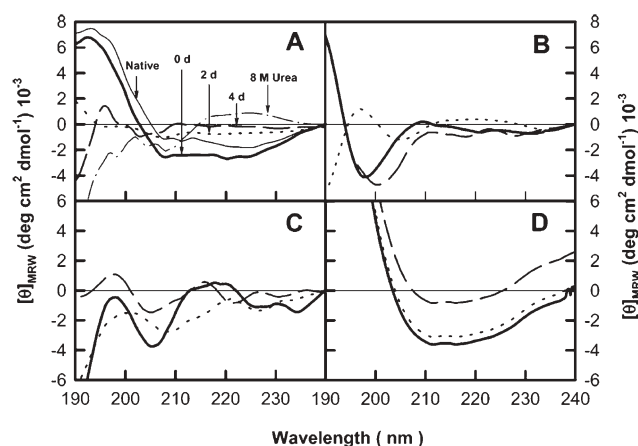


Fig. 6 Far-UV CD spectra of CaL-B in (A) water, (B) hexane, (C) [emim][Tf₂N], and (D) [btma][Tf₂N] at different incubation times and 50 °C ($t = 0$, bold line; $t = 2$ days, dotted line; $t = 4$ days, dashed line). (A) Native at 30 °C, thin line; unfolded in 8 M urea at 50 °C, dotted-dashed line. Reprinted with permission from T. de Diego, P. Lozano, S. Gmouh, M. Vaultier and J. L. Iborra, *Biomacromol.*, 2005, 6, 1457. Copyright (2005) American Chemical Society.⁹⁵

bond adsorption and the CD spectrum gives the content of regular secondary structural features, such as α -helix and β -strand. The far-UV CD spectra of the enzyme differ according to the assayed medium and incubation time, indicating that the protein has a particular distribution of the secondary structure in each condition (Fig. 6). CD analysis demonstrated a stabilisation of CaL-B by ILs associated to conformational evolution from α -helix to β -sheet secondary structures of the enzyme, resulting in a more compact enzyme conformation able to exhibit catalytic activity.

The intrinsic tryptophan fluorescence can be exploited to monitor the unfolding of enzymes in ILs. Cellulase from *Tricoderma reesi* is inactivated and unfolded when exposed to increasing concentrations of [bmim][Cl] (Fig. 7).⁹⁶

Similarly to cellulase, the intrinsic tryptophan fluorescence was exploited to monitor the change of folding of monellin in

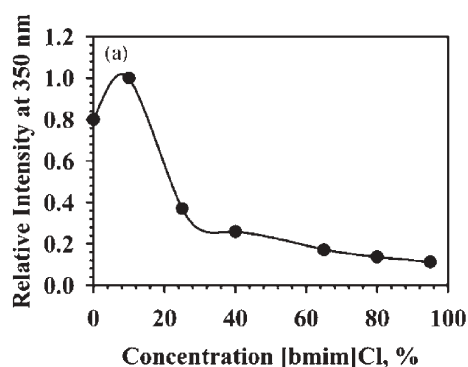


Fig. 7 Analysis by fluorescence spectroscopy of cellulase in [bmim][Cl] solutions. The relative fluorescence intensity, associated with the aromatic amino acids residues of the protein, decreases at increasing concentrations of IL due to the enzyme unfolding. M. B. Turner, S. K. Spear, J. G. Huddleston, J. D. Holbrey and R. D. Rogers, *Green Chem.*, 2003, 5, 443. Reproduced by permission of The Royal Society of Chemistry.⁹⁶

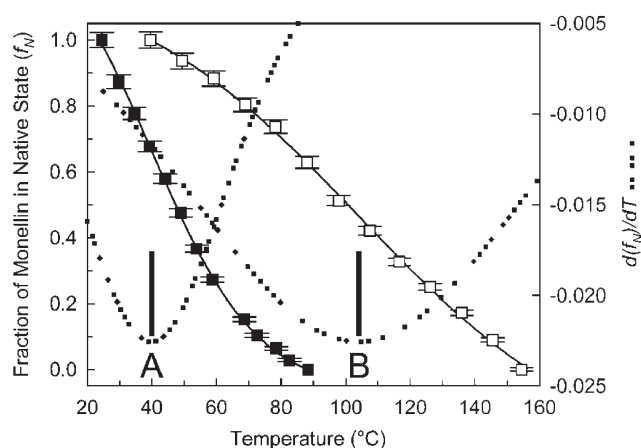


Fig. 8 Fluorescence-based thermal unfolding curves for monellin in water (■) and in [bmim][Tf₂N] equilibrated with 2.0% (v/v) water (□). S. N. Baker, T. M. McCleskey, S. Pandey and G. A. Baker, *Chem. Commun.*, 2004, 940. Reproduced by permission of The Royal Society of Chemistry.⁹⁷

[BuPy][Tf₂N] and in water (Fig. 8).⁹⁷ Comparing the unfolding curves in water and IL it emerges that the enzyme is considerably stabilised against thermal inactivation by the IL.

Infrared spectroscopy is a well-established technique for conformational analysis of proteins.⁹⁸ The C=O stretching vibration of the peptide bond is found at 1600–1700 cm^{-1} and is particularly informative on protein conformation. When FT-IR spectra of CaL-B in several ILs were compared with the spectrum of the protein in water, dramatic changes in the secondary structure of the enzyme were visible in ILs with anions [NO₃] and [lactate] (Fig. 9).⁹⁹ FT-IR data indicate that CaL-B undergoes structural changes in ILs, thus explaining the observed loss of activity.

LDI- and MALDI-MS¹⁰⁰ have the advantage that they can be employed for proteins without fluorophoric moieties or chromophores. They were applied for the analysis of enzymes and proteins dissolved in water-miscible ILs. Although these solvents are ionic it was possible to measure mass spectra of, among others, lysozyme and cytochrome c. The spectra showed a relation between the molecular mass of the analyte and the degree of ionisation depending on the nature of the ionic liquid. As expected, the ions of the liquids formed adducts with the proteins. These adducts were visible in the MALDI MS spectra.¹⁰¹

The quantitative analysis directly from ionic liquid-containing solutions enables the screening of enzyme activities and kinetic studies of enzyme-catalysed reactions in these solvents.

3. Biotransformations in supercritical fluids

The increasing demand for clean processes has led to the discovery that biotransformations can also be performed directly in environmentally benign, non-flammable supercritical fluids, SFs.¹⁰² The biocatalysis in supercritical fluids has been investigated over the last few years and a number of comprehensive reviews are available on the topic.^{103–105} SFs offer the opportunity to tune their physical properties by

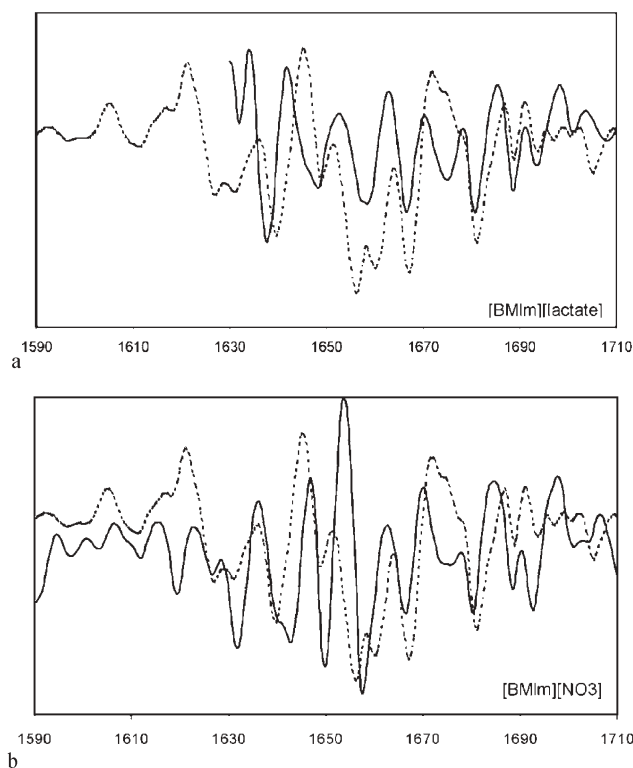


Fig. 9 FT-IR comparison of the second derivative spectra of CaL-B in (a) [bmim][lactate] and (b) in [bmim][NO₃] compared to the spectrum in aqueous solution (dotted line). R. Madeira Lau, M. J. Sordedra, G. Carrea, F. van Rantwijk, F. Secundo and R. A. Sheldon, *Green Chem.*, 2004, **6**, 483. Reproduced by permission of The Royal Society of Chemistry.⁹⁹

simple changes in pressure and temperature. The most used SF for biocatalysed processes is sc-CO₂, but also other supercritical fluids, such as sc-ethane, have been used successfully.¹⁰³

3.1 Properties of supercritical fluids

Supercritical fluids, sc-fluids, are materials above their critical temperature, T_c , and critical pressure, P_c (Fig. 10). Properties of supercritical fluids lie between the properties of liquids and gases.

The densities of supercritical fluids are comparable to those of liquids, while the viscosities are comparable to those of gases (Table 3 and 4).¹⁰³

In biocatalytic processes, the gas-like viscosity enhances mass transfer rates of reactants to the active sites of enzymes that are dispersed in the supercritical fluid. In this way, reactions that are limited by the rates of diffusion, rather than intrinsic kinetics, will proceed faster in supercritical fluids than in normal liquids.

A key feature of biocatalysis in supercritical fluids is the tunability of the medium. Small changes in pressure lead to significant changes in density, thus altering all density-dependent solvent properties (dielectric constant, solubility parameter and partition coefficient).

Since the changes in properties are predictable, supercritical fluid properties can be rationally controlled.

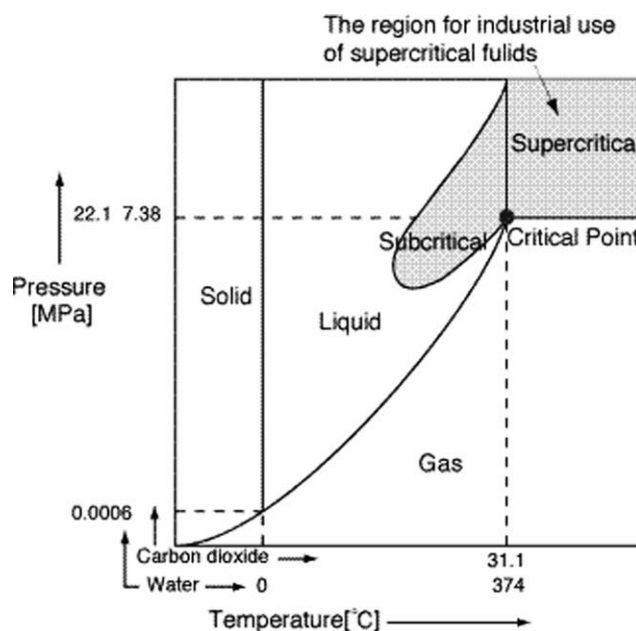


Fig. 10 Carbon dioxide phase diagram.

Table 3 Critical constants of supercritical fluids used in biocatalysis^a

SF	Critical temperature/K	Critical pressure/MPa
Butane	425.1	3.7960
Carbon dioxide	304.1	7.3773
Ethane	305.3	4.8728
Ethylene	282.3	5.0418
Fluoroform	299.3	4.8320
Propane	369.8	4.2477
Sulfur hexafluoride	318.7	3.7545

^a See <http://webbook.nist.gov> and references cited there.

Table 4 Properties of supercritical fluids (SFs) compared to the corresponding gasses and to organic solvents

Fluid	Viscosity, $\eta/\mu\text{Pa s}$	Density, $\rho/\text{g mL}^{-1}$
Gas ^a		
Butane	7.3949	0.0024
Carbon dioxide	15.046	0.0018
Ethane	9.3751	0.0012
Propane	8.1681	0.0018
SFs ^b		
sc-Butane	to be determined	0.2280
sc-CO ₂	2.1386	0.4670
sc-ethane	to be determined	0.2070
sc-Propane	to be determined	0.2200
Liquid ^a		
Hexane	296.29	0.6550
Toluene	to be determined	0.8620

^a 298 K, 1 atm. ^b At their T_c and P_c .

3.2 Enzymes in sc-fluids

Supercritical fluids are an environmentally friendly alternative to organic solvents as media for biocatalysis because, at the end of enzymatic processes, traces of sc-fluids can be removed by depressurisation. The use of supercritical fluids as non-aqueous solvents for enzyme-catalysed reactions was reported for the first time almost twenty years ago.^{106–108}

sc-Fluids allow the control of the reaction environment by varying the pressure and temperature. Another advantage is related to the downstream processing that might be

simpler than in organic solvents. By operating a cascade of depressurisations, product fractionation can be achieved.¹⁰⁹ Another possibility is the combination of a continuous flow reactor with an extraction column using sc-fluids as solvents in both steps. Among the solvents that can be used in supercritical conditions to conduct biocatalytic reactions, the most studied is carbon dioxide, CO₂, because of its low critical temperature (Table 3). Apart from being non-toxic, readily available and cheap, many native and immobilised enzymes such as lipases,^{110–114} cutinases,^{115,116} subtilisin Carlsberg,¹¹⁷ and β -D-galactosidase¹¹⁸ have proven to be stable, active and enantioselective in sc-CO₂. sc-CO₂ has also been used in enzymatic reactions catalysed by whole cells. As an example, the cells of *Bacillus megaterium* were employed for the CO₂ fixation reaction (decarboxylase catalysed) from pyrrole to pyrrole-2-carboxylate in sc-CO₂, and, as might be expected, higher yields were obtained under supercritical conditions (55%) than at atmospheric pressure (7%).¹¹⁹ Whole resting cells of *Geotrichum candidum* were used for the asymmetric reduction of various ketones (alcohol dehydrogenase catalysed) in sc-CO₂, showing enantioselectivity superior or equal to those for most other biocatalytic and chemical systems.^{120,121}

Although carbon dioxide is the most widely used sc-fluid, research has indicated that other sc-fluids are better suited to act as reaction medium for biocatalytic reactions.¹⁰³

Supercritical fluoroform has been used as reaction medium, in batch mode and under flow conditions, for the oxidation of *p*-cresol and *p*-chlorophenol by the enzyme polyphenol oxidase.¹⁰⁶ Cross-linked enzyme microcrystals (CLECs) of subtilisin Carlsberg and lipase Novozym 535 in supercritical ethane and compressed propane showed a 10 times higher activity than in supercritical carbon dioxide.^{122,123}

Enzyme activity is often reduced in supercritical carbon dioxide, due to the formation of carbonic acid in the presence of water and carbamates by reaction with amine groups of the enzyme. This is not the case for the supercritical ethane. It has therefore been used as a mixture with sc-CO₂ to reduce this acid base effect on cross-linked enzyme crystals (CLECs).¹²⁴ Transesterification rates obtained in sc-ethane are higher than those measured in acetonitrile and superior to those in hexane under similar conditions of enzyme hydration. This was attributed to the above mentioned improved mass transfer in sc-fluids.¹²²

Similar effects were also found in the cutinase-catalysed transesterification in sc-ethane and in sc-CO₂, where the enzyme activity dropped by more than one order of magnitude due to direct negative effects of sc-CO₂ on the enzyme.¹¹⁵ However, comparison with the more robust Novozym 435, a lipase immobilised on a macroporous support,¹²⁵ showed less pronounced deleterious effects due to sc-CO₂, and initial rates were found to be similar to those in sc-ethane.¹¹⁵

3.3 Stability of enzymes in sc-fluids

It was demonstrated that immobilised *Candida antarctica* lipase B (Novozym 435) is stable in sc-CO₂ for one month when stored at 40 °C and 14 MPa,¹¹⁵ and similar results have been reported for immobilised lipase from *Rhizomucor miehei*.¹²⁶

Studies on immobilised cutinase showed considerable stability and the enzyme maintained 90% of its initial activity upon exposure to sc-CO₂ at 45 °C and 130 bar for six days.¹¹⁶ The cutinase stability observed in sc-CO₂ was found to be significantly higher than in other non-conventional media such as microemulsions.

Immobilised lipase from *Rhizomucor miehei* and native lipases (from *Pseudomonas fluorescens*, *Rhizopus javanicus*, *Rhizopus niveus*, *Candida rugosa*) showed no activity change upon exposure to sc-CO₂, sc-*n*-butane or sc-*n*-propane for 24 h at a temperature of 40 °C and at a pressure of 300 bar.¹⁰² Despite the observed stability, a great difference in the relative activity of the biocatalysts in sc-CO₂ on the one hand and the other sc-fluids on the other hand, was observed. In fact, higher reaction rates were found in sc-*n*-butane or in a mixture of sc-*n*-butane/sc-*n*-propane than in sc-CO₂. The proposed explanation of this decreased relative activity of lipases was the interaction between CO₂ and the enzyme; *i.e.* carbamate formation with the lysine groups.¹⁰⁴ Another explanation of the observed reversible enzyme deactivation can be found in protonation effects due to the free carbonic acid formed by reaction of water with sc-CO₂. The acidic nature of sc-CO₂ and its effects on enzyme protonation have been underlined using Na₂CO₃/NaHCO₃ as a solid buffer in the reaction system. Na₂CO₃/NaHCO₃ was a good candidate for effecting changes in acid–base conditions in sc-CO₂, thus enhancing the catalytic activity of subtilisin Carlsberg CLECs.¹²⁴

3.4 Water content and its effect on enzyme activity in sc-fluids

Analogously to the behaviour of enzymes in organic solvents and in ionic liquids, the degree of enzyme hydration also plays a key role in the exhibited specific activity in the supercritical fluids. As an example, cholesterol oxidase in sc-CO₂ was less active in dry CO₂ than in the same system containing water.¹⁰³ The effect was found to be reversible, since the enzyme recovered its activity upon addition of water.

Similarly to the behaviour of immobilised enzymes in organic solvents, the carrier of the enzyme plays a key role. The material affects the enzyme activity, due to its ability to influence the partitioning of water molecules between the enzyme, the support and the medium.

In the comparative study by Barreiros *et al.* on the catalytic activity of CLECs in sc-fluids and in organic solvents, the same hydration hysteresis effects as in organic solvents were obtained. At the same time, however, the enzymes displayed superior activity in sc-fluids.¹²² Similarly to what happens in organic solvents, the solubility of water in such systems strongly depends on the nature of the supercritical fluid. As a matter of fact, hydrophilic SFs, such as sc-ethane or sc-butane, tend to dissolve water better than hydrophobic SFs, as sc-CO₂.

3.5 Effect of pressure

As mentioned above, pressure changes alter the polarity of the sc-fluid and allow modifying the reaction conditions. Research in conventional solvents has shown that solvent physical properties such as dielectric constant, dipole moment, log *P* and hydrophobicity have various effects on enzyme activity,

specificity and enantioselectivity. A variation of 13.8 MPa in the pressure of supercritical fluid fluoroform can translate into a 4-fold increase of its dielectric constant.¹²⁷ A variation of the pressure from 6.50 MPa to 28.90 MPa is sufficient to change the enantioselectivity of subtilisin Carlsberg and *Aspergillus* protease in supercritical fluoroform at 50 °C, and both enzymes become more stereoselective as the pressure is increased, in other words as fluoroform becomes more hydrophilic.¹⁰³

Also, in the case of lipase, it was found that the effect of supercritical fluoroform and ethane on the enzymatic activity of lipase was strongly dependent on the dielectric constant of the solvent.¹²⁸ Similar results were found for subtilisin.¹²⁹

Pressure has also been shown to affect the stability of some enzymes, and as the pressure is increased, some enzyme activities are enhanced, whereas others are decreased. But for the majority of enzymes, changes in pressure have no significant effects on the stability.¹⁰³

4. Combining ILs and SFs

4.1 Phase behaviours of ILs/SFs

Supercritical carbon dioxide (sc-CO₂) extraction has shown to be a viable method for solute recovery from an IL, due to the peculiar phase behaviour of this binary IL/sc-CO₂ system.

Preliminary investigations indicated that this is a very unusual biphasic system: while CO₂ readily dissolves in the liquid phase formed by the IL—reducing its viscosity—on the contrary the IL remains insoluble in the sc-CO₂.

Therefore two distinct phases are observed even under pressures up to 400 bar.

Also interesting is the volumetric behaviour of the IL/sc-CO₂ mixtures. It was observed that the total volume of a phase constituted by IL did not increase its volume even at very high concentrations of dissolved CO₂.¹³⁰

Due to these characteristics, sc-CO₂ can be used for the extraction of organic compounds dissolved in the IL phase and this has been successfully applied to several biocatalysed processes (see 4.2).

Another variation of the supercritical extraction is the use of sc-CO₂ to separate ILs and organic solvents. Solutions of MeOH and [bmim][PF₆], that are completely miscible at ambient conditions, were induced to form three phases in the presence of sc-CO₂.¹³¹

Upon increasing pressure of the system, a peculiar binary system forms, with an upper gas phase enriched by MeOH and a bottom phase constituted mainly from IL. The applied CO₂ pressure at which the second liquid phase appears is called the lower critical endpoint, while at the so-called K-point the MeOH enriched liquid phase merges with the vapour phase.

This behaviour can be exploited in all the biocatalysed transesterification processes where usually an alcohol is formed as by-product and should be eliminated to shift the equilibrium of the reaction.

4.2 Bioprocesses in ILs/SFs

sc-CO₂ has been widely described as an excellent solvent for hydrophobic compounds, and is billed as clean technology for

a range of industrial extractive processes.³¹ As mentioned before, sc-CO₂ might exert adverse effect on biocatalysts, due to pH changes caused by the carbonic acid that forms during the reaction, or due to conformational changes observed during pressurisation or depressurisation.

In order to overcome these limitations, a new concept for continuous biphasic biocatalysis, where a homogeneous enzyme solution is dissolved in ILs (working phase) and substrates and products reside largely in a supercritical phase (extractive phase), has been proposed (Fig. 11).¹³²

An aqueous solution of native *Candida antarctica* lipase B (CaL-B) was dissolved in [emim][Tf₂N] or [bmim][Tf₂N] and the synthesis of butyl butyrate was studied in a continuous packed bed reactor system. The reactor was coupled with a high-pressure sc-CO₂ extraction apparatus. The low water content of the system (<4% v/v) guaranteed high selectivity and good conversions. The ILs exerted a protective effect against enzyme deactivation by temperature and sc-CO₂ as demonstrated by the half-life time (ten reaction cycles).¹³²

A similar process, with continuous flow extraction by sc-CO₂, was used for the native CaL-B catalysed acylation of 1-octanol with vinyl acetate in [bmim][Tf₂N].¹³³ High yields, together with fully retained enzyme activity (after 24 h), make this methodology very promising in the development of sustainable synthetic biocatalysis in non-conventional media.

The same continuous flow extraction process, using native or immobilised CaL-B suspended in [bmim][Tf₂N], was used in

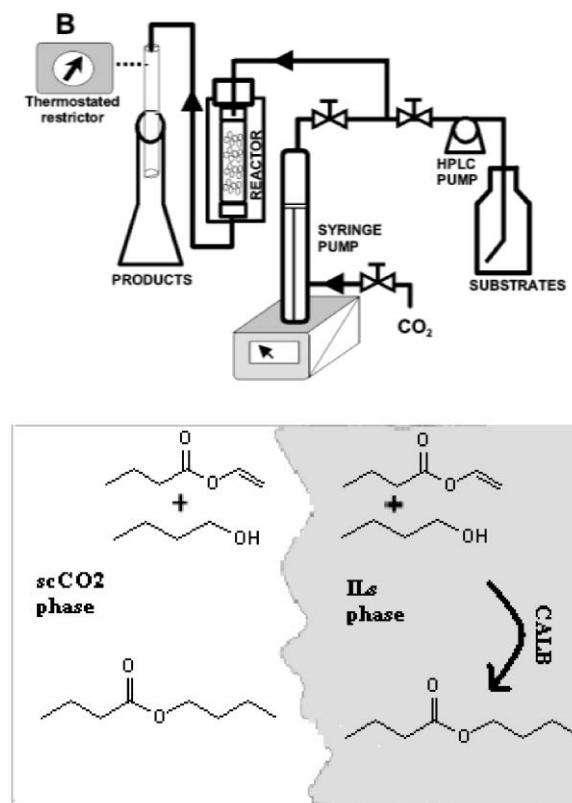


Fig. 11 Continuous biocatalytic processes using ionic liquids and supercritical carbon dioxide. P. Lozano, T. de Diego, D. Carrié, M. Vaultier and J. L. Iborra, *Chem. Commun.*, 2002, 692. Reproduced by permission of The Royal Society of Chemistry.¹³²

the kinetic resolution of chiral secondary alcohols.¹³⁴ After selective esterification, ester and unreacted alcohol are separated downstream by changing the properties of the sc-CO₂, *i.e.* by controlled density reduction by variation of temperature and/or pressure.

In another example, the enantioselective synthesis of glycidyl esters was described in a continuous biphasic reactor consisting of [emim][Tf₂N] containing the dissolved lipases and of an extractive phase formed by sc-CO₂.¹³⁵ These combined ILs/sc-CO₂ systems suggest a promising future for these biphasic systems. They balance the protecting effect that ILs exert towards lipases with the adverse effect of sc-CO₂ on the enzymatic activity, they allow good solubility of organic compounds in sc-CO₂ and they offer a low cost extraction technique.¹³⁶ However, before such techniques can be employed on a large-scale, more needs to be known about the toxicity of ILs.

Recently, the catalytic activity of CaL-B immobilised on different silica supports was investigated in sc-CO₂/ILs ([btma][Tf₂N] and [mtoa][Tf₂N]).¹³⁷ IL-coated immobilised enzyme improved its activity in sc-CO₂ by up to six times, with respect to organic solvents. The authors explain this finding by optimal hydrophobic interactions between the alkyl chains of the modified silica support (highest activity of the immobilised preparation was obtained with a butyl silica derivative) and the alkyl chains of the IL cations.

5. Solid-gas biocatalysis

At first sight it is surprising that enzymes can work at the solid-gas interphase.¹³⁸ But today solid-gas biocatalysis is a promising technology for fundamental research and for the development of new clean industrial processes. The use of enzymes or whole cells at the solid-gas interface offers some very interesting features, since total thermodynamic control of the system can easily be achieved.

Solid-gas biocatalysis presents many advantages compared to other systems (mono- or biphasic liquids): very high conversion yields compatible with a high production rate for a minimal plant scale, more efficient mass transfer, reduced diffusion limitations due to low gas viscosity and better stability of enzymes and cofactors. In addition, downstream processing is simplified due to the absence of a solvent phase and the scale-up is simpler due to the use of a gaseous circulating phase.¹³⁸

Many enzymes have been explored in solid-gas systems, such as alcohol oxidase from *Pichia pastoris* in ethanol oxidation,^{139,140} alcohol dehydrogenase for alcohol and aldehyde production,^{141,142} lipase from *Candida rugosa* and esterases for esters.¹⁴³

Solid-gas biocatalysis has not been restricted to the use of isolated enzymes. Whole cells are of particular interest in many fields of non-conventional biocatalysis, since they are cheap and since they allow the possibility to couple several enzymatic systems contained within the cell itself (cascade reactions).

Lyophilised *Saccharomyces cerevisiae* cells catalysed, in a solid-gas system at controlled a_w , the reduction of an aldehyde to the corresponding primary alcohol, with an efficient *in situ*

regeneration of the expensive nicotinamide cofactor.¹⁴⁴ The cellular matrix changes the conditions of hydration necessary for the expression of catalytic activity, and tests performed on the isolated enzyme and on whole cells showed that the isolated enzyme was active at an a_w as low as 0.1, whereas the whole cell required a minimal a_w of 0.4.¹⁴⁵

Similar results were also found for haloalkane dehalogenases, attractive biocatalysts for gas-phase bioremediation of pollutants. Due to their ability to convert short-chain aliphatic halogenated hydrocarbons to the corresponding alcohols, they can detoxify halogenated vapour emissions.

The study revealed that an optimal dehalogenase activity for the haloalkane dehalogenases from *Rhodococcus erythropolis* lyophilized cells is obtained at an a_w of 0.9, whereas the critical a_w of 0.4 is sufficient for the isolated enzyme to become active.¹⁴⁶ The activity and stability of lyophilized cells was also found to be dependent on the quantity of hydrochloric acid produced. pH control by the addition of a volatile Lewis base (triethylamine) to the gaseous phase was employed, thus preventing inhibition of dehalogenase by Cl⁻.

Systems consisting of several enzyme-catalysed reactions have been described. Two enzymatic systems, consisting of alcohol oxidase from cells of *Pichia pastoris* and isolated catalase (or peroxidases) were active in the same reactor. Thus, after oxidation of primary alcohols by alcohol oxidase, the isolated enzymes catalysed the elimination of produced by-products.¹⁴⁰ A further example is the complete degradation of trichloroethylene, in a continuous way, by cells of *Methylosinus trichosporium*, with the combination of methane monooxygenase, dehydrogenases and other monooxygenases in cascade.¹³⁸

5.1 The solid-gas bioreactor

Fig. 12 shows a schematic representation of a solid-gas bioreactor.

The packed bed reactor is composed of a solid phase, a biocatalyst in its native, immobilised or whole cell form, and a

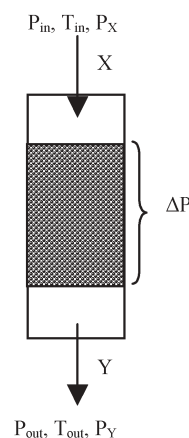


Fig. 12 Solid-gas biocatalysis in a packed bed reactor. The inlet gas is characterised by an inlet temperature, T_{in} and by an inlet pressure, P_{in} . P_X is the inlet partial pressure of X (reagent) and P_Y is the partial pressure of Y (product). The outlet after the reaction over the catalytic bed generates a pressure drop ΔP .¹³⁸

gas phase that flows through the reactor. The reagents give the composition of the inlet gas. The inlet gas is characterised by parameters such as molar composition, total pressure and temperature. The thermodynamic activity of each reagent a_X and of products a_Y can be calculated using the partial pressure of each compound on the saturation pressure of the pure compound. Of course, working with thermodynamic activity, which is an equilibrium parameter, it is necessary to ensure that the exchanges of molecules between the different phases are at the steady state.

The main strategy to create a gas with fixed thermodynamic activity is based on saturation of a carrier gas with the organic compound. A precise control of the molar composition of each compound contributing to the composition of the gas must be realized.¹⁴⁷ The thermodynamic control is realized by calculating the different partial pressures based on the different molar flow rates.

Another system to create a gas is the vaporization of organics in a carrier gas. In this liquid–gas flash vaporisation technique, a precise control of the different molar flow rates of each molecule contributing to the composition of the gas is required, too. This technique allows a better control of the molar flow rates compared to the saturated gases mixing technique, and complete vaporisation of the different molecules injected in the system is assured by performing solid–gas catalysis under reduced pressure.

5.2 Applications of solid–gas biocatalysis

Solid–gas technology represents a clean technology, since, compared to the organic liquid systems, the use of organic solvents can be reduced to zero.

Thanks to a thermodynamic approach, the optimisation of a solid–gas enzymatic esterification of natural alcohols and acids by Novozym 435 has been transferred successfully to the industrial scale for the production of fragrances and aromas.¹⁴⁸

A combined *in silico* optimisation and experimental determination of thermodynamic barriers allowed sample production at a kilogram level, and results were transferred to the pilot scale for validation.

Fig. 13 shows the industrial pilot for test production. The setup was developed on a closed loop of nitrogen, circulating in three different zones, thus reducing the nitrogen consumption in continuous operation. Liquid substrates (acid and alcohol), water and nitrogen are injected into a flash vapourisation unit using a pressurised loop. Once the liquid–gas transition is realized, the gas enters in a heat exchanger and the temperature is set to the bioreactor conditions.

The thermodynamic activities in the gas phase are obtained by controlling each partial pressure. A packed bed type reactor follows the heat exchanger, and the entire system is kept under reduced pressure. After biocatalysis, at the end of the process,

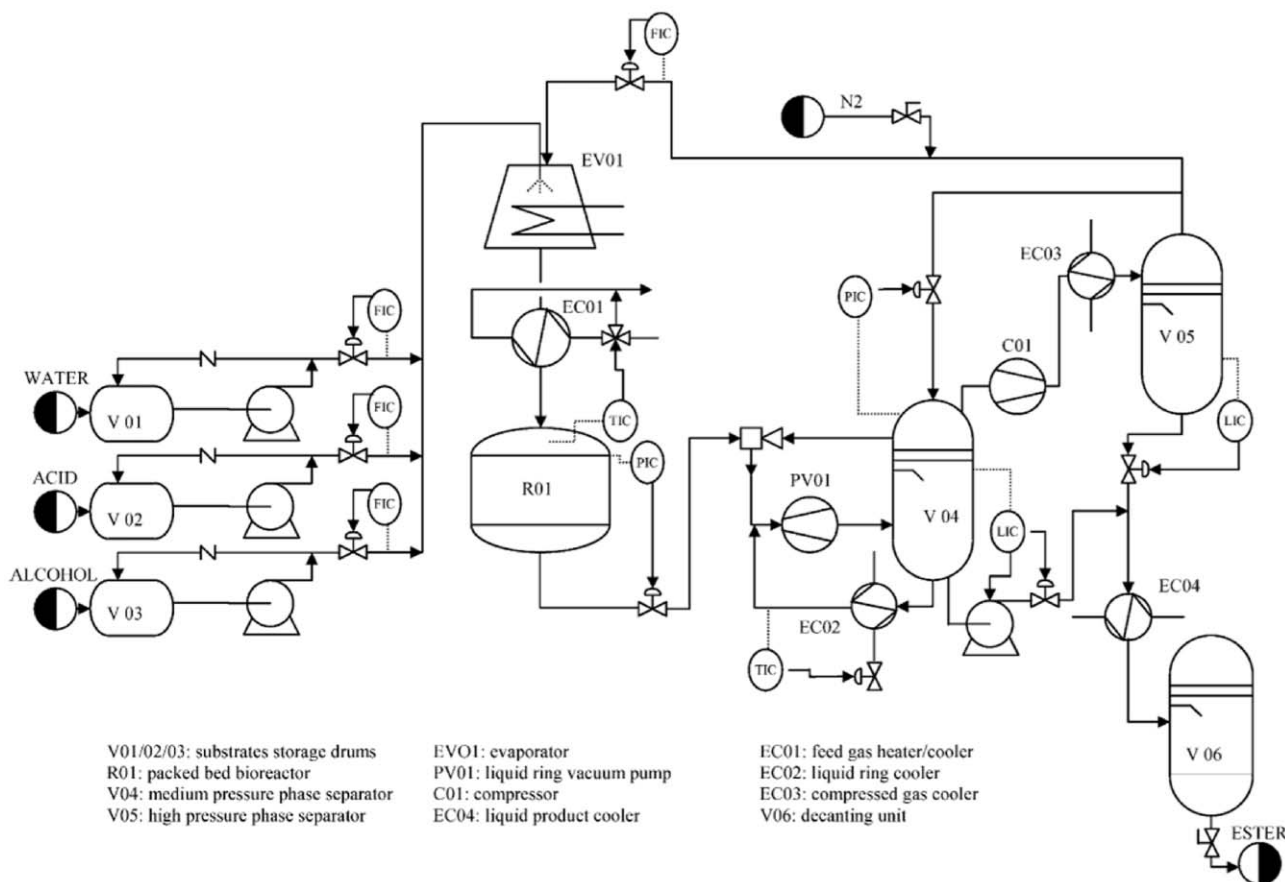


Fig. 13 Schematic diagram of the industrial continuous solid–gas bioreactor developed for the production of natural esters as a closed nitrogen loop.¹⁴⁸

condensable molecules are removed from the nitrogen by cooling and by increasing the absolute pressure. Nitrogen can then be recycled.

6. Conclusions

The application of enzymes in organic synthesis on a laboratory and industrial scale is by now a mature science. But with the introduction of ILs, sc-fluids and solid–gas interphase reactions new dimensions have been opened. ILs are only at the very beginning of their career as solvents. They close the gap between the polar and unpolar solvents that are suitable for enzymes, ensuring that enzymes can now be used over the entire polarity scale. At the same time, they enable carbohydrate chemistry that was unthinkable before. The degree of variation in these solvents is such that they have rightly been called designer solvents. Many of the ILs used today are composed of toxic ions or starting materials, and it can be expected that many of them will be replaced by environmentally friendly and biodegradable variants over the coming years.²⁷ Equally, it can be expected that their properties as a buffer will be explored more thoroughly, thereby opening new avenues to control the environment of the enzyme during the reaction, ensuring high enzyme stability.¹⁴⁹ Since their handling does not require any dedicated equipment in the laboratory, their already large popularity will increase. With the introduction of non-toxic and biodegradable ILs, their industrial application should be eased greatly.

Supercritical fluids are a mature technique already, and their power lies less in their number but in the variety of characteristics that one sc-fluid can have depending on the pressure. This already enables chemical industrial processes,⁵ and the enzyme-based processes are sure to follow. But due to the dedicated equipment necessary, their application in research is limited.

Enzyme catalysed reactions at the solid gas interphase have undergone a rapid development. Since starting materials and products need to be volatile, this technique is limited to smaller molecules, but laboratory scale experiments can very readily be transferred to large-scale transformations. Thus, this technique will definitely find a place in the production of high value added compounds.

Of particular interest is, however, the combination of ILs and supercritical fluids. This hands the chemist and engineer a wide range of possibilities to perform reactions and separate products in many yet undeveloped manners, opening an entirely new branch of process engineering.

Acknowledgements

Thanks are due to Prof. Lucia Gardossi, Prof. Cynthia Ebert and Dr Paolo Braiucă for useful discussions. Thanks are due to Nina Savko for graphical abstract drawing. The authors wish to thank the COST action D25, WG 4 for enabling this collaboration.

References

- 1 A. M. Klivanov, *Chemtech.*, 1986, **16**, 354.
- 2 K. Faber, *Biotransformations in Organic Chemistry*, Springer-Verlag, Berlin, Heidelberg, New York, 5th edn, 2004.
- 3 U. Bornscheuer and R. Kazlauskas, *Hydrolases in Organic Synthesis: Regio- or Stereoselective Biotransformations*, Wiley-VCH, Weinheim, New York, 1999.
- 4 Y. L. Khmel'nitsky and J. O. Rich, *Curr. Opin. Chem. Biol.*, 1999, **3**, 47.
- 5 R. A. Sheldon, I. Arends and U. Hanefeld, *Green Chemistry and Catalysis*, Wiley-VCH, Weinheim, 2007.
- 6 M. Breuer, K. Ditrach, T. Habicher, B. Hauer, M. Kessler, R. Stürmer and T. Zelinski, *Angew. Chem., Int. Ed.*, 2004, **43**, 788.
- 7 A. C. Hill, *J. Chem. Soc.*, 1898, **73**, 634.
- 8 J. H. Kastle and A. S. Loevenhart, *Am. Chem. J.*, 1900, **24**, 491.
- 9 E. A. Sym, *Biochem. Z.*, 1933, **258**, 304.
- 10 E. A. Sym, *Enzymologia*, 1936, **1**, 156.
- 11 P. J. Halling and L. Kvittingen, *Trends Biotechnol.*, 1999, **17**, 343.
- 12 A. M. Klivanov, *Nature*, 2001, **409**, 241.
- 13 P. J. Halling, *Enzyme Microb. Technol.*, 1994, **16**, 178.
- 14 G. Bell, P. J. Halling, B. D. Moore, J. Partridge and D. G. Rees, *Trends Biotechnol.*, 1995, **13**, 468.
- 15 A. Zaks and A. M. Klivanov, *J. Biol. Chem.*, 1988, **263**, 3194.
- 16 H. Sztajer, H. Lünsdorf, H. Erdmann, U. Menge and R. Schmid, *Biochim. Biophys. Acta*, 1992, **1124**, 253.
- 17 S. Hazarika, P. Goswami and N. N. Dutta, *Chem. Eng. J.*, 2002, **85**, 61.
- 18 A. M. Azevedo, D. M. F. Prazeres, J. M. S. Cabral and L. P. Fonseca, *J. Mol. Catal. B: Enzym.*, 2001, **5**, 147.
- 19 G. Pencrac'h and J. C. Baratti, *Enzyme Microb. Technol.*, 2001, **28**, 473.
- 20 A. M. Klivanov, *Trends Biotechnol.*, 1997, **15**, 97.
- 21 J. L. Schmitke, C. R. Wescott and A. M. Klivanov, *J. Am. Chem. Soc.*, 1996, **118**, 3360.
- 22 N. Krieger, T. Bhatnagar, J. C. Baratti, A. M. Baron, V. M. De Lima and D. Mitchell, *Food Technol. Biotechnol.*, 2004, **42**, 279.
- 23 P. T. Anastas, M. M. Kirchhoff and T. C. Williamson, *Appl. Catal., A*, 2001, **221**, 3.
- 24 J. D. Holbrey and K. R. Seddon, *Clean Prod. Process.*, 1999, **1**, 223.
- 25 R. Sheldon, *Chem. Commun.*, 2001, 2399.
- 26 A. Chowdhury, R. S. Mohan and J. L. Scott, *Tetrahedron*, 2007, **63**, 2363.
- 27 G. Imperato, B. König and C. Chiappe, *Eur. J. Org. Chem.*, 2007, 1049.
- 28 R. J. Bernot, M. A. Brueske, M. A. Evans-White and G. A. Lamberti, *Environ. Toxicol. Chem.*, 2005, **24**, 87.
- 29 M. T. Garcia, N. Gathergood and P. J. Scammells, *Green Chem.*, 2005, **7**, 9.
- 30 T. D. Landry, K. Brooks, D. Poche and M. Woolhiser, *Bull. Environ. Contam. Toxicol.*, 2005, **74**, 559.
- 31 S. V. Dzyuba and R. A. Bartsch, *Angew. Chem., Int. Ed.*, 2003, **42**, 148.
- 32 L. A. Blanchard, D. Hancu, E. J. Beckman and J. F. Brennecke, *Nature*, 1999, **399**, 28.
- 33 S. G. Kazarian, B. J. Briscole and T. Welton, *Chem. Commun.*, 2000, 2047.
- 34 C. Cadena, J. L. Anthony, J. K. Shah, T. I. Morrow, J. F. Brennecke and E. J. Maginn, *J. Am. Chem. Soc.*, 2004, **126**, 5300.
- 35 A. P. S. Kamps, D. Tuma, J. Xia and G. Maurer, *J. Chem. Eng. Data*, 2003, **48**, 746.
- 36 A. Ballesteros, F. J. Plou, J. L. Iborra and P. Halling, *Progress in Biotechnology*, Elsevier Science, New York, 1998, vol. 15, pp. 447–452.
- 37 S. Park and R. J. Kazlauskas, *Curr. Opin. Biotech.*, 2003, **14**, 432.
- 38 U. Kragl, M. Eckstein and N. Kaftzik, *Curr. Opin. Biotech.*, 2002, **13**, 565.
- 39 F. van Rantwijk, R. Madeira Lau and R. A. Sheldon, *Trends Biotechnol.*, 2003, **3**, 131.
- 40 Z. Yang and W. Pan, *Enzyme Microb. Technol.*, 2005, **37**, 19.
- 41 C. E. Song, *Chem. Commun.*, 2004, 1033.
- 42 J. A. Widegren, A. Laesecke and J. W. Magee, *Chem. Commun.*, 2005, 1610.
- 43 J. G. Huddleston, A. E. Visser, W. M. Reichert, H. D. Willauer, G. A. Broker and R. D. Rogers, *Green Chem.*, 2001, **3**, 156.
- 44 M. Koel, *Proc. Estonian Acad. Sci. Chem.*, 2000, **49**, 145.
- 45 R. Hagiwara and Y. Ito, *J. Fluor. Chem.*, 2000, **105**, 221.
- 46 H. Zhao and S. V. Malhotra, *Biotechnol. Lett.*, 2002, **24**, 1257.

- 47 H. Zhao, R. G. Luo and S. V. Malhotra, *Biotechnol. Prog.*, 2003, **19**, 1016.
- 48 A. J. Carmichael and K. R. Seddon, *J. Phys. Org. Chem.*, 2000, **13**, 591.
- 49 J. J. Golding, D. R. Macfarlane, L. Spiccia, M. Forsyth, B. W. Skelton and A. H. White, *Chem. Commun.*, 1998, 1593.
- 50 C. Reichardt, *Green Chem.*, 2005, **7**, 339.
- 51 D. R. MacFarlane, J. M. Pringle, K. M. Johansson, S. A. Forsyth and M. Forsyth, *Chem. Commun.*, 2006, 1905.
- 52 H.-P. Nguyen, P. Kirilov, H. Matondo and M. Baboulène, *J. Mol. Catal. A: Chem.*, 2004, **218**, 41.
- 53 J. Dupont and J. Spencer, *Angew. Chem., Int. Ed.*, 2004, **43**, 5296.
- 54 F. Hofmeister, *Arch. Exp. Pathol. Pharmacol.*, 1888, **24**, 247.
- 55 H. Zhao, O. Olubajo, Z. Song, A. L. Sims, T. E. Person, R. A. Lawal and L. A. Holley, *Bioorg. Chem.*, 2006, **34**, 15.
- 56 H. Zhao, S. M. Campbell, L. Jackson, Z. Song and O. Olubajo, *Tetrahedron: Asymmetry*, 2006, **17**, 377.
- 57 H. Zhao, *J. Mol. Catal. B: Enzym.*, 2005, **37**, 16.
- 58 K. R. Seddon, A. Stark and M.-J. Torres, *Pure Appl. Chem.*, 2000, **72**, 2275.
- 59 S. Park and R. J. Kazlauskas, *J. Org. Chem.*, 2001, **66**, 8395.
- 60 M.-J. Kim, M. Y. Choi, J. K. Lee and Y. Ahn, *J. Mol. Catal. B: Enzym.*, 2003, **26**, 115.
- 61 S. J. Nara, S. S. Mohile, J. R. Harjani, P. U. Naik and M. M. Salunkhe, *J. Mol. Catal. B: Enzym.*, 2004, **28**, 39.
- 62 K. Belafi-Bakó, N. Dörmö, O. Ulbert and L. Gubicza, *Desalination*, 2002, **149**, 267.
- 63 S. J. Nara, J. R. Harjani and M. M. Salunkhe, *Tetrahedron Lett.*, 2002, **43**, 2979.
- 64 P. Lozano, T. de Diego, D. Carrié, M. Vaultier and J. L. Iborra, *J. Mol. Catal. B: Enzym.*, 2003, **21**, 9.
- 65 S. H. Schöfer, N. Kaftzik, P. Wasserscheid and U. Kragl, *Chem. Commun.*, 2001, 425.
- 66 T. Itoh, Y. Nishimura, N. Ouchi and S. Hayase, *J. Mol. Catal. B: Enzym.*, 2003, **26**, 41.
- 67 M. Persson and U. T. Bornscheuer, *J. Mol. Catal. B: Enzym.*, 2003, **22**, 21.
- 68 S. S. Mohile, M. K. Potdar, J. R. Harjani, S. J. Nara and M. M. Salunkhe, *J. Mol. Catal. B: Enzym.*, 2004, **30**, 185.
- 69 R. Imrescu and K. Kato, *J. Mol. Catal. B: Enzym.*, 2004, **30**, 189.
- 70 R. M. Lau, F. van Rantwijk, K. R. Seddon and R. A. Sheldon, *Org. Lett.*, 2000, **26**, 4189.
- 71 M. Erbelinger, A. J. Mesiano and A. J. Russell, *Biotechnol. Prog.*, 2000, **16**, 1129.
- 72 J. A. Laszlo and D. L. Compton, *Biotechnol. Bioeng.*, 2001, **75**, 181.
- 73 P. Lozano, T. de Diego, J. P. Guegan, M. Vaultier and J. L. Iborra, *Biotechnol. Bioeng.*, 2001, **75**, 563.
- 74 M. Eckstein, M. Sessing, U. Kragl and P. Adlercreutz, *Biotechnol. Lett.*, 2002, **24**, 867.
- 75 W.-Y. Lou, M.-H. Zong and H. Wu, *Biocatal. Biotrans.*, 2004, **22**, 171.
- 76 W.-Y. Lou, M.-H. Zong and H. Wu, *Biotechnol. Appl. Biochem.*, 2005, **41**, 151.
- 77 C. Chiappe, E. Leandri, S. Lucchesi, D. Pieraccini, B. D. Hammock and C. Morisseau, *J. Mol. Catal. B: Enzym.*, 2004, **27**, 243.
- 78 M. Eckstein, M. V. Filho, A. Liese and U. Kragl, *Chem. Commun.*, 2004, 1084.
- 79 A. J. Walker and N. C. Bruce, *Chem. Commun.*, 2004, 2570.
- 80 N. Kaftzik, W. Kroutil, K. Faber and U. Kragl, *J. Mol. Catal. A: Chem.*, 2004, **214**, 107.
- 81 J. A. Laszlo and D. L. Compton, *J. Mol. Catal. B: Enzym.*, 2002, **18**, 109.
- 82 G. Hinckley, V. V. Mozhaev, C. Budde and Y. L. Khmel'nitsky, *Biotechnol. Lett.*, 2002, **24**, 2083.
- 83 K. Okrasa, E. Guibé-Jampel and M. Therisod, *Tetrahedron: Asymmetry*, 2003, **14**, 2487.
- 84 N. Kaftzik, P. Wasserscheid and U. Kragl, *Org. Proc. Res. Dev.*, 2002, **6**, 553.
- 85 A. Basso, S. Cantone, P. Linda and C. Ebert, *Green Chem.*, 2005, **7**, 671.
- 86 R. Marcilla, M. de Geus, D. Mecerreyes, C. J. Duxbury, C. E. Koning and A. Heise, *Eur. Polym. J.*, 2006, **42**, 1215.
- 87 R. A. Gross, A. Kumar and B. Kalra, *Chem. Rev.*, 2001, **101**, 2097.
- 88 J. Howarth, P. James and J. Dai, *Tetrahedron Lett.*, 2001, **42**, 7517.
- 89 H. Pfruender, M. Amidjojo, U. Kragl and D. Weuster-Botz, *Angew. Chem., Int. Ed.*, 2004, **43**, 4529.
- 90 W.-Y. Lou, M.-H. Zong and T. J. Smith, *Green Chem.*, 2006, **8**, 147.
- 91 H. Pfruender, R. Jones and D. Weuster-Botz, *J. Biotechnol.*, 2006, **124**, 182.
- 92 J. L. Kaar, A. M. Jesionowski, J. A. Berberich, R. Moulton and A. J. Russell, *J. Am. Chem. Soc.*, 2003, **125**, 4125.
- 93 O. Ulbert, T. Fráter, K. Bélafi-Bakó and L. Gubicza, *J. Mol. Catal. B: Enzym.*, 2004, **31**, 39.
- 94 R. A. Sheldon, R. M. Lau, M. J. Sordedra, F. van Rantwijk and K. R. Seddon, *Green Chem.*, 2002, **4**, 147.
- 95 T. de Diego, P. Lozano, S. Gmouh, M. Vaultier and J. L. Iborra, *Biomacromolecules*, 2005, **6**, 1457.
- 96 M. B. Turner, S. K. Spear, J. G. Huddleston, J. D. Holbrey and R. D. Rogers, *Green Chem.*, 2003, **5**, 443.
- 97 S. N. Baker, T. M. McCleskey, S. Pandey and G. A. Baker, *Chem. Commun.*, 2004, 940.
- 98 D. M. Byler and H. Susi, *Biopolymers*, 1986, **25**, 469.
- 99 R. Madeira Lau, M. J. Sordedra, G. Carrea, F. van Rantwijk, F. Secundo and R. A. Sheldon, *Green Chem.*, 2004, **6**, 483.
- 100 L. H. Cohen and A. I. Gusev, *Anal. Bioanal. Chem.*, 2002, **373**, 571.
- 101 M. Zabet-Moghaddam, R. Krüger, E. Heinzle and A. Tholey, *J. Mass Spectrom.*, 2004, **39**, 1494.
- 102 Z. Knez and M. Habulin, *J. Supercrit. Fluids*, 2002, **23**, 29.
- 103 A. J. Mesiano, E. J. Beckman and A. J. Russell, *Chem. Rev.*, 1999, **99**, 623.
- 104 S. Kamat, E. J. Beckman and A. J. Russell, *Crit. Rev. Biotechnol.*, 1995, **15**, 41.
- 105 J. Dordick, *Biocatalysts for Industry*, Plenum Publishing Corp., New York, 1991.
- 106 T. W. Randolph, H. W. Blanch, J. M. Prausnitz and C. R. Wilke, *Biotechnol. Lett.*, 1985, **7**, 325.
- 107 D. A. Hammond, M. Karel, A. M. Klibanov and V. J. Krukonis, *Appl. Biochem. Biotechnol.*, 1985, **11**, 393.
- 108 K. Nakamura, Y. M. Chi, Y. Yamada and T. Yano, *Chem. Eng. Commun.*, 1985, **45**, 207.
- 109 A. Marty, D. Combes and J. S. Condoret, *Biotechnol. Bioeng.*, 1994, **43**, 497.
- 110 T. Matsuda, T. Harada and K. Nakamura, *Green Chem.*, 2004, **6**, 440 and references cited therein.
- 111 T. Matsuda, R. Kanamaru, K. Watanabe, T. Harada and K. Nakamura, *Tetrahedron Lett.*, 2001, **42**, 8319.
- 112 T. Matsuda, R. Kanamaru, K. Watanabe, T. Kamitanaka, T. Harada and K. Nakamura, *Tetrahedron: Asymmetry*, 2003, **14**, 2087.
- 113 M. Rantakyla, M. Alkio and O. Aaltonen, *Biotechnol. Lett.*, 1996, **18**, 1089.
- 114 Y. Ikushima, N. Saito, K. Hatahara and O. Sato, *Chem. Eng. Sci.*, 1996, **51**, 2817.
- 115 S. Garcia, N. M. T. Lourenço, D. Lousa, A. F. Sequeira, P. Mimoso, J. M. S. Cabral, C. A. M. Afonso and S. Barreiros, *Green Chem.*, 2004, **6**, 466.
- 116 V. Sereti, H. Stamatis and F. N. Kolisis, *Biotechnol. Tech.*, 1997, **11**, 661.
- 117 P. Pasta, G. Mazzola, G. Carrea and S. Riva, *Biotechnol. Lett.*, 1989, **11**, 643.
- 118 T. Mori and Y. Okahata, *Chem. Commun.*, 1998, 2215.
- 119 T. Matsuda, Y. Ohashi, T. Harada, R. Yanagihara, T. Nagasawa and K. Nakamura, *Chem. Commun.*, 2001, 2194.
- 120 T. Matsuda, T. Harada and K. Nakamura, *Chem. Commun.*, 2000, 1367.
- 121 T. Matsuda, K. Watanabe, T. Kamitanaka, T. Harada and K. Nakamura, *Chem. Commun.*, 2003, 1198.
- 122 N. Fontes, M. C. Almeida, S. Garcia, C. Peres, J. Partridge, P. J. Halling and S. Barreiros, *Biotechnol. Prog.*, 2001, **17**, 355.
- 123 M. C. Almeida, R. Ruivo, C. Maia, L. Freire, T. Corrêa de Sampaio and S. Barreiros, *Enzyme Microb. Technol.*, 1998, **22**, 494.
- 124 N. Harper and S. Barreiros, *Biotechnol. Prog.*, 2002, **18**, 1451.

- 125 N. W. J. T. Heinsman, C. G. P. H. Schroën, A. van der Padt, M. C. R. Franssen, R. M. Boom and K. van't Riet, *Tetrahedron: Asymmetry*, 2003, **14**, 2699.
- 126 M. D. Romero, L. Calvo, C. Alba, M. Habulin, M. Primožič and Ž. Knez, *J. Supercrit. Fluids*, 2005, **33**, 77.
- 127 S. Kamat, E. J. Beckman and A. J. Russell, *J. Am. Chem. Soc.*, 1993, **115**, 8845.
- 128 S. Kamat, B. Iwaskewycz, E. J. Beckman and A. J. Russell, *Proc. Natl. Acad. Sci. U. S. A.*, 1993, **90**, 2940.
- 129 A. K. Chaudhary, S. V. Kamat, E. J. Beckman, D. Nurok, R. M. Kleyale, P. Hajdu and A. J. Russell, *J. Am. Chem. Soc.*, 1996, **118**, 12891.
- 130 L. A. Blanchard, Z. Gu and J. F. Brennecke, *J. Phys. Chem. B*, 2001, **105**, 2437.
- 131 A. M. Scurto, S. N. V. K. Aki and J. Brennecke, *J. Am. Chem. Soc.*, 2002, **124**, 10276.
- 132 P. Lozano, T. de Diego, D. Carrié, M. Vaultier and J. L. Iborra, *Chem. Commun.*, 2002, 692.
- 133 M. T. Reetz, W. Wiesenhöfer, G. Franciò and W. Leitner, *Chem. Commun.*, 2002, 992.
- 134 M. T. Reetz, W. Wiesenhöfer, G. Franciò and W. Leitner, *Adv. Synth. Catal.*, 2003, **345**, 1221.
- 135 P. Lozano, T. de Diego, D. Carrié, M. Vaultier and J. L. Iborra, *J. Mol. Catal. A: Chem.*, 2004, **214**, 113.
- 136 P. Lozano, T. de Diego, S. Gmouh, M. Vaultier and J. L. Iborra, *Biotechnol. Progr.*, 2004, **20**, 661.
- 137 P. Lozano, T. De Diego, T. Sauer, M. Vaultier, S. Gmouh and J. L. Iborra, *J. Supercrit. Fluids*, 2007, **40**, 93.
- 138 S. Lamare, M.-D. Legoy and M. Graber, *Green Chem.*, 2004, **6**, 445.
- 139 E. Barzana, A. Klibanov and M. Karel, *Appl. Biochem. Biotechnol.*, 1987, **15**, 25.
- 140 E. Barzana, A. Klibanov and M. Karel, *Biotechnol. Bioeng.*, 1989, **34**, 1178.
- 141 S. Pulvin, M. D. Legoy, R. Lortie, M. Pensa and D. Thomas, *Biotechnol. Lett.*, 1986, **8**, 783.
- 142 S. Pulvin, F. Parvaresh, D. Thomas and M. D. Legoy, *Ann. N. Y. Acad. Sci.*, 1988, **545**, 434.
- 143 N. Ross and H. Schneider, *Enzyme Microb. Technol.*, 1991, **13**, 370.
- 144 T. Maugard, S. Lamare and M. D. Legoy, *Biotechnol. Bioeng.*, 2001, **73**, 164.
- 145 I. Goubet, T. Maugard, S. Lamare and M. D. Legoy, *Enzyme Microb. Technol.*, 2002, **31**, 425.
- 146 B. Erable, T. Maugard, I. Goubet, S. Lamare and M. D. Legoy, *Process Biochem.*, 2005, **40**, 45.
- 147 S. Lamare and M. D. Legoy, *International Patent* WO 99/04894, 1999.
- 148 S. Lamare, B. Caillaud, K. Roule-Woiry, I. Goubet and M. D. Legoy, *Biocatal. Biotransform.*, 2001, **19**, 361.
- 149 G.-N. Ou, M.-X. Zhu, J.-R. She and Y.-Z. Yuan, *Chem. Commun.*, 2006, 4626.

Eco-friendly synthesis of 2,3-dihydroquinazolin-4(1*H*)-ones in ionic liquids or ionic liquid–water without additional catalyst†

Jiuxi Chen,^b Weike Su,^{*ab} Huayue Wu,^{*b} Miaochang Liu^b and Can Jin^a

Received 22nd January 2007, Accepted 10th April 2007

First published as an Advance Article on the web 4th May 2007

DOI: 10.1039/b700957g

2,3-Dihydroquinazolin-4(1*H*)-ones have been synthesized in high to excellent yields through direct cyclocondensation of anthranilamides and aldehydes in ionic liquids (ILs) or one-pot three-component cyclocondensation of isatoic anhydrides, ammonium acetate and aldehydes in ionic liquid–water solvent system without the use of any additional catalyst.

Quinazolinone derivatives are a class of fused heterocycles that have drawn much attention due to their potential biological and pharmaceutical activities.¹ A number of classical methods for the synthesis of 2,3-dihydroquinazolin-4(1*H*)-ones have been reported in the literature.^{2–5} Very recently we reported a novel method for the synthesis of 2,3-dihydroquinazolin-4(1*H*)-ones by reductive cyclization of *o*-nitrobenzamide or *o*-azidobenzamide with aldehydes and ketones promoted by metallic samarium and a catalytic amount of iodine or SmI₂.³ Recently, Shi⁴ has reported the preparation of 2,3-dihydroquinazolin-4(1*H*)-ones with the aid of a low-valent titanium reagent, whilst Salehi⁵ has reported a new method of one-pot synthesis of these compounds.

Due to the importance of quinazolinone derivatives in organic synthesis, the development of environmentally benign, high-yielding, and clean syntheses of 2,3-dihydroquinazolin-4(1*H*)-ones is in demand.

In recent years, ionic liquids have received recognition as green media in organic synthesis due to the ease of tuning their physical properties, such as good solvating capability, wide liquid range, negligible vapour pressure, tunable polarity, high thermal stability, and ease of recyclability.⁶ The rising number of publications is indicative of the potential of ILs as ‘designer solvents’ for various chemical reactions.

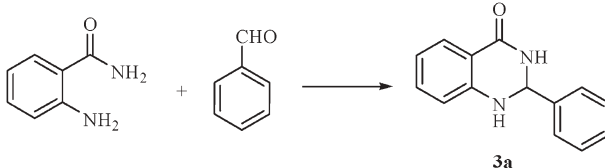
In light of our recent success in the ring-opening of epoxides with thiophenols in ionic liquids without the use of any additional catalyst,^{7a} and in continuation of our interest in green chemistry,⁷ we turned our attention to much more challenging reactions. Herein, we reported that ionic liquids or ionic liquid–water could be used as efficient reaction media for the preparation of 2,3-dihydroquinazolin-4(1*H*)-ones.

At the onset of the research, we investigated the model cyclocondensation reaction between anthranilamide and benzaldehyde at 75 °C under different reaction media. The results are illustrated

in Table 1. It was observed that ionic liquid was a type of feasible reaction medium in this cyclocondensation. After screening a variety of reaction media, [Bmim]PF₆ was determined to be the most effective medium for the generation the desired product (Table 1, entry 10). Compared with the reactions carried out in organic solvent, the condensation in ionic liquids required only 35–45 min to finish with good to excellent yields. Interestingly, when the reaction was carried out in DMSO, 2-phenyl-2,3-dihydroquinazolin-4(1*H*)-one (**3a**) was formed along with some of the oxidation product 2-phenylquinazolin-4(3*H*)-one (**4a**) (Table 1, entry 4). The weak oxidative ability of DMSO⁸ may account for the formation of **4a** from **3a**. Better yields of **3a** were obtained in the ionic liquids with imidazolium instead of pyridinium as the cation (Table 1, entries 5–12). The unique feature of the imidazolium ionic liquids used was based on their well-organized hydrogen-bonded polymeric supramolecular structure, which helped to introduce other molecules to form inclusion compounds.⁹ In light of the good results obtained, [Bmim]PF₆ was chosen as the reaction media as the research was extended to other anthranilamides and aldehydes without the use of any catalyst (Table 2).

Generally, the cyclocondensation reaction proceeded well and afforded the desired products **3a–3q** in good to excellent yields. As

Table 1 Synthesis of 2,3-dihydroquinazolin-4(3*H*)-ones under different reaction conditions^a

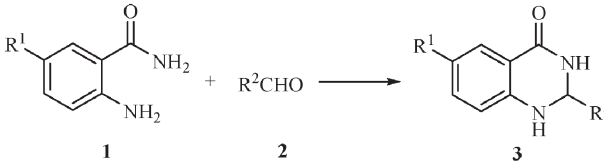
			
Entry	Reaction medium	Time/min	Yield (%) ^b
1	CH ₃ CN	60	31 (44)
2	CH ₃ NO ₂	60	33 (41)
3	DMF	60	36 (45)
4	DMSO	60	23 (34) ^c
5	[Emim]PF ₆	35	90
6	[Emim]BF ₄	35	91
7	[Emim]Br	40	88
8	[BPy]PF ₆	35	73
9	[BPy]BF ₄	45	81
10	[Bmim]PF ₆	35	92
11	[Bmim]BF ₄	40	90
12	[Bmim]Cl	40	85

^a For a typical experimental procedure, see ref. 11. ^b Isolated total yield (isolated total yield if the reaction was carried out at reflux temperature for 2 h). ^c 21% of 2-phenylquinazolin-4(3*H*)-one was formed.

^aCollege of Pharmaceutical Sciences, Zhejiang University of Technology, Zhejiang Key Laboratory of Pharmaceutical Engineering, Hangzhou, 310014, P. R. China. E-mail: suweike@zjut.edu.cn; Fax: +86 571 88320752

^bCollege of Chemistry and Materials Science, Wenzhou University, Wenzhou, 325027, P. R. China.

† Electronic supplementary information (ESI) available: Experimental details and characterisation data. See DOI: 10.1039/b700957g

Table 2 Synthesis of 2,3-dihydroquinazolin-4(1*H*)-ones in ionic liquids^a


Entry	R ¹	R ²	Time/min	Product	Yield (%) ^b
1	H	C ₆ H ₅	35	3a	89
2	H	<i>p</i> -(OCH ₃)C ₆ H ₄	35	3b	90
3	H	2,4-(OCH ₃) ₂ C ₆ H ₃	30	3c	91
4	H	<i>p</i> -(N(CH ₃) ₂)C ₆ H ₄	30	3d	94
5	H	<i>p</i> -(OH)C ₆ H ₄	30	3e	92
6	H	<i>p</i> -(F)C ₆ H ₄	35	3f	94
7	H	<i>p</i> -(Cl)C ₆ H ₄	40	3g	90
8	H	<i>o</i> -(NO ₂)C ₆ H ₄	50	3h	64 ^c
9	H	<i>m</i> -(NO ₂)C ₆ H ₄	45	3i	81
10	H	<i>p</i> -(NO ₂)C ₆ H ₄	45	3j	82
11	H	2-furyl	40	3k	85
12	H	2-pyridyl	40	3l	87
13	Cl	C ₆ H ₅	45	3m	84
14	Cl	<i>p</i> -(F)C ₆ H ₄	45	3n	87
15	Cl	<i>p</i> -(CH ₃)C ₆ H ₄	40	3o	85
16	Cl	<i>p</i> -(OCH ₃)C ₆ H ₄	40	3p	88
17	Cl	<i>p</i> -(NO ₂)C ₆ H ₄	50	3q	83

^a Reaction conditions: anthranilamide (5.5 mmol), aldehyde (5 mmol) and [Bmim]PF₆ (3.0 mL), 75 °C. ^b Isolated total yield. ^c Reaction was carried at 100 °C.

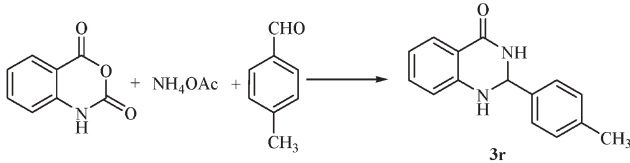
shown in Table 2, the reaction was compatible with a variety of electron-donating and electron-withdrawing substituents in the aryl aldehydes. Heteroaryl aldehydes could afford the corresponding products (**3k–3l**) with high yields as well (Table 2, entries 11–12). However, the steric effects exhibited by the aldehydes may play an important role and resulted in moderate yield of the product (Table 2, entry 8).

We further investigated the one-pot three-component synthesis of 2,3-dihydroquinazolin-4(1*H*)-ones from isatoic anhydrides, ammonium acetate and aldehydes.

Firstly, we applied the above optimal reaction conditions to the three-component reaction. However, when the scope of the reaction was explored, we quickly discovered that the reaction yields were unsatisfactory under the optimized reaction conditions. Thus, further optimization studies were performed in order to develop a better reaction system.

Recently, Yadav¹⁰ has reported that the conversion of oxiranes to thiiranes in ionic liquid and water solvent system. Enlightened by the research, we investigated the one-pot cyclocondensation reaction in the combination of ionic liquid and water solvent system (Table 3). The volume ratio of ionic liquids and water was examined and the best results were obtained by carrying out the reaction in [Bmim]BF₄–H₂O with a ratio of 3 : 2 (v/v) (Table 3, entry 3).

Using an ionic liquid–water solvent system instead of ionic liquid, the desired product was obtained in good yield. The water presumably plays an important role in the process due to the good water solubility of ammonium acetate, and hence the addition of water increases the solubility of ammonium acetate. However, in the absence of either water or ionic liquid, the reaction afforded the product in low yield or trace even after a long reaction time.

Table 3 Optimization of the one-pot three-component synthesis of 2,3-dihydroquinazolin-4(1*H*)-ones^a


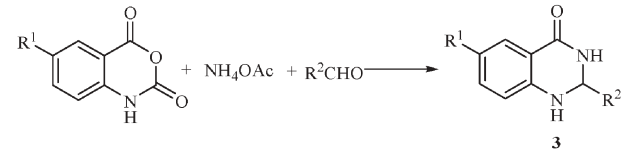
Entry	Reaction medium	Time/min	Yield (%) ^b
1	[Bmim]BF ₄	55	42
2	[Bmim]PF ₆	50	39
3	[Bmim]BF ₄ –H ₂ O (3 : 2) ^c	55	89
4	[Bmim]BF ₄ –H ₂ O (2 : 1) ^c	60	79
5	[Bmim]BF ₄ –H ₂ O (1 : 1) ^c	55	77
6	[Bmim]PF ₆ –H ₂ O (3 : 2) ^c	60	74
7	[Bmim]PF ₆ –H ₂ O (2 : 1) ^c	50	75
8	H ₂ O	100	trace

^a For a typical experimental procedure, see ref. 12. ^b Isolated total yield. ^c Volume ratio.

Therefore, the combination of ionic liquid and water was found to be an efficient reaction media for this transformation.

With the latter optimized conditions in hand, we explored the scope of the one-pot three-component cyclocondensation reaction (Table 4).

As shown in Table 4, an array of aldehydes bearing either electron-donating or electron-withdrawing groups on the aromatic ring were investigated. The substitution group on the phenyl ring did not make any difference in this reaction. The work-up procedure is very straightforward; that is, the products were isolated and purified by simple filtration. Our protocol avoids the use of organic solvents during the reaction process, making it superior to the previous methods. Several heteroaryl aldehydes were also examined and were found to give the expected products in excellent yields.

Table 4 One-pot synthesis of 2,3-dihydroquinazolin-4(1*H*)-ones in [Bmim]BF₄–H₂O^a


Entry	R ¹	R ²	Time/min	Product	Yield (%) ^b
1	H	<i>p</i> -(OCH ₃)C ₆ H ₄	60	3b	87
2	H	2,4-(OCH ₃) ₂ C ₆ H ₃	55	3c	90
3	H	<i>p</i> -(OH)C ₆ H ₄	55	3e	86
4	H	<i>p</i> -(NO ₂)C ₆ H ₄	70	3j	79
5	H	2-pyridyl	55	3l	82
6	Cl	C ₆ H ₅	70	3m	84
7	Cl	<i>p</i> -(F)C ₆ H ₄	60	3n	85
8	Cl	<i>p</i> -(CH ₃)C ₆ H ₄	55	3o	86
9	Cl	<i>p</i> -(OCH ₃)C ₆ H ₄	60	3p	87
10	Cl	<i>p</i> -(NO ₂)C ₆ H ₄	75	3q	77
11	H	<i>p</i> -(CH ₃)C ₆ H ₄	55	3r	89
12	H	<i>m</i> -(F)C ₆ H ₄	60	3s	86
13	H	<i>m</i> -(Cl)C ₆ H ₄	60	3t	82
14	H	<i>p</i> -(Br)C ₆ H ₄	60	3u	85

^a Reaction conditions: isatoic anhydride (5.5 mmol), ammonium acetate (8.0 mmol) and aldehyde (5.0 mmol) in [Bmim]BF₄ (3.0 mL)–H₂O (2.0 mL). ^b Isolated total yield.

All of the 2-substituted 2,3-dihydro-quinazolin-4(1*H*)-ones have been characterized by ^1H NMR, ^{13}C NMR, IR and MS spectra. The data of the known products were consistent with those reported in the literature. Taking **3a** as a example, in the ^1H NMR spectrum, protons appeared at δ 8.30 (s, 1 H), 7.61 (t, J = 6.8 Hz, 1 H), 7.50 (d, J = 7.2 Hz, 2 H), 7.32–7.41 (m, 3 H), 7.22–7.26 (m, 1 H), 7.12 (s, 1 H), 6.75 (d, J = 8.0 Hz, 1 H), 6.67 (t, J = 7.2 Hz, 1 H), 5.75 (s, 1 H). The NH proton at δ 8.30 (s, 1 H) and 6.75 (s, 1 H) does not appear due to a fast exchange in the presence of D_2O . In the ^1H NMR spectrum of **4a**, protons appeared at δ 11.80 (s, 1 H), 8.27–8.34 (m, 3 H), 7.79–7.87 (m, 2 H), 7.60 (t, J = 3.2 Hz, 3 H), 7.49–7.54 (m, 1 H). Similarly, The NH proton at δ 12.61 (s, 1 H) was exchanged with D_2O .

Finally, we checked the recycling of the ionic liquid–water solvent system. In the preparation of **3r**, the $[\text{Bmim}]\text{BF}_4\text{--H}_2\text{O}$ was reused for four runs without obvious loss of activity (with the yield of the product **3r** being 89%, 86%, 87%, and 84% yield, respectively).

In summary, the combination of simple experimental procedures and ease of recovery and reuse of this novel reaction media is expected to contribute to the development of a green strategy for the preparation of 2-substituted 2,3-dihydroquinazolin-4(1*H*)-ones. Compared to previous reported methodologies, the present protocol features simple operations, short reaction time, environmental friendliness, easy reusability of the ionic liquid, mild reaction conditions and good yields. Currently, studies on the extension of this protocol are ongoing in our laboratory.

Acknowledgements

We are grateful to the National Basic Research Program (No. 2003CB114402), National Natural Science Foundation of China (No. 20276123 and 20476098) and Wenzhou University Postgraduate Innovation Foundation (No. YCX0515) for financial support.

Notes and references

- M. G. Biressi, G. Cantarelli, M. Carissimi, A. Cattaneo and F. Ravenna, *Farmaco, Ed. Sci.*, 1969, **24**, 199; E. Hamel, C. M. Lin, J. Plowman, H. Wang, K. Lee and K. D. Paull, *Biochem. Pharmacol.*, 1996, **51**, 53; M. Hour, L. Huang, S. Kuo, Y. Xia, K. Bastow, Y. Nakanishi, E. Hamel and K. Lee, *J. Med. Chem.*, 2000, **43**, 4479; D. Gravier, J. P. Dupin, F. Casadebaig, G. Hou, M. Boisseau and H. Bernard, *Pharmazie*, 1992, **47**, 91; B. R. Baker, R. E. Schaub, J. P. Joseph, F. J. McEvoy and J. H. Williams, *J. Org. Chem.*, 1953, **18**, 133; J. F. Wolfe, T. L. Rathman, M. C. Sleeve, J. A. Campbell and T. D. Greenwood, *J. Med. Chem.*, 1990, **33**, 161.
- S. D. Sharma and V. Kaur, *Synthesis*, 1989, 677; J. A. Moore, G. J. Sutherland, R. Sowerby, E. G. Kelly, S. Palermo and W. Webster, *J. Org. Chem.*, 1969, **34**, 887; G. P. Cai, X. L. Xu, Z. F. Li, W. P. Weber and P. Lu, *J. Heterocycl. Chem.*, 2002, **39**, 1271; H. Asakawa and M. Matano, *Chem. Pharm. Bull.*, 1979, **27**, 1287; D. J. Connolly, D. Cusack, T. P. O'sullivan and P. J. Guiry, *Tetrahedron*, 2005, **61**, 10153 (review).
- W. K. Su and B. B. Yang, *Aust. J. Chem.*, 2002, **55**, 695; W. K. Su and B. B. Yang, *J. Chem. Res., Synop.*, 2002, 604.
- D. Q. Shi, L. C. Rong, J. X. Wang, X. S. Wang, S. J. Tu and H. W. Hu, *Chem. J. Chin. Univ.*, 2004, **25**, 2051; D. Q. Shi, J. X. Wang, L. C. Rong, Q. Y. Zhuang, S. J. Tu and H. W. Hu, *J. Chem. Res., Synop.*, 2003, 671; D. Q. Shi, L. C. Rong, J. X. Wang, Q. Y. Zhuang, X. S. Wang and H. W. Hu, *Tetrahedron Lett.*, 2003, **44**, 3199; D. Q. Shi, C. L. Shi, J. X. Wang, L. C. Rong, Q. Y. Zhuang and X. S. Wang, *J. Heterocycl. Chem.*, 2005, **40**, 173.
- M. Dabiri, P. Salehi, S. Otakesh, M. Baghbanzadeh, G. Kozhegarya and A. A. Mohammadi, *Tetrahedron Lett.*, 2005, **46**, 6123; P. Salehi, M. Dabiri, M. A. Zolfigol and M. Baghbanzadeh, *Synlett*, 2005, 1155; M. Baghbanzadeh, P. Salehi, M. Dabiri and G. Kozhegarya, *Synlett*, 2006, 344.
- T. Welton, *Chem. Rev.*, 1999, **99**, 2071; P. Wasserscheid and W. Keim, *Angew. Chem., Int. Ed.*, 2000, **39**, 3772; J. Dupont, R. F. de Souza and P. A. Z. Suarez, *Chem. Rev.*, 2002, **102**, 3667; D.-B. Zhao, M. Wu, Y. Kou and E.-Z. Min, *Catal. Today*, 2002, **74**, 157; T. Welton, *Coord. Chem. Rev.*, 2004, **248**, 2459; K. N. Marsh, J. A. Boxall and R. Lichtenthaler, *Fluid Phase Equilib.*, 2004, **219**, 93.
- (a) J.-X. Chen, H.-Y. Wu, C. Jin, X.-X. Zhang, Y.-Y. Xie and W.-K. Su, *Green Chem.*, 2006, **8**, 330; (b) J.-X. Chen, H.-Y. Wu, Z.-G. Zheng, C. Jin, X.-X. Zhang and W.-K. Su, *Tetrahedron Lett.*, 2006, **47**, 5383; (c) W.-K. Su, Z. Hong, W.-G. Shan and X.-X. Zhang, *Eur. J. Org. Chem.*, 2006, **2**, 723; (d) W.-K. Su, J.-J. Li, Z.-G. Zheng and Y.-C. Shen, *Tetrahedron Lett.*, 2005, **46**, 6037; (e) C.-M. Yu, X.-P. Dai and W.-K. Su, *Synlett*, 2007, 646; (f) W.-K. Su and C. Jin, *Org. Lett.*, 2007, **9**, 993.
- T. C. Igeorgiev, *Dyes Pigm.*, 1990, **12**, 243.
- J. Dupont, *J. Braz. Chem. Soc.*, 2004, **15**, 341.
- J. S. Yadav, B. V. S. Reddy, C. S. Reddy and K. Rajasekhar, *J. Org. Chem.*, 2003, **68**, 2525; J. S. Yadav, B. V. S. Reddy, B. Jyothirmai and M. S. R. Murty, *Tetrahedron Lett.*, 2005, **46**, 6559.
- Representative procedure: to a solution of anthranilamide (5.5 mmol) and benzaldehyde (5 mmol), $[\text{Bmim}]\text{PF}_6$ (2 mL) was added. The mixture solution was stirred at 75 °C for 35 min. The progress of the reaction was monitored by TLC. After completion of the reaction, the reaction was cooled to room temperature and the crude product was extracted with ethyl acetate (3 \times 10 mL). The extracted solution was dried over anhydrous magnesium sulfate and concentrated *in vacuo*. The crude product **3a** was purified by recrystallization from ethanol.
- Representative procedure: to a solution of isatoic anhydride (5.5 mmol), ammonium acetate (8.0 mmol) and *p*-methylbenzaldehyde (5.0 mmol), $[\text{Bmim}]\text{BF}_4$ (3.0 mL)- H_2O (2.0 mL) was added. The mixture solution was stirred at 80 °C for 55 min. The progress of the reaction was monitored by TLC. After completion of the reaction, the reaction mixture was cooled to room temperature and filtered to afford the crude product **3r**, which was purified by recrystallization from ethanol. In addition, the filtrate could be also reused for the next batch reaction. Selected data for compounds **3r**: R_f = 0.35 (petroleum ether–ethyl acetate = 1 : 1). Mp: 232.8–233.6 °C. ^1H NMR (400 MHz, $\text{DMSO}-d_6$): δ = 8.26 (s, 1 H), 7.62 (d, J = 7.6 Hz, 1 H), 7.38 (d, J = 8.0 Hz, 2 H), 7.17–7.25 (m, 3 H), 7.22–7.261 (m, 1 H), 7.07 (s, 1 H), 6.75 (d, J = 8.0 Hz, 1 H), 6.66 (t, J = 7.6 Hz, 1 H), 5.72 (s, 1 H), 2.28 (s, 3 H). ^{13}C NMR (100 MHz, $\text{DMSO}-d_6$): δ = 163.7, 148.0, 138.7, 137.8, 133.3, 128.9, 127.4, 126.9, 117.1, 115.0, 114.5, 66.5, 20.8. MS (EI, 70 eV): m/z (%) = 238 (M^+ , 47), 237 ($[\text{M} - 1]^+$, 92), 147 (100), 120 (48). **3n**: R_f = 0.35 (petroleum ether–ethyl acetate = 1 : 1). Mp: 249.2–250.4 °C. IR (KBr): 3430 (NH), 1672 (C=O) cm^{-1} . ^1H NMR (400 MHz, $\text{DMSO}-d_6$): δ (ppm) = 8.51 (s, 1 H), 7.54–7.57 (m, 3 H), 7.35 (s, 1 H), 7.22–7.31 (m, 3 H), 6.80 (d, J = 8.4 Hz, 1 H), 5.84 (s, 1 H). ^{13}C NMR (100 MHz, $\text{DMSO}-d_6$): δ (ppm) = 162.5, 162.2 (d, $^1J_{\text{CF}}$ = 243.4 Hz), 146.6, 137.4, 133.2, 129.1 (d, $^3J_{\text{CF}}$ = 8.3 Hz), 126.5, 121.0, 116.5, 116.1, 115.2 (d, $^2J_{\text{CF}}$ = 21.2 Hz), 65.9; m/z (EI) 278 ($[\text{M} + 2]^+$, 5), 276 (M^+ , 16), 181 (100), 183 (25), 154 (30), 95 (44). Found: C, 60.82; H, 3.69; anal. calcd for $\text{C}_{14}\text{H}_{10}\text{ClFN}_2\text{O}$: C, 60.77; H, 3.64. **3o**: R_f = 0.35 (petroleum ether–ethyl acetate = 1 : 1). Mp: 251.1–251.9 °C. IR (KBr): 3390 (NH), 1680 (C=O) cm^{-1} . ^1H NMR (400 MHz, $\text{DMSO}-d_6$): δ (ppm) = 8.44 (s, 1 H), 7.54 (d, J = 2.4 Hz, 1 H), 7.36 (d, J = 8.0 Hz, 2 H), 7.26–7.31 (m, 2 H), 7.19 (d, J = 8.0 Hz, 2 H), 6.77 (d, J = 8.4 Hz, 1 H), 5.74 (s, 1 H), 2.29 (s, 3 H). ^{13}C NMR (100 MHz, $\text{DMSO}-d_6$): δ (ppm) = 162.5, 146.6, 142.7, 137.9, 133.0, 129.2, 128.9, 126.8, 120.7, 116.4, 116.1, 66.2, 20.7. m/z (EI) 273 ($[\text{M} + 2]^+$, 32), 271 (M^+ , 95), 181 (100), 183 (25), 154 (34). Found: C, 66.01; H, 4.88; anal. calcd for $\text{C}_{15}\text{H}_{13}\text{ClN}_2\text{O}$: C, 66.06; H, 4.80. **3p**: R_f = 0.35 (petroleum ether–ethyl acetate = 1 : 1). Mp: 220.2–221.6 °C. IR (KBr): 3380 (NH), 1660 (C=O) cm^{-1} . ^1H NMR (400 MHz, $\text{DMSO}-d_6$): δ (ppm) = 8.40 (s, 1 H), 7.55 (s, 1 H), 7.42 (d, J = 6.4 Hz, 2 H), 7.26 (s, 2 H), 6.96 (d, J = 6.0 Hz, 2 H), 6.78 (d, J = 7.2 Hz, 1 H), 5.74 (s, 1 H), 3.75 (s, 3 H). ^{13}C NMR (100 MHz, $\text{DMSO}-d_6$): δ (ppm) = 162.4, 159.5, 146.7, 133.1, 132.9, 128.1, 126.4, 120.7, 116.4, 116.1, 113.7, 66.1, 55.1. m/z (EI) 290 ($[\text{M} + 2]^+$, 21), 289 ($[\text{M} + 1]^+$, 42), 288 (M^+ , 64), 287 ($[\text{M} - 1]^+$, 100), 183 (25), 181 (76), 183 (31), 154 (58). Found: C, 62.22; H, 4.67; anal. calcd for $\text{C}_{15}\text{H}_{13}\text{ClN}_2\text{O}_2$: C, 62.40; H, 4.54. **3q**: R_f = 0.35 (petroleum ether–ethyl acetate = 1 : 1). Mp: 220.1–220.8 °C. IR (KBr):

3440 (NH), 1668 (C=O) cm^{-1} . ^1H NMR (400 MHz, $\text{DMSO}-d_6$): δ (ppm) = 6.01 (s, 1 H), 6.85 (d, J = 8.8 Hz, 1 H), 7.32 (dd, J = 2.4, 8.8 Hz, 1 H), 7.58 (m, 2 H), 7.77 (d, J = 8.8 Hz, 2 H), 8.29 (d, J = 8.8 Hz, 2 H), 8.76 (s, 1 H). ^{13}C NMR (100 MHz, $\text{DMSO}-d_6$): δ (ppm) = 65.2, 116.0, 116.6, 121.2, 123.7, 126.5, 128.0, 133.4, 146.0, 147.5, 148.9, 162.2. m/z (EI) 305 ($[\text{M} + 2]^+$, 10), 303 (M^+ , 31), 181 (100), 183 (31), 154 (39). Found: C, 55.32; H, 3.25; anal. calcd for $\text{C}_{14}\text{H}_{10}\text{ClN}_3\text{O}_3$: C, 55.37; H, 3.32. **3s**: R_f = 0.4 (petroleum ether–ethyl acetate = 1 : 1). Mp: 266.1–267.4 $^\circ\text{C}$. IR (KBr): 3360 (NH), 1675 (C=O) cm^{-1} . ^1H NMR (400 MHz, $\text{DMSO}-d_6$): δ (ppm) = 8.42 (s, 1 H), 7.62 (d, J = 7.2 Hz, 1 H), 7.41–7.46 (m, 1 H), 7.15–7.35 (m, 5 H), 6.78 (d, J = 8.0 Hz, 1 H), 6.69 (t, J = 7.2 Hz, 1 H), 5.80 (s, 1 H); ^{13}C NMR (100 MHz, $\text{DMSO}-d_6$):

δ (ppm) = 163.5, 162.0 (d, $^1J_{\text{CF}}$ = 242.7 Hz), 147.6, 144.8, 133.5, 130.4 (d, $^3J_{\text{CF}}$ = 7.6 Hz), 127.4, 122.8, 117.3, 115.2 (d, $^2J_{\text{CF}}$ = 21.2 Hz), 115.0, 114.5, 113.6 (d, $^2J_{\text{CF}}$ = 22.0 Hz), 65.6; m/z (EI) 242 (M^+ , 30), 241 ($[\text{M} - 1]^+$, 40), 147 (100), 120 (50), 92 (25). Found: C, 69.33; H, 4.62; anal. calcd for $\text{C}_{14}\text{H}_{11}\text{FN}_2\text{O}$: C, 69.41; H, 4.58. **3u**: R_f = 0.35 (petroleum ether–ethyl acetate = 1 : 1). Mp: 205.7–206.3 $^\circ\text{C}$. IR (KBr): 3410 (NH), 1670 (C=O) cm^{-1} . ^1H NMR (400 MHz, $\text{DMSO}-d_6$): δ (ppm) = 8.35 (s, 1 H), 7.59–7.61 (m, 3 H), 7.44 (d, J = 8.4 Hz, 2 H), 7.23–7.27 (m, 1 H), 7.16 (s, 1 H), 6.74 (d, J = 8.4 Hz, 1 H), 6.68 (t, J = 7.6 Hz, 1 H), 5.76 (s, 1 H); m/z (EI) 304 ($[\text{M} + 2]^+$, 20), 302 (M^+ , 22), 147 (100), 120 (43), 91 (25). Found: C, 55.53; H, 3.55; anal. calcd for $\text{C}_{14}\text{H}_{11}\text{BrN}_2\text{O}$: C, 55.47; H, 3.66.

STOP!

searching...

Save valuable time searching for that elusive piece of vital chemical information.

Let us do it for you at the Library and Information Centre of the RSC.

We are your chemical information support, providing:

- Chemical enquiry helpdesk
- Remote access chemical information resources
- Speedy response
- Expert chemical information specialist staff

Tap into the foremost source of chemical knowledge in Europe and send your enquiries to

library@rsc.org

RSC Publishing

www.rsc.org/library

12120515

Atom economic synthesis of amides *via* transition metal catalyzed rearrangement of oxaziridines†

Chin Hin Leung,^a Adelina M. Voutchkova,^a Robert H. Crabtree,^{*a} David Balcells^b and Odile Eisenstein^{*b}

Received 24th April 2007, Accepted 22nd May 2007

First published as an Advance Article on the web 6th June 2007

DOI: 10.1039/b706164a

A mild synthetic route to amides involves imine oxidation to an oxaziridine followed by a transition-metal catalyzed rearrangement to the amide. This route shows potential for a greener pathway to amides. DFT studies showed a possible rearrangement pathway in the case of the Rh catalyst.

Introduction

Amide groups appear in a vast range of useful compounds, for example in pharmaceuticals. Traditional methods for synthesis of amides from carboxylic acids and amines have poor atom economy since they necessitate stoichiometric amounts of dehydrating agents such as carbodiimides, which consequently generate stoichiometric amounts of the corresponding urea as byproducts (eqn (1)).



Although acyl halides and esters can also react directly with amines to form amides, their preparation also generates undesirable waste (eqn (2)).



Atom-economic and environmentally more benign synthetic methods are thus highly desirable. One approach involves formation of imine by condensation of aldehyde and amine, oxidation of the imine to the oxaziridine, and subsequent isomerization of the oxaziridine to the amide, catalyzed by transition metal complexes (Scheme 1). This approach was proposed by Duhamel and Plaquevent¹ for peptide synthesis but using stoichiometric reagents. Using Mn, W, Ir and Rh catalysts, we now explore the potential of the oxaziridine route for a general synthesis of amides.

Oxaziridines were first synthesized independently in the 1950s by Krimm,² Emmons³ and Horner and Jurgens.⁴ Their unusual reactivity pattern is a consequence of the strained three-membered

ring and of the weak N–O bond. Oxaziridines are well known as both aminating and oxygenating reagents.⁵

The principal synthetic routes to oxaziridines involve the oxidation of imines with peracids.⁶ Other methods to oxidize imines include oxone,⁷ O₂/CoCl₂ (cat.),⁸ H₂O₂/benzonitrile⁹ or H₂O₂/urea¹⁰ and H₂O₂/Na₂WO₄ (cat.).¹¹ These alternatives to the harsh peracid methods usually generate stoichiometric amounts of undesirable waste. For example, in the O₂/Co(II) system, an aldehyde has to be used as coreductant. The atom economic method of Rao and coworkers,¹¹ using the catalyst Na₂WO₄ and the green oxidant H₂O₂,¹² goes at room temperature in moderate yield.

Rearrangement of oxaziridines to amides usually requires harsh conditions. Treatment of certain oxaziridines with a strong base such as NaH in HMPA¹³ or LDA¹⁴ gives amides, but can also lead to decomposition.¹⁵ Both thermal and photochemical isomerization of oxaziridines are known, but nitrones are sometimes formed instead of amides.¹⁶

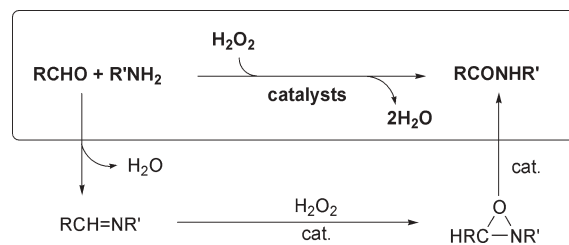
Oxaziridine rearrangements to amides with transition metal complexes are mostly stoichiometric.¹⁷ Apart from an early example by Emmons using FeSO₄,³ catalytic oxaziridine rearrangements have been found with iron or manganese porphyrin catalysts with high (10–20%) catalyst loadings.¹⁸

While direct oxidation of imines to amides is sometimes possible, this usually requires stoichiometric oxidants such as KMnO₄¹⁹ or *m*CPBA/BF₃·OEt₂.²⁰

Results and discussion

Catalytic synthesis of oxaziridines

Imines were synthesized from the corresponding amines and aldehydes by direct condensation. In some cases, this even occurred in water, following the prior work by Tashiro *et al.*²¹ Otherwise Al₂O₃, a potentially recyclable reagent, was used as the reaction medium in a solvent-free reaction. Oxaziridines were then prepared from the corresponding imines by the known mild



Scheme 1

^aDepartment of Chemistry, Yale University, 225 Prospect Street, New Haven, CT, 06520-8017, USA. E-mail: robert.crabtree@yale.edu; Fax: +1 (203) 432 6344; Tel: +1 (203) 432 3925

^bInstitut Charles Gerhardt, Université Montpellier 2, CNRS – cc-1501 Place Eugène Bataillon, 34095, Montpellier, France. E-mail: odile.eisenstein@univ-montp2.fr; Fax: +33 467144839; Tel: +33 467143306

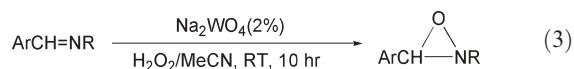
† Electronic supplementary information (ESI) available: Experimental details, computational references, optimized structures with E, H and G. See DOI: 10.1039/b706164a

Table 1 Catalysts for the rearrangement of oxaziridine **1**^a

Entry	Catalyst ^b	Loading (mol%)	Solvent	% Yield amide ^c
1	Pd(OAc) ₂	5	MeCN	14
2	Pd(PPh ₃) ₂ Cl ₂	5	MeCN	30
3	[Rh(cod)Cl] ₂	2.5	Toluene	57
4	[Rh(PPh ₃) ₂ (cod)]BF ₄	5	MeCN	12
5	[Rh(NHC) ₂ (cod)]PF ₆	5	MeCN	56
6	[Rh(py) ₂ cod] PF ₆	5	Toluene	61
7	Rh ₂ (octanoate) ₄	2.5	Toluene	50
8	[IrCp*Cl] ₂	2.5	Toluene	36
9	[Ir(cod)Cl] ₂	2.5	Toluene	58
10	[Ir(py) ₂ cod] PF ₆	5	Toluene	58
11	TPPMnCl (2)	5	MeCN	83
12	[(L) ₂ Mn ₂ (μ-O) ₂ (H ₂ O) ₂](ClO ₄) ₃ (3)	2.5	MeCN	74
13	Pd/C	5	Toluene	0
14	Rh/alumina	5	Toluene	0
15	MnO ₂	10	Toluene	0

^a Reaction time 12 h in refluxing solvent. ^b NHC = 1,3-dimethyl-imidazole-2-ylidene; cod = 1,5-cyclooctadiene; TPPMnCl is tetraphenylporphyrin chloro manganese(III); L = 4'-phenyl-2,2':6,2''-terpyridine. ^c Yields based on ¹H NMR integrations using 1,3,5-trimethoxybenzene as internal standard.

method using Na₂WO₄ (cat., 2 mol%) and H₂O₂ in MeCN (eqn (3): Ar = *p*-NO₂C₆H₄, *p*-MeOC₆H₄, *p*-ClC₆H₄, R = Cy; Ar = Ph, R = Cy, *n*Bu, *t*Bu, *i*Pr, C₂H₄Ph).²²



Catalytic rearrangement to amides

The rearrangement of the 2-cyclohexyl-3-phenyloxaziridine (**1**; Ar = Ph, R = Cy) to the corresponding amide was used for screening catalysts and conditions (Table 1).²³ Common heterogeneous catalysts (Rh/alumina, Pd/C) showed no activity. The commercially available [Rh(cod)Cl]₂ and [Ir(cod)Cl]₂ and some simple cationic derivatives all showed good activity (entries 3–6, 9, 10), but yields were lowered if air was not excluded. The catalyst Rh₂(octanoate)₄ was less active but unaffected by air.

Manganese complexes were tested based on the previously reported activity.¹⁹ Indeed, the two homogeneous manganese species showed the best activities for the rearrangement step (entries 11 and 12), and exclusion of air was not necessary. Manganese dioxide, on the other hand, was inactive.

The Mn catalyzed rearrangement showed some generality (Table 2) but yields of 2-*t*-butyl-3-phenyloxaziridine (entry 3) and 2-cyclohexyl-3-(*p*-nitrophenyl)oxaziridine (entry 7) were poor. TPPMnCl (**2**) did not catalyze the rearrangement of 2-*t*-butyl-3-phenyloxaziridine at all, but the sterically less hindered Mn dimer (**3**) achieved a low yield (36%, entry 3).

DFT study of the Rh-catalyzed oxaziridine rearrangement

DFT studies²⁴ have been carried out using Gaussian 03²⁵ for [Rh(cod)Cl]₂ where the catalyst is most likely the mononuclear Rh(cod)Cl. Although the Mn catalysts are somewhat more active, the mechanism in these cases has proved to be much harder to tackle, so we defer discussion of this point until the full paper. The substrate was modelled by replacing Cy and Ph by Me. A reasonable reaction mechanism for this catalyst consists of the

Table 2 Yields for different substrates

Entry	R ₁	R ₂	Cat. ^a	Yield (step 1)	Yield (step 2)	Overall yield
1	Ph	Cy	2	81	83	67
2	Ph	<i>n</i> Bu	3	62	90	56
3	Ph	<i>t</i> Bu	3	50	36	18
4	Ph	<i>i</i> Pr	3	61	95	58
5	Ph	C ₂ H ₄ -Ph	3	71	46	33
6	<i>p</i> -Cl	Cy	3	83	73	61
7	<i>p</i> -NO ₂	Cy	2	90	25	23
8	<i>p</i> -OMe	Cy	2	80	85	68

^a The better catalyst is shown in this column.

oxidative addition of the oxaziridine N–O bond to [Rh(cod)Cl] followed by β-H elimination and, finally, reductive elimination. The potential energy surface and a schematic representation of the intermediates and transition states are shown in Fig. 1.

The coordination of the substrate to [Rh(cod)Cl] leads to the square-planar Rh(I) intermediate **I1**, with the oxaziridine coordinated to Rh via N. This process is exothermic with a Δ*E* of –27.9 kcal mol^{–1}. Only potential energy (*E*) needs to be considered because the oxaziridine rearrangement is a unimolecular process.

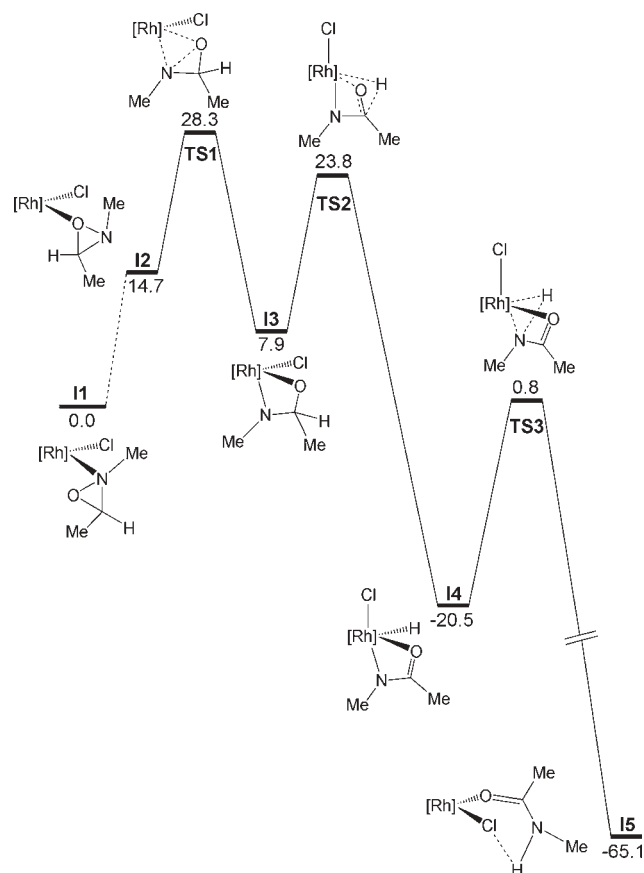


Fig. 1 DFT potential energy surface for the Rh-catalyzed rearrangement. Energies are given in kcal mol^{–1} and [Rh] = Rh(cod).

TS1 is the transition state for oxidative addition of the oxaziridine. At **TS1**, O is coplanar with the plane defined by Rh, Cl and cod C=C bond mid-points, and the N–O bond is perpendicular to that plane. **TS1** is connected to the intermediate **I2**, on the reactant side of the reaction, and to **I3**, on the product side. In **I2**, the oxaziridine is bound to Rh *via* O and **I2** is less stable than **I1** by 14.7 kcal mol^{−1}. **I3** is a square pyramidal Rh(III) species with a four-membered metallacycle in which N occupies the apical site. The step **I1** → **TS1** → **I3** has a ΔE of +7.9 kcal mol^{−1} and a ΔE^\ddagger of +28.3 kcal mol^{−1}, indicating that the oxidative addition is relatively slow and moderately endothermic.

It is remarkable that the N–O cleaving step starts from the O-bound complex **I2** and not from the more stable N-bound complex **I1**. This is consistent with the fact that the N–O bond, with a bondlength of 1.486 Å in the free substrate, shortens to 1.477 Å in **I1** and lengthens to 1.500 Å in **I2**. To cleave the N–O bond, Rh needs to transfer electron density into the σ^*_{NO} orbital, while avoiding the repulsive interaction from the heteroatom lone pairs. This situation is only obtained when Rh is coplanar with the three-membered ring, which is best achieved by coordination of Rh to the in-plane sp^2 lone pair on oxygen.

The metallacycle **I3** undergoes β -H elimination through the transition state **TS2** leading to the formation of the hydride **I4**. The Rh–O bond is weakened on going from C–O to C=O and the resulting hydride complex (**I4**) is octahedral, N and Cl being mutually *trans*. The exothermic and lower energy barrier β -H elimination, with $\Delta E = -28.4$ kcal mol^{−1} and $\Delta E^\ddagger = +15.9$ kcal mol^{−1}, is more favourable than the endothermic and higher energy barrier oxidative addition. β -H elimination may be assisted by the N lone pair, *via* hyperconjugation of the lone pair into σ^*_{CH} and delocalization of the lone pair into the developing π system of the C–O bond.

At the transition state **TS3** for the reductive elimination, the apical N bends over the Rh₂O₂H plane in order to approach the hydride while the Rh–N and Rh–H bonds elongate. **TS3** connects to the square-planar intermediate **I5** in which the amide is coordinated to Rh *via* O. At **I5**, the Rh–N bond is broken and the new N–H bond forms a hydrogen-bond with the Cl.

The **I4** → **TS3** → **I5** step has a ΔE of −44.6 kcal mol^{−1} and a ΔE^\ddagger of +21.3 kcal mol^{−1}. These values indicate that the N–H reductive elimination is more exothermic than the β -H elimination but involves a moderately higher energy barrier. N–H reductive elimination has been relatively rarely observed.^{26–28} However, the energy released by the overall reaction ($\Delta E = -65.1$ kcal mol^{−1}) is a driving force for going over moderately high energy barriers.

The final amide decooordination from **I5** releases the product and recycles the catalyst. The bond dissociation energy of the amide (+30.3 kcal mol^{−1}) is slightly larger than that of the oxaziridine maybe because of the H-bond between N–H and Cl. However, the bond dissociation energies of the reactant and product are sufficiently similar to keep the catalyst active.

Conclusions

Our data suggests that an atom economic route to amides from imines may be possible using the oxidation/rearrangement strategy of Scheme 1. This would entail a redesign of the overall synthesis *versus* the conventional routes. Better catalysts are desirable for both steps, however, because generality is still not optimal. DFT

studies could not provide a pathway for the metal-free oxaziridine rearrangement in agreement with the need for a catalyst. In contrast with this, in the case of the Rh-catalyzed reaction, the calculations show that the reaction pathway consisting of substrate coordination, oxidative addition (rate-determining), β -H elimination, reductive elimination and then product decooordination is reasonable.

Acknowledgements

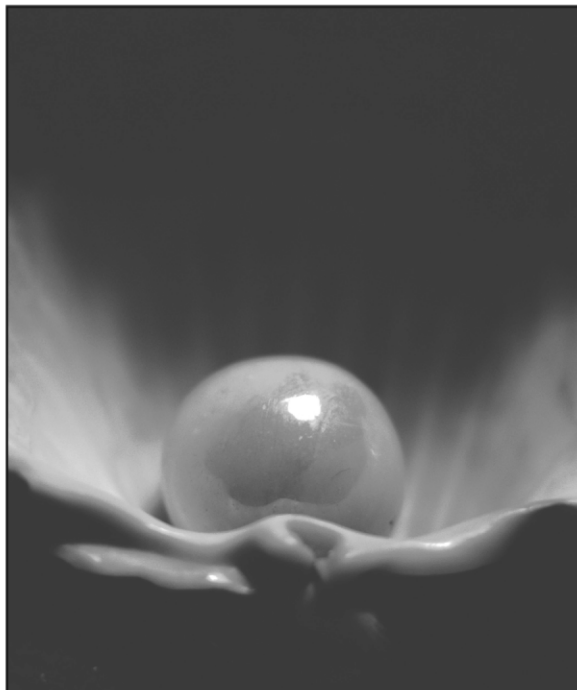
R.H.C, C.H.L., and A.V. thank the U.S. DOE and Johnson Matthey Co. for support. O.E. and D.B. thank the CNRS and the Ministère de l'Education Nationale for funding. D.B. thanks SANOFI-Aventis for a post-doctoral fellowship and R.H.C. also thanks them for funding.

Notes and references

- 1 J. C. Plaquevent, D. Benard and B. Goument, *New J. Chem.*, 1991, **15**, 579–585 and references therein.
- 2 For reviews on early oxaziridine work, see: (a) H. Krimm, *Chem. Ber.*, 1958, **91**, 1057–1068; (b) J. F. Dupin, *Bull. Soc. Chim. Fr.*, 1967, 3085–3092.
- 3 W. D. Emmons, *J. Am. Chem. Soc.*, 1957, **79**, 5739–5754.
- 4 L. Horner and E. Jurgens, *Chem. Ber.*, 1957, **90**, 2184–2189.
- 5 For select examples, see: (a) P. C. B. Page, C. Limousin and V. L. Murrell, *J. Org. Chem.*, 2002, **67**, 7787–7796; (b) L. Bohe, M. Lusinchi and X. Lusinchi, *Tetrahedron*, 1999, **55**, 155–166; (c) Y. Hata and M. Watanabe, *J. Am. Chem. Soc.*, 1979, **101**, 6671–6676.
- 6 K. Kloc, E. Kubicz, J. Mlochowski and L. Syper, *Synthesis*, 1987, 1084–1087.
- 7 D. Mohajer, N. Iranpoor and A. Rezaeifard, *Tetrahedron Lett.*, 2004, **45**, 631–634.
- 8 (a) L. Martiny and K. A. Jorgensen, *J. Chem. Soc., Perkin Trans. 1*, 1995, 699–704; (b) B. J. Aurret, D. R. Boyd and P. B. Coulter, *J. Chem. Soc., Chem. Commun.*, 1984, 463–464.
- 9 J. Kraiem, Y. Kacem, J. Khiari and B. Ben Hassine, *Synth. Commun.*, 2001, **31**, 263–271.
- 10 J. A. Damavandi, B. Karami and M. A. Zolfigol, *Synlett*, 2002, 933–934.
- 11 M. Shailaja, A. Manjula and B. V. Rao, *Synlett*, 2005, 1176–1178.
- 12 B. S. Lane and K. Burgess, *Chem. Rev.*, 2003, **103**, 2457–2473.
- 13 G. M. Rubottom, *Tetrahedron Lett.*, 1969, 3887–3889.
- 14 (a) S. E. Dinizo and D. S. Watt, *J. Am. Chem. Soc.*, 1975, **97**, 6900–6901.
- 15 (a) M. Newcomb and R. A. Reeder, *J. Org. Chem.*, 1980, **45**, 1489–1493; (b) D. R. Boyd, K. M. McCombe and N. D. Sharma, *J. Chem. Soc., Perkin Trans. 1*, 1986, 867–872.
- 16 (a) L. H. Sternbach, E. Reeder and B. A. Koechlin, *J. Org. Chem.*, 1962, **27**, 4671–4672; (b) D. R. Boyd, P. B. Coulter, W. J. Hamilton, W. B. Jennings and V. E. Wilson, *Tetrahedron Lett.*, 1984, **25**, 2287–2288.
- 17 J. Aube, X. Peng, Y. G. Wang and F. Takusagawa, *J. Am. Chem. Soc.*, 1992, **114**, 5466–5467 and references therein.
- 18 K. Suda, T. Umehara and F. Hino, *Chem. Pharm. Bull.*, 1990, **38**, 839–841.
- 19 J. Larsen, K. A. Jorgensen and D. Christensen, *J. Chem. Soc., Perkin Trans. 1*, 1991, 1187–1190.
- 20 S. Y. Kim, G. I. An and H. Rhee, *Synlett*, 2003, 112–114.
- 21 A. Simion, C. Simion, T. Kanda, S. Nagashima, Y. Mitoma, T. Yamada, K. Mimura and M. Tashiro, *J. Chem. Soc., Perkin Trans. 1*, 2001, 2071–2078.
- 22 In slight modification of the published procedure,⁹ 2 mol% of Na₂WO₄ (instead of 10 mol%) was found to be adequate. Further experimental details are described in the ESI†.
- 23 A mixture of oxaziridine (0.25 mmol) 1,3,5-trimethoxybenzene (10 mg) and metal in solvent (5 ml) was heated at reflux for 12 h. For Pd/Rh/Ir cases, air was excluded. Yields were determined by ¹H NMR peak integration 1,3,5-trimethoxybenzene as internal standard.
- 24 DFT calculations were carried out using the hybrid B3PW91 functional. The basis set was the ECP-adapted SDDALL with a set of polarization functions for Rh and Cl and the all-electron 6-31G(d,p) for all other

atoms. Geometry optimizations were carried out without any geometrical constraints. The analytical calculation of frequencies was performed in order to classify each stationary point as a minimum or a transition state. Each transition state was relaxed towards reactants and products using the vibrational data to confirm its nature. All energies in the text are potential energies. The zero-point, thermal and entropy corrections were evaluated to compute enthalpies and Gibbs free energies, which are given in the ESI†. It was verified that the free energy profiles and the potential energy profiles are similar. The references for the level of calculations are given in the ESI†.

- 25 M. J. Frisch, G. W. Trucks, H. B. Schlegel, G. E. Scuseria, M. A. Robb, J. R. Cheeseman, J. A. Montgomery, Jr., T. Vreven, K. N. Kudin, J. C. Burant, J. M. Millam, S. S. Iyengar, J. Tomasi, V. Barone, B. Mennucci, M. Cossi, G. Scalmani, N. Rega, G. A. Petersson, H. Nakatsuji, M. Hada, M. Ehara, K. Toyota, R. Fukuda, J. Hasegawa, M. Ishida, T. Nakajima, Y. Honda, O. Kitao, H. Nakai, M. Klene, X. Li, J. E. Knox, H. P. Hratchian, J. B. Cross, V. Bakken, C. Adamo, J. Jaramillo, R. Gomperts, R. E. Stratmann, O. Yazyev, A. J. Austin, R. Cammi, C. Pomelli, J. Ochterski, P. Y. Ayala, K. Morokuma, G. A. Voth, P. Salvador, J. J. Dannenberg, V. G. Zakrzewski, S. Dapprich, A. D. Daniels, M. C. Strain, O. Farkas, D. K. Malick, A. D. Rabuck, K. Raghavachari, J. B. Foresman, J. V. Ortiz, Q. Cui, A. G. Baboul, S. Clifford, J. Cioslowski, B. B. Stefanov, G. Liu, A. Liashenko, P. Piskorz, I. Komaromi, R. L. Martin, D. J. Fox, T. Keith, M. A. Al-Laham, C. Y. Peng, A. Nanayakkara, M. Challacombe, P. M. W. Gill, B. G. Johnson, W. Chen, M. W. Wong, C. Gonzalez and J. A. Pople, *GAUSSIAN 03 (Revision D.01)*, Gaussian, Inc., Wallingford, CT, 2004.
- 26 M. Kanzelberger, X. Zhang, T. J. Emge, A. S. Goldman, J. Zhao, C. Incarvito and J. F. Hartwig, *J. Am. Chem. Soc.*, 2003, **125**, 13644–13645.
- 27 D. M. Roundhill, *Chem. Rev.*, 1992, **92**, 1–27.
- 28 D. S. Glueck, L. J. N. Winslow and R. G. Bergman, *Organometallics*, 1991, **10**, 1462–1479.



Looking for that **special** research paper from applied and technological aspects of the chemical sciences?

TRY this free news service:

Chemical Technology

- highlights of newsworthy and significant advances in chemical technology from across RSC journals
- free online access
- updated daily
- free access to the original research paper from every online article
- also available as a free print supplement in selected RSC journals.*

*A separately issued print subscription is also available.

Registered Charity Number: 207890

RSCPublishing

www.rsc.org/chemicaltechnology

22030683

Green Chemistry

Cutting-edge research for a greener sustainable future

www.rsc.org/greenchem

Volume 9 | Number 9 | September 2007 | Pages 913–1028



ISSN 1463-9262

RSC Publishing

Green Solvents for Processes
Themed Issue

Wallis *et al.*
Improving the catalytic properties of
K-10 montmorillonite

Cantone *et al.*
Biocatalysis in non-conventional
media



1463-9262(2007)9:9;1-3

Assessing and improving the catalytic activity of K-10 montmorillonite†

Philip J. Wallis,^a Will P. Gates,^{ab} Antonio F. Patti,^{*ac} Janet L. Scott‡^a and Euneace Teoh^a

Received 31st January 2007, Accepted 10th April 2007

First published as an Advance Article on the web 3rd May 2007

DOI: 10.1039/b701504f

K-10 montmorillonite, commonly used as a heterogeneous acid catalyst, was found to vary in the extent of acid-treatment, with some batches exhibiting significantly reduced catalytic activity in Brønsted acid-catalysed reactions. K-10 was thus further treated with HCl of varying concentrations to increase its activity in acid-catalysed reactions. Acid-treated clays exhibited significant enhancements in catalytic activity in three test reactions; tetrahydropyranylation of ethanol, diacetylation of benzaldehyde and esterification of succinic anhydride. Acid-treatment of K-10 was shown to result in protonation, and loss of layer stacking of the clay structure, as determined by powder X-ray diffraction, inductively coupled plasma–optical emission spectroscopy (ICP-OES), diffuse reflectance infrared Fourier transform (DRIFT) spectroscopy and Brunauer–Emmett–Teller (BET) specific surface area measurements. Quantifiable physical changes to the K-10 correlated with measurable increases in catalytic activity. Standard procedures for assessing acid-treated montmorillonite clay catalysts, such as K-10, and procedures for obtaining the most effective catalyst for acid-catalysed reactions, involving analytical and synthetic techniques, were devised.

Introduction

K-10 montmorillonite is a commercially available smectite clay, which has been acid-treated with sulfuric acid, and is used as a catalyst in organic synthesis. K-10 has featured prominently in clay-mediated organic synthesis for many years: it is an effective catalyst for a range of reactions, is safe to handle and is easily separated from reaction mixtures. The utility of clays as catalysts in organic synthesis is reflected in a huge number of reports of synthetic procedures utilising such catalysts, and the reader is referred to a number of recent reviews.¹ Specifically, K-10 montmorillonite is widely considered to be a green heterogeneous catalyst.² Chemists often employ K-10 as purchased, without any further treatment of the clay and accepting the consequences of its use without question. However, in our experience, different batches of K-10 montmorillonite “fresh” from the bottle give highly variable results. Thus, to ensure product quality for laboratory experimentation, we find that K-10 should be characterised and possibly acid-treated before use.

Montmorillonite clay is a hydrated 2 : 1 layered dioctahedral aluminosilicate of the smectite group of clays.³ It is composed of two tetrahedral (predominantly silicate) sheets which are bonded to either side of an octahedral (predominantly aluminate) sheet. Isomorphous substitution of Mg²⁺ for the

octahedral aluminium, and of Al³⁺ for the tetrahedral silicon, results in charge deficit. This layer charge is balanced by hydrated exchangeable cations (e.g., Na⁺ or Ca²⁺) which occupy the surfaces between clay layers, termed the interlayer.³

With respect to catalytic applications, various aspects of acid-activation of montmorillonite have been studied in depth;⁴ however, where previous studies have focused on acid treatment of virgin montmorillonite, the aim of this study is to assess commercially acid treated montmorillonite. Acid activation results in at least four significant changes in the smectite: (1) exchange of the hydrated interlayer charge compensating cations for H⁺ and their release into solution; (2) delamination, or loss of layer stacking of individual clay platelets into dis-oriented aggregates; (3) dissolution of the individual clay platelets and release of the constituent cations into solution; and (4) formation of a hydrous, poorly crystalline and highly porous phase.⁵ In general, changes 1 and 2 precede 3 and 4 in time, but harsh acid-treatment can result in all occurring simultaneously. The final acid activation products arising from the acid-treatment of smectites are hydrous and poorly crystalline silica that may or may not contain some aluminium.⁶ Prolonged acid-treatment can result in complete structural breakdown of the smectite component as inferred from changes in the infrared spectra.⁷ The process of ‘autotransformation’, whereby acid-treated clays are found to self-digest in the solid state, and thus increase the proportion of exchange sites occupied by Al³⁺ or Mg²⁺, is also a significant process relevant to acid-treated clay catalysts.⁸ Autotransformation of acid treated montmorillonite must be considered when using old batches of K-10, as the catalytic activity will decline over time.

The extent of acid-treatment has profound implications for the use of clays as acid catalysts, particularly in synthetic organic chemistry where researchers may use an acid-treated

^aCentre for Green Chemistry, Monash University, Melbourne, Australia. E-mail: Antonio.Patti@sci.monash.edu.au; Fax: +61 03 99054597; Tel: +61 03 99051620

^bDepartment of Civil Engineering, Monash University, Melbourne, Australia

^cSchool of Applied Sciences and Engineering, Monash University, Churchill, Australia. E-mail: Tony.Patti@sci.monash.edu.au

† Electronic supplementary information (ESI) available: Additional experimental data. See DOI: 10.1039/b701504f

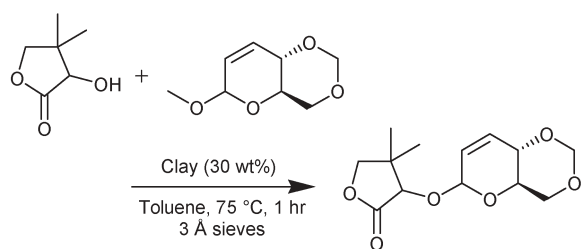
‡ Present address: Unilever Home and Personal Care R&D, Bebington, Wirral, UK.

clay catalyst as-purchased and uncharacterised. Dissolution of the clay and formation of hydrous, amorphous, silica-rich phases in part, promote the catalytic activity of the acid-treated material for either Brønsted and Lewis acid-catalysed reactions.^{8,9} The ability of clay catalysts to promote Brønsted or Lewis acid-catalysed reactions, depends on the exchangeable cations present. Thus, products can be created with properties ranging from an *acidic clay*, represented by H⁺ exchange and delamination, to an *acid digested product*, represented by formation of hydrous silica.

In our study, recently purchased K-10 montmorillonite (referred to herein as K-10A) was treated with hydrochloric acid at various concentrations and temperatures. Treated and untreated clays were utilised in well described acid-catalysed reactions, including tetrahydropyranylation of ethanol,^{10,11} acetylation of benzaldehyde¹² and esterification of succinic anhydride.¹³ Tetrahydropyranylation was included to demonstrate the importance of exchangeable H⁺ to the reaction, where the solvent, ethanol, was also a reagent and thus access to reactive sites was not limited. The acetylation reaction, using reagents dissolved in a solvent, was included to demonstrate the need for greater exposed surface area caused by stronger acid treatment. Finally, the esterification example was selected from the literature where low conversions were obtained with as-supplied K-10, which could be improved by further acid treatment of K-10 to illustrate that the acid treatment proposed in this paper has merit. The important alterations in clay structure and composition were probed using powder X-ray diffraction (XRD), diffuse reflectance infrared Fourier transform (DRIFT) spectroscopy, Brunauer–Emmett–Teller (BET) method for specific surface area,¹⁴ and inductively coupled plasma optical emission spectroscopy (ICP-OES) analysis of supernatants post acid-treatment. The objective of this study was to perform an in-depth assessment of acid-treated K-10 montmorillonite by a variety of physical and synthetic techniques, in order to provide synthetic “green” chemists with tools to achieve the optimal performance of acid activated clay catalysts.

Results and discussion

A routine experiment, the transacetalisation of pantolactone with an auxiliary (Scheme 1), usually catalysed by K-10, was attempted using a batch of K-10 as received (K-10A).¹⁵ Under standard reaction conditions, only starting materials were recovered. Further attempts using more rigorously dried



Scheme 1 Transacetalisation of pantolactone with methyl-2,3-dideoxy-4,6-*O*-methylene- α -D-erythro-hex-enopyranoside, under standard conditions for catalytic comparison.

solvents and K-10A dried at 120 °C under vacuum, again yielded only starting materials. Repeating the reaction using a different batch of K-10 (K-10B) resulted in high (98%) conversion, but only when reactions were allowed to proceed overnight (>12 hours).

To determine possible differences in the composition of the two K-10 batches, powder XRD diffraction patterns were collected. Both K-10A and K-10B were composed predominantly of montmorillonite, with significant quantities of muscovite, quartz and opalised silica and small quantities of feldspar. The most notable difference was that of the relative intensity and location of the basal 001 reflections. With increasing acid-treatment, a decrease in intensity of the basal 001 peak corresponds to disruption of the layered structure of the clay. Relative intensity is reported with respect to other clay reflections in the XRD pattern which are not affected by acid-treatment. The powder XRD pattern of K-10A exhibited an intense basal reflection at 5.74° 2 θ , corresponding to a *d*-spacing of 15.40 Å, whereas K-10B exhibited a weak reflection at 5.94° 2 θ corresponding to a *d*-spacing of 14.88 Å. These differences are likely to be a result of acid-treatment, as the intensity of the basal reflection of montmorillonite relates to the preservation of aggregates composed of well oriented stacks of individual clay platelets.⁴ Higher intensity basal reflections indicate a greater number of repeating clay platelets within the aggregate. A lower intensity indicates a loss of laminar stacking due to poorer orientation of clay platelets, dissolution of the clay platelets and an increased presence of acid digestion products, and possibly the interstratification of numerous interlayer spacings.

Mild acid-treatment can potentially affect the specific surface area, where more strongly delaminated and partially dissolved clays exhibit higher external specific surface areas (as measured by the BET technique). Also, the slight difference in the size of the interlayer (0.52 Å) indicated a possible difference in the composition of cations present: intercalation of protons would result in a smaller interlamellar spacing than intercalation with either hydrated Ca²⁺ or Na⁺. In terms of reactivity, the lack of available protons would fail to promote any Brønsted acid-catalysed reactions at the basal surfaces, and the lower surface area may affect the rate of reaction due to diffusion limitations.

In a pilot study, two acid-treatments were performed on K-10A utilising HCl at 1.0 M and 10 M. The clay was subjected to acid-treatment for six hours at room temperature (21 °C) and recovered by centrifugation. The sample was then repeatedly washed with deionised water until Cl[−] could no longer be detected by a silver nitrate test, and dried at 120 °C. The materials thus prepared were analysed by powder XRD, and notable differences included a significant shift to a smaller interlayer spacing (change of 0.69 Å), as well as a decrease in the intensity of the basal 001 reflection (at 6.01° 2 θ corresponding to a *d*-spacing of 14.71 Å). When the acid-treated clays were compared with the batch K-10A and K-10B for catalytic activity using the synthetic reaction previously described (with a standard set of conditions less forcing than those previously used), K-10A (10 M HCl) yielded significantly higher conversion to product (Table 1) compared with K-10B (23% *versus* 3%) under these conditions, as determined by GC

Table 1 Transacetalisation of pantolactone with methyl-2,3,-dideoxy-4,6-*O*-methylene- α -D-erythro-hex-enopyranoside, conversion at 60 minutes

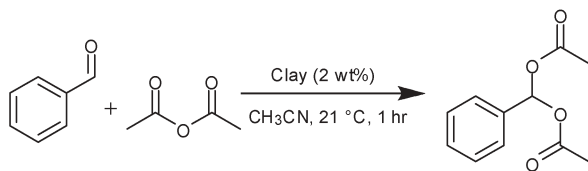
Catalyst	Conversion (%)
K-10A	0
K-10B	3
K-10A (1.0 M HCl treated)	7
K-10A (10 M HCl treated)	23
Silica gel	0
Silica gel (0.1 M HCl)	0

analysis. Furthermore, in general, transacetalisation reactions with other alcohols were complete within 3 hours using K-10A (10 M HCl), as compared with overnight (>12 hours) using K-10B.

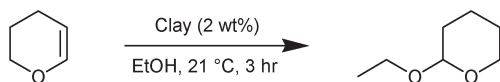
These results prompted a more comprehensive study of the acid-treatment procedure, including analysis by ICP-OES of the acidic supernatants post-treatment, and acid-treated clays by XRD, IR and N₂ adsorption isotherms for surface area determination. Four acid-treatments, ranging in severity, were performed: 0.1 M HCl, 1.0 M HCl, 10 M HCl at 21 °C and 5 M HCl at 80 °C. All treatments were for 6 hours. Treatments were performed in duplicate, using 10 g of K-10A and 200 ml of acid in each case. The resulting acid-treated clays obtained are herein designated: (K-10A) untreated K-10, (K-10A1) 0.1 M HCl treated K-10, (K-10A2) 1.0 M HCl treated K-10, (K-10A3) 10 M HCl treated K-10, (K-10A4) 5 M HCl at 80 °C treated K-10, (K-10B) an additional batch of untreated K-10, and (K-10C) a further additional batch of untreated K-10. The rationale for these treatments was that the 1.0 M HCl and 10 M HCl treatments had improved the catalytic activity of the clay previously, 0.1 M HCl was used to determine whether a fairly dilute acid could be used to cost effectively and more safely achieve an effect for syntheses requiring mildly acidic clays, and 5 M HCl at 80 °C had been used by others to effect a more thorough digestion of montmorillonite.^{6,7}

All four treated clays, as well as K-10A and K-10B, were utilised in two common examples of acid-catalysed transformations: the diacetylation of benzaldehyde (Scheme 2), used to protect aldehydic functional groups and previously shown to be catalysed by acidic clay,¹² and the tetrahydropyranylation of ethanol (Scheme 3).¹⁶

Results for the diacetylation of benzaldehyde (Fig. 1) and the tetrahydropyranylation of ethanol (Fig. 2) show negligible



Scheme 2 Clay-catalysed diacetylation of benzaldehyde to form phenylmethylenediacetate.



Scheme 3 Clay-catalysed tetrahydropyranylation of ethanol to form 2-ethoxy-tetrahydro-2H-pyran.

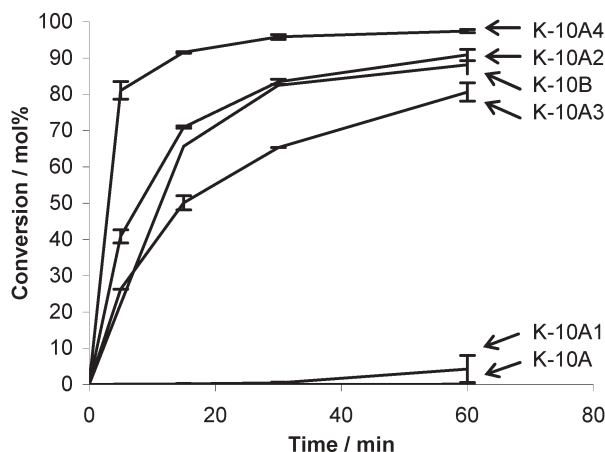


Fig. 1 Diacetylation of benzaldehyde, promoted by: untreated K-10A, 0.1 M HCl treated K-10A1, 1.0 M HCl treated K-10A2, 10 M HCl treated K-10A3, 5 M 80 °C HCl treated K-10A4 and untreated K-10B.

conversion using the untreated K-10A, to quantitative conversion for the strongly acid-treated K-10A4. The changes in reactivity with acid-treatment are significant, and follow the general trend of increasing catalytic activity with stronger acid-treatment of the clay. The two different reactions exhibit different trends of reactivity; the tetrahydropyranylation of ethanol is rapidly promoted by all catalysts, even the lightly acid-treated K-10A1, whereas the degree of diacetylation of benzaldehyde by different treated clays is more differentiated by the degree of acid-treatment, with the weakly treated K-10A1 giving almost no conversion. This may be due to different reaction limiting processes, with the tetrahydropyranylation limited by the availability of protons at the clay surface, and the diacetylation limited by the accessibility of active sites.

Analysis of the acid-treatment supernatants by ICP-OES (Fig. 3) revealed significant differences in the amount of leaching between acid-treatments. With K-10A as the starting

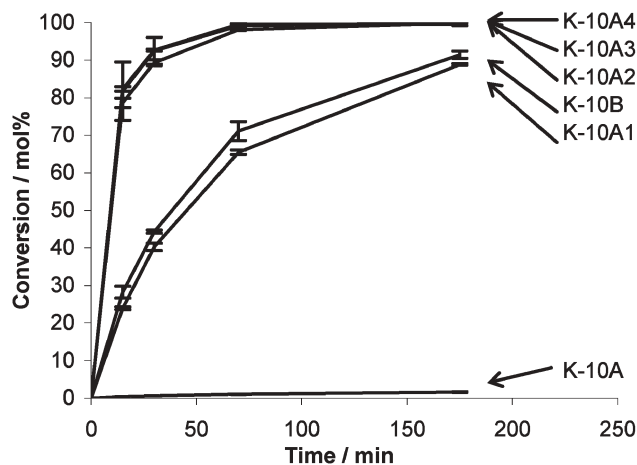


Fig. 2 Tetrahydropyranylation of ethanol, promoted by: untreated K-10A, 0.1 M HCl treated K-10A1, 1.0 M HCl treated K-10A2, 10 M HCl treated K-10A3, 5 M 80 °C HCl treated K-10A4 and untreated K-10B.

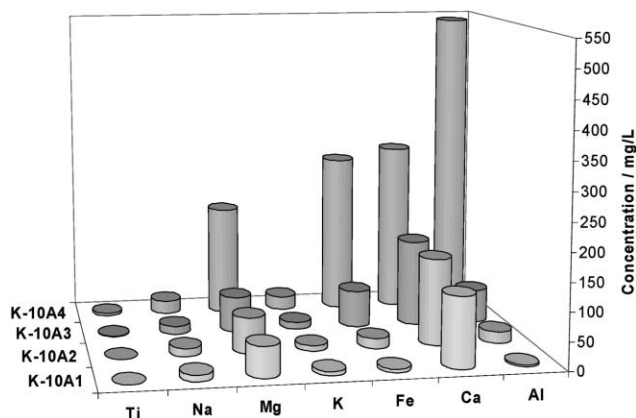


Fig. 3 Concentrations of cations from acidic supernatants (K-10A1–K-10A4) as determined by ICP-OES. Concentration of analytes in mg L^{-1} from 0.7 L of supernatant, treating 10 g of K-10A.

material, we observed that significant amounts of Ca^{2+} and Mg^{2+} were released with light acid treatment (K-10A1). The high levels indicate that the original clay material may have been Ca^{2+} saturated and that this batch of clay largely escaped acid-treatment during the industrial preparation of K-10. Mg^{2+} can be both an exchange cation and a structural cation, but its ready removal, with even the 0.1 M HCl treatment, indicated the presence of a significant amount of exchangeable Mg^{2+} .³

With stronger acid-treatments, removal of additional Mg^{2+} occurred, most likely originating from the clay structure. The Al^{3+} was progressively removed from the octahedral sheets with increasing acid-treatment, with the harshest conditions leaching significant quantities from the clay. Fe^{3+} followed the same trend as Al^{3+} . The rate and extent of clay dissolution has previously been found to increase with the degree of Mg^{2+} and Fe^{3+} substitution for Al^{3+} in the octahedral sheet.⁷ Small amounts of Na^+ and K^+ were leached from the material, most likely originating from the feldspar and muscovite impurities, respectively, but possibly also arising from the smectite inter-layers. The peak corresponding to muscovite in the powder XRD was relatively unaltered, which is consistent with the resistance of muscovite to acid attack. Negligible, but measurable, levels of Ti^{4+} were also leached from the clay.

Powder XRD provided a means for assessing the extent of delamination with acid-treatment (Fig. 4). As acid-treatments increased in severity, the layered structure of the clay was lost, as evidenced by the decrease in intensity of the basal 001 peak. The retention of other clay-related peaks, including the two-dimensional hk index pairs 02–11 20–13 and 06–33,¹⁷ indicated some preservation of the two-dimensional lattice. Note that these decreased, but were still present in the harshest treatment. The quartz impurity was significant in all of the K-10 samples analysed, and was retained despite acid-treatment. From a visual comparison of the powder XRD spectra, it appeared that untreated K-10B lay somewhere between the two stronger acid-treatments K-10A3 and K-10A4, in terms of structural disruption and surface area, although this did not give an idea of the saturation of protons at the surface. Indeed, acid-treated montmorillonite may undergo partial auto-transformation in the solid state when in storage, where the surface

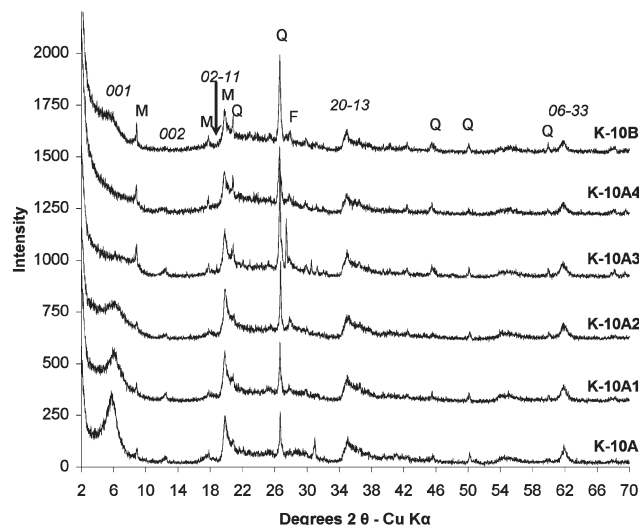


Fig. 4 Stacked powder XRD spectra of treated (K-10A1, K-10A2, K-10A3, K-10A4) and untreated (K-10A, K-10B), indicating impurities (Q: quartz, M: muscovite, F: feldspar) with reflections and hk index pairs attributed to montmorillonite.

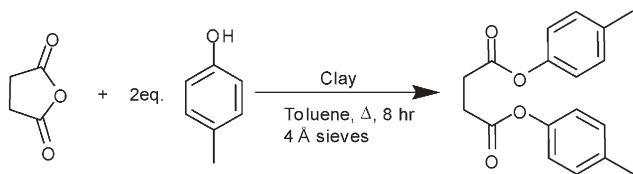
protons attack octahedral sites, and are replaced at exchange sites with metals from the lattice.⁸ Therefore, clays which are determined to have been highly acid-treated by powder XRD, but are still of sub-optimal catalytic activity, could in theory be rejuvenated by a simple acid-wash with a dilute mineral acid.

The external specific surface area of the clay increased with increasing severity of acid-treatment. In this context, external specific surface area, as determined from N_2 adsorption isotherms using the BET method, can also be used to estimate the extent of dissolution of the clay structure.¹⁰ From specific surface measurements made of our acid-treated clays (Table 2) it could be seen that the surface area of K-10A increased from a relatively low $83 \text{ m}^2 \text{ g}^{-1}$ to $270 \text{ m}^2 \text{ g}^{-1}$ for the strongest acid-treatment. The surface area of K-10B was between that of the 10 M HCl (K-10A3) and 5 M HCl at 80°C (K-10A4) treatments, in agreement with the powder XRD data.

Specific surface area measurements give a good indication of the degree of clay acid-treatment: however, they do not allow quantification of the proportion of surface sites saturated with protons. As discussed above, clay that has been strongly acid-treated will have reduced catalytic activity if the remaining exchangeable cations are not protons, a situation which may arise through the process of autotransformation.⁸ In this context, an example was found in the literature where a strongly acid-treated clay gave significantly reduced catalytic activity compared with other H^+ exchanged clays.¹³ In this published example, the esterification of succinic anhydride

Table 2 Specific surface area of treated clays determined by N_2 BET

Clay	Specific surface area/ $\text{m}^2 \text{ g}^{-1}$
K-10A untreated K-10	83
K-10A1 (0.1 M HCl K-10A)	88
K-10A2 (1.0 M HCl K-10A)	110
K-10A3 (10 M HCl K-10A)	130
K-10A4 (5 M 80°C K-10A)	270
K-10B untreated K-10	220



Scheme 4 Clay-catalysed esterification of succinic anhydride to form the succinic acid di-*p*-tolyl ester.

(Scheme 4), K-10 montmorillonite with a specific surface area of $254.6 \text{ m}^2 \text{ g}^{-1}$ yielded 10% of the di-ester, whereas H^+ -montmorillonite with a specific surface area of $33.3 \text{ m}^2 \text{ g}^{-1}$ gave 71% yield under the same conditions.¹³ This result indicated that the K-10 used may not have had sufficient protons at exchange sites when used straight from the bottle, whereas the freshly treated H^+ -montmorillonite, despite having a much lower specific surface area, most likely had a full complement of protons at exchange sites.

The esterification of succinic acid was thus performed using untreated (K-10A-C) and treated (K-10A1-4) K-10 montmorillonite under conditions (see Experimental) similar to those published.¹³ The results are presented as a percentage of conversion from succinic anhydride *versus* time (Fig. 5).

The results show that untreated K-10A gives 9% conversion to the di-ester, in accordance with the literature example.¹³ However, the acid-treated clays gave up to 91% conversion (K-10A4), which was a clear indication that whilst loss of layer stacking is important in optimising activity, protonation of the available exchange sites is essential for the reaction to proceed.

Some further effects of acid-treatment of clay can be observed using FTIR.^{4,7} Infrared spectra of clays were obtained using DRIFT, and spectra were normalised with

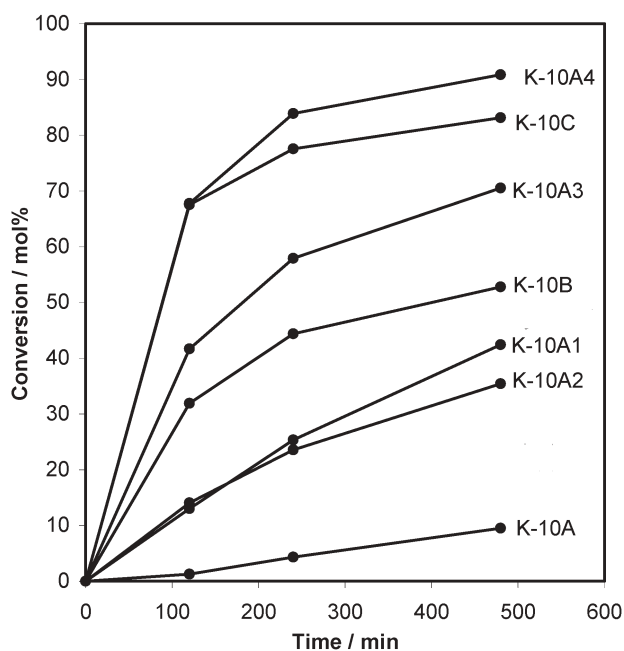


Fig. 5 Esterification of succinic anhydride, promoted by: untreated K-10A, 0.1 M HCl treated K-10A1, 1.0 M HCl treated K-10A2, 10 M HCl treated K-10A3, 5 M 80°C HCl treated K-10A4, untreated K-10B and untreated K-10C.

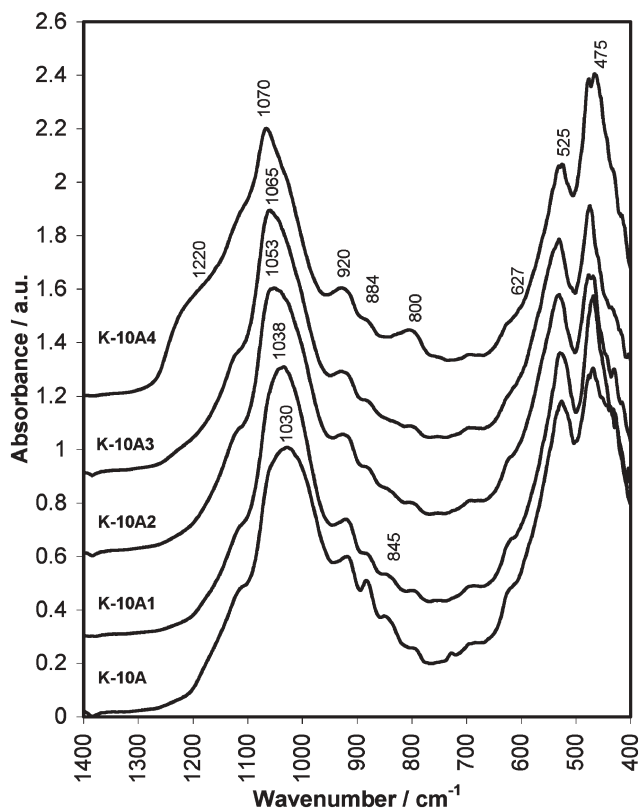


Fig. 6 DRIFT spectra of treated and untreated clays: untreated K-10A, 0.1 M HCl treated K-10A1, 1.0 M HCl treated K-10A2, 10 M HCl treated K-10A3 and 5 M 80°C HCl treated K-10A4. Spectra have been normalised to Si–O stretch, smoothed using a 7-point boxcar function, and stacked.

regards to intensity to the Si–O stretch at $\sim 1030 \text{ cm}^{-1}$, in order to compare the appropriate wavenumber shifts and changes in intensity (Fig. 6). The clearest trend is the shift to higher wavenumber of the main Si–O stretch associated with silica tetrahedra in the clay.^{18,19} As the acid-treatment increases in severity, this peak shifts from $\sim 1030 \text{ cm}^{-1}$ to $\sim 1070 \text{ cm}^{-1}$, indicative of changes to the bonding environment surrounding the tetrahedra. In this case the loss of layer charge due to the removal of (1) substituted cations that provide layer charge and (2) loss of interlayer exchangeable cations that neutralised that charge. The result is Si–O in a different environment due to internal (1) and external (2) factors.²⁰ The most strongly acid-treated clay (5 M HCl 80°C) showed the greatest shift, and also the appearance of a large shoulder centred on 1220 cm^{-1} next to the Si–O band, and a new band near 800 cm^{-1} , both characteristic of amorphous silica.¹⁸ The peaks relating to AlAl–OH (920 cm^{-1}), AlFe–OH (884 cm^{-1}) and AlMg–OH (845 cm^{-1}) deformation bands,¹⁸ decreased in intensity with increasing acid-treatment, with the Mg leaching out rapidly in agreement with ICP-OES data. Furthermore, the Si–O–Al (525 cm^{-1}) lattice deformation band decreased in intensity in relation to the Si–O–Mg (475 cm^{-1}) lattice deformation band.

Infrared can be used to estimate the degree of acid digestion, and hence the potential reactivity of montmorillonite, by observing the location of the Si–O stretch, ranging from

1030 cm^{-1} to 1070 cm^{-1} . In summary, the IR spectra show that the acid-treatment mostly caused exchange of interlayer exchangeable cations, delamination of the layer stacking, and only partially show destruction of the layers. The 5 M HCl at 80 °C for 6 hours is not a harsh enough treatment to completely convert the clay to amorphous silica, which would be characterised by a shift of the Si–O stretch closer to 1100 cm^{-1} and the complete disappearance of the AlAl–OH, AlFe–OH, AlMg–OH, Si–O–Al and Si–O–Mg bands.¹⁸

In summary, the physical effects of the treatment of K-10 montmorillonite with HCl includes protonation of surface exchange sites, proton attack at sites of isomorphous substitution and the resulting removal of Mg^{2+} , dissolution of octahedral sites resulting in removal of Fe^{3+} and Al^{3+} , and the resulting increase in surface area associated with delamination of the smectite and formation of a poorly crystalline silica phase.

Conclusion

In our laboratory we found that acid-treated K10 montmorillonite had variable catalytic activity. Acid-treatment improved the catalytic activity of untreated K-10. Analysis of acid-treated materials by IR, XRD and BET specific surface area indicated that only the harshest acid-treatment resulted in significant dissolution of the smectite and production of hydrous silica.

In general, acid-treatment of K-10 improved the catalytic activity for three synthetic reactions: (1) diacetylation of benzaldehyde, (2) tetrahydropyranylation of ethanol and (3) esterification of succinic anhydride. One batch of untreated K-10 (K-10A) yielded no product conversion in acid-catalysed reactions, whereas other untreated batches yielded moderate (K-10B) and high (K-10C) conversion to product in acid-catalysed reactions. These differences in reactivity reflect either differences in the degree of initial acid treatment by the manufacturers or differences in age of the K-10 product. Reaction yields of both diacetylation and esterification generally increased with strength of acid-treatment, indicating the importance of a highly acid-treated material for this reaction. In contrast, even the mildest acid-treatment provided a material with significantly enhanced catalytic activity for tetrahydropyranylation reactions. Thus, acetylation or esterification is suitable for determining the degree of clay delamination, and tetrahydropyranylation is suitable for determining the degree of clay protonation.

Experimental

Materials and methods

Benzaldehyde, 3,4-dihydro-2H-pyran, pantolactone, acetic anhydride, silver nitrate, succinic anhydride, *p*-cresol and K-10 montmorillonite (K-10A batch 03412CA, K-10B batch 11007BI, K-10C batch 13721JD) were purchased from Sigma–Aldrich chemical company. Ethanol (99.7%), acetonitrile, HPLC-grade acetone, toluene and hydrochloric acid (34%) were purchased from Merck. All reagents and solvents were used as purchased from the supplier without any further purification.

Powder XRD spectra were collected on a Philips PW1140 diffractometer from 2–70° 2 θ at 4° min^{-1} with a step size of 0.02° using a Cu K α source (λ = 1.54 nm). A 1° divergence slit, 1° receiving slit and 0.2° scatter aperture were used. Samples were prepared as front-loaded packed powders in aluminium sample holders.

Diffuse reflectance infrared Fourier transform (DRIFT) spectra were collected using a “Harrick” single bounce mirror assembly on a BIORAD Excalibur Series FTS 3000MX Fourier transform spectrophotometer. A cooled DTGS solid-state detector was employed with an extended KBr beam-splitter, and the sample compartment was purged with dry nitrogen gas prior to and during collection. Spectra were collected in the mid-IR region (400–4000 cm^{-1}) at a resolution of 2 cm^{-1} with 1024 scans co-added. Powdered clay samples were diluted (2.5%) in solid KBr, with KBr as the reference background.

Gas chromatography (GC) was performed on an Agilent 6850 Series II Network GC System, equipped with an FID detector and an HP-1 column (30 m \times 0.32 mm ID). Helium was used as a carrier gas at a flow-rate of 2.0 ml min^{-1} , and a temperature program of 100–300 °C at 10 °C min^{-1} was employed. Detector response factors (from multiple-point calibration curves) were determined for all of the starting materials and reaction products.

Inductively coupled plasma optical emission spectroscopy (ICP-OES) was carried out using a Varian VistaPro ICP-OES with simultaneous CCD and axial view torch detectors. Specific surface areas were determined using the Brunauer–Emmett–Teller (BET) method. Nitrogen vapour adsorption data was obtained for the vapour pressure range (P/P_0) of 0.05 to 0.25. Samples were degassed at 105 °C overnight under vacuum. Surface area was determined based on the linear portion of the BET plot. A silver nitrate (AgNO_3) test was used to determine the presence of chloride ions in washing supernatants after treatment of the clay samples. If halide ions are present, the insoluble precipitate AgCl is formed, and can be visually detected.

Acid-treatment procedures

K-10 montmorillonite (K-10A) (10 g) was placed in a 250 ml round-bottom flask. 0.1 M hydrochloric acid (200 ml) was added, and the suspension was stirred at room temperature (21 °C) for 6 h. The mixture was added to a 1 L polypropylene centrifuge tube containing 250 ml of deionised water, and the residues were washed with a further 250 ml of deionised water. The clay was centrifuged (5000 rpm) for 5 min, and a sample of the supernatant taken for analysis by ICP-OES, and refrigerated until analysis, which occurred within 7 days. The remaining supernatant was discarded, and the clay repeatedly resuspended in deionised water until no Cl^- could be detected in the supernatant by a silver nitrate test, and then washed once more. The clay was recovered, dried in a vacuum oven at 120 °C overnight, then ground in a mortar and pestle and ball-milled for 2 minutes. The final material was a finely divided powder with a beige colour. This procedure was performed in duplicate for each acid-treatment, including 0.1 M HCl, 1.0 M HCl, 10 M HCl at 21 °C and 5 M HCl at 80 °C.

General procedure for transacetalisation of pantolactone with methyl-2,3,-dideoxy-4,6-*O*-methylene- α -D-erythro-hex-enopyranoside

Pantolactone (450 mg, 3.49 mmol) and methyl-2,3,-dideoxy-4,6-*O*-methylene- α -D-erythro-hex-enopyranoside (200 mg, 1.16 mmol) were dissolved in dry toluene (5 mL) followed by the addition of 10 M HCl treated K-10 montmorillonite (60 mg, 30% by weight) and 3A molecular sieves. The reaction mixture was heated to 75 °C. After 20 h the clay was filtered off, and the solvent was evaporated to give a yellow oil. The ratio of *R*- α : *S*- α = 68 : 32 was assessed by GC, which showed 93% conversion.

General procedure for diacetylation of benzaldehyde¹²

Benzaldehyde (1.0 g, 9.4 mmol) and acetic anhydride (1.44 g, 14 mmol) were added together in a test-tube. K-10 (0.0220 g \pm 0.0002 g) was added, the tube sealed, and the mixture stirred at room temperature (21 °C) for 1 h. GC samples were taken at 5, 15, 30 and 60 min by removing a drop of the reaction mixture, diluting with HPLC-grade acetone, and filtering through a Teflon disc filter (0.45 μ m) directly into a GC vial.

General procedure for tetrahydropyranylation of ethanol^{10,11}

Ethanol (1.38 g, 30 mmol) and 3,4-dihydro-2*H*-pyran (2.53 g, 30 mmol) were added together in a test-tube. K-10 (0.0500 \pm 0.0002 g) was added, the tube sealed, and the mixture stirred at room temperature (21 °C) for 3 h. GC samples were taken at 15, 30, 70 and 175 min by removing a drop of the reaction mixture, diluting with HPLC-grade acetone, and filtering through a Teflon disc filter (0.45 μ m) directly into a GC vial.

General procedure for esterification of succinic anhydride with *p*-cresol¹³

Succinic anhydride (0.5080 g) was dissolved in toluene (32.5 ml) with heating. The hot solution was pipetted in portions (8 \times 3.25 ml) into test-tubes. *p*-Cresol (1.6231 g) was dissolved in toluene (17.5 ml) and pipetted in portions (8 \times 1.75 ml) into each tube. The mixtures were heated to reflux (111 °C), and two 4A molecular sieve pellets were added to each tube. K-10 (0.0500 g \pm 0.0002 g) was added to each tube, and stirred at reflux for 8 hours. GC samples were removed at 2, 4 and 8 h, diluted with HPLC-grade acetone and filtered through a Teflon disc filter (0.45 μ m) directly into a GC vial.

Acknowledgements

The authors acknowledge the financial support of the Australian Research Council Special Research Centre for Green Chemistry and PW gratefully acknowledges support in the form of an Australian Postgraduate Award.

References

- 1 J. H. Purnell, *Catal. Lett.*, 1990, **5**, 203–210; R. S. Varma, *Tetrahedron*, 2002, **58**, 1235–1255; M. Balogh and P. Laszlo, *Organic Chemistry Using Clays*, Springer-Verlag, Berlin, 1993, pp. 1–184; G. Nagendrappa, *Resonance*, 2002, **7**, 64–77.
- 2 G. D. Yadav, P. K. Goel and A. V. Joshi, *Green Chem.*, 2001, **3**, 92–99; G. D. Yadav and N. S. Doshi, *Green Chem.*, 2002, **4**, 528–540; K. Toshima, K. Uehara, H. Nagai and S. Matsumura, *Green Chem.*, 2002, **4**, 27–29; T. Jin, S. Zhang and T. Li, *Green Chem.*, 2002, **4**, 32–34; R. Ballini, G. Bosica, R. Maggi, M. Ricciutielli, P. Righi, G. Sartori and R. Sartorio, *Green Chem.*, 2001, **3**, 178–180; P. J. Wallis, K. J. Booth, A. F. Patti and J. L. Scott, *Green Chem.*, 2006, **8**, 333–337.
- 3 B. Velde, *Introduction to Clay Minerals: Chemistry, Origins, Uses and Environmental Significance*, Chapman & Hall, London, 1992, pp. 1–198.
- 4 C. Breen, J. Madejová and P. Komadel, *Appl. Clay Sci.*, 1995, **10**, 219–230.
- 5 R. Fahn, *Proc. Soc. Mining Engineers*, 1979, 1–13.
- 6 I. Tkáč, P. Komadel and D. Müller, *Clay Miner.*, 1994, **29**, 11–19.
- 7 J. Madejová, J. Bujdák, M. Janek and P. Komadel, *Spectrochim. Acta, Part A*, 1998, **54**, 1397–1406.
- 8 C. N. Rhodes and D. R. Brown, *J. Chem. Soc., Faraday Trans.*, 1995, **91**, 1031–1035.
- 9 W. P. Gates, J. S. Anderson, M. D. Raven and G. J. Churchman, *Appl. Clay Sci.*, 2002, **20**, 189–197.
- 10 C. N. Rhodes and D. R. Brown, *Catal. Lett.*, 1994, **24**, 285–291.
- 11 G. F. Woods and D. N. Kramer, *J. Am. Chem. Soc.*, 1947, **69**, 2246.
- 12 L. Jankovič and P. Komadel, *J. Catal.*, 2003, **218**, 227–233.
- 13 C. R. Reddy, P. Iyengar, G. Nagendrappa and B. S. Jai Prakash, *J. Mol. Catal. A: Chem.*, 2005, **229**, 31–37.
- 14 S. Brunauer, P. H. Emmett and E. Teller, *J. Am. Chem. Soc.*, 1938, **60**, 309–319.
- 15 C. R. Strauss, J. L. Scott, D. Saylik and N. Malic, Resolution of chiral alcohols via transacetalization with enantiomerically pure chiral auxiliaries, *PCT Int. Appl.*, WO 2005/070911 A1, 2005.
- 16 S. Hoyer and P. Laszlo, *Synthesis*, 1986, 655–657.
- 17 G. W. Brindley, in *Crystal Structures of Clay Minerals and their X-ray Identification*, ed. G. W. Brindley and G. Brown, Mineralogical Society, London, 1980, pp. 125–195.
- 18 J. Madejová, *Vib. Spectrosc.*, 2003, **31**, 1–10.
- 19 V. C. Farmer, in *The Infrared Spectra of Minerals*, ed. V. C. Farmer, Mineralogical Society, London, 1974, pp. 331–363.
- 20 W. P. Gates, P. Komadel, J. Madejová, J. Bujdák, J. W. Stucki and R. J. Kirkpatrick, *Appl. Clay Sci.*, 2000, **16**, 257–271; P. Komadel, J. Madejová, M. Janek, W. P. Gates, R. J. Kirkpatrick and J. W. Stucki, *Clays Clay Miner.*, 1996, **44**, 228–236.

Enzymatic acylation of levoglucosan in acetonitrile and ionic liquids†

Paola Galletti,* Fabio Moretti, Chiara Samorì and Emilio Tagliavini

Received 8th February 2007, Accepted 29th March 2007

First published as an Advance Article on the web 17th April 2007

DOI: 10.1039/b702031g

The regioselective acylation of carbohydrates is of great interest in many industrial fields. Levoglucosan (1,6-anhydroglucopyranose), an anhydro-sugar easily obtainable through the pyrolytic treatment of cellulose, can be used as an excellent alternative feedstock to get chemicals of interest from renewable resources. Levoglucosan has been acylated in good yields with diverse acyl donors, such as vinyl esters and carboxylic acids with long and short chains in alternative green solvents: CH₃CN, a traditional organic solvent with low ecotoxicity, and ionic liquids. The surfactant properties of 4-*O*-lauryl-levoglucosan have been evaluated and resulted in the range of oil soluble emulsifiers.

Introduction

Enzymatic acylation of sugars has been extensively exploited to obtain sugar fatty acid esters which can be used as non-ionic surfactants in the medicinal, cosmetic and food industries, thanks to their amphiphilic properties. Many enzymes are able to transform regioselectively the most reactive primary hydroxy group in positions 6 of hexopyranoses¹ to obtain derivatives which have been used as additives in detergent formulations,² as emulsifiers in food,³ or can be involved in the synthesis of anti-tumors or anti-inflammatory drugs.⁴

Levoglucosan (1,6-anhydroglucopyranose), an anhydro-sugar derived from glucose, is the main product of cellulose pyrolysis and can be considered as an excellent alternative feedstock to get chemicals of interest from renewable resources;⁵ in levoglucosan, the positions 1 and 6 form an acetalic function and all the remaining secondary hydroxy groups are in the axial position; for these reasons, levoglucosan is less reactive than glucose either to chemical or enzymatic attack, in particular the regioselective acylation of a single secondary OH function represents a very challenging task.

Enzymatic acetylation on levoglucosan was successfully accomplished in the 1990s by means of several lipases using vinyl acetate as both the acyl donor and the reaction solvent.⁶ To our knowledge, other acyl donors or the use of other solvents in which the enzymatic acylation of levoglucosan is performed have never been reported. In particular, the use of carboxylic acids instead of vinyl esters would be environmentally beneficial for both the reduced formation of by-products and the reaction atom economy.⁷ Exploiting lipophilic, long-chain carboxylic acid derivatives as acyl donors for the acylation of highly polar sugars is quite problematic for the different solubility of the two reagents in organic solvents. Few polar solvents, such as pyridine, DMSO, DMF and THF, are

able to dissolve carbohydrates, but these solvents usually inactivate the enzyme and cannot be used in food manufacturing for safety reasons; on the contrary, acetonitrile is able to dissolve levoglucosan in very high concentrations and is recognized as poorly toxic.⁸

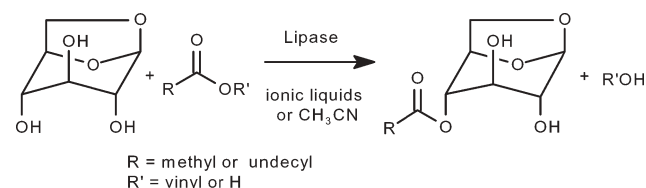
Room temperature ionic liquids are considered green recyclable solvents alternative to the traditional volatile organic solvents, because of their unique chemical and physical properties. In particular, 1,3-dialkylimidazolium-based ionic liquids have emerged as alternative reaction media for both transition metal and enzymatic catalysis.⁹ Thanks to their peculiar solvating properties they are particularly interesting for enzymatic transformations of carbohydrates, especially with lipophilic acyl donors as in the case of long-chain carboxylic acids.^{1b,10}

Herein we present our data on the enzymatic acylation of levoglucosan with a variety of acyl donors and enzymes in green solvents; in particular, we compared the enzymatic activity in CH₃CN with that in three ionic liquids.

Results and discussion

We have performed the enzymatic acylation of levoglucosan using various enzymes, acyl donors and solvents (Scheme 1). Results are reported in Tables 1 and 2.

As ionic liquids we have chosen the commercially available and widely used [BMIm][BF₄], together with [MOEMIm][BF₄] and [MOEMIm][dca], which have been prepared by anion exchange starting from the corresponding chlorides.¹¹ [MOEMIm][dca] in particular is a recently introduced ionic liquid useful in carbohydrate chemistry¹² and characterized by a low toxicity against aquatic organisms.¹³ For acyl donors we



Scheme 1

Interdepartmental Research Centre for Environmental Sciences (CIRSA), University of Bologna, Via S. Alberto 163, 48100 Ravenna, Italy. E-mail: paola.galletti@unibo.it; Fax: +39 0544 937411; Tel: +39 0544 937353

† Electronic supplementary information (ESI) available: Evaluation of surfactant active properties. See DOI: 10.1039/b702031g

Table 1 Enzymatic acetylation of levoglucosan **1** in CH₃CN and ionic liquids^a with vinyl acetate **2a** and acetic acid **2b**

$\text{1} + \text{2 a: R = CH=CH}_2 \text{ or 2 b: R = H} \xrightarrow[\text{55}^\circ\text{C}]{\text{lipase, solvent}} \text{3a, 3b, 4a, 4b, 4c} + \text{ROH}$

Entry	Solvent	Enzyme ^b	2 (2 equiv.) ^c	Yield (%) ^d				
				3a	3b	4a	4b	4c
1	CH ₃ CN	Porcine liver esterase	2a	2	—	—	—	—
2	CH ₃ CN	<i>Candida rugosa</i>	2a	—	—	—	—	—
3	CH ₃ CN	<i>Candida cylindracea</i>	2a	—	—	—	—	—
4	CH ₃ CN	Chymotrypsin	2a	—	—	—	—	—
5	CH ₃ CN	PS (free form)	2a	63	—	2	—	3
6	CH ₃ CN	PS	2a	74	—	9	—	11
7	CH ₃ CN	CAL B	2a	59	—	2	—	2
8	CH ₃ CN	PS	2b	6	—	—	—	—
9	CH ₃ CN	CAL B	2b	5	—	—	—	—
10	CH ₃ CN	PS	2a	76	—	14	—	10
11	[MOEMIm][BF ₄]	CAL B	2a	43	—	8	—	7
12	[MOEMIm][BF ₄]	CAL B	2b	31	—	—	—	—
13	[BMIm][BF ₄]	CAL B	2a	22	—	4	—	3
14	[BMIm][BF ₄]	CAL B	2b	29	—	—	—	—
15	[MOEMIm][dca]	CAL B	2a	61	5	6	9	9
16	[MOEMIm][dca]	CAL B	2b	10	1	1	2	1
17	[MOEMIm][BF ₄]	PS	2a	39	—	7	—	10
18	[MOEMIm][BF ₄]	PS	2b	27	10	3	3	5
19	[BMIm][BF ₄]	PS	2a	18	—	1	—	5
20	[BMIm][BF ₄]	PS	2b	15	—	—	—	—
21	[MOEMIm][dca]	PS	2a	30	—	1	2	2
22	[MOEMIm][dca]	PS	2b	25	—	—	—	—

^a MOEMIm = 1-Methoxyethyl-3-methylimidazolium; BMIm = 1-butyl-3-methylimidazolium; dca = dicyanamide. ^b PS = lipase from *Pseudomonas cepacea* immobilized on ceramic particles; CAL B = lipase immobilized from *Candida antarctica* lipase B, Novozym[®] 435. ^c When **2b** is used 4 Å MS were added to the reaction mixture. ^d Yields of the products purified by column chromatography as a mixture of **3a** and **3b** and as a mixture of **4a**, **4b** and **4c**; the composition of each mixture was established by GC and confirmed also by ¹H NMR analysis.

used vinyl acetate and vinyl laurate, together with the corresponding carboxylic acids, acetic and lauric acids.

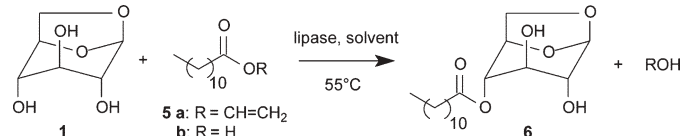
In a typical procedure, levoglucosan was dissolved in the chosen solvent and incubated with the enzyme in the presence of the acyl donor at 55 °C. When we used carboxylic acids, we added 4 Å molecular sieves to trap *in situ* water formed in the reaction and avoid product hydrolysis. Acylation was monitored by TLC and GC–MS; after five days the enzyme and the molecular sieves were filtered off and the products isolated by flash chromatography. Results using vinyl acetate and acetic acid as acyl donors are reported in Table 1.

First experiments were devoted to an enzyme screening. As enzymes we screened several lipases, either in their free form or supported on ceramic particles; as expected, supported lipases afforded better results in both CH₃CN and in ionic liquids. In particular, free enzymes like Porcine liver esterase, lipases from *Candida rugosa*, *C. cylindracea*, and chymotrypsin do not catalyze the reaction in CH₃CN (entries 1–4); the best results were obtained with immobilized lipases from *Pseudomonas cepacea* (PS, immobilized on ceramic particles) and from *Candida antarctica* B (CAL B, Novozym[®] 435). As the results in Table 1 show, 4-*O*-acetyl levoglucosan **3a** is the main product in any reaction condition, but conversion of **1** and

yields are highly variable. The formation of mixtures of diacetates **4a–c** and occasionally of **3b** is also observed.

When vinyl acetate is used as the acyl donor, acetonitrile is a good solvent for the enzymatic acetylation of levoglucosan, and good yields are obtained with both CAL B and PS (Table 1, entries 6, 7 and 10). Also, ionic liquids showed good performances and the yields obtained in [MOEMIm][dca] with vinyl acetate (entry 15) are high and similar to those in CH₃CN (entries 7). Using acetic acid as the acyl donor, the reaction proceed poorly in CH₃CN (entries 8 and 9), whereas a 30% yield could be obtained in [MOEMIm][BF₄] with both enzymes (entries 12 and 18). Results in [BMIm][BF₄] are always inferior to those in [MOEMIm][BF₄], with both immobilized lipases and acyl donors, suggesting that the enzymatic activity is strongly influenced by the change of the cation. For what concerns the anion modification, comparing data obtained in [MOEMIm][BF₄] and [MOEMIm][dca], a strong anion influence on reaction yields using PS does not appear, whereas results with CAL B and vinyl acetate in [MOEMIm][dca] are much better.

In order to obtain more lipophilic sugar derivatives and extend the reaction scope, we also performed the enzymatic acylation by reacting **1** with vinyl laurate **5a** or lauric acid **5b**,

Table 2 Reaction of **1** in CH₃CN and ionic liquids with vinyl laurate **5a** and lauric acid **5b**


Entry	Solvent	Enzyme ^a	5 (2 equiv.)	6 Yield (%) ^b
1	CH ₃ CN	PS	5a ^c	26
2	CH ₃ CN	PS	5a	58
3	CH ₃ CN	PS	5a ^d	73
4	CH ₃ CN	<i>Candida cylindracea</i>	5a ^c	6
5	CH ₃ CN	CAL B	5a	24
6	CH ₃ CN	PS	5b ^e	13
7	CH ₃ CN	CAL B	5b ^e	40
8	[MOEMIm][BF ₄]	CAL B	5a	13
9	[MOEMIm][BF ₄]	CAL B	5b ^e	9
10	[BMIm][BF ₄]	CAL B	5a	10
11	[BMIm][BF ₄]	CAL B	5b ^e	7
12	[MOEMIm][dca]	CAL B	5a	19
13	[MOEMIm][dca]	CAL B	5b ^e	37
14	[MOEMIm][BF ₄]	PS	5a	7
15	[MOEMIm][BF ₄]	PS	5b ^e	5
16	[BMIm][BF ₄]	PS	5a	11
17	[BMIm][BF ₄]	PS	5b ^e	6
18	[MOEMIm][dca]	PS	5a	4
19	[MOEMIm][dca]	PS	5b ^e	5

^a PS = lipase from *Pseudomonas cepacea* immobilized on ceramic particles; CAL B = lipase immobilized from *Candida antarctica* lipase B, Novozym[®] 435. ^b Yields of the isolated product purified by column chromatography. ^c Reaction carried out at room temperature. ^d 3 equiv. of **5a** were used. ^e When **5b** is used 4 Å MS were added to the reaction mixture.

again comparing the results obtained in CH₃CN with those in ionic liquids (Table 2).

The acylation reaction with long-chain acyl donors was performed under the same reaction conditions as used for acetylation and afforded **6** as the sole product; no regioisomeric laurate esters or diacylated derivatives were observed. As Table 2 shows, using vinyl laurate as the acyl donor the best results were obtained in CH₃CN with immobilized lipase from *Pseudomonas cepacea* (entries 2 and 3). Enzyme CAL B worked better in combination with lauric acid and [MOEMIm][dca] (entry 13); in fact, the yield of **6** is the double of that obtained with vinyl esters in the same solvent (entry 12). Both [BMIm][BF₄] and [MOEMIm][BF₄] proved to be unsuitable solvents for this reaction, affording disappointing yields of **6**. This trend confirms what was observed for the acetylation reaction.

The preliminary assessment of the surfactant active properties of products **3a** and **6** has been carried out by measuring the surface tension modification induced and the HLB (hydrophile–lipophile balance) value. The HLB value has been estimated by the ¹H NMR spectrum through integration of the proton signals from the lipophilic and hydrophilic parts of the molecule.¹⁴ In the case of compound **3a**, a HLB value of 15.6 resulted, which corresponds to a hydrophilic oil-in-water emulsifier; in the case of compound **6**, we obtained a HLB value of 5.9 which indicates a lipophilic water-in-oil emulsifier.¹⁵ The surface tension modification has been measured using the pendant drop method.¹⁶ While compound **3a** is able to significantly lower the surface tension of water only at high concentration, compound **6** shows good surfactant properties at very low surface concentration

(51 mN m^{−1} at 0.003 ng mm^{−2} and 45 mN m^{−1} at 0.019 ng mm^{−2}). Thus, as expected, HLB values and surface tension modifications suggest the possibility of fine tuning the surfactant properties of levoglucosan esters by choosing the most suitable chain length.

Conclusion

In conclusion we can say that both acetonitrile and [MOEMIm][dca] are useful green, poorly toxic solvents for the lipase-catalyzed acylation of levoglucosan with short- or long-chain acylating reagents, while other ionic liquids are less suitable solvents. The cheapest and easily available carboxylic acids can effectively substitute vinyl esters as acylating agents, but in this case the ionic liquids are the solvent of choice.

The reaction times are quite long, but notwithstanding the intrinsic lesser reactivity of levoglucosan if compared with glucose, it is important to note that isolated yields obtained with free carboxylic acid in levoglucosan acylation are comparable with those reported in the literature for glucose.¹⁰ The herein described procedures together with the evaluation of promising product surfactant properties significantly enhance the potentialities of levoglucosan, the most easily available anhydro-sugar from biomass conversion.

Experimental

General

Most chemicals were purchased from Aldrich and used without further purification; [BMIm][BF₄] was purchased from Merck, [MOEMIm][BF₄] and [MOEMIm][dca] were

prepared according to ref. 11. Reactions were monitored by means of TLC using silica gel sheets (Merck 60 F₂₅₄); the products were separated by flash chromatography on silica gel (Aldrich, 230–400 mesh); melting points were determined on a Electrothermal 9100 and were uncorrected; FT-IR spectra were measured on a Nicolet 380 FT spectrometer as films between NaCl plates and reported in cm⁻¹; optical rotations were measured on a Perkin Elmer Polarimeter 343, [α]_D values are given in 10¹ deg cm² g⁻¹; ¹H and ¹³C NMR spectra were recorded using a 5 mm probe on a Varian Gemini 200, Varian Inova 300 or VARIAN Mercury 400 spectrometer, all chemical shifts have been quoted relative to deuterated solvent signals with chemical shifts (δ) given in ppm and coupling constants (*J*) values given in Hz. GC–MS spectra were obtained using a VARIAN 3400 gas chromatograph on a SUPELCO SPB-5 capillary column (temperature programme: 50 °C for 5 min then 10 °C min⁻¹ to 300 °C) coupled with a mass spectrometer (ion trap) SATURN 2000 or SATURN II; HPLC–MS: Agilent Technologies HP1100, column ZORBAX-Eclipse XDB-C8 Agilent Technologies, mobile phase: H₂O–CH₃CN, gradient: from 10 to 100% of CH₃CN in 25 min then 100% of CH₃CN, flux 0.5 cm³ min⁻¹, coupled with an Agilent Technologies MSD1100 single-quadrupole mass spectrometer, full-scan mode from *m/z* 50 to 2600, scan time 0.1 s in positive ion mode, ESI spray voltage 4500 V, nitrogen gas 35 psig, drying gas flow 11.5 cm³ min⁻¹, fragmentor voltage 20 V; surface tension measurements have been performed by a SINTECH PAT1 tensiometer at ISAC-CNR, Bologna, Italy.

[MOEMIIm][BF₄]. A mixture of 2-chloroethyl methyl ether (21.9 cm³, 0.24 mol) and 1-methylimidazole (15.9 cm³, 0.20 mol) was stirred at 80 °C for two days under nitrogen. The mixture was cooled to room temperature and ethyl acetate (70 cm³) was added, causing precipitation of 1-methoxyethyl-3-methylimidazolium chloride as a white solid. The solid was recovered by filtration, washed with ethyl acetate and diethyl ether and added to a suspension of NaBF₄ (25.2 g, 0.23 mol) in acetone (75 cm³). The mixture was stirred for two days at room temperature; the sodium halide precipitate was removed by filtration and the filtrate concentrated to an oil by rotary evaporation. The oil was diluted with CH₂Cl₂ (100 cm³) and filtered through silica gel. The solution was washed twice with a small amount of saturated sodium carbonate aqueous solution (CH₂Cl₂–NaHCO₃ aq, 10 : 1) and dried over anhydrous Na₂SO₄. The solvent was removed by rotary evaporation, giving a yellow oil (14.89 g, 32%), (Found: C, 36.78; H, 5.79; N, 12.21. C₇H₁₃BF₄N₂O requires: C, 36.88; H, 5.75; N, 12.29%). δ_{H} (300 MHz, acetone-*d*₆) 3.36 (3H, s, OCH₃), 3.74 (2H, t, *J* 4.5, OCH₂CH₂N), 3.96 (3H, s, CH₃N), 4.38 (2H, t, *J* 4.5, OCH₂CH₂N), 7.27 (1H, m, NCH=CHN), 7.40 (1H, m, NCH=CHN), 8.81 (1H, s, N=CHN); δ_{C} (75 MHz, acetone-*d*₆) 36.4, 50.1, 58.7, 70.7, 123.7, 124.3, 137.8.

[MOEMIIm][dca]. A mixture of 2-chloroethyl methyl ether (21.9 cm³, 0.24 mol) and 1-methylimidazole (15.9 cm³, 0.20 mol) was stirred at 80 °C for two days under nitrogen. The mixture was cooled to room temperature, and ethyl acetate (70 cm³) was added, causing precipitation of 1-methoxyethyl-3-methylimidazolium chloride as a white solid. The solid was

recovered by filtration, washed with ethyl acetate and diethyl ether and added to a suspension of NaN(CN)₂ (20.5 g, 0.23 mol) in acetone (75 cm³). The mixture was stirred for two days at room temperature; the sodium halide precipitate was removed by filtration and the filtrate concentrated to an oil (37.05 g) by rotary evaporation. The oil was diluted with acetone and filtered through silica gel (30 g). The solvent was removed by rotary evaporation, giving a light yellow oil (30.78 g, 74.2%), (Found: C, 52.11; H, 6.39; N, 33.73. C₉H₁₃N₃O requires: C, 52.16; H, 6.32; N, 33.79%). δ_{H} (400 MHz, acetone-*d*₆) 3.35 (3H, s, OCH₃), 3.81 (2H, t, *J* 5.2 Hz, OCH₂CH₂N), 4.07 (3H, s, CH₃N), 4.53 (2H, t, *J* 5.2, OCH₂CH₂N), 7.71 (1H, m, NCH=CHN), 7.75 (1H, m, NCH=CHN), 9.08 (1H, s, N=CHN); δ_{C} (100 MHz, acetone-*d*₆) 36.1, 49.8, 70.2, 120.0, 123.3, 123.9, 137.4.

General procedure for the lipase-catalyzed acylation of 1,6-anhydroglucopyranose

In a typical experiment, 1,6-anhydroglucopyranose (levoglucosan) (0.25 mmol, 40.5 mg) and the chosen acyl donor (0.5 mmol) were introduced into a flask, after that the solvent (5 cm³ of CH₃CN or 0.6 cm³ of ionic liquids) and the supported enzyme (7 mg) were added. The mixture was stirred at 50–60 °C for about five days, and the course of the reaction was monitored by means of TLC and GC–MS. To stop the reaction the enzyme was filtered off and the products of the reaction separated by flash chromatography. The monoesters were easily separated from the diesters, which were obtained as a mixture. Compounds **3a,b** and **4a–c** are known⁶ and have been identified by comparison of ¹H NMR spectra and GC–MS analysis.

4-*O*-Acetyl-1,6-anhydroglucopyranose (3a). δ_{H} (300 MHz, CDCl₃) 2.17 (3H, s, CH₃COO), 3.58 (1H, m, H-2), 3.79 (1H, m, H-3), 3.81 (1H, dd, *J* 7.8 and 5.4, H-6 *exo*), 4.23 (1H, dd, *J* 0.5 and 7.8, H-6 *endo*), 4.60 (1H, d, *J* 5.4, H-5), 4.74 (1H, s, H-4), 5.51 (1H, s, H-1); GC rt 18.4 min; *m/z* (EI) 205 (*M*⁺ + 1, 40%), 187 (*M*⁺ – OH, 25), 127 (35), 115 (45), 97 (55), 69 (90), 60 (100).

2-*O*-Acetyl-1,6-anhydroglucopyranose (3b). δ_{H} (200 MHz, CDCl₃) 2.12 (3H, s, CH₃COO), 3.62 (2H, m, H-4 + H-3), 3.83 (1H, m, H-6 *exo*), 4.08 (1H, d, *J* 7.2, H-6 *endo*), 4.60 (1H, m, H-5), 4.76 (1H, s, H-2), 5.46 (1H, s, H-1); GC rt 19.1 min; *m/z* (EI) 205 (*M*⁺ + 1, 1%), 187 (*M*⁺ – OH, 5), 145 (20), 97 (55), 73 (100).

2,4-*O*-Diacetyl-1,6-anhydroglucopyranose (4a). δ_{H} (200 MHz, CDCl₃) 2.16 (3H, s, CH₃COO), 2.17 (3H, s, CH₃COO), 2.76 (1H, s, OH), 3.79 (2H, m, H-3, H-6 *exo*), 4.18 (1H, d, *J* 7.6, H-6 *endo*), 4.61 (3H, m, H-2 + H-4 + H-5), 5.49 (1H, s, H-1); GC rt 20.3 min; *m/z* (EI) 247 (*M*⁺ + 1, 35%), 229 (*M*⁺ – OH, 10) 157 (10), 115 (45), 98 (55), 69 (100).

3,4-*O*-Diacetyl-1,6-anhydroglucopyranose (4b). δ_{H} (200 MHz, CDCl₃) 2.17 (3H, s, CH₃COO), 2.18 (3H, s, CH₃COO), 3.80 (2H, m, H-2 + H-6 *exo*), 4.18 (1H, d, *J* 8.4, H-6 *endo*), 4.61 (2H, m, H-4 + H-5), 4.80 (1H, m, H-3), 5.49 (1H, s, H-1); GC

rt 19.7 min; m/z (EI) 247 ($M^+ + 1$; 5%), 229 ($M^+ - OH$, 7), 187 ($M^+ - OAc$, 15), 98 (70), 81 (100).

2,3-*O*-Diacetyl-1,6-anhydroglucopyranose (4c). δ_H (300 MHz, $CDCl_3$) 2.12 (3H, s, CH_3COO), 2.15 (3H, s, CH_3COO), 2.81 (1H, d, J 10.8, OH), 3.59 (1H, d, J 10.8, H-4), 3.83 (1H, dd, J 6 and 7.5, H-6 *exo*), 4.11 (1H, d, J 7.5, H-6 *endo*), 4.60 (1H, d, J 6, H-5), 4.63 (1H, s, H-3), 4.82 (1H, s, H-2), 5.45 (1H, s, H-1); GC rt 19.3 min; m/z (EI) 247 ($M^+ + 1$, 15%); 229 ($M^+ - OH$, 25), 187 ($M^+ - OAc$, 30), 157 (25), 115 (100), 81 (75).

4-*O*-Lauryl-1,6-anhydroglucopyranose (6). White crystals, mp 75–78 °C, (Found: C, 62.9; H, 9.2. $C_{18}H_{32}O_6$ requires: C, 62.8; H, 9.4%). $[\alpha]_D = -58$ (c 1.5 in CH_2Cl_2). ν_{max} (CH_2Cl_2)/ cm^{-1} : 3350br (OH), 3230br (OH) and 1732s (ester); δ_H (400 MHz, $CDCl_3$) 0.89 (3 H, t, J 6.4, CH_3CH_2), 1.27 [16 H, m, $CH_3(CH_2)_8$], 1.65 (3 H, m, $CH_2CH_2COO + OH$), 2.40 (2H, t, J 7.6, CH_2CH_2COO), 2.68 (1H, bs, OH), 3.57 (1 H, m, H-2), 3.78 (1 H, m, H-3), 3.81 (1H, dd, J 5.6 and 8.0, H-6 *exo*), 4.24 (1H, dd, J 0.6 and 8.0, H-6 *endo*), 4.58 (1H, d, J 5.6, H-5), 4.74 (1H, d, J 1.6, H-4), 5.51 (1H, s, H-1); δ_C (50 MHz, $CDCl_3$) 14.1, 22.6, 24.9, 29.0, 29.2, 29.3, 29.4, 29.6 (2C), 31.8, 34.2, 65.7, 70.0, 71.3, 72.5, 74.3, 102.0, 172.8; GC rt 28.8 min; m/z (EI) 345 ($M^+ + 1$, 1%), 201 (40), 183 (70), 165 (10), 155 (20), 143 (5), 129 (20), 109 (40), 98 (75), 81 (40), 69 (75), 57 (100); m/z (ESI) 345 [$M + H$] $^+$, 362 [$M + H_2O$] $^+$, 367 [$M + Na$] $^+$.

Acknowledgements

We acknowledge the ministry MiUR and the University of Bologna for funding. We thank Dr Stefano Decesari of ISAC – CNR, Area della ricerca Via Gobetti 101, 40129 Bologna, Italy for measurements and discussion about surface tension.

References

- (a) M. J. Kim, M. Y. Choi, J. K. Lee and Y. Ahn, *J. Mol. Catal. B: Enzym.*, 2003, **26**, 115–118; (b) F. Ganske and U. T. Bornscheuer, *Org. Lett.*, 2005, **7**, 3097–3098; (c) X. Zhang, T. Kobayashi, S. Adachi and R. Matsuno, *Biotechnol. Lett.*, 2002, **24**, 1097–1100;
- (d) P. Degn, L. H. Pedersen, J. Duus and W. Zimmermann, *Biotechnol. Lett.*, 1999, **21**, 275–280; (e) J. A. Arcos, M. Bernabè and C. Otero, *Biotechnol. Bioeng.*, 1998, **57**, 53–60; (f) B. C. Youan, A. Hussain and N. T. Nguyen, *AAPS PharmSci*, 2003, **5**(2), article 22.
- M. J. Donnelly and J. D. Bu'Lock, *J. Am. Oil Chem. Soc.*, 1988, **65**, 284–289; A. Ducret, A. Giroux, M. Trani and R. Lortie, *J. Am. Oil Chem. Soc.*, 1996, **73**, 109–113; G. Sekeroglu, S. Fadiloglu and E. Ibanoglu, *J. Sci. Food Agric.*, 2002, **82**, 1516–1522.
- J. P. Gibbons and C. J. Swanson, *J. Am. Oil Chem. Soc.*, 1959, **36**, 553–559.
- P. J. Garregg, *Acc. Chem. Res.*, 1992, **25**, 575–580.
- Z. J. Witzczak, in *Levoglucosenone and Levoglucosans: Chemistry and Applications*, ed. Z. J. Witzczak, ATL press, Mount Prospect, 1994, ch. 10, 13 and 14.
- C. Chon, A. Heisler, N. Junot, F. Levayer and C. Rabiller, *Tetrahedron: Asymmetry*, 1993, **4**, 2441–2444; N. Junot, C. Tellier and C. Rabiller, *J. Carbohydr. Chem.*, 1998, **17**, 99–115.
- B. M. Trost, *Science*, 1991, **254**, 1471–1477.
- D. J. Couling, R. J. Bernot, K. M. Docherty, J. K. Dixon and E. J. Maginn, *Green Chem.*, 2006, **8**, 82–90; J. Ranke, K. Mölter, F. Stock, U. Bottin-Weber, J. Poczo butt, J. Hoffmann, B. Ondruschka, J. Filser and B. Jastorff, *Ecotoxicol. Environ. Saf.*, 2004, **58**, 396–404; R. J. Bernot, M. A. Brueseke, M. A. Evans-White and G. A. Lamberti, *Environ. Toxicol. Chem.*, 2005, **24**(1), 87–92; M. T. Garcia, N. Gathergood and P. J. Scammells, *Green Chem.*, 2005, **7**, 9–14.
- Z. Yang and W. Pan, *Enzyme Microb. Technol.*, 2005, **37**, 19–28; B. J. Frost, *J. Am. Chem. Soc.*, 2006, **128**, 7112.
- F. Ganske and U. T. Bornscheuer, *J. Mol. Catal.*, 2005, **36**, 40–42.
- S. Park and R. J. Kazlauskas, *J. Org. Chem.*, 2001, **66**, 8395–8401; L. C. Branco, J. N. Rosa, J. J. M. Ramos and C. A. M. Afonso, *Chem.–Eur. J.*, 2002, **8**, 3671–3677.
- Q. Liu, M. H. A. Janssen, F. van Rantwijk and R. A. Sheldon, *Green Chem.*, 2005, **7**, 39–42.
- C. Samori, A. Pasteris, P. Galletti and E. Tagliavini, *Environ. Toxicol. Chem.*, 2007, submitted.
- A. Rabaron, G. Cavè, F. Puisieux and M. Seiller, *Int. J. Pharm.*, 1993, **99**, 29–36; G. Ben-Et and D. Tatarsky, *J. Am. Oil Chem. Soc.*, 1972, **49**, 499–500; J. R. Berquerio, M. Bao and J. J. Casares, *An. Quim.*, 1978, **74**(529–530), 1941–1942.
- R. T. Otto, U. T. Bornscheuer, C. Syltatk and R. D. Schmid, *J. Biotechnol.*, 1998, 231–237; F. A. Husband, D. B. Sarney, M. J. Barnard and P. J. Wilde, *Food Hydrocolloids*, 1998, **12**, 237–244; C. J. Drummond and D. Wells, *Colloids Surf., A*, 1998, **141**, 131–142.
- A. W. Adamson, *Physical Chemistry of Surfaces*, Wiley Interscience, New York, 5th edn, 1990, ch. III and IV.

Tunable mesoporous materials optimised for aqueous phase esterifications

Vitaly L. Budarin,^a James H. Clark,^{*a} Rafael Luque,^a Duncan J. Macquarrie,^a Apostolis Koutinas^b and Colin Webb^b

Received 16th March 2007, Accepted 24th April 2007

First published as an Advance Article on the web 11th May 2007

DOI: 10.1039/b704055e

Sulfonated forms of carbonaceous mesoporous materials, named Starbons[®], are active and reusable catalysts for the aqueous phase esterification of dicarboxylic acids. The optimum temperature of preparation of the Starbons[®] is dependant on the physical properties of the acid substrates.

Introduction

The drive towards greener process chemistry has resulted in the partial or even complete replacement of organic solvents with water in a few organic reactions but these tend to involve unusual circumstances (aggregation of hydrophobic compounds, use of supercritical conditions, presence of surfactants, *etc.*) and remain the exception.^{1–3} The need to develop more and better aqueous phase chemistry will become greater as future biorefineries produce aqueous fermentation broths of biomass platform molecules. The best known “green” catalysts, based on non-toxic, and easy to separate and reuse porous solids, are rarely^{4,5} considered to be suitable for chemistry in water due to problems related with mass transfer resistance (*e.g.* zeolites) or loss of active sites in the presence of a polar medium (*e.g.* HPA–silica). Indeed, great effort is generally taken to remove water, which tends to compete with the organic substrate for the catalyst pores and deactivates the catalyst’s active sites.⁴

We envisage that an optimized catalyst surface that can carry out organic transformations in aqueous media will be mesoporous⁶ and with tunable hydrophobicity.⁷ This will optimise the concentration of the substrate in the pores, overcoming the diffusional problems present in microporous materials and the competitive adsorption of water on active sites. The recently discovered mesoporous Starbons[®]⁸ provide the possibility for achieving a new class of tunable, mesoporous carbonaceous materials. Simple treatment of these materials with sulfuric acid then provides a series of porous solid acids that can work under a range of conditions including dilute aqueous solutions. Our new aqueous catalytic chemistry relies on the ability to adjust the surface properties and hydrophobicity–hydrophilicity balance of Starbon[®] acids by carbonisation of the parent materials at different temperatures (250–750 °C).

Here we report for the first time our preliminary results from the aqueous phase esterification of dicarboxylic acids, which show how the Starbon[®] acids can be optimised to suit different substances.

Results and discussion

The Starbon[®] acids were characterized using different techniques, including high resolution transmission electronic microscopy (HRTEM), scanning electron microscopy (SEM), nitrogen physisorption measurements, and diffuse reflectance infrared Fourier transform (DRIFT). The activities of the materials in the esterification of succinic, fumaric and itaconic acids were subsequently studied.

HRTEM micrographs of sulfonated Starbon[®]-450 show that the functionalized material is amorphous, although some more organized domains are evident. SEM micrographs of materials before and after sulfonation showed that they were not remarkably different in terms of particle size and morphology after functionalisation, although high temperature Starbons[®] appeared to be affected by the temperature of carbonisation, showing a high degree of cracked particles in both sulfonated and non sulfonated samples. In general, Starbons[®] have a small microporous volume and a significant volume in the mesoporous region (5–15 nm).

After sulfonation the materials remain largely mesoporous, although their surface areas and mean pore diameters are reduced. The key textural features of these materials along with those of a commercial carbon and a zeolite are shown in Table 1.

DRIFT experiments (Fig. 1) confirmed the sulfuric acid treatment did not significantly change the materials surface structures, in good agreement with the SEM micrographs. However, sulfonation gave rise to several peaks in the 1300–600 cm^{−1} region that can be attributed to –SO₃H groups in different environments.⁹ On absorption of pyridine (Py) both Brønsted (1640, 1485 cm^{−1}) and Lewis (1632, 1439 cm^{−1}) acid sites are evident. Interestingly, the quantity of the Brønsted

Table 1 Textural features of Starbon[®] acids and other solid acids

Solid with temperature of preparation for Starbon [®]	Specific surface area/m ² g ^{−1}	Pore volume/cm ³ g ^{−1}	Mean pore diameter/nm
Starbon [®] -350	390	0.53	4.9
Starbon [®] -350–SO ₃ H	210	0.49	7.5
Starbon [®] -700	480	0.44	3.7
Starbon [®] -700–SO ₃ H	230	0.47	8.3
DARCO	1276	1.3	4.1
Zeolite β25	680	0.28	0.6

^aGreen Chemistry Centre of Excellence, Department of Chemistry, The University of York, York, UK. E-mail: jhcl@york.ac.uk; Fax: +44 1904 432705; Tel: +44 1904 432567

^bSatake Centre for Grain Process Engineering, Manchester University, Manchester, UK M60 1QD. Tel: +44 1613 064379

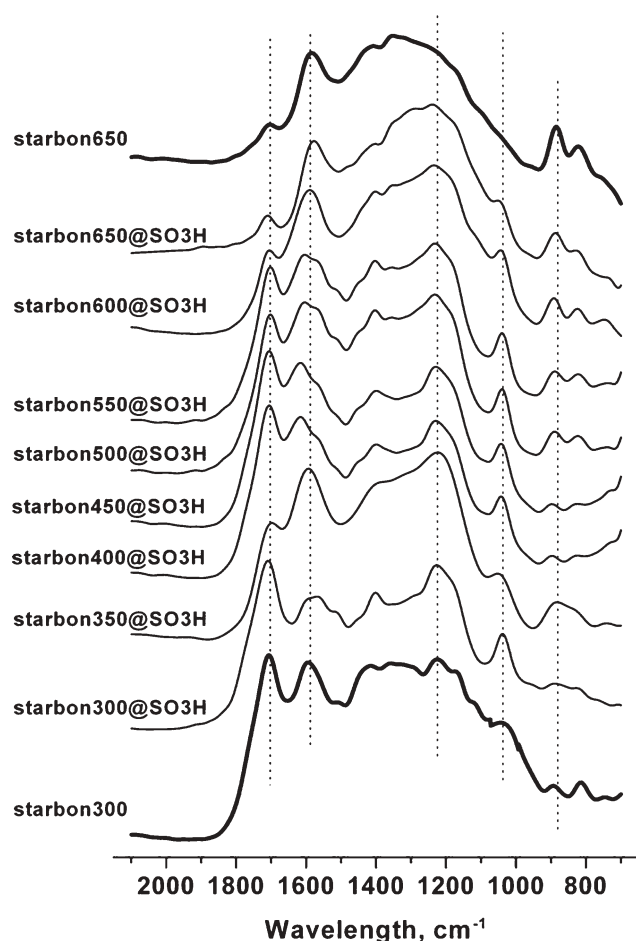


Fig. 1 DRIFT measurements of Starbon[®] acids (300 to 650 °C) compared to the parent materials (300 and 650 °C, top and bottom) in the 2000–600 cm⁻¹ range.

acid sites did not significantly change with increasing Starbons[®] preparation temperature, while stronger Lewis acid sites became more evident at lower temperatures (<550 °C). In general, the total acidity of the Starbon[®] acids did not appreciably change in low temperature materials (<600 °C), in good agreement with –SO₃H loading data obtained from TG-IR (thermogravimetry-infrared spectroscopy coupled analysis) measurements (Fig. 2). The ability to produce different acidic species on the catalysts surface has enabled us to generate catalytically active materials that can be employed in a wide range of reactions.¹⁰

The reactions of typical carboxylic acids in aqueous alcohol demonstrate the excellent activities and particular characteristics of Starbon[®] acids. Esterification reactions of organic diacids in water were chosen because they can offer several interesting features. Firstly, (di)carboxylic acids are included in the top biomass platform molecules as forecast for near future large scale applicability.¹¹ Secondly, esterifications are one of the most useful transformations for organic acids, especially for a dicarboxylic acid since the diester can be used as an intermediate in the manufacture of polymers. Thirdly, traditional esterification methods are unselective, use soluble mineral acids that have to be separated at the end of the reaction, and lead to hazardous waste.¹²

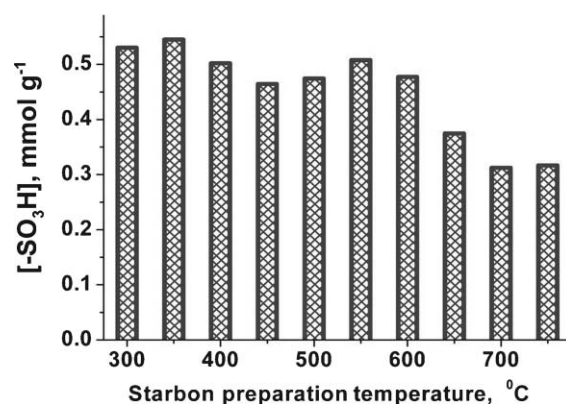


Fig. 2 Influence of Starbon[®] temperature preparation on the active acid sites (–SO₃H, mmol g⁻¹) loading measured by TG-IR.

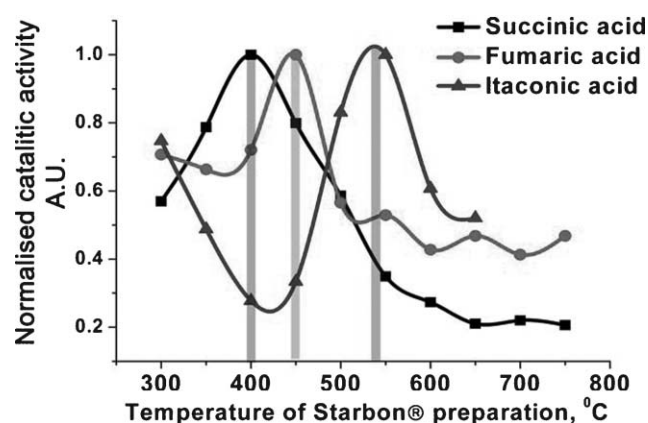


Fig. 3 Normalised catalytic activity of Starbon[®] acids in the esterification of succinic, fumaric and itaconic acids depending of the parent Starbon preparation temperature. Maximum catalytic activities were: succinic acid (400 °C, $k = 32 \times 10^{-5} \text{ s}^{-1}$); fumaric acid (450 °C, $k = 5.0 \times 10^{-5} \text{ s}^{-1}$); itaconic acid (550 °C, $k = 15.4 \times 10^{-5} \text{ s}^{-1}$).

Starbon[®] acids based on Starbons[®] prepared at different temperatures showed an optimum catalytic activity for each one of the diacids screened in the esterification, with sharply reduced activities below or above this maximum. Perhaps the most interesting feature of the Starbon[®] acids catalysis is the substrate-dependent maximum of catalytic activity (Fig. 3). Activities peaked at *ca.* 400 °C (succinic), 450 °C (fumaric) and 550 °C (itaconic acid).

The physical properties of the three diacids are significantly different (Table 2) and in particular, the polarity of itaconic acid and its derivatives are substantially different to fumaric and succinic acid. This might well influence the adsorption–desorption processes that take place on the Starbons[®] surface,

Table 2 Reaction rate constants (k , s⁻¹), physical properties [acidity, pK₁ and pK₂; dipole moment of the acid (μ_{acid}) and the monoester (μ_{mono})] and position of the maximum catalytic activity (peak position) for the different diacids screened in the esterification reaction

Acid	k/s^{-1}	pK ₁	pK ₂	μ_{acid}	μ_{mono}	Peak position
Succinic	32×10^{-5}	4.19	5.57	0.00	0.71	400 °C
Itaconic	15×10^{-5}	3.84	5.55	3.23	3.63	550 °C
Fumaric	5×10^{-5}	3.03	4.47	2.50	2.87	450 °C

Table 3 Catalytic activity of different acids in the esterification of succinic acid in aqueous ethanol

Acid catalyst	Rate of conversion of succinic acid over first hour of reaction/mol g catalyst ⁻¹ h ⁻¹	Time to achieve 90% formation of the diester/min ^a
H ₂ SO ₄	0.51	1440
β-25	0.24	>1440 ^b
DARCO [®] -SO ₃ H	0.29	1150
Starbon [®] -400-SO ₃ H	1.2	410

^a Mono- and diester are the only products formed. ^b 70% diester after 1440 min with only very slow further production thereafter.

explaining the different optimum temperatures of catalyst preparation.

Materials generated at high temperature (>650 °C) exhibited, in general, a relatively poor activity for all substrates screened in the model reaction, in good agreement with Py adsorption data (loss of Brønsted acid sites). Remarkably, the optimized sulfonated Starbons[®] were an order of magnitude more active than commercial solid acids and microporous carbonaceous materials (Table 3), reminiscent of those recently reported as catalysts for biodiesel production.¹³ The catalysts are completely reusable and can be recycled up to four times without appreciable loss of catalytic activity (>90% of the initial activity is retained after 3 reuses).

In conclusion, Starbon[®] acids are tunable, mesoporous materials that can be optimized to carry out organic reactions in aqueous media. Surface properties and the type and strength of acid centres can be controlled by the preparation temperature of the parent materials. The ability to rapidly produce useful, less water-soluble, and hence easily separable products (e.g. diesters), is probably attributable to the surface characteristics in the Starbon[®] acids enabling the inward diffusion of polarisable substrates, rapid reaction in-pore, and the outward diffusion of hydrophobic products. We can foresee our methodology being extended to almost all of the 'top' bioplateform molecules, including the production of other important chemicals and intermediates such as amides, imides and polymers *etc.*

Experimental

The Starbon[®] synthesis method comprises of three key stages. Firstly, corn starch is gelatinised by heating in water for 48 h and subsequently cooled to 5 °C for one to two days to yield a porous gel block. The water in the block is then exchanged with ethanol and oven dried to yield a predominantly mesoporous starch. In the final stage the mesoporous starch is doped with a catalytic amount of an organic acid (e.g. 0.1 mmol of *p*-toluenesulfonic acid per 1 g of starch) and heated under vacuum at a temperature of 180 °C for 6 h. Obtained samples were heated to various temperatures (up to 750 °C) in 3.5 mL alumina sample caps in a Netzsch STA analyser.

SEM micrographs were recorded on a JEOL JSM-6490LV. Samples were Au/Pd coated on a high resolution sputter

SC7640 at a sputtering rate of 1500 V per min, up to a thickness of 7 nm. HRTEM micrographs were recorded on a Philips CM200 field emission gun transmission electron microscope (FEGTEM). DRIFT spectra were recorded on a Brüker EQUINOX-55 instrument equipped with a liquid N₂ cooled MCT detector. Resolution was 2 cm⁻¹ and 1024 scans were averaged to obtain the spectra in the 4000–600 cm⁻¹ range. Spectra were recorded using KBr as a reference. The samples for DRIFT studies were prepared by mechanically grinding all reactants to a fine powder (sample : KBr, 1 : 1000 ratio). Infrared spectra of adsorbed Py were carried out in an Brüker EQUINOX-55 equipped with an environmental chamber. Py was adsorbed at room temperature for a certain period of time and then spectra were recorded at 100 °C according to the methodology reported by Luque *et al.*¹⁴ TG-IRs were recorded using a Netsch STA409 interfaced to Equinox-55 FTIR.

As-synthesized materials were then suspended in H₂SO₄ 99.999% purity (10 mL acid g⁻¹ material) and heated for 4 h at 80 °C. After sulfonation, samples were subsequently washed with distilled water until the washings were neutral, extracted with toluene (4 h at boiling toluene), and water (3 h, 80 °C) and finally oven dried (100 °C) overnight before being tested in the catalytic reaction.

A typical catalytic test was performed as follows: 1 mmol acid, 30 mmol EtOH (2.4 mL) and 50 mmol water (0.9 mL) were added to a round bottom flask with 0.1 g of sulfonated Starbon[®], increasing the temperature to 80 °C. Samples were withdrawn periodically from the reaction mixture and the mixture was left reacting for 5 h. Products were analysed by GC using an Agilent 6890 N GC model equipped with a 7683B series autosampler. Response factors of the reaction products were determined with respect to the different acids employed from GC analysis using known compounds in calibration mixtures of specified compositions.

Acknowledgements

We thank EPSRC for support and colleagues in the Green Chemistry Centre, especially Mr Paul Elliott for technical support, Mr Robin White and Mr Peter Shuttleworth for providing the expanded starch as a starting material and Dr Andrew Brown (Leeds University) for his help and interesting discussions.

References

- 1 C. R. Strauss, in *Handbook of Green Chemistry and Technology*, ed. J. H. Clark and D. J. Macquarrie, Blackwell Science, Oxford, 2002.
- 2 V. M. Lindstrom, *Chem. Rev.*, 2002, **102**, 2751.
- 3 W. Wei, C. C. K. Keh, C. J. Li and R. S. Varma, *Clean Technol. Environ. Policy*, 2004, **6**, 250.
- 4 T. Okuhara, *Chem. Rev.*, 2002, **102**, 3641.
- 5 J. G. Zeikus, M. K. Jain and P. Elankovan, *Appl. Microbiol. Biotechnol.*, 1999, **51**, 545.
- 6 A. Taguchi and F. Schüth, *Microporous Mesoporous Mater.*, 2005, **77**, 1.
- 7 S. Iimura, K. Manabe and S. Kobayashi, *Tetrahedron*, 2004, **60**, 7673.
- 8 V. Budarin, J. H. Clark, J. J. E. Hardy, R. Luque, K. Milkowski, S. J. Tavener and A. J. Wilson, *Angew. Chem., Int. Ed.*, 2006, **45**, 3782.

- 9 M. Di Serio, P. Iengo, R. Gobetto, S. Bruni and E. Santacesaria, *J. Mol. Catal. A: Chem.*, 1996, **112**, 235.
- 10 V. Budarin, J. H. Clark, R. Luque and D. J. Macquarrie, *Chem. Commun.*, 2007, 634.
- 11 T. Werpy and G. Pedersen, *Top Value Chemicals from biomass*, 2004, <http://www1.eere.energy.gov/biomass/pdfs/35523.pdf>.
- 12 J. H. Clark, *Acc. Chem. Res.*, 2002, **35**, 791.
- 13 T. Toda, A. Takagaki, M. Okamura, J. N. Kondo, S. Hayashi, K. Domen and M. Hara, *Nature*, 2005, **438**, 178.
- 14 R. Luque, J. M. Campelo, D. Luna, J. Marinas and A. A. Romero, *Microporous Mesoporous Mater.*, 2005, **84**, 11.

		<p>Comments received from just a few of the thousands of satisfied RSC authors and referees who have used ReSource - the online portal helping you through every step of the publication process.</p> <p>authors benefit from a user-friendly electronic submission process, manuscript tracking facilities, online proof collection, free pdf reprints, and can review all aspects of their publishing history</p> <p>referees can download articles, submit reports, monitor the outcome of reviewed manuscripts, and check and update their personal profile</p> <p>NEW!! We have added a number of enhancements to ReSource, to improve your publishing experience even further.</p> <p>New features include:</p> <ul style="list-style-type: none"> ● the facility for authors to save manuscript submissions at key stages in the process (handy for those juggling a hectic research schedule) ● checklists and support notes (with useful hints, tips and reminders) ● and a fresh new look (so that you can more easily see what you have done and need to do next) <p>Go online today and find out more.</p> <p style="text-align: right; font-size: small;">Registered Charity No. 207890</p>
	<p>'I wish the others were as easy to use.'</p>	
<p>'ReSource is the best online submission system of any publisher.'</p>		

RSC Publishing
www.rsc.org/resource

Investigations into the efficacy of methylphosphonic acid functionalised 1,4,7-triazacyclononane ligands in bleaching catalysis

Kirtida Shastri,^a Eileen W. C. Cheng,^a Majid Motevalli,^a John Schofield,^b Jennifer S. Wilkinson^b and Michael Watkinson^{*a}

Received 7th July 2006, Accepted 9th May 2007

First published as an Advance Article on the web 22nd May 2007

DOI: 10.1039/b609710c

In an attempt to reduce the dye and fabric damage caused by manganese complexes of 1,4,7-trimethyl-1,4,7-triazacyclononane previously employed as low temperature bleaching catalysts in domestic laundry formulations, a novel series of analogues with chelating phosphonic acid pendant arms has been prepared. In order to identify possible bleaching catalysts more rapidly, and with reduced environmental impact, a bleaching screening test has been developed that seeks to identify metal–ligand combinations that may represent active low temperature bleaching catalysts. Of the four methylphosphonic acid containing ligands tested in combination with a range of transition metal salts, only two metal–ligand combinations with manganese salts displayed sufficient activity to take forward for further testing, with the efficacy of the ligands in the oxidative removal of stains decreasing as the number of pendant arms increased. Both of the active ligand systems produced greater dye damage than existing bleach activators, with the ligand with a single methylphosphonic acid pendant arm being particularly aggressive towards stained fabrics sensitive to oxidative damage. This indicates that the systematic addition of chelating pendant arms, whilst tempering the activity of the complexes as bleaching catalysts, unfortunately does not provide a solution to the problem of dye and fabric damage. In contrast to the activity observed in the bleaching screen, the activity of the manganese–ligand combinations in the epoxidation of some alkene substrates was found to bear no relation to the number of methylphosphonic acid pendant arms.

Introduction

Most people share a common desire to keep their clothes and general domestic laundry stain free. Whilst many stains can be removed through the physically abrasive action of washing, many other common stains are rather more persistent. As the unwanted colour of stains generally results from the presence of conjugated π -systems, it is possible to chemically remove the stains through oxidative bleaching. This has an obvious two-fold effect. Firstly, the loss of the colour due to the oxidation of the π -system. Secondly, the oxidation process frequently results in an oxidised stain product with increased hydrophilicity, resulting in its easier removal from the previously stained surface. As a result of this, oxygen based bleaches have been used in laundry applications for many years. Although hydrogen peroxide is very effective at temperatures over 60 °C, it cannot be incorporated directly into washing powders. A convenient solution to this issue comes through the use of sodium perborate and sodium percarbonate, which act as a solid source of peroxide causing less damage to dyes and fabrics than, for example, sodium hypochlorite, and are effective at more modest temperatures

(40–60 °C) through the use of bleach activators. Bleach activators such as teraacetylenediamine (TAED), **1**, and sodium nonanoyloxybenzenesulfonate (SNOBS), **2**, react with the perhydroxyl anion present in basic laundry and generate more reactive peracyl species *in situ* which provide more effective bleaching at lower temperatures, Fig. 1.¹

Nonetheless, despite the effectiveness of modern detergents at relatively low temperatures, there is a considerable environmental drive to reduce both their operational temperature (to reduce energy usage in water heating) and of course to reduce effluent levels. A possible solution that addresses both of these issues is the incorporation of environmentally benign bleaching catalysts within the washing powders to activate the peroxide bleach at even lower temperatures. In this regard the report by Hage *et al.* of a series of potent low temperature bleaching catalysts based on manganese complexes of the azamacrocyclic ligand **3** was an extremely exciting development.² Unfortunately, the impressive bleaching performance

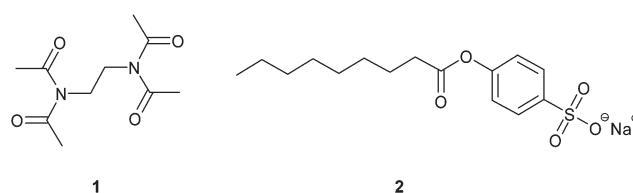


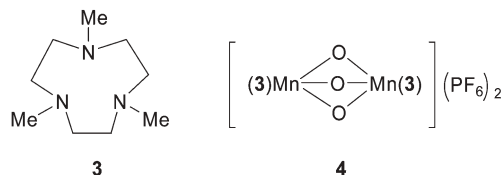
Fig. 1 The structures of two of the bleaching activators currently employed in detergents and catalytic bleaching systems.

^aSchool of Biological and Chemical Sciences, Queen Mary, University of London, Mile End Road, London, E1 4NS, UK.

E-mail: m.watkinson@qmul.ac.uk

^bWarwick International Limited, Mostyn, Holywell, Flintshire, CH8 9HE, UK

was also shown to be accompanied by unwanted dye and fabric damage and the detergent formulation containing the bleaching catalyst **4**, was quickly removed from the market. Nevertheless, the catalyst continues to be marketed in dishwasher formulations and significant effort continues to be invested in the development of new catalytic systems, as the environmental benefits are potentially so great.³



It must be emphasised, however, that regardless of the presence or absence of bleaching catalysts, any laundry process involving the persistent usage of bleaching agents will ultimately result in some degree of fabric and dye damage, and thus the levels of damage observed through the use of current commercial washing powders are considered to be acceptable. Therefore, to be commercially viable any new bleaching catalyst must show a demonstrable increase in stain removal properties at low temperatures whilst not producing an increase in dye or fabric damage *c.f.* existing formulations.

We speculated that the unwanted damage resulting from the prolonged use of **4** in detergents was a consequence of its decomposition during the washing cycle, causing deposition of manganese salts onto fabrics, although it has been shown that certain azo-dyes are susceptible to oxidative degradation under comparable conditions.⁴ We postulated that the introduction of chelating *N*-pendant arms within the macrocyclic ligand framework might provide an increase in the stability of the metal complexes whilst retaining their bleaching profile. Hage *et al.* demonstrated in their seminal report² that the

incorporation of pendant arms in analogues of **3**, *viz.* **5**, Fig. 2, resulted in a complex which was active as an epoxidation catalyst between pH 7 and 10, but which was inactive in the bleaching of stained cloths. In an extension of this report, De Vos and Bein subsequently reported that **6** and **7** could also be used in the epoxidation of alkenes.⁵ Whilst the rate of the catalytic reactions was slower for these ligands, there were some advantages, which included: a reduced rate of the decomposition of the oxidant; a broader range of solvents in which catalysis occurred and improved stereoretention of the alkene configuration in the epoxide products. Moreover, Bolm has demonstrated **8** to be the most effective variant of **3** yet reported in the asymmetric epoxidation of alkenes.⁶ Overviews of this chemistry have appeared recently.^{3,7}

The approach we decided to adopt was to investigate the effect that systematic changes in the ligand structure had on bleaching activity and on dye damage by incorporating a variety of chelating methylphosphonic acid pendant arms in the ligand framework, **9–12** (Fig. 3). Although such pendant arms have been extensively studied in the tetraazamacrocycles, their use in the coordination complexes of the triazamacrocycles is far less studied. At the outset of our investigations only four coordination complexes of **9** had been structurally characterised^{8–10} and to the best of our knowledge there were no reports of the synthesis of **10–12**, nor of their application in bleaching catalysis. We therefore sought to develop efficient routes towards the synthesis of the new ligands and to investigate their efficacy in bleaching catalysis.

Results and discussion

Ligand synthesis

All of the ligand precursors were synthesised by adaptation of procedures developed by us and others. Ligand **9** could be

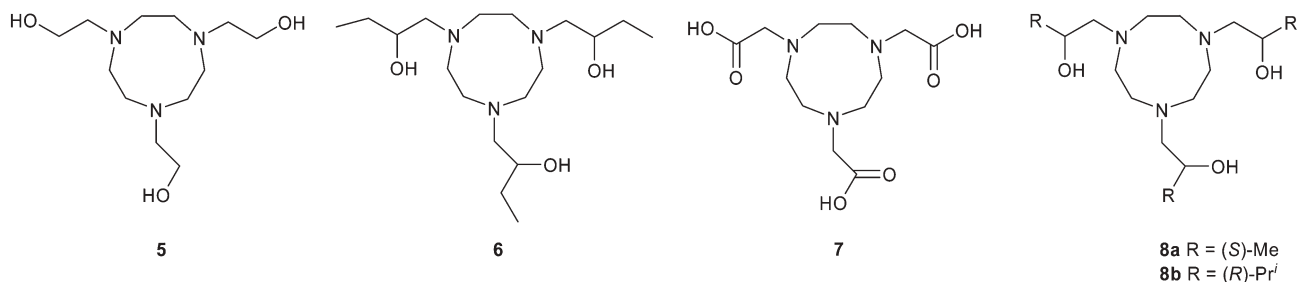


Fig. 2 *N*-Functionalised derivatives of **3** that have been employed in the epoxidation of alkenes in the presence of manganese salts.

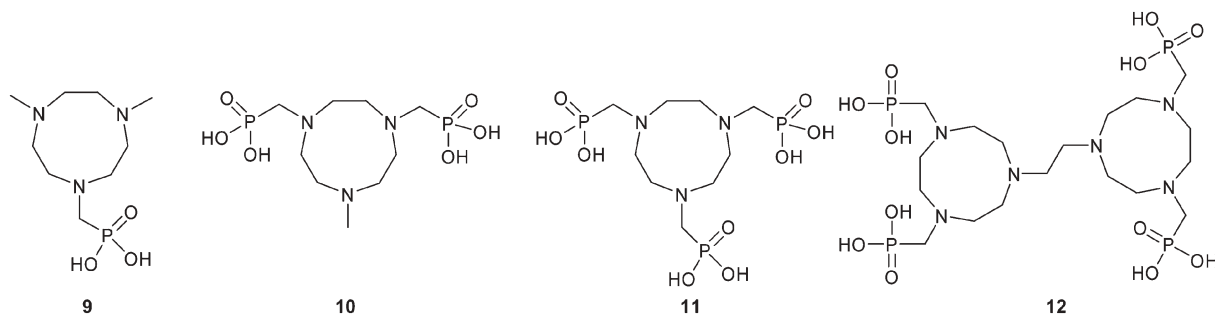
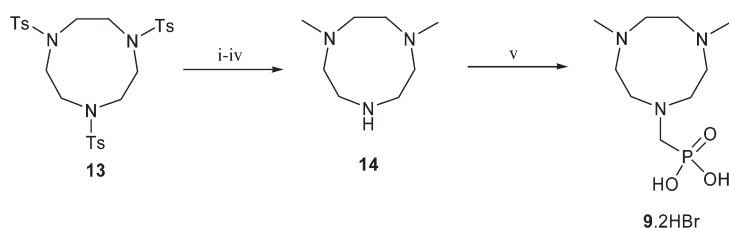


Fig. 3 Ligands prepared in this study.



Scheme 1 Reagents and conditions: i, HBr/AcOH, Δ ; ii, CH₂O, HCO₂H, Δ ; iii, H₂SO₄ (conc.), Δ ; iv, HBr(conc.); v, H₃PO₃, HCl(conc.), CH₂O.

isolated as its hydrobromide salt from the hydrobromide salt of 1,4-dimethyltriazacyclononane, **14**,^{11–14} in good yield by adapting the procedure reported by Sherry *et al.* for the formation of aminophosphonic acids,¹⁵ as illustrated (Scheme 1). This procedure was found to be very reliable provided that solid paraformaldehyde was used as the electrophile and that the molar ratios of the reactants, the total volume of the reaction mixture and its acidity, as well as the addition time of the paraformaldehyde and total reaction time were carefully controlled, as reported. Single crystals

suitable for X-ray diffraction studies of **9**·2HBr were formed by slow evaporation (Fig. 4).

The structure confirms the formulation proposed with two bromide anions and the macrocyclic ligand in the asymmetric unit in addition to two water molecules. The macrocyclic ligand is protonated on nitrogen atoms N(2) and N(3) and two of the oxygen atoms of the phosphonate group, allowing for the formation of an intricately hydrogen bonded dimer (Fig. 4). The bond lengths and bond angles of the ligand **9** are comparable to those observed in other aminoalkylphosphonic acid ligands and are consistent with the proposed formulation.¹⁶ The bond lengths around protonated nitrogen atoms in such systems are expected to be significantly longer than those around unprotonated nitrogen atoms. The lengthening of the appropriate C–N bonds is observed in **9**·2HBr, (Table 1). The mean C–N value around N(2) and N(3) are 1.495 Å and 1.513 Å, respectively, whilst that about N(1) is 1.466 Å, suggesting that N(1) is not protonated. The bond lengths between the phosphorus atom and oxygen atoms O(2) and O(3) of 1.576(5) Å and 1.542(5) Å are consistent with their protonation as they are at the high end of the range found for P–OH in related aminoalkylphosphonic acid ligands. The P(1)–O(1) bond length of 1.510(5) Å reflects its double bond character. Other selected bond lengths and angles are given in Table 1.

The intermolecular hydrogen bonds between the phosphonic acid groups results in the formation of 8-membered hydrogen-bonded ring connections, P(O)⋯H–O–P, between adjacent

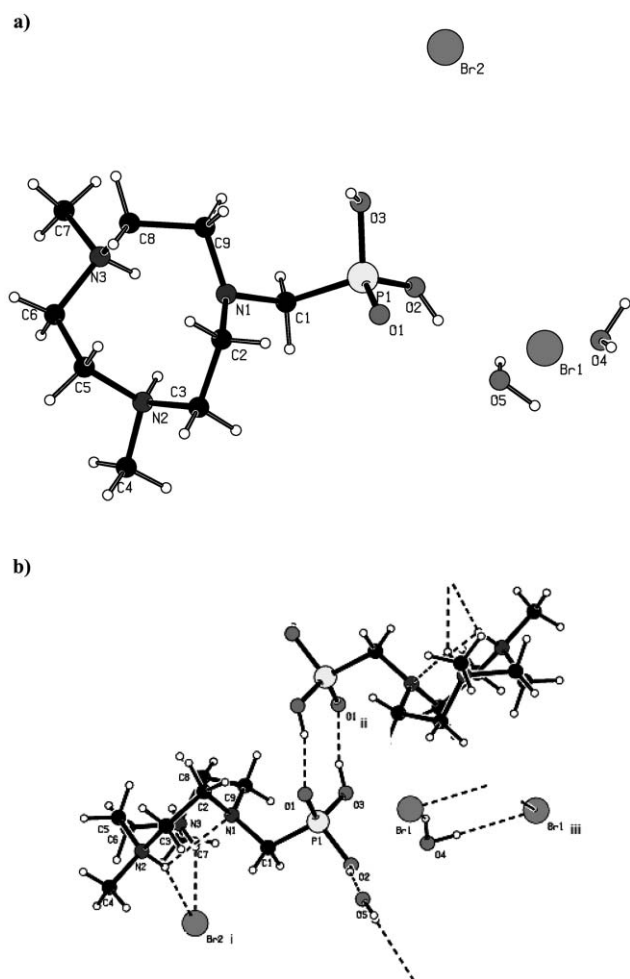
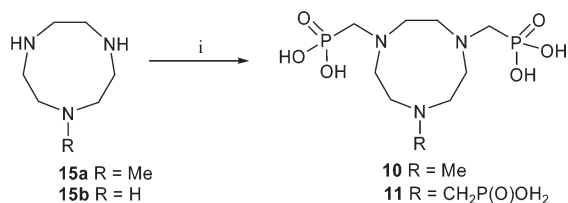


Fig. 4 PLUTON¹⁷ plots showing (a) the single crystal X-ray structure of **9**·2HBr and atomic labelling scheme (b) the hydrogen bonding network (symmetry codes: (i) $x - 1, y, z$ (ii) $-x + 1, -y + 1, -z + 1$ (iii) $-x, y + 1, -z$).

Table 1 Selected bond lengths (Å), angles (°) and hydrogen bond distances D⋯A (Å), for **9** with esds

N(1)–C(1)	1.464(8)	N(3)–C(8)	1.518(8)
N(1)–C(9)	1.449(8)	C(2)–C(3)	1.540(9)
N(1)–C(2)	1.486(8)	C(5)–C(6)	1.525(9)
N(2)–C(3)	1.505(8)	C(8)–C(9)	1.532(9)
N(2)–C(5)	1.507(8)	C(1)–P(1)	1.813(6)
N(2)–C(4)	1.474(8)	P(1)–O(1)	1.510(5)
N(3)–C(6)	1.527(8)	P(1)–O(2)	1.576(5)
N(3)–C(7)	1.493(8)	P(1)–O(3)	1.542(5)
N(1)–C(1)–P(1)	116.8(4)	O(1)–P(1)–O(2)	113.5(3)
C(1)–P(1)–O(1)	113.8(3)	O(2)–P(1)–O(3)	103.5(3)
C(1)–P(1)–O(2)	103.7(3)	O(1)–P(1)–O(3)	114.0(3)
C(1)–P(1)–O(3)	107.3(3)		
N(1)–C(1)–P(1)	116.8(4)		
N(2)–H(2)⋯Br(2)#1	3.150(6)	O(2)–H(2C)⋯O(5)	2.561(6)
N(3)–H(3)⋯Br(2)#1	3.043(6)	O(3)–H(3C)⋯O(1)#2	2.539(7)
N(2)–H(2)⋯N(1)	2.797(7)	O(4)–H(41)⋯Br(1)#3	3.314(5)
N(3)–H(3)⋯N(1)	2.836(7)	O(4)–H(42)⋯Br(1)	3.291(4)



Scheme 2 Reagents and conditions: *i*, H₃PO₃, HCL(conc.), CH₂O.

molecules with a crystallographically imposed inversion centre. The major hydrogen bonding interactions in **9** are intermolecular in nature between O(3)–H···O(1) involving the phosphonic acid P=O and P–OH atoms, with an O···O distance of 2.539(7) Å. The remaining one is the O–H···O interaction between one of the water molecules H(51)–O(5)–H(52) and O(2)–H(2C), with an O···O distance of 2.561(6) Å. In addition to this intermolecular hydrogen bonding, intramolecular hydrogen bonds between N(2)–(H)···N(1) 2.797(7) Å and N(3)–(H)···N(1) 2.836(7) Å appear to stabilise the macrocyclic ring conformation and minimise Coulombic interactions.

Similarly ligands **10** and **11** could be prepared in good yield by adapting the same experimental protocol using known 1,4,7-triazacyclononane analogues, Scheme 2. To the best of our knowledge this represents the first report of **10** and, although **11** has been reported previously,^{8–10,18} the procedure adopted herein is higher yielding and full spectroscopic characterisation of the ligand is presented.

Ligand **12** was prepared using our previously reported direct synthesis of binucleating azamacrocyclic ligands¹⁹ and other reported methods,^{13–15} Scheme 3, and has been comprehensively characterised using a range of techniques including single crystal X-ray diffraction, Fig. 5.

The crystal structures of ligand **12** reveals that the macrocyclic ligand adopts a conformation in which the two macrocyclic rings and the methylene phosphonic acid substituents are positioned in opposite directions as a result of a crystallographically imposed inversion centre.

Comparison of the geometry of **12** with other amino-alkylphosphonic acid ligands suggests that two of the nitrogen atoms N(1) and N(2) are protonated, whereas N(3) is not. The average C–N bond lengths around N(1) (1.479 Å) and N(2) (1.483 Å) are longer and closer to the mean value of 1.495 Å found in aminophosphonic acids than the average C–N bond

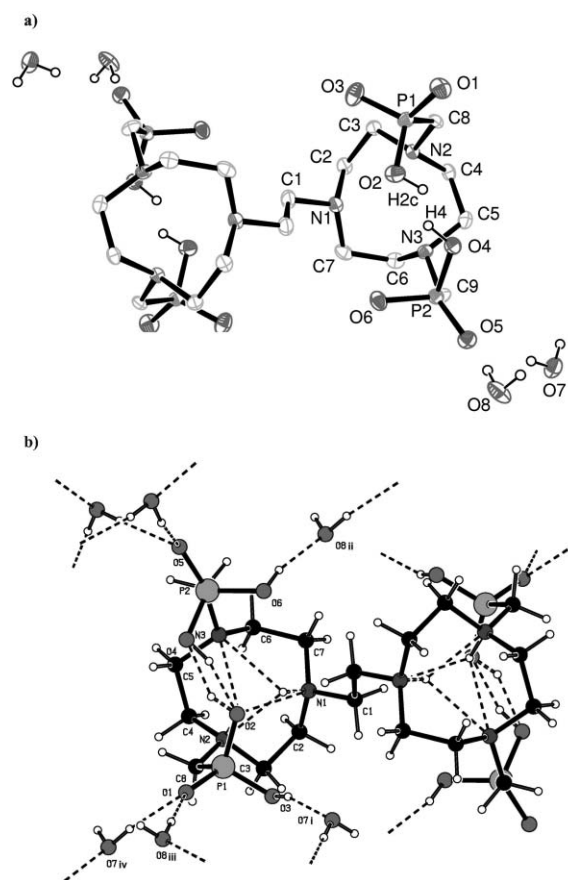
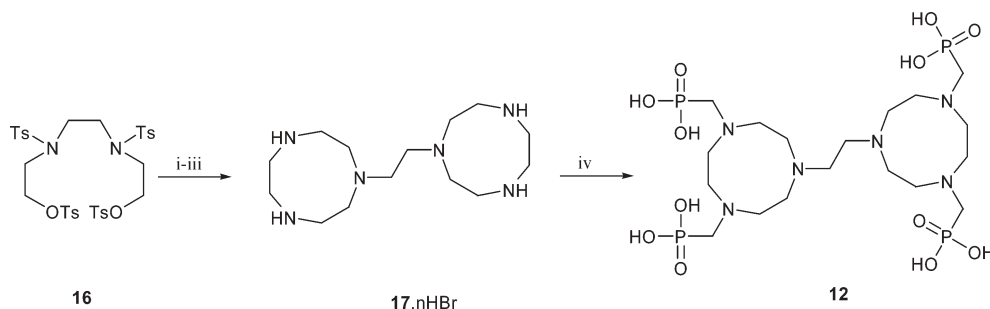


Fig. 5 (a) ORTEP²⁰ plot of the single crystal X-ray structure of ligand **12** showing the labelling scheme of the non-hydrogen atoms, except for H2c and H4 which show the disordered positions of the H atoms between O(2) O(4) with 0.33(6) and 0.67(6) occupancy, and (b) the hydrogen bonding network (symmetry codes: (i) $x + 1/2, -y + 5/2, -z + 1/2$ (ii) $-x - 1/2, y - 1/2, -z - 1/2$ (iii) $-x - 1/2, y - 1/2, -z + 1/2$ (iv) $-x - 1/2, y + 1/2, -z + 1/2$ (Pluton)).¹⁷

length around N(3) (1.467 Å).^{16,18} However, protonation of both nitrogen atoms results in an impossibly short H···H separation and we have found that the structure is best refined with a disordered hydrogen with half occupancy at N(1) and N(2). The phosphorus atoms have distorted tetrahedral geometries. The bond lengths between the phosphorus atoms and the oxygen atoms of P(1)–O(1) = 1.494(2), P(1)–O(2) = 1.517(2) Å and P(1)–O(3) = 1.556(2) Å, P(2)–O(4) = 1.533(2) Å,



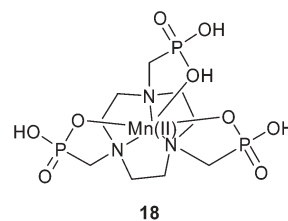
Scheme 3 Reagents and conditions: *i*, H₂N(CH₂)₂NH₂, K₂CO₃, CH₃CN, Δ; *ii*, H₂SO₄(conc.), Δ; *iii*, HBr (conc); *iv*, H₃PO₃, HCL (conc.), CH₂O.

Table 2 (a) Selected bond lengths (Å), angles (°) and hydrogen bonding interactions D...A (Å) observed in ligand **12** with esds

C(1)–N(1)	1.476(4)	P(1)–O(2)	1.517(2)
C(2)–N(1)	1.483(4)	P(1)–O(3)	1.556(2)
C(7)–N(1)	1.486(4)	P(2)–O(4)	1.533(2)
C(3)–N(2)	1.485(4)	P(2)–O(5)	1.492(2)
C(4)–N(2)	1.492(4)	P(2)–O(6)	1.566(2)
C(8)–N(2)	1.486(4)	C(8)–P(1)	1.805(3)
C(5)–N(3)	1.464(4)	C(9)–P(2)	1.814(3)
C(6)–N(3)	1.469(4)	C(2)–C(3)	1.527(4)
C(9)–N(3)	1.475(4)	C(4)–C(5)	1.513(4)
P(1)–O(1)	1.494(2)	C(6)–C(7)	1.518(5)
N(2)–C(8)–P(1)	116.4(2)	C(5)–N(3)–C(6)	114.0(3)
O(1)–P(1)–O(3)	113.58(14)	C(9)–N(3)–C(6)	113.4(2)
O(2)–P(1)–O(3)	107.31(14)	C(5)–N(3)–C(9)	111.0(2)
O(1)–P(1)–O(2)	116.62(14)	C(4)–N(2)–C(8)	111.1(2)
O(5)–P(2)–O(6)	114.12(13)	C(8)–N(2)–C(3)	114.2(2)
O(5)–P(2)–O(4)	112.04(13)	C(4)–N(2)–C(3)	112.9(2)
O(4)–P(2)–O(6)	105.24(13)		
O(3)–H(3) ... O(7)#1	2.575(3)	O(6)–H(6) ... O(8)#2	2.576(3)
O(7)–H(7C) ... O(1)#3	2.703(4)	O(8)–H(8D) ... O(1)#4	2.862(4)
N(1)–H(1) ... N(2)	2.667(4)	N(2)–H(2) ... N(1)	2.667(4)
O(4)–H(4) ... O(2)	2.442(3)	O(2)–H(2c) ... O(4)	2.442(3)

P(2)–O(5) = 1.492(2) Å and P(2)–O(6) = 1.566(2) Å are consistent with their formulation as PO₃H[−] *i.e.* each bears a single protonated oxygen atom and they are consequently anionic, although the H atom along the O(2)–O(4) vector is disordered. All of the protons associated with the two water molecules that hydrate the structure (which have half-occupancy over two sites) were also located in the difference map, further supporting this formulation. Their presence results in an extensive hydrogen bonded array which is illustrated in Fig. 5b. Selected bond lengths and angles are presented in Table 2.

Our efforts to prepare authenticated coordination complexes of the ligands **9–12** have met with mixed success, although we have consistently been able to prepare an analytically pure complex of ligand **11**. The infrared spectrum of the manganese(II) complex formed, **18**, shows clear differences to that of the free ligand and is consistent with the presence of P=O (1124 cm^{−1}) and P–O (1039 cm^{−1} and 908 cm^{−1}) groups. The disappearance of the strong C=O asymmetric stretch from the manganese(II) acetate starting material indicates that the phosphonic acids also serve as anions. The EPR spectrum of **18**, recorded as a frozen water glass, gave a sharp 6-line signal centred at *g* = 2.005, consistent with magnetically dilute manganese(II),²¹ which together with the elemental analysis and mass spectrometry data, allied with very closely related structural data,^{8–10} are entirely consistent with the formation of the structure proposed, although an MnO₆ coordination sphere or oligomeric/polymeric material cannot be discounted. Unfortunately, despite extensive efforts, attempts to isolate single crystal suitable for X-ray diffraction were unsuccessful, as were our attempts to prepare analytically pure complexes of ligands **9**, **10** and **12**. ESMS of the materials formed *in situ* by mixing manganese salts with ligands **9** and **10** are much more complex than for **18**, but suggest that species of the type [MnL] and [Mn₂L₂] may be present in solution.



Screening for bleaching activity

As part of our ongoing programme to increase the rate at which we are able to identify potential bleaching catalysts, we sought to develop a fast and reliable qualitative assay of bleaching activity. Before the development of this test this process typically took over six months as a result of the need to resort to lengthy wash-test results for each catalyst. The concept behind the test and its process are simple; however, it is important to explain how the protocol was established.

We speculated that a potential ligand system could be mixed with a metal salt and the relative rate of bleaching of dyes that mimicked stains by this mixture be compared to a series of blanks and standards. If it were assumed that a metal complex had formed *in situ*, any increased bleaching activity over the blanks would be indicative of a potential bleaching catalyst. There is of course a risk when using such an approach that active catalysts might be missed, however, in our development of the conditions used for this test we have been very careful to attempt to eliminate this possibility. The key factor underpinning our approach was that the screening test would translate as an indicator of wash-test success and our criteria were thus that the conditions used must be representative of a wash-test (in terms of pH, concentration, time-scale *etc.*), be reliable, be able to distinguish between inactive, active and highly active catalyst systems and differentiate between peroxide bleaching, metal salt bleaching and catalyst bleaching. Ambient temperature was preferred for operational simplicity and we additionally anticipated that this would make qualitative visual comparison of solutions rather easier due to the slower reactions.

A wide range of dyes to represent laundry stains covering all of the major dye classes were initially screened in the presence of known bleaching catalysts (including **4**) under conditions typical of European laundry in the presence of peracetic acid (to mimic the action of **1** in the presence of hydrogen peroxide). From these initial experiments we decided that three dyes might be suitable for monitoring purposes, specifically crocetin, crystal scarlet and erichrome cyanine RC. Similar validations were carried out at 40 °C for peroxide bleaching which again confirmed these dyes to be suitable. Ultimately crocetin was chosen as the most reliable dye molecule. We are aware that dyes in solution are not the same as dyes or stains on fabrics, and that the sensitivity and reactivity of the unsaturated chromophore of crocetin to bleaching agents is very different to that of other stain chromophores such as the polyphenols found in tea, coffee and wine. Nonetheless, our extensive validation of this method indicates that it does provide a reliable guide of activity in bleaching catalysts.

The activity of the ligands is assayed using an array of metal salts that may have potential applicability in oxidative bleaching catalysts *e.g.* VCl_3 , $\text{MnSO}_4 \cdot \text{H}_2\text{O}$, $\text{MnCl}_2 \cdot 4\text{H}_2\text{O}$, $\text{Mn}(\text{OAc})_3 \cdot 2\text{H}_2\text{O}$, $\text{FeCl}_3 \cdot 4\text{H}_2\text{O}$ and $\text{CuSO}_4 \cdot 5\text{H}_2\text{O}$. The test employs a series of reference solutions whose activities are compared to the test solution. The first reference solution is a blank containing carbonate buffer, a sequestrant and the crocetin dye. The second contains carbonate buffer, a sequestrant, the metal salt being tested in combination with the ligand, dye and peracetic acid to monitor the rate of bleaching by the free metal ions alone. The final reference solution is an identical mixture to the screening solutions with the exception of the addition of the active preformed catalyst **4**, which is treated as a benchmark for activity. The activity of all candidate ligands was compared to these reference solutions. A suitable candidate ligand–metal combination is deemed to be one which gives superior bleaching activity to the peracid and metal salt standard but with comparable or lower activity than **4**. In this context bleaching refers to gradual bleaching over a period of time (usually 24 hours), rather than rapid bleaching and then inactivation—any metal–ligand combinations behaving in this way are deemed to be unsuitable. In addition, a candidate ligand–metal combination should not lead to the precipitation of insoluble oxides.

A typical screen is performed at room temperature using the standard stock solutions described at pH 10 (see Experimental for further details). As the rate of crocetin bleaching is dependent on the age of the solution, due to the gradual aerial oxidation of the crocetin substrate that occurs, the rate of bleaching is typically assessed over a 24 h period with freshly prepared solutions, however, as the solution ages, bleaching occurs more rapidly. In these cases the effectiveness of the screening test can be maintained by cooling the solutions to *ca.* 4 °C. It is important to emphasise that the key is the *relative activity* of the reference solutions *c.f.* the possible candidate bleaching combinations, *i.e.* the test is not a quantitative measure of activity. Ligands **9–12** were screened for activity in this way and, as it was not known whether the metal to ligand stoichiometry would be important, 1 : 1 and 1 : 2 ratios of metal to ligand were used in the test solutions. No discernable differences were observed between these combinations indicating that 1 : 1 metal : ligand ratios were optimal in this series of ligands. The manganese catalysts prepared *in situ* from ligand **9** and **10** were found to be very active bleaching catalysts, showing significantly greater bleaching activity than the reference free manganese salt and comparing favourably with the activity of **4**. In addition, it was found that these compounds also formed active bleaching species in the presence of iron(III) chloride. Disappointingly, no activity was observed for combinations of metal salts with **11** and **12**. *N. B.* All further references to ligand activity in bleaching refer to the activity of ligand–manganese complexes formed *in situ* (see Experimental).

Assessment of stain removal

The ligand systems thus identified as potential bleach catalysts by the screen were investigated further using standard European wash-test conditions (see Experimental).

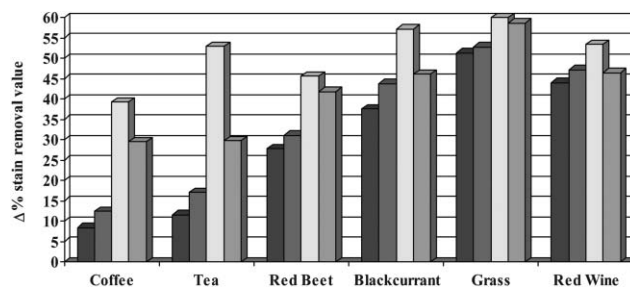


Fig. 6 Assessment of the bleaching activity of **9** evaluated using the terg-o-tometer test in the presence of $\text{Mn}(\text{OAc})_3 \cdot 2\text{H}_2\text{O}$ (concentration equivalent to 50 ppm of metal), bars from left to right: blank, **1**, **4**, **9**.

In addition, it was decided to investigate the activity of ligand **11** in comparison to complex **18** to support the efficacy of the bleaching assay. The stain removal results of the *in situ* formed complexes were compared with a catalyst-free system (using only **1** as the activator) as well as to catalyst **4**. As anticipated, the activity of the complex formed *in situ* from ligand **11** and complex **18** were comparable, supporting the validity of the screening method, and neither showed a significant increase in stain removal activity over **1** alone.

In contrast, both ligands **9** and **10** showed enhanced stain removal properties when tested in a 1 : 1 metal : ligand ratio. A representative example of the wash-test results for ligand **9** in the presence of manganese(III) acetate dosed at 50 ppm is shown in Fig. 6 (formulations employing both manganese(III) acetate and manganese(II) chloride gave similarly increased performance over **1**). It is important to stress that the wash-test data between different data-sets cannot and should not be compared. Comparison within each data-set is valid as the wash-test is performed at the same time with the same batch of stained swatches; however, comparison between different wash-tests and swatch batches is not. This is because variations in batches of stained swatches are large, rendering them non-comparable. Moreover, even using the same batches of stained swatches in different sets of wash-tests can lead to significant variation in the levels of stain removal. In this instance, the data presented in Fig. 6 and 7 refer to four readings taken from two different cloths. The standard deviation of all measurements was less than 1.5% (with one exception in Fig. 6 for compound **3** with red wine which gave a standard deviation of 5.5%). Our premise is that a deviation of 3.0% or more has

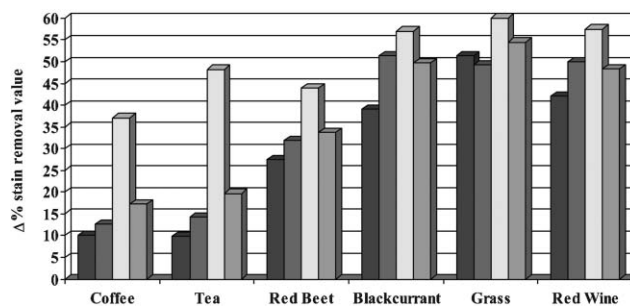


Fig. 7 Assessment of the bleaching activity of **10** evaluated using the terg-o-tometer test in the presence of $\text{Mn}(\text{OAc})_3 \cdot 2\text{H}_2\text{O}$ (concentration equivalent to 100 ppm of metal), bars from left to right: blank, **1**, **4**, **10**.

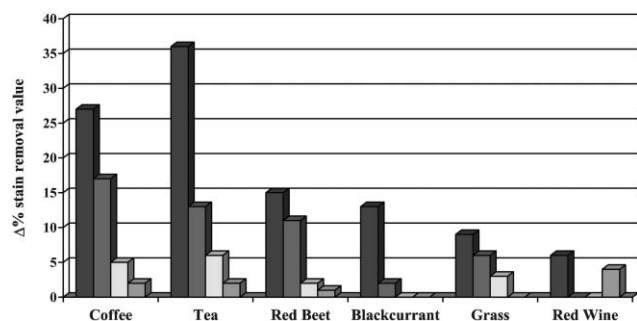


Fig. 8 Comparison of the catalytic bleaching activity of ligands **9–11** evaluated using the terg-o-tometer test in the presence of $\text{Mn}(\text{OAc})_3 \cdot 2\text{H}_2\text{O}$ (concentration equivalent to 50 ppm of metal), bars from left to right: **4**, **9**, **10**, **11**.

meaning, as this is the minimum that can be visually detected. Thus, as the standard deviations are below this threshold value we believe that the results are statistically significant.

Evaluation of the second active ligand system **10**, identified by the screen, was also performed using the terg-o-tometer test. The stain removal results for **10** were performed in the presence of two different concentrations of metal salts equivalent to 50 ppm and 100 ppm of metal within the formulation (see Experimental). When ligand **10** was dosed at 50 ppm manganese, benefits were seen for coffee and grass stains. When the concentration of manganese was increased to 100 ppm, a benefit was also seen for tea and red beet stains, Fig. 7.

Thus, the stain removal tests clearly show that there is a definite trend in the effectiveness of ligands **9–11** when combined with manganese salts, Fig. 8. Their effectiveness as bleaching catalysts is systematically reduced upon the addition of each additional phosphonic acid pendant arm, as had been anticipated at the outset of this study. Ligand **11** with three phosphonic acid pendant arms showed negligible catalytic bleaching activity with manganese salts, whereas ligands **9** and **10** provided active bleaching systems, and their dye damage was thus also assessed in comparison to catalyst **4**.

Assessment of dye damage

The bleaching stain removal wash test results clearly gave hope that ligands **9** and **10** might provide suitable bleaching catalysts. Therefore the dye damage caused by these formulations was investigated with dyed fabrics that have been shown to be rather sensitive to bleaching agents using a protocol that has recently been shown to be reliable in inter-laboratory testing.²² In order to show that dye fading is not restricted to vat dyes, reactive dye and direct dyes were included (see Experimental). Dye fading is easily measured using a Datacolor International Spectraflash 500 spectrophotometer and is assessed in terms of the total colour difference between the starting fabric and its condition after the specified wash cycle, ΔE . Thus the larger the value of ΔE , the greater is the level of dye damage. The twelve test-dyed cotton swatches were washed for the predetermined time in a terg-o-tometer at the selected temperature in one litre of solution prior to assessment of ΔE .

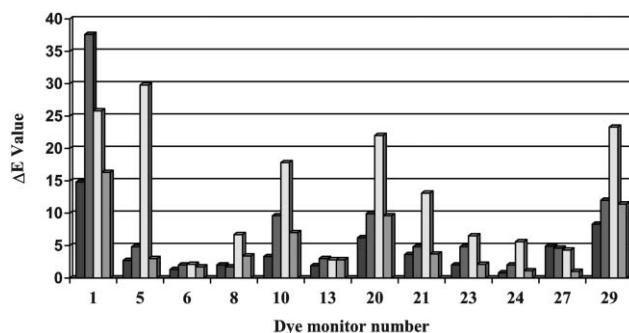


Fig. 9 Comparison of the dye damage in standard stain swatches, bars from left to right: **1**, **4**, **9**, **10**.

Standard formulations of **1** and **4** were used as benchmarks for comparison, with damage due to **1** being viewed as acceptable and that due to **4** as being unacceptable. Additionally, the effect of the addition of manganese(III) acetate to **1** was investigated which revealed no difference from **1** alone, indicating that manganese(III) acetate is not damaging to the dye selection used in this study. Unfortunately, ligand **9** in combination with manganese(III) acetate gave bigger ΔE values for each fabric than did **1**, and in the majority of cases led to significantly more damage than **4**, Fig. 9. We are unsure as to the reasons for the aggressive nature of manganese combinations with ligand **9** towards dye damage, especially given its reduced activity *c.f.* **4** in the bleaching experiments. Although dye damage for **10** in combination with manganese(III) acetate was significantly less than for **9**, significant damage was unfortunately still evident with certain dyes, which is comparable to that seen for complex **4**, Fig. 9. Thus, given its significantly lower bleaching profile we conclude that manganese complexes of **10** are unlikely to be efficacious as laundry bleaching catalysts.

Activity in the epoxidation of selected alkene substrates

Given that there continues to be much interest in the epoxidation of alkenes using the environmentally benign hydrogen peroxide as the oxidant,⁷ we were interested to investigate the activity of the metal–ligand combinations in the epoxidation of certain alkene substrates. We adapted the approach reported by De Vos,⁵ although we found that catalytic activity was superior at 298 K rather than 273 K. Given the previous observations we had made in the bleaching experiments, we were rather surprised to find that **11** displayed far superior activity in epoxidation catalysis when compared to **9** in combination with a number of manganese salts, Table 3. This is based on the reasonable expectation that as the coordination sphere in complex **18** is likely to be saturated that the complex should be incapable of activating hydrogen peroxide. However, Hage,² De Vos,⁵ and Bolm⁶ have all demonstrated the efficacy of manganese complexes of analogues of **3** that are all potentially hexadentate in epoxidation catalysis, thus the activity is not without precedent and indicates the presence of an equilibrium of a species in which at least one, and possibly more, of the phosphonate moieties are not coordinated. Given the potency

Table 3 Summary of the epoxidation of selected alkene substrates by *in situ* formed manganese complexes in acetone at 298 K⁵

Entry	L	Metal salt	Substrate	% Conversion ^a	% Epoxide yield ^b	TON ^c
1	9	MnSO ₄ ·H ₂ O	Cyclooctene	23	0.6	~1
2	10	MnSO ₄ ·H ₂ O	Cyclooctene	65	25	50
3	11	MnSO ₄ ·H ₂ O	Cyclooctene	63	27	54
4	11	MnCl ₂ ·4H ₂ O	Cyclooctene	74	33	66
5	11	Mn(OAc) ₂ ·4H ₂ O	Cyclooctene	75	33	66
6	11	Mn(ClO ₄) ₂ ·6H ₂ O	Cyclooctene	77	38	76
7	9	MnSO ₄ ·H ₂ O	Styrene	42	12	24
8	10	MnSO ₄ ·H ₂ O	Styrene	100	58	116
9	10	Mn(ClO ₄) ₂ ·6H ₂ O	Styrene	100	56	112
10	11	MnSO ₄ ·H ₂ O	Styrene	42	42	84
11	10	MnSO ₄ ·H ₂ O	1-Octene	37	3	6
12	11	MnSO ₄ ·H ₂ O	1-Octene	52	2	4

^a A series of blank experiments indicated that alkene oxidation only occurred when the manganese salt and ligand were present. ^b Yields of epoxides in comparison to alkene conversion indicate that other products may form, however, to date we have been unable to identify these satisfactorily. ^c Based on epoxide yield.

of combinations of manganese with **9** in bleaching catalysis, its very low activity in epoxidation catalysis perhaps indicates a different mode of action. Similarly the potency of combinations of **10** with manganese, which provided the highest conversion and epoxide yield for styrene (Table 3, entries 8 and 9) is not in keeping with the bleaching experiments. The fact that very little difference is observed in the epoxidation of cyclooctene with **11** in combination with a number of manganese(II) salts (Table 3, entries 2–6) and for **10** in the epoxidation of styrene (Table 3, entries 8 and 9) appears to indicate that the active complexes formed for each ligand may well be the same in each case, with the anion playing little part in the primary coordination sphere of the metal. Unfortunately, until we are able to prepare authenticated complexes of **9** and **10** to investigate these possible differences, this will remain entirely speculative.

Conclusion

We have been able to prepare a series of novel ligands based on the 1,4,7-triazacyclononane core that have been selectively *N*-functionalised with phosphonic acid pendant arms. The rapid screening test that we have developed for bleaching activity indicated the potential efficacy of manganese complexes of **9** and **10** formed *in situ* as bleaching catalysts which was subsequently supported by bleaching stain removal tests. As anticipated, the effectiveness of the ligands in the removal of stains decreased as the number of pendant arms increased. Unfortunately, both combinations of ligands **9** and **10** with manganese lead to greater dye damage than did **1** alone, with **9** being a particularly aggressive bleaching catalyst of stained fabrics sensitive to oxidative damage, leading to more severe dye damage than is produced by **4**. This therefore suggests that the systematic addition of chelating pendant arms, whilst tempering the activity of the complexes as bleaching catalysts, unfortunately does not provide a solution to the problem of dye and fabric damage.

Experimental

All the reagents were used as supplied or were prepared using reported methods and used without further purification unless

otherwise stated. NMR spectra were obtained on a Jeol JNM-EX270 spectrometer (δ_{H} 270 MHz, δ_{C} 67.9 MHz, δ_{H} 109.3 MHz) in CDCl₃ unless otherwise stated. All *J* values are given in Hertz. Infrared spectra were obtained on a Perkin–Elmer FTIR 1720X spectrometer with a solid state ATR attachment. UV-visible spectra were recorded on a Hewlett–Packard 8453 diode array UV-vis spectrophotometer. Electrospray mass spectra were recorded on a Finnigan MAT 900 XLT instrument at the Engineering and Physical Science Research Council (EPSRC) National Mass Spectrometry Service centre, The University of Wales, Swansea. Elemental analysis was obtained using a Carlo Erba 1106 elemental analyser. Electron paramagnetic resonance (EPR) spectra were recorded on a Bruker 200D X-band spectrometer. The resonant position is referred to as the *g* value and the hyperfine splitting is ascribed as *A* and is measured in Gauss (G).

1-(Methylenephosphonic acid)4,7-bis-(methyl)-1,4,7-triazacyclononane dihydrobromide, **9**

The hydrobromide salt of **14** (1.00 g, 4.20 mmol) and anhydrous phosphorus acid (690 mg, 8.41 mmol) were dissolved in water (1.2 cm³) and concentrated hydrochloric acid (0.5 cm³) added. The mixture was heated to reflux and dry solid paraformaldehyde (190 mg, 6.30 mmol) was added in small portions over 1 h. This mixture was heated at reflux for a further hour. The solution was then cooled to 0 °C and then added dropwise to a stirred solution of ice-cold diethyl ether and absolute ethanol (2 : 1), (30 cm³) under vigorous stirring (rate of addition 1 drop every 3–4 s). The final mixture was stirred for an additional hour and the solvent was decanted. The precipitate obtained was dissolved in the minimum amount of hot methanol and the solution filtered whilst hot. To this solution petroleum ether (40 : 60) was added dropwise, which gave a white solid. The solid was recrystallised from hot methanol to yield **9**·2HBr as a white solid (0.80 g, 57%). Mp 240–241 °C; $\tilde{\nu}_{\text{max}}/\text{cm}^{-1}$ 2811, 2250, 1649, 1450, 1417, 1380, 1336, 1214 (P=O), 1163, 971, 930, 728; $\delta_{\text{H}}(\text{D}_2\text{O})$ 3.00 (2H, d, *J* 12.0, NCH₂P), 3.06 (6H, s, CH₃N), 3.07–3.27 (4H, br m, PCH₂NCH₂), 3.40–3.54 (4H, br m, PCH₂NCH₂CH₂NCH₃), 3.76 (4H, br,

CH_3NCH_2). δ_{C} 44.9 (CH_3N), 49.4 ($\text{CH}_3\text{NCH}_2\text{CH}_2\text{NCH}_3$), 51.4 ($\text{PCH}_2\text{NCH}_2\text{CH}_2\text{NCH}_3$), 52.1 (d, J 152.5, NCH_2P), 53.6 ($\text{PCH}_2\text{NCH}_2\text{CH}_2\text{NCH}_3$); δ_{P} 22.4; m/z (ES)⁺ 252.1472 ($\text{M} + \text{H}^+$, $\text{C}_9\text{H}_{23}\text{N}_3\text{O}_3\text{P}^+$ requires 252.1472), 503.3 (38%) ($2\text{M} + \text{H}^+$), 252.0 (100) ($\text{M} + \text{H}^+$), 171.9 (93) ($\text{C}_9\text{H}_2\text{N}_3^+$), 142.9 (23) ($\text{C}_7\text{H}_{16}\text{N}_3^+$), 129.9 (16) ($\text{C}_6\text{H}_{15}\text{N}_3^+$). Slow evaporation of an aqueous solution led to crystals suitable for single crystal X-ray diffraction.

1-Methyl-4,7-bis-(methylenephosphonic acid)-1,4,7-triazacyclononane dihydrobromide, **10**

Macrocycle **15a** (1.48 g, 4.20 mmol) and anhydrous phosphorus acid (1.59 g, 19.4 mmol) were dissolved in water (1.79 mL) and concentrated hydrochloric acid (0.76 mL) added. The mixture was heated at reflux and dry solid paraformaldehyde (437 mg, 14.6 mmol) was added in small portions over 1 h. This mixture was further refluxed for 60 min. The solution was then cooled to 0 °C in an ice bath and then added dropwise (at a rate of 1 drop every 3–4 s) to a vigorously stirred mixture of cold diethyl ether and absolute ethanol (1 : 1) (30 mL). The final mixture was stirred for an additional 1 h and the solvent was decanted. The precipitate obtained was dissolved in hot methanol and the solution filtered. Petroleum ether was added to the filtrate, which gave a white solid. The solid was recrystallised from hot methanol to yield **10** as a white solid (1.00 g, 51%). mp 98–100 °C; $\tilde{\nu}_{\text{max}}/\text{cm}^{-1}$ 2730, 2302, 1631, 1450, 1384, 1332, 1155 (P=O), 1118, 1096, 1052, 912, 724, 588; $\delta_{\text{H}}(\text{D}_2\text{O})$ 3.00 (3H, s, CH_3N), 3.18 (4H, d, J 10.0, NCH_2P), 3.35 (4H, s, $\text{CH}_3\text{NCH}_2\text{CH}_2\text{NCH}_2\text{P}$), 3.48–3.53 (8H, br m, $\text{CH}_3\text{NCH}_2\text{CH}_2\text{NCH}_2\text{P}$ and $\text{PCH}_2\text{NCH}_2\text{CH}_2\text{NCH}_2\text{P}$); δ_{C} 44.6 (CH_3N), 50.4 ($\text{CH}_3\text{NCH}_2\text{CH}_2\text{NCH}_2\text{P}$), 51.6 ($\text{CH}_3\text{NCH}_2\text{CH}_2\text{NCH}_2\text{P}$), 52.5 ($\text{PCH}_2\text{NCH}_2\text{CH}_2\text{NCH}_2\text{P}$), 53.3 (d, J 144.2, NCH_2P); δ_{P} 14.8; m/z (ES)⁺ 332.1132 ($\text{M} + \text{H}^+$, $\text{C}_9\text{H}_{24}\text{N}_3\text{O}_6\text{P}_2^+$ requires 332.1135), 663.5 (7%) ($2\text{M} + \text{H}^+$), 332.2 (64) ($\text{M} + \text{H}^+$), 250.1 (36) ($\text{C}_9\text{H}_{21}\text{N}_3\text{O}_3\text{P}^+$), 170 (26) ($\text{C}_9\text{H}_{20}\text{N}_3^+$).

1,4,7-Triazacyclononane-1,4,7-triyltris(methylenephosphonic acid) trihydrochloride, **11**

Macrocycle **11** has previously been reported,^{8–10,18} however, no experimental data other than a single crystal X-ray structure and elemental analysis were reported. An improvement in yield of the hydrochloride salt of **11** was achieved using the following method.

The hydrobromide salt of **15b** (7.00 g, 18.8 mmol) and anhydrous phosphorus acid (9.26 g, 113 mmol) were dissolved in water (15 mL) and concentrated hydrochloric acid (5.6 mL) added. The mixture was heated to reflux and dry solid paraformaldehyde (2.54 g, 84.7 mmol) was added in small portions over 1 h. This mixture was refluxed for a further 60 min. After cooling to room temperature, the dark brown reaction mixture was added dropwise, with cooling, to cold absolute ethanol (15 mL), which was stirred vigorously (addition rate 1 drop every 3–4 s). The final mixture was stirred for an additional hour and the resultant precipitate collected by filtration. The solid was thoroughly washed with ethanol and ether. The crude product was recrystallised from

the minimum amount of hot water to yield **11** as a white solid (6.0 g, 61%). Mp 255–257 °C; $\tilde{\nu}_{\text{max}}/\text{cm}^{-1}$ 2302, 1653, 1454, 1093 (P=O), 926, 709, 591; $\delta_{\text{H}}(\text{D}_2\text{O})$ 3.29 (6H, d, J 11.0, NCH_2P), 3.47 (12H, s, $\text{NCH}_2\text{CH}_2\text{N}$); due to the zwitterionic nature of the compound measurement of the ^{13}C NMR was not possible; δ_{P} 13.3; m/z (ES)⁺ 412.0791 ($\text{M} + \text{H}^+ - 3\text{HCl}$, $\text{C}_9\text{H}_{25}\text{N}_3\text{O}_9\text{P}_3^+$ requires 412.0798), 823 (3%) ($2\text{M} + \text{H}^+ - 6\text{HCl}$), 412 (100) ($\text{M} + \text{H}^+ - 3\text{HCl}$), 330 (32) ($\text{C}_9\text{H}_{22}\text{N}_3\text{O}_6\text{P}_2^+$), 248 (24) ($\text{C}_9\text{H}_{19}\text{N}_3\text{O}_3\text{P}^+$).

1,2-bis(4,7-Methylenephosphonic acid)-1,4,7-triazacyclonon-1-yl)-ethane, **12**

The hydrobromide salt of **17** (0.32 g, 0.40 mmol) and anhydrous phosphorus acid (300 mg, 3.29 mmol) were dissolved in water (0.80 mL) and concentrated hydrochloric acid (0.32 mL) added. The mixture was heated to reflux and dry solid paraformaldehyde (70 mg, 2.4 mmol) was added in small portions over 1 h. This mixture was refluxed for a further 1 h. The dark brown solution was then cooled to 0 °C in ice. The cold brown reaction mixture was then added to cold absolute ethanol (1.1 mL) dropwise under vigorous stirring (rate of addition 1 drop every 3–4 s). The final mixture was stirred for an additional hour and the resultant precipitate collected by filtration. The solid was thoroughly washed with ethanol and ether and recrystallised from the minimum amount of hot water to yield **12** as a white solid (0.27 g, 84%). Mp 276–277 °C; $\tilde{\nu}_{\text{max}}/\text{cm}^{-1}$ 2921, 2651, 1739, 1453, 1382, 1236 (P=O), 1090, 898; $\delta_{\text{H}}(\text{D}_2\text{O})$ 3.20 (8H, br, bridge $\text{CH}_2\text{NCH}_2\text{CH}_2\text{N}$), 3.24 (4H, br, bridge CH_2), 3.39 (8H, d, J 12.0, NCH_2P), 3.55 (16H, br s, $\text{NCH}_2\text{CH}_2\text{N}$); due to the zwitterionic nature of the compound measurement of the ^{13}C NMR was not possible; δ_{P} 11.4; m/z (ES) 661.2041 ($\text{M} + \text{H}^+ - 4\text{HCl}$, $\text{C}_{18}\text{H}_{45}\text{N}_6\text{O}_{12}\text{P}_4^+$ requires 661.2040), 661 (37%) ($\text{M} + \text{H}^+ - 4\text{HCl}$), 581.4 (27) ($\text{C}_{18}\text{H}_{44}\text{N}_6\text{O}_9\text{P}_3^+$), 497.5 (5) ($\text{C}_{18}\text{H}_{39}\text{N}_6\text{O}_6\text{P}_2^+$), 344.2 (5) ($\text{C}_{18}\text{H}_{36}\text{N}_6^+$). Slow evaporation of an aqueous solution led to crystals suitable for single crystal X-ray diffraction.

Synthesis of $[\text{Mn}(\mathbf{9})]\cdot 3\text{H}_2\text{O}$, **18**

Ligand **9** (5.21 g, 10.0 mmol) was stirred in water (20 cm³) and sodium hydroxide (1.20 g, 30.0 mmol) added. The mixture was heated to 55 °C for 5 min. To this clear solution manganese(II) acetate tetrahydrate (2.46 g, 10.0 mmol) dissolved in water (10 mL) was added. The reaction mixture was heated for one hour and the reaction solution changed from colourless to pale pink. The solvent was evaporated and the precipitate obtained washed with hot ethanol and methanol to yield **17** as a white powder (4.00 g, 76%). mp > 300 °C; Found: C, 20.0; H, 5.3; N, 7.6. $\text{C}_9\text{H}_{29}\text{MnN}_3\text{NaO}_{12}\text{P}_3\cdot 3\text{H}_2\text{O}$ requires: C, 19.9; H, 5.4; N, 7.8; $\tilde{\nu}_{\text{max}}/\text{cm}^{-1}$ 2324, 1560, 1421, 1145, 1064, 915, 719; UV-vis λ_{max} 190 nm (6280 mol dm⁻³ cm⁻¹); m/z (ES)⁺ 462.9868 ($\text{M} - \text{H}^+$, $\text{C}_9\text{H}_{21}\text{N}_3\text{O}_9\text{MnP}_3^+$ requires 462.9866).

Screening of catalytic systems

The screening tests were carried out using the following standard stock solutions: (i) a buffer solution (5 kg) was

prepared by dissolving sodium hydrogen carbonate (84 g) and sodium carbonate (106 g) in deionised water; (ii) an aqueous solution of Dequest 2066 (2.5% w/v); (iii) all ligands and catalysts were diluted with deionised water (to 1×10^{-3} M); (iv) aqueous metal salts were diluted to (1×10^{-3} M) with deionised water; (v) the oxidant used was either 36–40 wt% peracetic acid in acetic acid solution or 27% hydrogen peroxide solution; (vi) reference catalyst solution containing complex **4** (1×10^{-3} M) dissolved in deionised water; (vii) crocetin dye (25 mg) was dissolved in deionised water (100 mL) and the solution heated to 40 °C in an ultrasonic bath for 2 h or until the dye crystals dissolved.

The screening test employs the following solutions, which were made by the addition of the standard stock solutions in the order stated: (1) a blank solution of buffer solution (stock solution (i), 98 mL), Dequest 2066 solution (stock solution (ii), 1 mL) and dye solution (stock solution (vii), 1 mL); (2) standard solution 1 comprising buffer solution (stock solution (i), 98 mL), Dequest 2066 solution (stock solution (ii), 1 mL), either 36–40 wt% peracetic acid in acetic acid solution (0.095 mL) or 27% hydrogen peroxide solution (0.065 mL) and dye solution (stock solution (v), 1 mL); (3) standard solution 2 containing buffer solution (stock solution (i), 97 mL), Dequest 2066 solution (stock solution (ii), 1 mL), metal salt solution (stock solution (iv), 1 mL), either 36–40 wt% peracetic acid in acetic acid solution (0.095 mL) or 27% hydrogen peroxide solution (0.065 mL) and dye solution (stock solution (vii), 1 mL); (4) standard solution 3 comprising buffer solution (stock solution (i), 97 mL), Dequest 2066 solution (stock solution (ii), 1 mL), reference catalyst solution (stock solution (vi), 1 mL), either 36–40 wt% peracetic acid in acetic acid solution (0.095 mL) or 27% hydrogen peroxide solution (0.065 mL) and dye solution (stock solution (vii), 1 mL).

The behaviour of these standard solutions was then compared to two test solutions: (T1) test solution 1 made up with buffer solution (stock solution (i), 96 mL), ligand solution (stock solution (iii), 1 mL) and metal salt solution (stock solution (iv), 1 mL) and the mixture stirred and then left for 30 min before a solution of Dequest 2066 (stock solution (ii), 1 mL), either 36–40 wt% peracetic acid in acetic acid solution (0.095 mL) or 27% hydrogen peroxide solution (0.065 mL) and dye solution (stock solution (vii), 1 mL) were added; (T2) test solution 2 comprising buffer solution (stock solution (i), 97 mL), complex solution (stock solution (iii), 1 mL), Dequest 2066 solution (stock solution (ii), 1 mL), either 36–40 wt% peracetic acid solution in acetic acid (0.095 mL) or 27% hydrogen peroxide solution (0.065 mL) and dye solution (stock solution (vii), 1 mL).

Compounds were first screened in the presence of peracetic acid. Samples that bleached more effectively than the reference standard solutions 2 and 3 were then also screened with hydrogen peroxide. Whilst this approach may seem anti-thetical due to the possibility of ligand oxidation/destruction by peracetic acid, it is our observation that this approach provides a more reliable indicator of bleaching activity of potential catalysts. The results were obtained by simple visual observation of the colour change over a 24 h period at room temperature of the solution over time as the yellow

solution turned colourless or very light yellow. This provided the preliminary results and identified potential bleaching candidates.

Wash-test analysis

A terg-o-tometer Model 7243-S (United States Testing Co., Inc.) and a Datascolor International Spectraflash 500 spectrophotometer were used for the wash test analysis.

Evaluation of bleaching efficacy

Wash test analyses were carried out at Warwick International Ltd using standard company conditions. Stained swatches were obtained from the Centre for Testmaterials, Stoomloggerweg 11, 3133 KT Vlaardingen, Netherlands (email info@cftbv.nl).

The test was carried out at 40 °C for 20 min at 150 rpm in the terg-o-tometer using a dosage of 5 g of reagents L⁻¹ of deionised water. The catalysts were added to a standard formulation of **1** at a level of 0.01 mmol of metal L⁻¹ of deionised water. These catalysts were produced by dissolving ligands and metal salts in deionised water (10 L) and they were allowed to react for a set time (30 min) to yield the catalytic solution. The wash tests were carried out by the addition of the reagents to the terg-o-tometer pot in the following order: (i) resultant catalytic solutions (1 L); (ii) reagents (5 g) added sequentially = uncoated **1** (activator) (0.25 g), NaBO₃·H₂O (0.5 g) and finally IECA*²¹ (4.25 g); (3) one of six bleachable stained swatches (BC2—coffee stains, BC3—tea stains for low temperatures, BC5—red beet stains, CS12—red wine, CS8—grass stains, E114—oil/carbon black stains) was added to each terg-o-tometer pot. After the first wash cycle stained fabrics were rinsed, ironed and the stain removal results measured as Z% brightness using the Datascolor International Spectraflash 500 spectrophotometer.

Evaluation of dye damage

The twelve cotton fabrics used in this study were a specifically selected part of the standard monitor set (40 cloths in total)²² and can be obtained from Colour Synthesis Solutions Ltd., Textiles and Paper, School of Materials The University of Manchester, PO Box 88, Sackville Street, Manchester, M60 1QD, UK.

Specifically: fabric 1, black sulfur dye; 5, vat blue dye (indanthrone); 6, yellow vat dye (antraquinone + azo units in structure); 8 yellow direct dye treated with a cationic after treatment agent; 10, black direct dye; 13, rubine direct dye; 20 navy/black reactive dye (applied at pale depth of shade); 21, navy/black reactive dye (applied at heavy depth of shade); 23, green reactive dye (nickel phthalocyanine); 24, turquoise reactive dye (copper phthalocyanine); 27, three reactive trichromatic combinations which exhibit no oxidative-bleach; 29, three reactive trichromatic combinations which exhibit two oxidative-bleach sensitive dyes.

The colour damage profile (CDP) test that forms part of the international standard ISO 105-C09 (colour fastness to domestic laundering—oxidative bleach response in the presence of a low temperature bleach activator) was utilised for this

evaluation. The method is intended to reflect the effect of multicycle laundering using an activated bleach detergent by domestic procedures. Previous 'in-house' studies have indicated that this is a suitable method for evaluating dye damage incurred when using catalyst formulations. A Rotawash instrument or equivalent is stipulated in the CDP test, however a Roaches Pyrotec instrument was utilised for this study as it provided a more efficient way of performing multiple evaluations whilst maintaining the principle of the method. Each fabric was cut into a 5 cm × 10 cm swatch. Each formulation was prepared in tap water (1 L) by dispersing the ECE reference detergent²³ (10.0 g L⁻¹), uncoated **1** (1.8 g L⁻¹) and NaBO₃·H₂O (7.7 g L⁻¹) at 25 °C. In addition, manganese(III) acetate (0.0086 g L⁻¹) and the ligand (0.0083 g for **9** and 0.0130 g for **10**) were added. The solution was stirred at 400 rpm for 10 min (±1 min) before adding it (60 g) to each Pyrotec pot. The pots were placed in the Pyrotec at 25 °C before ramping the temperature to 60 °C at 1.5 °C min⁻¹. The temperature was maintained at 60 °C for 30 min, before the fabrics were removed and placed in a beaker containing ambient water (2 L). The rinsing solution was stirred gently for 1 min before the beaker was placed under a cold running tap for 10 min. Each fabric was squeezed to remove the excess liquor and then dried flat between two layers of paper tissue. The fabrics were allowed to air dry prior to evaluation. The new ligand formulations were compared to two blank solutions made up in the same way as outlined above the first without any metal salt and the second a catalytic standard containing **4** (0.0144 g L⁻¹). [$\Delta E = (\Delta L^2 + \Delta a^2 + \Delta b^2)^{1/2}$ Where ΔL = lightness, Δa = red(+) to green(-) and Δb = yellow(+) to blue(-).]²⁴

Epoxidation catalysis

All reactions were performed by a slight modification of the reported procedure⁵ as follows: to a solution of the substrate (1 mmol) in acetone (0.6 g) was added the metal salt (5 µmol) in water (0.1 cm³), ligand (7.5 µmol) in stock solution (i) (0.1 cm³). The resultant mixture was then diluted with stock solution (i) (three times the volume of H₂O₂ solution to be added subsequently) and the solution adjusted to pH 7 with glacial acetic acid. An internal *n*-decane standard (0.02 cm³) was added and the mixture stirred at room temperature for 30 min. A solution of H₂O₂ (35% wt/vol) was diluted with acetone in a 1 : 3 v/v ratio and 6 molar equivalents of this solution added to the reaction mixture and the reactions stirred for 4 h. All reactions were assessed as reported by GC.⁵

X-ray crystallography

Crystal data for **9**. C₉H₂₈Br₂N₃O₅P, $M = 449.13$, Triclinic, $a = 7.6030(7)$, $b = 9.1105(9)$, $c = 13.0353(15)$ Å, $\alpha = 89.455(4)^\circ$, $\beta = 75.731(4)^\circ$, $\gamma = 86.145(6)^\circ$, $V = 873.06(15)$ Å³, space group P1, $Z = 2$, $D_c = 1.708$ mg m⁻³, $\mu(\text{Mo-K}\alpha) = 4.754$ mm⁻¹, reflections measured 14229, reflections unique 3798 with $R_{\text{int}} = 0.0966$, $T = 120(2)$ K, Final R indices [$I > 2\sigma(I)$] $R1 = 0.1243$, $wR2 = 0.3384$ and for all data $R1 = 0.1570$, $wR2 = 0.3619$.

CCDC reference number 6149132. For crystallographic data in CIF or other electronic format see DOI: 10.1039/b609710c

Crystal data for **12**. C₁₈H₅₂N₆O₁₆P₄, $M = 732.54$, Monoclinic, $a = 20.450(4)$, $b = 7.329(2)$, $c = 10.310(7)$ Å, $\beta = 99.28(2)^\circ$, $V = 1525.0(7)$ Å³, space group P2₁/n, $Z = 2$, $D_c = 1.595$ mg m⁻³, $\mu(\text{Mo-K}\alpha) = 0.330$ mm⁻¹, reflections measured 2883, reflections unique 2643 with $R_{\text{int}} = 0.0234$, $T = 160(2)$ K, final R indices [$I > 2\sigma(I)$] $R1 = 0.0402$, $wR2 = 0.0944$ and for all data $R1 = 0.0928$, $wR2 = 0.1099$.

CCDC reference number 6149131. For crystallographic data in CIF or other electronic format see DOI: 10.1039/b609710c

Acknowledgements

We are grateful to the EPSRC for the provision of a studentship (KS) under the CNA Scheme, for the National Mass Spectrometry Service, University of Wales, Swansea and for the National X-Ray Crystallography Service, University of Southampton.

References

- 1 N. J. Milne, *J. Surfactants Deterg.*, 1998, **1**, 253–261.
- 2 R. Hage, J. E. Iburg, J. Kerschner, J. H. Koek, E. L. M. Lempers, R. J. Martens, U. S. Racherla, S. W. Russell, T. Swarthoff, M. R. P. van Vliet, J. B. Warnaar, L. van der Wolf and B. Krijnen, *Nature*, 1994, **369**, 637–639.
- 3 R. Hage and A. Lienke, *Angew. Chem., Int. Ed.*, 2006, **45**, 206–222; R. Hage and A. Lienke, *J. Mol. Catal. A: Chem.*, 2006, **251**, 150–158.
- 4 B. C. Gilbert, J. R. Lindsay Smith, M. S. Newton, J. Oakes and R. Pons i Prats, *Org. Biomol. Chem.*, 2003, **1**, 1568–1577.
- 5 D. E. De Vos and T. Bein, *J. Organomet. Chem.*, 1996, **520**, 195–200.
- 6 C. Bolm, D. Kadereit and M. Valacchi, *Synlett*, 1997, 687–688.
- 7 K. Sibbons, K. Shastri and M. Watkinson, *Dalton Trans.*, 2006, 645–661.
- 8 M. Y. Antipin, A. P. Baranov, M. I. Kabachnik, T. Y. Medved, Y. M. Polikarpov, Y. T. Struchkov and B. K. Scherbakov, *Dokl. Akad. Nauk SSSR*, 1986, **287**, 130–134.
- 9 M. I. Kabachnik, M. Y. Antipin, B. K. Shcherbakov, A. P. Baranov, Y. T. Struchkov, T. Y. Medved and Y. M. Polikarpov, *Koord. Khim.*, 1988, **14**, 536–542.
- 10 S.-S. Bao, G.-S. Chen, Y. Wang, Y.-Z. Li, L.-M. Zheng and Q.-H. Luo, *Inorg. Chem.*, 2006, **45**, 1124–1129.
- 11 J. S. Bradshaw, K. E. Krakowiak and R. M. Izatt, *Aza-crown Macrocycles*, Wiley, New York, 1989, ch. 4, p 145.
- 12 G. H. Searle and R. J. Geve, *Aust. J. Chem.*, 1984, **37**, 959–970.
- 13 K. Wieghardt, I. Tolksdorf and W. Herrmann, *Inorg. Chem.*, 1985, **24**, 1230–1235.
- 14 A. J. Blake, J. P. Danks, W. S. Li, V. Lippolis and M. Schröder, *J. Chem. Soc., Dalton Trans.*, 2000, 3034–3040.
- 15 I. Lázár, D. C. Hrnčir, W.-D. Kim, G. E. Kiefer and A. D. Sherry, *Inorg. Chem.*, 1992, **31**, 4422–4424.
- 16 N. Choi and M. McPartlin, *Aminophosphonic and Aminophosphinic Acids*, ed. V. P. Kukhar and H. R. Hudson, Wiley, UK, 2000, ch 10, p327–361.
- 17 (a) A. L. Spek, *Acta Crystallogr., Sect. A: Found. Crystallogr.*, 1990, **46**, C34; (b) A. L. Spek, *PLATON, A Multipurpose Crystallographic Tool*, Utrecht University, Utrecht, The Netherlands, 1998.
- 18 (a) W. Clegg, P. B. Iveson and J. C. Lockhart, *J. Chem. Soc., Dalton Trans.*, 1992, 3291–3298; (b) C. F. G. C. Geraldes, A. D. Sherry and W. P. Cacheris, *Inorg. Chem.*, 1989, **28**, 3336–3341.
- 19 S. Pulacchini, K. Shastri, N. C. Dixon and M. Watkinson, *Synthesis*, 2001, 2381–2383.
- 20 L. J. Farrugia, ORTEP-3 for Windows, *J. Appl. Crystallogr.*, 1997, **30**, 565.
- 21 R. V. Parish, *NMR, NQR, EPR, and Mössbauer Spectroscopy in Inorganic Chemistry*, Ellis Horwood, Chichester, UK, 1990, ch. 5.
- 22 Developed by AISE as part of the new bleach care testing protocol described in ISO 105-C09 for colour fastness (2001); see also G. C. A. Luijk, R. Hild, E. S. Krijnen, R. Lodewick,

T. Rechenbach, G. Reinhardt and D. A. S. Phillips, *Tenside Surfactants Deterg.*, 2004, **41**, 156–162.

23 For further information see: http://www.testgewebe.de/mainframe_us.html.

24 For a discussion of ΔE and issues associated with colour difference measurement see for example *Colour Physics for Industry* (1987), ed. R. McDonald, Society of Dyers and Colourists, Bradford, UK, ch. 4, p. 97–115, ISBN 0901956457.

Find a SOLUTION

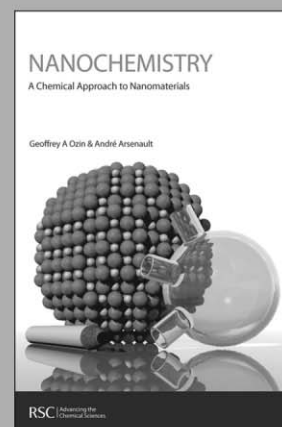
... with books from the RSC

Choose from exciting textbooks, research level books or reference books in a wide range of subject areas, including:

- Biological science
- Food and nutrition
- Materials and nanoscience
- Analytical and environmental sciences
- Organic, inorganic and physical chemistry

Look out for 3 new series coming soon ...

- RSC Nanoscience & Nanotechnology Series
- Issues in Toxicology
- RSC Biomolecular Sciences Series



RSC Publishing

www.rsc.org/books

Renewable plant-based soybean oil methyl esters as alternatives to organic solvents

Scott K. Spear,^{*a} Scott T. Griffin,^b Kimberly S. Granger,^b Jonathan G. Huddleston^c and Robin D. Rogers^{*b}

Received 13th February 2007, Accepted 3rd May 2007

First published as an Advance Article on the web 24th May 2007

DOI: 10.1039/b702329d

The physico-chemical properties of soybean oil methyl ester (SBME), better known as biodiesel, of importance to its use as a solvent in liquid–liquid separations have been examined. Partition coefficients of several organic species between SBME–water have been determined and compared to log *P* (1-octanol–water). The free energy of transfer of a methylene group has been obtained and the solvent properties of the SBME–water system determined from distribution data of a small solute set using Abraham's generalized solvation equation. Solute distribution behavior is similar to that found for conventional organic solvent–water systems, but is most similar to other vegetable oils such as olive oil. When ionizable solutes are partitioned in the SBME–water system at differing pH, the neutral species show the highest distribution. Partitioning is dependent on the solute's ability to form hydrogen bonds between water and its charged state. Metal ions (*e.g.*, Fe³⁺, Co²⁺, and Ni²⁺) exhibit moderate partitioning to the SBME phase from water only in the presence of extractants. Actinides (UO₂²⁺, Am³⁺) exhibit significant partitioning to the SBME from aqueous solutions with the use of octyl(phenyl)-*N,N*-diisobutylcarbamoylmethyl phosphine oxide (CMPO). Soybean oil methyl ester may be a suitable “green” alternative for the replacement of volatile organic solvents in liquid–liquid extractions in selected applications.

Introduction

An important component of green chemistry is the search for new solvents with which to replace volatile organic compounds (VOCs). Ideally, such solvents should be of low toxicity, low volatility, and derived from renewable resources.¹ We have a long standing interest in the design and development of environmentally benign solvents for liquid–liquid extraction.^{2–4} One possible route to renewable solvents having a ‘green’ character with some potential to address pollution prevention/remediation concerns, may be to base the starting materials upon agrochemicals rather than petroleum based raw materials.^{5,6} Here, we examine the solvent properties of transesterified soybean oil, better known as biodiesel, as related to liquid–liquid partition from water.

World production of vegetable oils is recorded at 88.7 million metric tons, with over 10 million metric tons of vegetable oils produced in the United States.⁷ U. S. oilseed crops include soybean (by far the predominant seed oil crop), corn, cotton, sunflower, flax, and rapeseed (canola). The major use for vegetable oils is, obviously, in food products, however, some vegetable oils and their ester derivatives are finding increasing industrial usage. Two important uses of transesterified soybean oil are in soybean oil inks and in diesel fuel.⁸

Also, vegetable oils have recently found use as a cheap, non-toxic solvent for the synthesis of nanoparticles⁹ and quantum dots.¹⁰ Regulatory pressure to reduce VOC emissions is leading to an increasing use of such solvents in the coatings industry.¹¹

Soybean oil methyl esters (SBMEs, *e.g.*, SoyGold[®] 1000) are composed of a mixture of fatty acids (Table 1). Palmitic and stearic acid are saturated fatty acids and comprise approximately 15% of the final mixture. The remaining three major fatty acids, oleic acid, linoleic acid, and linolenic acid have varying degrees of unsaturation and comprise approximately 83% of the final mixture. By far the major fatty acid present in soybean oil is linoleic acid. Linoleic acid is an 18-carbon long-chain fatty acid with double bonds at the 9- and 12-carbon atoms.

SBME is produced by the transesterification of soybean oil and methanol. It is non-toxic, non-hazardous, and biodegradable. It is neither a hazardous air pollutant (HAP), nor an ozone-depleting chemical (ODC).

Transesterification chemistry (used in the production of SoyGold[®] 1000) is a more modern innovation, and involves the combination of organically derived oils or fats with a small chain alcohol such as methanol or ethanol in the presence of a catalyst (most often the catalyst is a base) to form fatty acid esters. This process is akin to saponification chemistry, the alkaline hydrolysis of fatty acid esters, in which triglycerides are reacted with sodium or potassium hydroxide to produce glycerol and fatty acid salts (soap). SBME has a high flash point (218 °C) and low vapor pressure (<2 mm Hg).¹³

Materials such as SBME may have an important role to play in replacing the previous generation of solvents with materials of a more benign nature derived from renewable resources. However, there is a need to understand the physico-chemical

^aAlabama Institute for Manufacturing Excellence, The University of Alabama, Tuscaloosa, AL 35487, USA. E-mail: SSpear@bama.ua.edu; Fax: +1 205 3483510; Tel: +1 205 3480464

^bCenter for Green Manufacturing and Department of Chemistry, The University of Alabama, Tuscaloosa, AL 35487, USA. E-mail: RDRogers@bama.ua.edu; Fax: +1 205 3480823; Tel: +1 205 3484323

^cMillipore Bioprocessing Ltd., Medomsley Road, Consett, County Durham, UK DH8 6SZ

Table 1 Major fatty acids (%) and ratio of # of carbons to carbon-carbon double bonds in soybean oil^{a,b}

Ratio (name)	16 : 0 (Palmitic)	18 : 0 (Stearic)	18 : 1 (Oleic)	18 : 2 (Linoleic)	18 : 3 (Linolenic)	Other
%	11	4	22	53	7.5	2.5
Structure						

^a From data compiled in ref. 12. ^b Cis-unsaturation.

properties of these materials before they can find widespread application. The solvent property data we report here is intended to inform that understanding, and begin to place SBME in context with other common solvents.

Experimental

Reagents and tracers

SoyGold[®] 1000, was used as received from Ag Environmental Products L.L.C. (Lenexa, KS, USA). Extractants 1-(2-pyridylazo)-2-naphthol, PAN, and (1-thiazolylazo)-2-naphthol, TAN, were obtained from Lancaster Synthesis, Inc. (Windham, NH, USA) and used as received. Octyl(phenyl)-*N,N*-diisobutylcarbamoylmethyl phosphine oxide, CMPO, was obtained from Strem Chemicals (Newburyport, MA, USA) and used without further purification. All water was purified using a Barnstead (Dubuque, IA, USA) commercial deionization and polishing system. All other chemicals were of reagent grade.

The ¹⁴C-labeled organic solutes were purchased from Sigma (St. Louis, MO, USA). Upon receipt, the tracers were diluted to an activity of *ca.* 0.06–0.08 $\mu\text{Ci } \mu\text{L}^{-1}$ for use as the ‘spike’ in the partitioning experiments. The hydrophilic tracers were diluted in deionized water and the hydrophobic tracers were diluted in their unlabelled form.

The cobalt tracer (as ⁶⁰CoCl₂ in 0.5 M HCl) was obtained from New England Nuclear (Boston, MA, USA). The iron tracer (as ⁵⁹FeCl₃ in 0.1 M HCl) and the nickel tracer (as ⁶³NiCl₂ in 0.1 M HCl) were both obtained from Amersham Pharmacia Biotech (Piscataway, NJ, USA). The actinide tracers (²³³UO₂Cl₂ and ²⁴¹AmCl₃) were obtained from Isotope Products Laboratories (Valencia, CA, USA). All metal ion radiotracers, except for ²³³U, were used as received for partitioning studies, or diluted with deionized water to an activity of *ca.* 0.03 $\mu\text{Ci } \mu\text{L}^{-1}$.

Stock solutions of the uranyl nitrate radiotracer solution were cleaned of impurities (²²⁸Th and its daughters from decay of ²³²U impurities) using TEVA resin (Eichrom Industries, Darien, IL, USA).¹⁴ 20 μL of ²³³UO₂²⁺ stock solution was diluted in 10 mL of 5 M HCl and the solution was added to a column comprised of 1 g TEVA resin preconditioned with 5 M HCl. After loading, 20 mL of 0.5 M HCl was added to the column to elute ²³³U, which was collected, evaporated to dryness and dissolved in 0.1 M HNO₃.

Water content

The equilibrium water content of SBME was determined using a volumetric Aquastar Karl Fischer titrator (EM Science, Gibbstown, NJ, USA) with Composite 5 solution as the titrant

and anhydrous methanol as the solvent. Each sample was at least 0.1 g and triplicate measurements were performed on each sample.

Radioanalytical measurements

Cobalt-60, iron-59, nickel-63, and americium-241 were analyzed by their characteristic gamma ray emission with a Packard Cobra II Auto-Gamma counting system (Packard Instrument Co., Inc., Meriden, CT, USA). Carbon-14 and uranium-233 activities were followed by beta decay analysis using Ultima Gold scintillation cocktail and a Packard Tri-Carb 1900 TR Liquid Scintillation Analyzer (Packard Instrument Co., Inc., Meriden, CT, USA).

Partitioning studies

Equal volumes of water and SoyGold[®] were added to form the biphasic system studied. In liquid-liquid partition studies, the organic and metal ion species distribution ratios were determined radiometrically using previously described methods.¹⁵ For each determination, equal aliquots of SoyGold[®] and water were mixed. Each system was equilibrated by vortexing for 2 min, followed by 2 min of centrifugation (2000 g). A tracer quantity of organic or metal ion species was then added to the two-phase system. The system was then twice vortexed for 2 min followed by 2 min of centrifugation (2000 g). Equal aliquots of each phase were then removed for radioanalysis. The distribution ratio (*D*) was calculated by the ratio of the activity in the top SoyGold[®] phase divided by the activity in the lower aqueous phase.

The distribution ratios reported here are the average of at least two measurements and are typically accurate to $\pm 5\%$. Where necessary, the aqueous phase pH was measured using a Fisher Accumet pH meter and adjusted to acidic conditions using sulfuric acid or to basic conditions using sodium hydroxide. Multiple linear regression analyses were performed using Stat Box v2.5 (Grimmer Logiciels, 34 Rue de Dunkerque, Paris, France).

Solvent characterization

The SBME used in this study (SoyGold[®] 1000) is identified as methyl soyate with the CAS registry number 67784-80-9.¹³ It can be described as a pale yellow liquid with a mild odor. SBME is insoluble in water and is incompatible with strong oxidizing agents. While no specific fire hazard problems during shipment have been reported, the possibility of spontaneous combustion (“oily rag” problem) is inherent. With a boiling point over 315 °C at 760 mm Hg and a specific gravity of 0.882 g mL⁻¹ at 25 °C, SBME has most commonly been used

as 'biodiesel' in the United States. In the following discussion, we address the effectiveness of SBMEs as environmentally-friendly, alternative organic diluents.

Results and discussion

Organic solute partitioning

Partitioning data for 20 solutes partitioned as the neutral species in an SBME–water biphasic system are shown in Fig. 1, where they are compared to published values of these solutes' octanol–water partition coefficient ($\log P$). As is to be expected, there is a significant relationship between the octanol–water partition coefficient and the partition coefficient in the SBME–water system. However, there are also, again as is to be expected, significant differences in detail.

The relationship between the octanol–water partition coefficient and the distribution in the SBME–water system can be summarized in the form of eqn (1):

$$\log D(\text{SBME}) = b + m(\log P) \quad (1)$$

where $\log D(\text{SBME})$ is the distribution in the SBME–water system, $\log P$ is the distribution in the 1-octanol–water system, and b and m are constants. Here, $b = -0.69$ and $m = 1.04$ ($R^2 = 0.88$). Thus, the distribution coefficient in the SBME–water system is in general somewhat less than one order of magnitude lower (*ca.* 0.7 log) than that in the 1-octanol–water system, and a 1-octanol–water partition coefficient of about 0.7 marks the transition between water and oil phase preference in the SBME–water system.

Determination of ΔG_{CH_2}

ΔG_{CH_2} is generally recognized as a measure of hydrophobicity related to the relative free energy of cavity formation to accommodate a solute in each of the two phases in a *l-l* biphasic system.^{17,18} As a result of the limited molecular interactions possible for solutes, it is characterized here by an incremental increase in methylene groups. However, solutes

differ in their relative hydrophobicity, and this arises from differences in the total of all solute–solvent interactions possible in each of the phases. Such complexity is not always captured by relationships to 1-octanol–water partitioning or by quantities such as the free energy of transfer of a methylene group, and thus it is usually necessary to measure several such properties for any given system. Here we discuss our determinations of ΔG_{CH_2} for the SBME–water system.

Fig. 2 shows the distribution of several *n*-alcohols in relation to their alkyl chain length in the SBME–water system, as well as literature data for their distribution in an olive oil–water system¹⁶ and the conventional 1-octanol–water system. These relationships can be described by eqn (2):

$$\ln K = C + En_c \quad (2)$$

where K is the partition coefficient, C is a constant related to the hydration properties of the phases, n_c refers to the number of carbons in the alkyl chain of the solutes partitioned, and E is a constant defined as the average $\ln K$ increment per CH_2 group.^{17–19} From this data the free energy of transfer of a methylene group (ΔG_{CH_2}) may be obtained from eqn (3) in kcal mol^{-1} :

$$\Delta G_{\text{CH}_2} = -RTE \quad (3)$$

where R is the universal gas constant, T is the absolute temperature, and E is the slope of the line in Fig. 2 (plotted from eqn (2)).^{17–19}

Table 2 presents ΔG_{CH_2} values for various solvent systems to allow comparison with the present SBME system and with the olive oil–water system. Also included in Table 2 are ΔG_{CH_2} values for selected ionic liquid (IL) salt–salt²⁰ and polyethylene

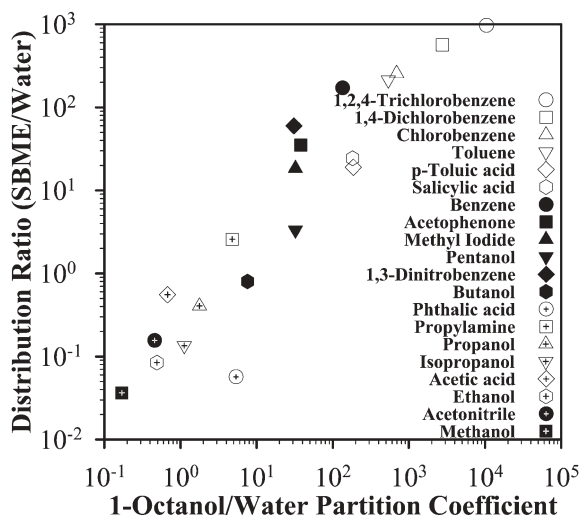


Fig. 1 Correlation of partitioning data between SBME–water and 1-octanol–water biphasic systems.

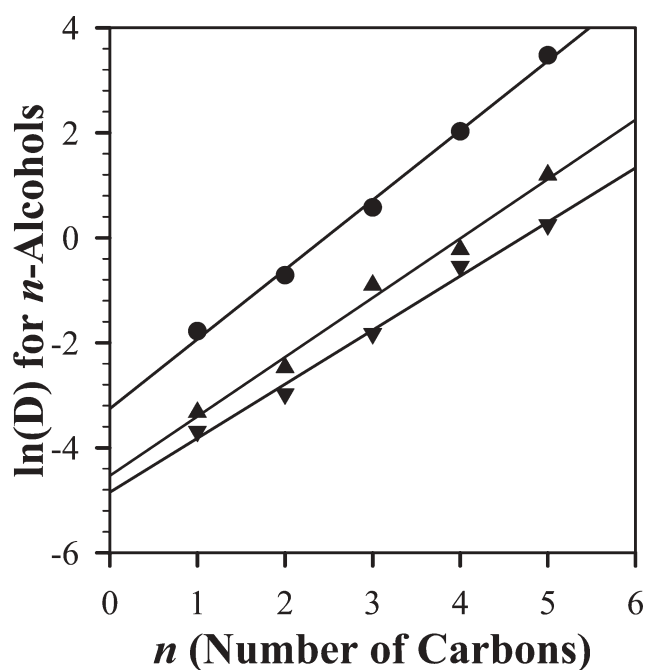


Fig. 2 Distribution of short chain alcohols in the SBME–water (\blacktriangle) system compared to distribution in the olive oil–water (\blacktriangledown) and 1-octanol–water (\bullet) systems.

Table 2 Free energy of transfer of a methylene group for various solvent–water systems

Solvent–water system	$-\Delta G_{\text{CH}_2}/\text{kcal mol}^{-1}$	Ref.	Solvent–water system	$-\Delta G_{\text{CH}_2}/\text{kcal mol}^{-1}$	Ref.
Hexane	1.10	18	Diisopropyl ether	0.68	18
Chloroform	0.85	18	SBME	0.67	— ^a
Benzene	0.84	18	Xylene	0.64	18
Octanol	0.79	18	Olive oil	0.61	— ^b
Octane	0.77	18	<i>n</i> -Butanol	0.54	18
Dodecane	0.77	18	Methyl ethyl ketone (MEK)	0.43	18
Methyl isobutyl ketone (MIBK)	0.72	18	PEG–salt (general)	0.142–0.696	4
IL salt–salt : 1-butyl-3-methylimidazolium chloride/K ₃ PO ₄ or K ₂ HPO ₄ or K ₂ CO ₃	0.304–0.728	20	PEG-2000 (40% w/w)/(NH ₄) ₂ SO ₄ (1.68 M)	0.214	4

^a Present work. ^b Calculated in present work with data from Ref. 16.

glycol (PEG)–salt aqueous biphasic systems (ABS)⁴ that have been studied in our laboratory. From Table 2, one notes that based on the ΔG_{CH_2} for the various solvents listed, SBME is very near to that observed for xylene and would suggest that SBME is a likely alternative to xylene as a solvent. Indeed, Hendrickson *et al.* have discovered that SBME is a suitable replacement for xylene as a developing solvent for photopolymerizable printing plates.²¹

Table 2 and Fig. 2 illustrate the similarity between the solvent properties of the currently investigated SBME–water system and literature data for the olive oil–water system. The free energy of transfer between the phases of the SBME system is much less than that typical of solvents dominated by van der Waals forces and much more similar to solvents typified by molecular interactions or by a significant water content at equilibrium. However, the equilibrium water content of the SBME phase is relatively low (0.35% wt/wt), and since it might be expected that the predominant intermolecular forces in an SBME phase would be dispersion forces, it is possible that molecular packing features contribute to the relative weakness of cavity forces in the olive oil and SBME phases implied by the relatively low free energy of CH₂ transfer value obtained in these systems.

Linear free energy relationships

The complexity of solute–solvent interactions is generally assumed to be encapsulated in some form of a generalized solvation equation which can be represented by eqn (4):⁴

$$\text{Some Property (SP)} = \text{cavity terms} + \text{polarity terms} + \text{hydrogen bonding terms} + \text{constant} \quad (4)$$

Linear free energy relationships (LFER) based upon the generalized solvation equation have been widely used to model many processes, such as partitioning in aqueous–organic systems, solubility, and transport across biological membranes.^{22–24} Abraham's generalized solvation equation, eqn (5):

$$\log SP = c + rR_2 + s\pi_2^H + a\sum\alpha_2^H + b\sum\beta_2^H + vV_x \quad (5)$$

has been used to characterize solvation in a wide variety of solvent systems including the description of partition in various aqueous–organic systems^{25–27} and aqueous–micellar systems.^{28,29} We have previously used Abraham's approach to

characterize solute distribution in a PEG-2000/(NH₄)₂SO₄ ABS⁴ and for ionic liquids (ILs).³⁰

In essence, the log of *SP*, in this case the partition coefficient of a series of solutes in a given system, can be related to the solute property descriptors of each solute through eqn (5). The solute distribution ratios for a very limited set of solutes determined in the SBME–water system and their corresponding Gibbs's energy related solute property descriptors are shown in Table 3.^{24,26,31}

The descriptors are the McGowan volume (*V_x*), the excess molar refraction (*R₂*), the solute dipolarity–polarizability (π_2^H), and the solutes' overall hydrogen-bond acceptor basicity and hydrogen-bond donor acidity, $\sum\beta_2^H$ and $\sum\alpha_2^H$, respectively. The sign and magnitude of the regression coefficients obtained from eqn (5) (*r*, *s*, *a*, *b*, and *v*), by multiple linear regression of the solute descriptors on the log of the partition coefficient, may be considered proportional to the solvent properties of the phases corresponding to the appropriate solute descriptor. Thus, *r* corresponds to the relative strengths of the solute–solvent interactions determined by the excess molar refractivity of the solute, and *a* corresponds to the relative solvent hydrogen-bond basicity of the phases, and so on. Finally, *c* is a constant of proportionality.

Table 3 Abraham's property descriptors and distribution coefficients in SBME–water of various solutes

Solute	Abraham parameters						Ref.	log <i>D</i>
	π_2^H	$\sum\alpha_2^H$	$\sum\beta_2^H$	<i>V_x</i>	<i>R₂</i>			
1,2,4-Trichlorobenzene	0.081	0	0	1.0836	0.98	23		2.99
1,4-Dichlorobenzene	0.75	0	0.02	0.9612	0.825	23		2.75
Chlorobenzene	0.65	0	0.07	0.8388	0.718	23		2.41
Toluene	0.52	0	0.14	0.8573	0.601	23		2.33
<i>p</i> -Toluic acid	0.90	0.60	0.38	1.073	0.73	25		1.28
Salicylic acid	0.84	0.71	0.38	0.9904	0.89	26		1.39
Benzene	0.52	0	0.14	0.7164	0.61	23		2.23
Acetophenone	1.01	0	0.49	1.0139	0.818	23		1.54
Methyl iodide	0.43	0	0.13	0.5077	0.676	23		1.27
Pentanol	0.42	0.37	0.48	0.8718	0.219	23		0.52
Butanol	0.42	0.37	0.48	0.7309	0.224	23		−0.096
Phthalic acid	1.60	0.82	0.75	1.147	0.85	26		−1.24
Propylamine	0.35	0.16	0.61	0.631	0.225	23		0.41
Propanol	0.42	0.37	0.48	0.59	0.236	23		−0.39
Isopropanol	0.36	0.33	0.56	0.59	0.212	23		−0.87
Acetic acid	0.65	0.61	0.45	0.4648	0.265	23		−1.26
Ethanol	0.42	0.37	0.48	0.4491	0.246	23		−1.07
Acetonitrile	0.90	0.04	0.33	0.4042	0.237	23		−0.81
Methanol	0.44	0.43	0.47	0.3082	0.278	23		−1.44

Table 4 Relative contributions of the coefficients of the generalized solvation equation^a

Variable	Coefficient	Correlation/Y	Student's <i>t</i>	Probability
<i>a</i>	-1.67	-0.61	2.87	0.0117
<i>b</i>	-3.61	-0.80	4.80	0.0002
<i>v</i>	3.20	0.59	6.98	4.41×10^{-6}
Constant	-0.012			

^a Adjusted $R^2 = 0.90$; multiple $R^2 = 0.96$; *F* statistic = 55.34

The use of as few as twenty solutes in a multiple linear regression is unlikely to give very satisfactory results, and thus the results we report can only be considered a preliminary characterization of the solvent properties of the SBME–water partitioning system. Nevertheless, Table 4 shows the relative contributions of the regression coefficients to the partitioning of the solutes in the SBME–water system. Only solute acidity, solute basicity, and solute volume are significant at the 95% level. The most significant factor is solute basicity, for which the regression coefficient is large and negative. The SBME phase is significantly less acidic than the aqueous phase and basic (in the sense of Lewis) solutes have a strong preference for the aqueous phase.

The next most significant parameter is volume, which is comparatively small and (typical of solvent–water partitioning) positive. The *v* parameter may be considered to be a measure of the relative hydrophobicity of the system and is similar to ΔG_{CH_2} in that it reflects the difference in the free energy required for cavity formation between the water and SBME phases. Typically, this parameter is large in solvent–water systems (Table 4) reflecting the fact that for most solvents, there are few intermolecular forces hindering cavity formation other than dispersion forces, whereas the free energy of cavity formation in aqueous phases is dominated by its extensively hydrogen bonded nature. There is a significant penalty to cavity formation in the aqueous phase due to the structuredness of water. However, the magnitude of this parameter is not as great as for most pure van der Waals solvents, which usually indicates either there is significant structure to the SBME phase, or that (and of course it amounts to the same thing) there is significant water present in the organic phase at equilibrium; for example, in the 1-octanol–water system. However, in the case of SBME, we have measured an equilibrium water content of only 0.35% wt/wt. It may be thought in the case of olive oil and SBME that molecular shape features play a role in determining the magnitude of this parameter.

Finally, the *a* coefficient is relatively small and negative, suggesting that the oil phase is less basic than the aqueous phase, it is also the least significant factor of those which are significant at the 95% confidence level. Again, it should be remembered that the solute set is small and the above interpretation tentative.

The full solvation equation for the 20 solute SBME–water partition is given in eqn (6):

$$\text{Log } D_{(\text{SBME})} = -0.11 - 0.78\pi_2^H - 1.58\sum\alpha_2^H - 2.90\sum\beta_2^H + 3.19V_x - 0.59R_2 \quad F = 35.5 \quad (6)$$

The coefficients are slightly different from those shown in Table 4 because in Table 4 only three terms are used (*a*, *b*, and *v*), and in eqn (6) all 5 terms have been used (*a*, *b*, *v*, *s*, and *r*). Both equations give the same result for Log *D* within statistical limits; however, the effect of the extra terms is to change the values of the terms in the first equation. The effect ought to be small because the extra terms are of small statistical significance, nevertheless, they do have an effect.

These results may be directly compared to a similar LSER derived for the olive oil–water system²⁷ shown in eqn (7).

$$\text{Log } D_{(\text{OO})} = -0.011 - 0.8\pi_2^H - 1.47\sum\alpha_2^H - 4.92\sum\beta_2^H + 4.17V_x + 0.58R_2 \quad F = 5841 \quad (7)$$

The similarity in the roles of solute acidity, basicity, and volume in the SBME–water systems and the olive oil–water system is readily apparent. Surprisingly, even terms which were least significant in the regression of eqn (6), follow the olive oil–water regression quite closely.

Partitioning vs. pH

The partition of several ionizable organic species was examined in relation to changes in the aqueous phase pH in the SBME–water system. Quite frequently in chemical processing by liquid–liquid extraction, recourse is to perform forward (partition into the extracting organic phase) and back (partition into a fresh aqueous phase) partitioning to effect purification of particular species (*e.g.*, in the liquid–liquid extraction of penicillin).³² Fig. 3 shows partitioning data for several ionizable organic compounds in SBME–water systems. The data confirm that distribution is higher for the uncharged form than for the charged form. For acidic species this means that there is a relative preference for the organic (SBME) phase at low pH and a relative preference for the aqueous phase at

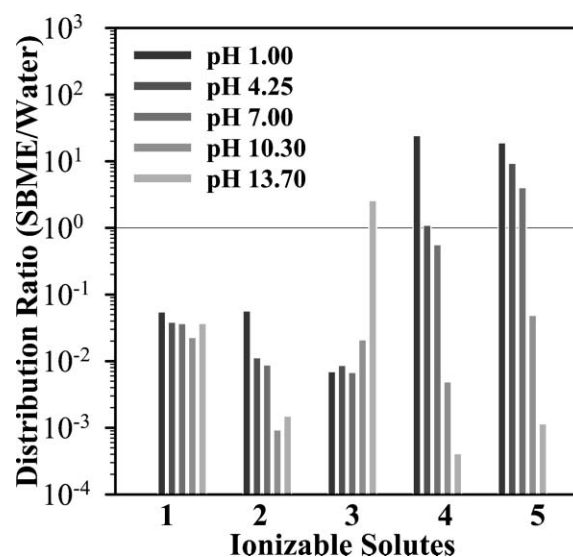


Fig. 3 pH dependent partitioning of ionizable solutes: 1 acetic acid ($pK_a = 4.75$); 2 phthalic acid ($pK_{a1} = 2.89$, $pK_{a2} = 5.51$); 3 propylamine ($pK_a = 10.71$); 4 salicylic acid ($pK_{a1} = 2.97$, $pK_{a2} = 13.40$); 5 *p*-toluic acid ($pK_a = 4.36$).

high pH. This phase preference is reversed where the ionizable group is basic. For the relatively weak acids and the base shown in Fig. 3, a forward and back extraction of these species is possible in principle, although there may still be mass transfer concerns to be addressed.

Metal ion partitioning

In general, the distribution and extraction of metal ion species into organic phases is limited by the requirement to solvate (hydrate) the metal ion in the organic phase.³³ This usually can only be achieved by the use of an extractant which can replace the metal ion hydration layer and provide a molecular surface compatible with solvation in the organic phase. Fig. 4 illustrates the partition of several metal ion species in the SBME–water system and demonstrates that this system is no exception. In all cases the metal ion species partitions strongly to the aqueous phase unless an extractant is included in the system.

For the transition metal ions (Co^{2+} , Ni^{2+} , Fe^{3+}) examined, no useful extraction is achieved in the absence of an extractant. In the presence of the extractants PAN and TAN, the distribution coefficient of all the metal ions increases, except at the lowest pH. This increase is pH dependent, being highest under the most basic conditions. This is commonly found in the extraction of metal ion species by solvent extraction and is due to the increase in the complexation constant with pH and forms a useful technical means of metal ion purification. Extractants and organic phases may be loaded at high pH and unloaded at low pH in a similar forward and back extraction process as mentioned above for the extraction of organic acids and bases. Additionally, some selectivity in metal ion separation may be secured by this means. In the SBME–water system, there appears to be little difference between the performance of PAN and TAN which are most effective in the extraction of Co^{2+} , but appear not practically useful for the extraction of Ni^{2+} and Fe^{3+} . Undoubtedly, suitable extractants could be found for the extraction of these and other metal ion species using the SBME–water system.

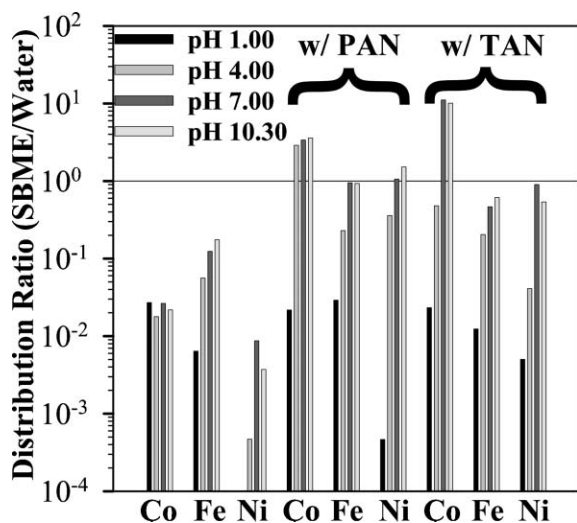


Fig. 4 The distribution of metal ions (Co^{2+} , Fe^{3+} , Ni^{2+}) in the absence and presence of PAN and TAN (each at 0.1 mM) vs. pH.

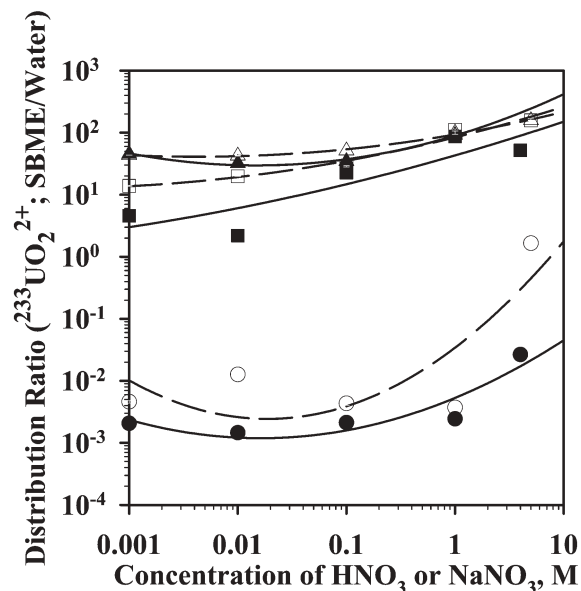


Fig. 5 The distribution of UO_2^{2+} in the SBME–water system without extractant (●), with 0.2 M CMPO (■), and with 0.2 M CMPO–1.2 M TBP (▲) vs. HNO_3 (filled symbols, solid lines) or NaNO_3 (open symbols, dashed lines). Distribution ratio from SBME–water = 0.0044.

In the TRUEX process for the extraction of uranium and transuranic ions, 0.2 M CMPO is used as the extractant, 1.2–1.4 M tri-*n*-butylphosphate (TBP) as a phase modifier, and the diluent is paraffinic hydrocarbons.³⁴ Schultz and Horwitz,³⁴ using the TRUEX formulation, reported the highest distribution values for UO_2^{2+} and Am^{3+} to be 10^3 and 10, respectively, at 6 M HNO_3 . Mathur *et al.*, using dodecane as the diluent, 0.2 M CMPO and 1.2 M TBP, reported distribution ratios of 10^2 for UO_2^{2+} and 10 for Am^{3+} at 1–6 M HNO_3 .³⁵ We have examined the partitioning of UO_2^{2+} (Fig. 5) and Am^{3+} (Fig. 6)

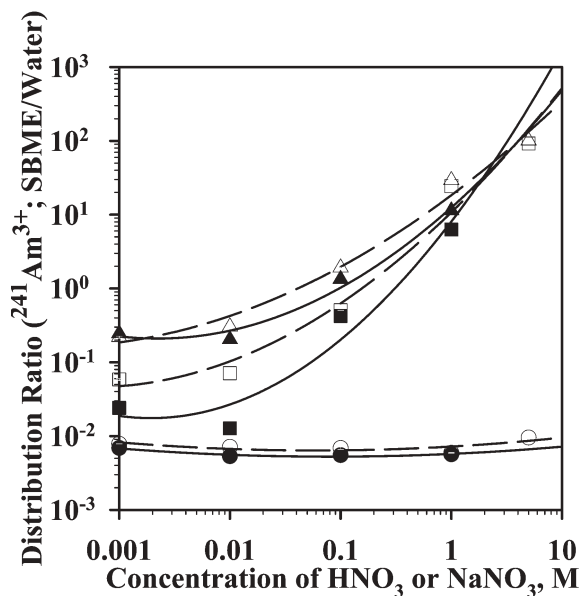


Fig. 6 The distribution of Am^{3+} in the SBME–water system without extractant (●), with 0.2 M CMPO (■), and with 0.2 M CMPO–1.2 M TBP (▲) vs. HNO_3 (filled symbols, solid lines) or NaNO_3 (open symbols, dashed lines). Distribution ratio from SBME–water = 0.0082.

in a similar system but with SBME as a replacement for the paraffinic hydrocarbon diluent. Without CMPO, the distribution ratios fall well below 1, indicating the preference for the aqueous phase. For the uranyl cation, addition of 0.2 M CMPO significantly improves the distribution ratios up to 10^2 at all nitric acid and NaNO_3 concentrations studied.

As with the uranyl cation, the distribution ratios for Am^{3+} are well below 1 and although there is an increase in preference for the SBME phase with the addition of CMPO, the distribution ratios are still below 1 and favor the aqueous phase up to 0.1 M NO_3^- , where they then begin to increase above 1 and favor the SBME phase approaching 10^2 at 5 M NO_3^- . This behavior would allow the separation of UO_2^{2+} from Am^{3+} in this system.

The inclusion of 1.2 M TBP for either UO_2^{2+} or Am^{3+} only made small improvements in the distribution ratios and does not appear to be needed as a phase modifier in the SBME–water systems as observed for traditional dodecane–water systems;^{34,35} the distribution values remain comparable without its use. The elimination of TBP could simplify and reduce the costs of these systems.

Conclusions

We have examined the partitioning of neutral, ionizable, and metal ion solutes in biphasic systems formed with soybean oil methyl ester and water. For neutral solutes, distribution behavior is similar to comparative solvent–water systems and is most similar to the olive oil–water system as judged by application of the Abraham generalized solvation equation. For the ionizable solutes, distribution behavior in this system is similar to the behavior of similar solutes in the presence of organic diluents in traditional solvent extraction. Extraction of metal ions using SBME is dependent on the presence of coordinating extractants to carry metal ions into the SBME phase. Such behavior is comparable to traditional organic solvent extraction. Soybean oil methyl esters thus represent a class of solvents that can be considered as a medium for the development of liquid–liquid extraction processes. Solute behavior during extraction is comparable to that found for traditional solvents, thus current models and process practices may, in many cases, be easily adapted to the use of this solvent–water system.

Acknowledgements

This research was supported by the Division of Chemical Sciences, Geosciences, and Biosciences, Office of Basic Energy Research, U. S. Department of Energy (Grant DE-FG02-96ER14673). The authors wish to thank Ag Environmental Products of Lenexa, Kansas for the gracious gift of the soybean oil methyl ester, SoyGold® 1000, used in this study.

References

- 1 P. T. Anastas, Green Chemistry as Applied to Solvents, in *Clean Solvents: Alternative Media for Chemical Reactions and Processing*, ed. M. A. Abraham, L. Moens, ACS Symposium Series 819, American Chemical Society, Washington, DC, 2002, pp. 1–9.
- 2 J. G. Huddleston, H. D. Willauer, R. P. Swatoski, A. E. Visser and R. D. Rogers, Room Temperature Ionic Liquids as Novel Media for 'Clean' Liquid–Liquid Extraction, *Chem. Commun.*, 1998, **16**, 1765–1766.
- 3 S. K. Spear, A. E. Visser, H. D. Willauer, R. P. Swatoski, S. T. Griffin, J. G. Huddleston and R. D. Rogers, Green Separation Science & Technology: Replacement of Volatile Organic Compounds in Industrial Scale Liquid/Liquid or Chromatographic Separations, in *Green Chemistry and Engineering*, ed. P. T. Anastas, L. G. Heine, T. C. Williamson, ACS Symposia Series 766, American Chemical Society, Washington, DC, 2001, pp. 206–221.
- 4 H. D. Willauer, J. G. Huddleston and R. D. Rogers, Solvent Properties of Aqueous Biphasic Systems Composed of Polyethylene Glycol and Salt Characterized by the Free Energy of Transfer of a Methylene Group between the Phases and by a Linear Solvation Energy Relationship, *Ind. Eng. Chem. Res.*, 2002, **41**, 2591–2601.
- 5 N. E. Kob, Dibasic Ester: A Low Risk, Green Organic Solvent Alternative, in *Clean Solvents: Alternative Media for Chemical Reactions and Processing*, ed. M. A. Abraham, L. Moens, ACS Symposium Series 819, American Chemical Society, Washington, DC, 2002, pp. 238–253.
- 6 L. R. Lynd, C. E. Wyman and T. U. Gerngross, Biocommodity Engineering, *Biotechnol. Prog.*, 1999, **15**, 777–793.
- 7 Oil Crops Situation and Yearbook Outlook, Market and Trade Economics Division, Economic Research Service, U. S. Department of Agriculture, October 2001, OCS–2001.
- 8 M. O. Bagby, Products from Vegetable Oils: Two Examples, in *Agricultural Materials As Renewable Resources: Nonfood and Industrial Applications*, ed. G. Fuller, T. A. McKeon, D. D. Bills, ACS Symposium Series 647, American Chemical Society, Washington, DC, 1996, pp. 248–257.
- 9 Y. Koltypin, N. Perkas and A. Gedanken, Commercial Edible Oils as New Solvents for Ultrasonic Synthesis of Nanoparticles: The Preparation of Air Stable Nanocrystalline Iron Particles, *J. Mater. Chem.*, 2004, **14**, 2975–2977.
- 10 S. Sapra, A. L. Rogach and J. Feldman, Phosphine-Free Synthesis of Monodisperse CdSe Nanocrystals in Olive Oil, *J. Mater. Chem.*, 2006, **16**, 3391–3395.
- 11 B. Lavers, A Fresh Look at Solvents – Vegetable vs. Mineral Oils, *Asia Pac. Coat. J.*, 2000, **13**, 14–18.
- 12 *The Lipid Handbook*, ed. F. D. Gunstone, J. L. Harwood and F. B. Padley, Chapman & Hall, London, 2nd edn, 1994, pp. 53–146.
- 13 Ag Environmental Products, L. L. C. 2001, *Material Safety Data Sheet*, http://www.soygold.com/products/solvents/SG1000/SG1000_MSDS.pdf, last accessed 02/05/2007.
- 14 E. P. Horwitz, M. L. Dietz, R. Chiarizia, H. Diamond, S. L. Maxwell, III and M. R. Nelson, Separation and Preconcentration of Actinides by Extraction Chromatography using a Supported Liquid Anion Exchanger: Application to the Characterization of High-Level Nuclear Waste Solutions, *Anal. Chim. Acta*, 1995, **310**, 63–78.
- 15 J. G. Huddleston, S. T. Griffin, J. Zhang, H. D. Willauer and R. D. Rogers, in *Methods in Biotechnology, Vol. 2: Bioremediation Protocols*, ed. D. Sheehan, Humana Press, Totowa, NJ, 1998, pp. 1–17.
- 16 T. Kaneko, P.-Y. Wang and A. Sato, Partition Coefficients of Some Acetate Esters and Alcohols in Water, Blood, Olive Oil and Rat Tissues, *Occup. Environ. Med.*, 1994, **51**, 68–72.
- 17 B. Y. Zaslavsky, L. M. Miheeva, N. N. Mestechkina and S. V. Rogozhin, Physico-Chemical Factors Governing Partition Behaviour of Solutes and Particles in Aqueous Polymeric Biphasic Systems: I. Effect of Ionic Composition on the Relative Hydrophobicity of the Phases, *J. Chromatogr.*, 1982, **253**, 139–148.
- 18 B. Y. Zaslavsky, L. M. Miheeva and S. V. Rogozhin, Parameterization of Hydrophobic Properties of Aqueous Polymeric Biphasic Systems and Water–Organic Solvent Systems, *J. Chromatogr.*, 1981, **212**, 13–22.
- 19 B. Y. Zaslavsky, N. D. Gulaeva, E. A. Djafarov, E. A. Masimov and L. M. Miheeva, Phase Separation in Aqueous Poly(ethylene glycol)-(NH₄)₂SO₄ Systems and Some Physicochemical Properties of the Phases, *J. Colloid Interface Sci.*, 1990, **137**, 147–156.
- 20 N. J. Bridges, K. E. Gutowski and R. D. Rogers, Investigation of Aqueous Biphasic Systems Formed from Solutions of Chaotropic Salts with Kosmotropic Salts (Salt–Salt ABS), *Green Chem.*, 2007, **9**, 177–183.

- 21 C. M. Hendrickson and D. C. Bradford, Developing Solvent for Photopolymerizable Printing Plates. *US Pat. 6 582 886*, 2003.
- 22 M. H. Abraham, H. S. Chadha, F. Martins, R. C. Mitchell, M. W. Bradbury and J. A. Gratton, Hydrogen Bonding. Part 46. A Review of the Correlation and Prediction of Transport Properties by an LFER Method: Physicochemical Properties, Brain Penetration and Skin Permeation, *Pestic. Sci.*, 1999, **55**, 78–88.
- 23 J. A. Platts, M. H. Abraham, D. Butina and A. Hersey, Estimation of Molecular Linear Free Energy Relationship Descriptors by a Group Contribution Approach. 2. Prediction of Partition Coefficients, *J. Chem. Inf. Comput. Sci.*, 2000, **40**, 71–80.
- 24 M. H. Abraham, J. Andonian-Haftvan, G. S. Whiting, A. Leo and R. S. Taft, Hydrogen Bonding. Part 34. The Factors that Influence the Solubility of Gases and Vapours in Water at 298 K, and a New Method for its Determination, *J. Chem. Soc., Perkin Trans. 2*, 1994, 1777–1791.
- 25 A. Pagliara, G. Caron, G. Lisa, F. Weizheng, P. Gaillard, P.-A. Carrupt, B. Testa and M. H. Abraham, Solvatochromic Analysis of Di-n-butyl ether/Water Partition Coefficients as Compared to Other Solvent Systems, *J. Chem. Soc., Perkin Trans. 2*, 1997, 2639–2643.
- 26 M. H. Abraham, H. S. Chadha, G. S. Whiting and R. C. Mitchell, Hydrogen Bonding. 32. An Analysis of Water-Octanol and Water-Alkane Partitioning and the $\Delta\log P$ Parameter of Seiler, *J. Pharm. Sci.*, 1994, **83**, 1085–1100.
- 27 M. H. Abraham, C. E. Green and J. A. Platts, University College London, London, Private communication, 2000.
- 28 F. H. Quina, E. O. Alonso and J. P. S. Farah, Incorporation of Nonionic Solutes into Aqueous Micelles: A Linear Solvation Free Energy Relationship Analysis, *J. Phys. Chem.*, 1995, **99**, 11708–11714.
- 29 M. F. Vitha and P. W. Carr, An LSER Study of the Effects of Surfactant Chain Length on the Chemical Interactions Governing Retention and Selectivity in Micellar Electrokinetic Capillary Chromatography using Sodium Alkyl Sulfate Elution Buffers, *Sep. Sci. Technol.*, 1998, **33**, 2075–2100.
- 30 J. G. Huddleston, G. A. Broker, H. D. Willauer and R. D. Rogers, Free-Energy Relationships and Solvatochromatic Properties of 1-Alkyl-3-Methylimidazolium Ionic Liquids, in *Ionic Liquids: Industrial Applications for Green Chemistry*, ed. R. D. Rogers, K. R. Seddon, ACS Symposium Series 818, American Chemical Society, Washington D. C., 2002, pp. 270–288.
- 31 M. H. Abraham, Scales of Solute Hydrogen-Bonding: Their Construction and Application to Physicochemical and Biochemical Processes, *Chem. Soc. Rev.*, 1993, 73–83.
- 32 T. A. Hatton, Liquid–Liquid Extraction of Antibiotics, in *Comprehensive Biotechnology: The Principles, Applications and Regulations of Biotechnology in Industry, Agriculture and Medicine*, ed. M. Moo-Young, Pergamon, Oxford, 1985, pp. 439–449.
- 33 *Principles and Practices of Solvent Extraction*, ed. J. Rydberg, C. Musikas and G. R. Choppin, Marcel Dekker, Inc., New York, 1992.
- 34 W. W. Schultz and E. P. Horwitz, The Truex Process and the Management of Liquid TRU Waste, *Sep. Sci. Technol.*, 1988, **23**, 1191–1210.
- 35 J. N. Mathur, M. S. Murali, P. R. Natarajan, L. P. Badheka and A. Banerji, Extraction of Actinides and Fission Products by Octyl(phenyl)-N,N-diisobutylcarbamoylmethyl-phosphine Oxide from Nitric Acid Media, *Talanta*, 1992, **39**, 493–496.

Renewable hydrogen: carbon formation on Ni and Ru catalysts during ethanol steam-reforming

Jeppe Rass-Hansen,^a Claus Hviid Christensen,^{*a} Jens Sehested,^b Stig Helveg,^b Jens R. Rostrup-Nielsen^b and Søren Dahl^{*b}

Received 26th February 2007, Accepted 3rd May 2007

First published as an Advance Article on the web 29th May 2007

DOI: 10.1039/b702890c

Biomass is probably the only realistic green and sustainable carbonaceous alternative to fossil fuels. By degradation and fermentation, it can be converted into bioethanol, which is a chemical with a range of possible applications. In this study, the catalytic steam-reforming of ethanol for the production of hydrogen is investigated, along with quantitative and qualitative determinations of carbon formation on the catalysts by TPO and TEM experiments. A Ru/MgAl₂O₄ catalyst, a Ni/MgAl₂O₄ catalyst as well as Ag- and K-promoted Ni/MgAl₂O₄ catalysts were studied. The operating temperature was between 673 and 873 K, and a 25 vol% ethanol–water mixture was employed. Deactivation of the catalysts by carbon formation is the main obstacle for industrial use of this process. Carbon formation was found to be highly affected by the operating temperature and the choice of catalyst. The effect of Ag addition was a rapid deactivation of the catalyst due to an enhanced gum carbon formation on the Ni crystals. Contrary to this, the effect of K addition was a prolonged resistance against carbon formation and therefore against deactivation. The Ru catalyst operates better than all the Ni catalysts, especially at lower temperatures.

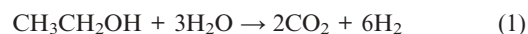
Introduction

The continuously increasing oil prices and the need for a CO₂-neutral energy production have in recent years increased the interest in different bio-fuels. Lately, bioethanol in particular has achieved significant attention for several reasons. First of all, it can be produced in large amounts from biomass by a relatively simple fermentation, it is considered CO₂-neutral, it is easy to handle, and it is non-toxic.^{1,2}

Here, the catalytic steam-reforming (SR) of ethanol for hydrogen production is investigated. In particular, the objectives of this paper are to quantitatively determine the effect of temperature and the role of the catalytic metal on the formation rate for coke on the technical catalysts during the SR. This is important to eventually implement ethanol SR in stationary and/or mobile units.

It is well known³ that highly pure ethanol in small quantities can be mixed with gasoline to increase the octane number. Additionally, it is possible to run cars on any mixture of ethanol and gasoline with an engine adjustment. These cars are called flexible fuel vehicles (FFVs). The production of highly pure ethanol is, however, still quite expensive and generally not cost-competitive with gasoline.^{3,4} But the world ethanol production has more than doubled from 2000 to 2005 and is expected to increase significantly.⁵ Together with technological improvements and lack of oil this will continue to favor ethanol prices compared to gasoline prices.

When ethanol is burned in a combustion engine, the energy efficiency of the fuel is limited by the Carnot efficiency and can reach only about 25%.⁶ This fuel efficiency can be significantly increased when ethanol is first converted to hydrogen and then used in a fuel cell with an efficiency of more than 50%.^{6–8} Besides that, it will not be necessary to first produce the highly pure ethanol required for fuel in combustion engines by expensive distillation since the reaction of ethanol SR [eqn (1)] requires at least three moles of water for every mole of ethanol:

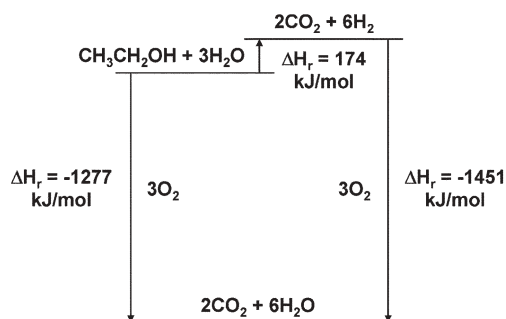


The use of agricultural feedstocks for a form of CO₂-neutral energy production relies on the photosynthesis of carbohydrates with high energy contents. These can, by degradation and fermentation, be converted into ethanol and CO₂. Especially in Brazil and the USA this is done on large scales (around 16 billion L in each country)⁹ by fermentation of sugar-cane and corn, respectively. Further catalytic conversion of ethanol into hydrogen requires energy, but the higher efficiency from using hydrogen in fuel cells, probably, makes the effort worthwhile. Fig. 1 shows in an energy level diagram the idea and potential of using biohydrogen *versus* bioethanol for energy applications. Theoretically, the total efficiency could be raised by about 70% with the given energy efficiencies, or even higher when considering distillation issues and the efficient use of waste heat.

The catalytic SR of ethanol has recently been reviewed by Haryanto *et al.*¹⁰ The conversion of ethanol to hydrogen and CO₂ is possible with many different catalysts, but in particular Rh and Ni catalysts have shown promising results.^{10–14} One major problem is, however, the formation of coke on the less noble catalysts and the resulting deactivation.¹⁰

^aCenter for Sustainable and Green Chemistry, Department of Chemistry, Technical University of Denmark, DK-2800 Kgs. Lyngby, Denmark. E-mail: chc@kemi.dtu.dk; Tel: +45 45252402

^bHaldor Topsøe A/S, Nymøllevej 55, DK-2800 Kgs. Lyngby, Denmark. E-mail: sda@topsøe.dk; Tel: +45 45272487



Energy output for ethanol combustion with an energy efficiency of 25 %:
 $0.25 \cdot 1277 \text{ kJ/mol} = 319 \text{ kJ/mol}$

Energy output for hydrogen utilization in fuel cells with an energy efficiency of 50 %:
 $0.50 \cdot 1451 \text{ kJ/mol} - 174 \text{ kJ/mol} = 552 \text{ kJ/mol}$

Total energy efficiency could potentially be raised by 73 %

Fig. 1 Energy level diagram comparing the combustion of ethanol with the transformation of ethanol to hydrogen and use in a fuel cell.

Fierro *et al.*¹¹ found that Rh and Ru catalysts gave the highest hydrogen selectivity among different noble metals for oxidative SR. Moreover, they found that addition of Cu to Ni catalysts enhanced the lifetime of the catalyst by lowering the coke depositions. Auapr tre *et al.*¹² showed that Ni and Rh catalysts were very active for non-oxidative SR, and later that a combination with Rh on a $\text{Ni}_{1-x}\text{Mg}_x\text{Al}_2\text{O}_4$ support gave particularly promising results.¹³ Frusteri *et al.*¹⁴ reported that Ni catalysts have the highest selectivity towards hydrogen, and Rh catalysts to be almost as selective but far more resistant to carbon formation. They also describe how doping a Ni catalyst with an alkali metal can improve the catalyst performance with regard to ethanol conversion.¹⁵ Furthermore, they suggested that carbon formation is significantly lowered by using a basic rather than an acidic support.¹⁵ Similarly, Liguras *et al.*¹⁶ described how the acidity of the support influences the carbon formation on the catalyst, mainly because acidic supports lead to the formation of ethylene, which is known to be a carbon-forming species in SR reactions.^{17,18}

Here, a Ru- and a Ni-catalyst was prepared on a non-acidic support (MgAl_2O_4) and tested for the SR of ethanol. Moreover, nickel catalysts doped with small amounts of potassium and silver were prepared to analyze the effect on carbon formation on the catalysts.

Experimental

Catalyst synthesis

Pure Ni, and Ag- and K-doped 10 wt% $\text{Ni/MgAl}_2\text{O}_4$ catalysts were prepared by the *incipient wetness impregnation technique*. A high surface area spinel (MgAl_2O_4) with a pore volume of 427 mL kg^{-1} and a specific surface area of $72 \text{ m}^2 \text{ g}^{-1}$ was used as support material. This support was chosen due to its stability at high water pressures and temperatures, and because it does not contain acidic sites. The spinel tablets were crushed to a fraction of 300–710 μm and dried for 1 h at 373 K. The solution for the impregnation was prepared by dissolving the desired amount of the different metal compounds, as nitrate salts, in water under moderate heating. After impregnation,

Table 1 List of pure and promoted catalysts

Sample	Composition
Ni	10 wt% Ni/ MgAl_2O_4
Ag/Ni	1 wt% Ag–10 wt% Ni/ MgAl_2O_4
K/Ni	1 wt% K–10 wt% Ni/ MgAl_2O_4
Ru	2 wt% Ru/ MgAl_2O_4

the catalysts were dried for 2 h at 373 K and finally calcined at 773 K for 4 h.

A 2 wt% Ru/ MgAl_2O_4 catalyst was prepared similarly from a nitrosyl nitrate aqueous solution $[\text{Ru}(\text{NO})(\text{NO}_3)_3]$ but without the calcination step. The different catalysts are listed in Table 1.

Catalytic measurements

The catalytic experiments were performed in a tubular fixed-bed quartz reactor with an inner diameter of 6 mm. For each test, 200 mg of catalyst material was loaded into the reactor and secured by quartz wool. The reactor was placed in an electrically heated oven. Before each run, the loaded catalyst was reduced and activated by heating at 5 K min^{-1} to 773 K for 2 h in a gas flow of 100 mL min^{-1} of equal amounts of hydrogen and nitrogen (the Ru catalyst was reduced at 873 K).

After reduction, SR experiments were conducted with a nitrogen gas flow of 80 mL min^{-1} and an ethanol–water liquid flow of $40 \mu\text{L min}^{-1}$. The liquid was pumped by a Gynkotek 480 high precision pump and vaporized by heating tape at 493 K. The ethanol–water mixture consisted of 25 vol% ethanol, which gave a total molar gas flow ratio to the catalyst bed of ethanol–water–nitrogen of about 1 : 10 : 20.

A Leybold-Heraeus BINOS was used for analyzing the reaction stream by continuously measuring the CO and CO_2 contents in the exit gas after condensation of any liquids in an ice bath. The condensate was mainly water and occasionally a minor amount of unreacted ethanol, and trace amounts of other liquid species. Some experiments were further analyzed by GC measurements on a HP 5890A gas chromatograph (both FID and TCD).

Temperature programmed oxidation (TPO)

The same experimental setup was used for analyzing the amount of coke formed on the catalysts during SR. The TPO experiments were carried out by heating the oven to 873 K at 10 K min^{-1} in a gas flow of 20 mL min^{-1} consisting of a mixture of 91.5% nitrogen and 8.5% oxygen. By this method, the coke was completely oxidized to CO and CO_2 , which was very convenient for making accurate measurements on the BINOS.

Transmission electron microscopy (TEM)

High resolution TEM images were obtained from selected catalysts after reaction in order to characterize the morphology and structure of the carbon deposits. The pictures were recorded with a Philips CM200 FEG transmission electron microscope operating with a primary electron energy of 200 kV and a point resolution of 1.9 \AA . About 30 pictures were taken for each catalyst at varying magnifications to identify reasonable trends.

Results

Steam-reforming experiments

During SR, ethanol decomposes mainly *via* two different routes: either by dehydration forming ethylene, or by dehydrogenation forming acetaldehyde.^{10,14,19} These two intermediate products can be further catalytically decomposed and steam-reformed to an equilibrated mixture of methane, carbon dioxide, carbon monoxide, hydrogen and water (*cf.* Fig. 2). Experiments performed under the chosen conditions (200 mg catalyst material, a molar mixture of ethanol–water–nitrogen of 1 : 10 : 20, temperatures from 673 to 873 K and a gas flow to the catalyst bed of 120 mL min⁻¹) all reached equilibrium²⁰ as fresh catalysts, meaning that equilibrium was always reached during the first 6 h of run time. Hereafter, carbon formation and the resulting catalyst deactivation influenced the ethanol conversion and product distribution for some of the catalysts. At equilibrium conditions, all ethanol is converted to the products shown in Fig. 2, and the amount of hydrogen produced is determined by the operating temperature. The BINOS was used to continuously identify the CO and CO₂ concentrations in the exit gas, and together with occasional GC measurements, a total carbon balance was achieved.

The BINOS signals from SR experiments performed at 673 K are shown in Fig. 3 and 4. After a 16 h run time, the Ni-based catalysts all showed large amounts of coke depositions on the catalyst pellets. There were, however, significant differences in the deactivation patterns for the different catalysts. Deactivation can obviously be seen by unconverted ethanol in the exit gas, but more conveniently (in this setup) by a drop in the CO₂ concentration, and a rise in the CO concentration. Fig. 3 illustrates these patterns and how the Ag-promoted nickel catalyst shows a rapid deactivation after *ca.* 7 h, and the pure Ni catalyst deactivates more slowly after *ca.* 10 h, whereas the K/Ni catalyst barely deactivates during the first 16 h. The Ru catalyst does not seem to deactivate at all (*cf.* Fig. 4). These time indications are only suitable for a fast comparison between the different nickel catalysts, and they are very dependent on the dimensions of the catalyst bed. The deactivation appears as a profile that develops down through the entire catalyst bed. At the start of a run, the gas is equilibrated in the first part of the bed and this is also where the carbon is deposited. Along with carbon depositions formed on the catalyst, the equilibration part is shifted down through the bed. This proceeds until all of the catalyst is eventually partly covered with coke, and equilibration of the gas stream is

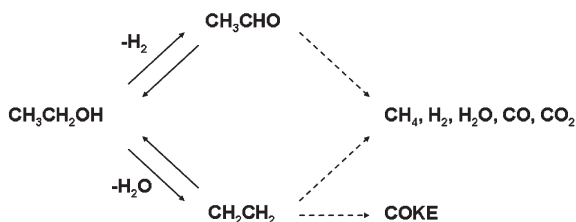


Fig. 2 Ethanol reaction pathways. Ethanol can be directly dehydrogenated to acetaldehyde or dehydrated to ethylene. Both of these species can in multiple steps be further converted to a synthesis-gas mixture, equilibrated by ordinary SR and WGS reactions.

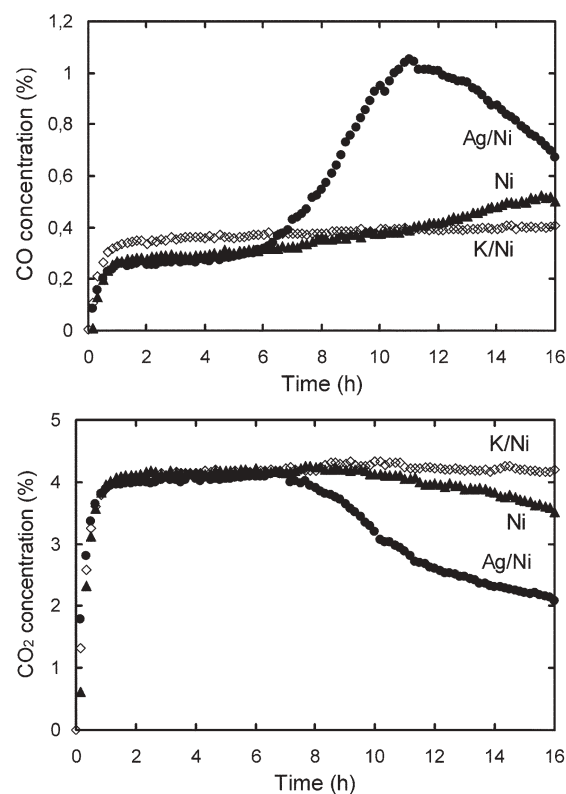


Fig. 3 CO and CO₂ signals from the BINOS in experiments performed at 673 K.

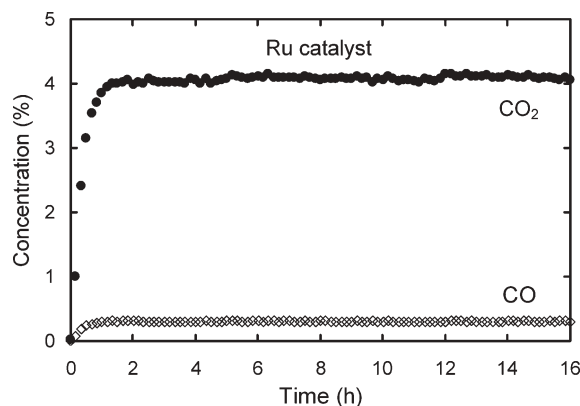


Fig. 4 CO and CO₂ signals from the BINOS for the Ru catalyst operated at 673 K.

therefore no longer possible, or until the top part of the reactor is totally clogged by carbon.

The combined analytical experiments show for the silver-promoted nickel catalyst that the first thing that happens during deactivation is a decrease in the CO₂ concentration and a simultaneous increase in the CO concentration. Then, the ethanol conversion starts decreasing and so does the production of methane whereas acetaldehyde and small amounts of ethylene start to appear in the gas stream. It is around this point that the highest CO concentration is reached, as seen in Fig. 3. Following this, acetaldehyde and ethylene reach a maximum before going towards zero. Since acetaldehyde is much more abundant than ethylene in the gas stream during

Table 2 TPO experiments for catalysts operated at 673 K for 16 h

Catalyst	TPO/mg C	TPO/(mg C) h ⁻¹	Comment
Ni	73.5	4.6	Deactivation
Ag/Ni	66.2	4.1	Rapid deactivation
K/Ni	26.9	1.7	Slow deactivation
Ru	1.70	0.1	No deactivation

the deactivation, it seems likely that the main reaction path for ethanol is through acetaldehyde. However, both reaction paths are possible and less ethylene is expected in the exit gas due to the higher coke-forming potential of ethylene, *cf.* Fig. 2.

At 873 K, all catalysts established an equilibrium and none of them seemed to deactivate. Even after a run time of six days, there was no deactivation of the Ni/MgAl₂O₄ catalyst.

TPO experiments

Table 2 shows the results from the TPO experiments following the SR experiments illustrated in Fig. 3 and 4. From these experiments it is seen that less carbon depositions are formed on the Ag/Ni catalyst than on the pure Ni catalyst, even though the Ag/Ni catalyst deactivates more rapidly. The K/Ni catalyst has only about one-third of the amount of carbon formed on the Ni catalyst, but still more than 15 times the amount of carbon formed on the Ru catalyst. In general, the rate of coke formation was between 0.01 and 5 mg h⁻¹, which is an almost negligible amount in the total carbon balance, where around 240 mg carbon is reacted per hour.

Discussion

Formation of carbon and deactivation

One of the main challenges for industrial use of ethanol SR is carbon depositions on the catalysts formed during the SR.^{10,19} Carbon is formed through several well known reactions, but, in particular, ethylene is an important precursor for carbon formation, as illustrated in Fig. 2.¹⁰ Rostrup-Nielsen *et al.*^{17,18} have previously described the different reaction paths for coke formation and the types of coke formed on the catalysts during the SR of hydrocarbons, as summarized in Table 3. From the table, it is clear that a lot of different parameters influence the carbon formation. Some of the most important are temperature and steam/carbon ratio, but the catalytic metal, the support material, the exact process conditions, the surface structure of the catalytic metal, the presence of promoters, *etc.*,

are also critical parameters for the formation of carbon on the catalysts.

One approach to lower the rate of carbon formation on nickel catalysts is to promote them with another metal that blocks the most reactive sites (the step sites).²¹ Blocking of these sites on the nickel crystals can have a far more pronounced effect on the rate of coke formation than on the rate of reforming.^{11,18} Besenbacher *et al.*²² designed a Au/Ni surface alloy catalyst for SR with gold blocking the most reactive sites. Hereby, a slightly less active but far more robust catalyst was achieved compared to an unpromoted nickel catalyst.²² Thus, the nickel catalysts doped with potassium and silver were prepared. In addition to step-site blocking, potassium is also expected to increase the steam adsorption and thereby lower the formation of coke on the catalyst.¹⁷ A high steam pressure is known to decrease carbon formation,¹⁷ and therefore a high water to ethanol ratio will also decrease coking problems.

The above considerations and the results from the TPO and SR experiments suggest that different types of carbon are formed on the catalysts, but only some types are leading to rapid deactivation. Therefore, the carbon deposits on selected catalysts were studied by TEM. It was apparent that on all the Ni-based catalysts various types of carbon formations were observed. However, the four TEM images in Fig. 5 exemplify the most abundant or archetypal carbon structures formed on each catalyst.

On Fig. 5, it is seen that the nickel crystals are generally around 10 nm in diameter. A mixture of amorphous carbon, whisker carbon and gum was formed on all the nickel catalysts. Apparently, the gum formation is more predominant on the Ag/Ni catalyst than on any of the other catalysts where whisker carbon formation seems to dominate. According to Rostrup-Nielsen *et al.*,^{17,18} gum formation leads to rapid catalyst deactivation caused by carbon encapsulation of the metal on the catalyst pellets (*cf.* Table 3). This can perhaps explain why the Ag/Ni catalyst deactivates more rapidly than the other catalysts. The Ag particles are expected to block the most reactive sites on the Ni crystals, the step-sites, and thereby significantly lower the ethanol SR reaction rate. This will cause a much higher ethanol concentration on the surface and therefore a higher carbon formation rate.

On the other Ni catalysts, where whisker carbon dominates, less deactivation should be observed due to the fact that whisker carbon does not immediately lead to deactivation of the catalyst.¹⁸ Whisker carbon or carbon nanotubes is a result

Table 3 Carbon-forming reactions and nature of the coke deposits

Reaction		Carbon type	Phenomena	Critical parameters
2CO ↔ C + 2CO ₂	(2)	Whisker carbon	Break-up of catalyst pellets	Low H ₂ O/C ratio, high temperature, presence of olefins and aromatics
CO + H ₂ ↔ C + H ₂ O	(3)			
CH ₄ ↔ C + 2H ₂	(4)			
C _n H _m → nC + m/2H ₂	(5)			
C _n H _m → olefins → coke	(6)	Pyrolytic coke	Encapsulation of catalyst pellet, deposits on tube wall	High temperature, residence time, presence of olefins
C _n H _m → (CH ₂) _n → gum	(7)	Gum	Blocking of metal surface	Low H ₂ O/C ratio, low temperature, presence of olefins and aromatics, absence of H ₂

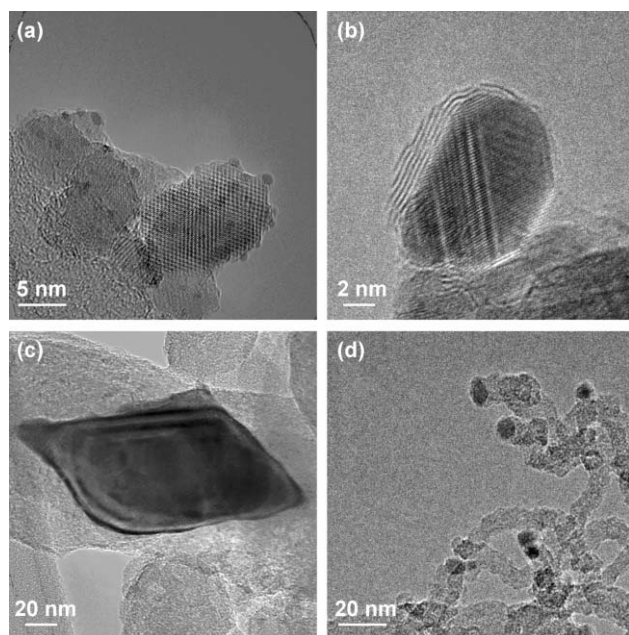


Fig. 5 TEM images of typical carbon formations on the different catalysts: (a) Ru catalyst, the image shows an ensemble of supported Ru particles without carbon deposits; (b) Ag/Ni catalyst, the image shows a Ni particle encapsulated by gum (graphitic layers); (c) K/Ni catalyst, the image shows an 'octopus' carbon nanofiber formed around a Ni particle; (d) Ni catalyst, the image shows numerous carbon nanofibers with Ni particles located at their tip apices.

of adsorbed carbon atoms, which forms on a Ni particle, diffuses and nucleates into a carbon fiber. In this process, most of the nickel crystal remains open for catalysis and only part of it is blocked by the growing carbon fiber. However, eventually the catalyst particle will be completely destroyed as described in Table 3.¹⁸

The K/Ni catalyst was very special in the way that among the small Ni crystals several relatively large particles (around 100 nm) were also present resulting in carbon formed in the so-called 'octopus' structure, where several fibers are growing from one nickel crystal (*cf.* Fig. 5).²³ These large particles create a kind of whisker carbon formation, which perhaps partly can explain the almost complete lack of deactivation observed with the K-promoted catalyst. Another important observation is, of course, that far less carbon is formed on the K/Ni catalyst, which could also be the reason for the very slow deactivation. The reason why less carbon is formed on the K/Ni catalyst can probably be ascribed to a better steam adsorption as discussed.¹⁷

Essentially no carbon was observed on the ruthenium catalyst, which is in agreement with earlier published work on methane SR.²⁴ As seen in Fig. 5, the Ru particles are distributed quite uniformly on the spinel with a crystal size of *ca.* 1–2 nm.

Fig. 6 clearly illustrates the effect of temperature on the amount of carbon formed on the catalysts. Experiments performed at high temperatures *e.g.* 873 K show no catalyst deactivation and almost no carbon formations on any of the catalysts, even after running for a week. These results are somewhat surprising since methane decomposition on

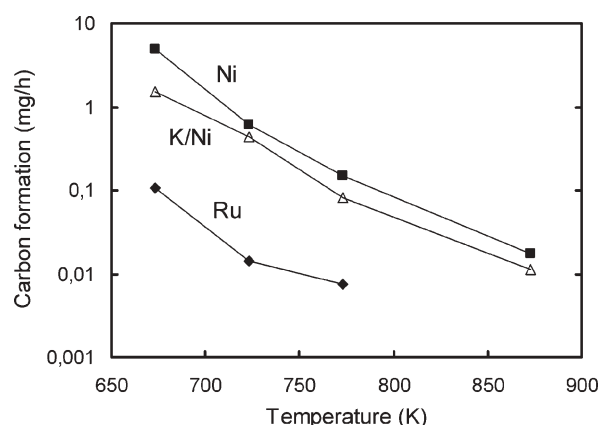


Fig. 6 Carbon formation as a function of temperature.

supported nickel catalysts usually leads to increasing carbon formation with increasing temperature.¹⁸ This might be explained by diffusion limitations at high temperatures resulting in a very low ethanol concentration at the catalyst surface and therefore in a very low rate of carbon formation. It is clear that promotion by potassium has a positive effect on the nickel catalyst because it significantly lowers the coking rate. The silver-promoted catalyst is not included in this diagram because the rapid deactivation gives incomparable results regarding the hourly normalized carbon formation. The Ru catalyst is by far the best of the tested catalysts, especially at lower temperatures around 673 K.

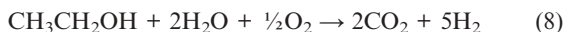
Applications

Ethanol SR can be implemented either in mobile or stationary units. For 'on-board' SR in vehicles, relatively low temperatures should be applied in order to meet the requirements of the polymer electrolyte membrane fuel cell (PEMFC). This type of FC is probably the most convenient to use in cars, because of its high power density and its ability to vary the output very fast, which, for example, is required to reach the power demands for a quick start-up. To run the SR 'on-board' it will be necessary to burn some of the ethanol to make the required heat for the endothermic SR reaction. Cavallaro *et al.*^{14,25} suggest instead to use a molten carbonate FC (MCFC). MCFCs, as well as solid oxide FCs (SOFCs), are convenient when running due to their operating temperature of around 900–1200 K, which provides the system with the necessary heat for the SR reaction, improves the hydrogen production and lowers the coking rate. Moreover, the MCFC and SOFC can use a less clean hydrogen fuel than the PEMFC. However, the high temperatures needed for the MCFC or SOFC are also the main disadvantage of the system for use in vehicles where they cannot meet the flexibility requirements.²⁶ They are more likely to be used in a stationary system. The optimal hydrogen production is, however, according to equilibrium calculations²⁰ at high temperatures. Therefore a better alternative might be to integrate a SR and water gas shift (WGS) reactor in extension to the bio-refinery producing the ethanol. Westermann and Ahning²⁷ describe a new type of bio-refinery in which bio-material rich in lignocelluloses (*e.g.* straw) can be used in combination with

manure for a combined ethanol and methane production. In this bio-refinery the methane produced could be used directly as a fuel for the endothermic SR process. Another possibility is to add a SOFC or a MCFC to the system to produce electricity, and then use the generated heat at 900–1200 K to run the endothermic SR reaction.

Moreover, for implementation of 'on-board' ethanol SR in vehicles, no carbon formations are allowed on the catalyst during the lifetime of the vehicle. It will be far too inconvenient if the catalyst is something that has to be replaced over time. For stationary applications the requirements for the catalyst could perhaps be a little less strict concerning the carbon formations. It might be acceptable, after a certain period of time, that the catalyst should be replaced, or at least oxidized to get rid of possible carbon depositions. Nevertheless, carbon depositions should by all means be minimized.

An alternative to lower the coke depositions and the costs for the endothermic SR, which has gained a lot of interest,^{11,28} is to do oxidative SR [eqn (8)]. For this exothermic reaction no external heat is necessary to do the SR. Moreover, the oxygen decreases the coke depositions by oxidizing the solid carbon to CO and CO₂. However, the total amount of hydrogen produced by oxidative SR is significantly less than from non-oxidative SR.



Conclusions

Bioethanol is a fast growing industrial chemical, whose main use is as an additive to gasoline for fueling automobiles. However, simple calculations indicate that this is an inefficient use of the chemical. Instead, bioethanol could be converted to hydrogen and used in fuel cells, which have much higher energy efficiencies.

Catalytic conversion of bioethanol by SR has turned out to be a very promising route to hydrogen. But severe difficulties with catalyst deactivation caused by coke depositions exist.

In this paper it is clarified how important the temperature is on the rate of carbon formation on the catalysts. It is shown that at 873 K both Ru- and Ni-based catalysts perform without any deactivation under the chosen conditions. Below 773 K, however, a noble metal like Ru is needed to avoid coke depositions.

It is illustrated how the addition of other metals to the Ni/MgAl₂O₄ catalyst influence the type of carbon deposition formed on the catalysts. Doping with K prolonged the lifetime of the catalyst by lowering the rate of carbon formation, whereas Ag promotion lowered the lifetime of the catalyst probably, due to a more pronounced gum carbon formation.

Both the Ru/MgAl₂O₄ catalyst and the Ni/MgAl₂O₄-based catalysts had high selectivity towards hydrogen since the reaction mixture was equilibrated. This also meant the total conversion of ethanol.

The K–Ni/MgAl₂O₄ catalyst is very cheap and a promising candidate for high temperature SR in stationary systems. However, low temperature SR could be even more interesting

regarding its use in mobile units, and here the Ru/MgAl₂O₄ catalyst shows great potential. The challenges for the implementation in mobile units are, on the other hand, probably much more difficult than in stationary systems.

Acknowledgements

The Center for Sustainable and Green Chemistry is sponsored by the National Danish Research Foundation.

References

- 1 E. C. Wanat, K. Venkataraman and L. D. Smith, *Appl. Catal., A*, 2004, **276**, 155–162.
- 2 L. F. Brown, *Int. J. Hydrogen Energy*, 2001, **26**, 381–397.
- 3 H. Bayraktar, *Renewable Energy*, 2005, **30**, 1733–1747.
- 4 *Bio-methane & Bio-hydrogen: status and perspectives of biological methane and hydrogen production*, ed. J. H. Reith, R. H. Wijffels and H. Barten, Dutch Biological Hydrogen Foundation, ZG Petten, Netherlands, 2003.
- 5 RNCOS, *Biofuel Market Worldwide (2006)*, July 1, 2006, 85 pp., pub. ID: CICQ1316286, <http://www.rncos.com>.
- 6 L. Schlapbach and A. Züttel, *Nature*, 2001, **414**, 353–358.
- 7 I. Chorkendorf and J. W. Niemantsverdriet, in *Concepts of Modern Catalysis and Kinetics*, Wiley-VCH, Weinheim, 2003.
- 8 J. R. Rostrup-Nielsen, *Phys. Chem. Chem. Phys.*, 2001, **3**, 283–288.
- 9 F. O. Licht, *World Ethanol and Biofuels Report*, vol. 4, no. 17 (9 May 2006), Table: 'Ethanol: World Production, by Country', p. 395.
- 10 A. Haryanto, S. Fernando, N. Murali and S. Adhikari, *Energy Fuels*, 2005, **19**, 2098–2106.
- 11 V. Fierro, O. Akdim and C. Mirodatos, *Green Chem.*, 2003, **5**, 20–24.
- 12 F. Auprêtre, C. Descorme and D. Duprez, *Catal. Commun.*, 2002, **3**, 263–267.
- 13 F. Auprêtre, C. Descorme, D. Duprez, D. Casanave and D. Uzio, *J. Catal.*, 2005, **233**, 464–477.
- 14 F. Frusteri, S. Freni, L. Spadaro, V. Chiodo, G. Bonura, S. Donato and S. Cavallaro, *Catal. Commun.*, 2004, **5**, 611–615.
- 15 F. Frusteri, S. Freni, V. Chiodo, L. Spadaro, O. Di Blasi, G. Bonura and S. Cavallaro, *Appl. Catal., A*, 2004, **270**, 1–7.
- 16 D. K. Liguras, D. I. Kondarides and X. E. Verykios, *Appl. Catal., B*, 2003, **43**, 345–354.
- 17 J. R. Rostrup-Nielsen, *Steam Reforming Catalysts*, Teknisk Forlag, Copenhagen, 1975.
- 18 J. R. Rostrup-Nielsen, J. Sehested and J. K. Nørskov, *Adv. Catal.*, 2002, **47**, 65–139.
- 19 P. D. Vaidya and A. E. Rodrigues, *Chem. Eng. J.*, 2006, **117**, 39–49.
- 20 Equilibrium calculations are performed with the program Outokumpu HSC Chemistry 5.1.
- 21 R. T. Vang, K. Honkala, S. Dahl, E. K. Vestergaard, J. Schnadt, E. Lægsgaard, B. S. Clausen, J. K. Nørskov and F. Besenbacher, *Nat. Mater.*, 2005, **4**, 160–162.
- 22 F. Besenbacher, I. Chorkendorff, B. S. Clausen, B. Hammer, A. M. Molenbroek, J. K. Nørskov and I. Stensgaard, *Science*, 1998, **279**, 1913–1915.
- 23 C. A. Bernardo, I. Alstrup and J. R. Rostrup-Nielsen, *J. Catal.*, 1985, **96**, 517–534.
- 24 J. R. Rostrup-Nielsen and J.-H. B. Hansen, *J. Catal.*, 1992, **144**, 38–49.
- 25 S. Cavallaro, *Energy Fuels*, 2000, **14**, 1195–1199.
- 26 N. M. Sammes, Y. Du and R. Bove, in *Biofuels for Fuel Cells*, ed. P. Lens, P. Westermann, M. Haberbauer and A. Moreno, IWA, London, UK, 2005, ch. 14, pp. 235–247.
- 27 P. Westermann and B. Ahring, in *Biofuels for Fuel Cells*, ed. P. Lens, P. Westermann, M. Haberbauer and A. Moreno, IWA, London, UK, 2005, ch. 11, pp. 194–205.
- 28 G. A. Deluga, J. R. Salge, L. D. Schmidt and X. E. Verykios, *Science*, 2004, **303**, 993–997.

Metal- and solvent-free conditions for the acylation reaction catalyzed by carbon tetrabromide (CBr₄)†

Liang Zhang,^a Yong Luo,^a Renhua Fan^{*a} and Jie Wu^{*ab}

Received 20th February 2007, Accepted 11th May 2007

First published as an Advance Article on the web 30th May 2007

DOI: 10.1039/b702646c

An efficient and useful catalyst—carbon tetrabromide (CBr₄)—was discovered to be highly effective for the acylation of phenols, alcohols, and thiols under metal- and solvent-free conditions.

Introduction

Organocatalysis has attracted much attention in the last few years as result of both the novelty of the concept and, more importantly, the fact that the efficiency and selectivity of many organocatalytic reactions meet the standards of established organic reactions.¹ Catalysts of the same class may promote similar reactions or less closely related reactions. For instance, DABCO and its analogues show high efficiency in Morita–Baylis–Hillman reactions,^{2a} cyanation of ketones,^{2b} as well as ring-opening of aziridines^{2c} or epoxides.^{2d} Carbon tetrabromide (CBr₄) is another example of this catalyst class, which is able to mediate an astonishing variety of transformations.³ Although carbon tetrabromide is considered a poisonous, irritating solid (skin contact can cause severe irritation; avoid inhalation of fumes; toxicity: irritating to skin, eyes and respiratory tract, irritating to mucous membranes, narcotic in high concentrations; possible liver and kidney damage; SCU-MUS LD₅₀ 298 mg kg⁻¹; IVN-MUS LD₅₀ 56 mg kg⁻¹),⁴ in recent years it has been utilized as a mild Lewis acid imparting high regio- and chemo-selectivity in various organic transformations.³ Very recently, we also found that it was highly effective as catalyst in the three-component reactions of aldehydes, amines and diethylphosphite under solvent-free conditions.^{3a} Herein, we would like to disclose its other applications as an efficient catalyst for acylation of alcohols, phenols, and thiols under metal- and solvent-free conditions.

It is well-known that the protection of phenols, alcohols, and thiols is one of the most frequently employed reactions in

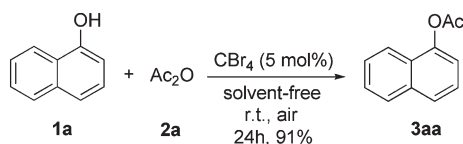
organic synthesis, since phenols, alcohols, and thiols are sensitive to chemical transformations in the synthesis of some multifunctional targets. The protection can be achieved by acylation with acid anhydrides in the presence of a suitable catalyst. So far, Lewis bases (e.g., DMAP and Bu₃P) and Lewis acids (e.g., halides and triflates of transition and rare earth metals) have been employed as catalysts for this transformation.⁵ Recently, continuous efforts for methodology development illustrate the importance of heteroatom acylation.^{6,7} However, the development of a simple, low cost protocol is still desirable. As acylation is among the most important acid-mediated reactions, development of a reaction that uses a catalytic amount of an economic and readily available catalyst that does not contain a metal would be of great interest.

Furthermore, due to the growing concern for the influence of the organic solvent on the environment as well as on human body, organic reactions without use of conventional organic solvents have attracted the attention of synthetic organic chemists. Although a number of modern solvents, such as fluorous media,⁸ scCO₂,⁹ ionic liquids¹⁰ and water¹¹ have been extensively studied recently, not using a solvent at all is definitely the best option. Development of solvent-free organic reactions is thus gaining prominence.¹²

Results and discussion

As described above, carbon tetrabromide (CBr₄) has received considerable attention as a catalyst in various organic transformations recently.³ Inspired by these results, we conceived that CBr₄ may also act as an efficient organocatalyst in acylation reactions. Initial studies were performed by using CBr₄ (5 mol%) as catalyst in the reaction of 1-naphthalenol **1a** with acetic anhydride **2a** under solvent-free conditions at room temperature (Scheme 1). To our delight, we observed the formation of the corresponding product **3aa**. Complete conversion and 91% isolated yield was obtained after 24 h. Only a trace amount of product was detected in the absence of carbon tetrabromide. The reaction was retarded when 1 mol% of catalyst was employed. Further examination showed that the reaction was completed in 6 h at 60 °C and 96% of **3aa** was obtained.

To demonstrate the generality of this method, we next investigated the scope of this reaction under the optimized conditions (solvent free, 5 mol% of CBr₄, air, 60 °C) and the



Scheme 1 Initial study for acylation reaction.

^aDepartment of Chemistry, Fudan University, 220 Handan Road, Shanghai, 200433, China. E-mail: jie_wu@fudan.edu.cn; Fax: +86 21 6510 2412; Tel: +86 21 5566 4619

^bState Key Laboratory of Organometallic Chemistry, Shanghai Institute of Organic Chemistry, Chinese Academy of Sciences, 354 Fenglin Road, Shanghai, 200032, China

† Electronic supplementary information (ESI) available: General experimental procedure and product characterisations. See DOI: 10.1039/b702646c

Table 1 Reaction of substrate **1** with acid anhydride **2** catalyzed by carbon tetrabromide^a

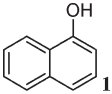
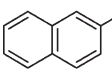
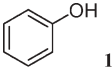
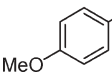
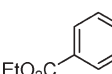
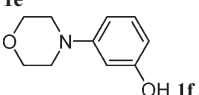
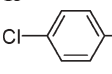
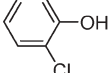
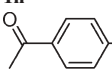
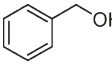
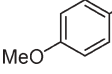
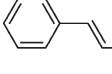
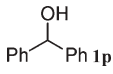
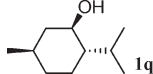
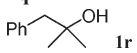
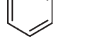
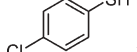
$\text{R}^1(\text{Ar})\text{XH} + (\text{R}^2\text{CO})_2\text{O} \xrightarrow[\text{solvent-free, 3-6 hours}]{\text{CBr}_4 (5 \text{ mol}\%)} \text{R}^1(\text{Ar})\text{XCOR}^2$				
Entry	Substrate 1	Acid anhydride	Product	Yield (%) ^b
X = O, S				
1		(CH ₃ CO) ₂ O 2a	3aa	96
2	1a	(CH ₃ CH ₂ CO) ₂ O 2b	3ab	96
3		(CH ₃ CO) ₂ O 2a	3ba	92
4	1b	(CH ₃ CH ₂ CO) ₂ O 2b	3bb	93
5		(CH ₃ CO) ₂ O 2a	3ca	76
6	1c	(CH ₃ CH ₂ CO) ₂ O 2b	3cb	55
7		(CH ₃ CO) ₂ O 2a	3da	96
8	1d	(CH ₃ CH ₂ CO) ₂ O 2b	3db	94
9		(CH ₃ CO) ₂ O 2a	3ea	70
10	1e	(CH ₃ CH ₂ CO) ₂ O 2b	3eb	60
11		(CH ₃ CO) ₂ O 2a	3fa	92
12	1f	(CH ₃ CH ₂ CO) ₂ O 2b	3fb	80
13		(CH ₃ CO) ₂ O 2a	3ga	62
14	1g	(CH ₃ CH ₂ CO) ₂ O 2b	3gb	83
15		(CH ₃ CO) ₂ O 2a	3ha	95
16	1h	(CH ₃ CH ₂ CO) ₂ O 2b	3hb	95
17		(CH ₃ CO) ₂ O 2a	3ia	83
18	1i	(CH ₃ CH ₂ CO) ₂ O 2b	3ib	95
19		(CH ₃ CO) ₂ O 2a	3ja	96
20	1j	(CH ₃ CH ₂ CO) ₂ O 2b	3jb	96
21		(CH ₃ CO) ₂ O 2a	3ka	97
22	1k	(CH ₃ CH ₂ CO) ₂ O 2b	3kb	86
23		(CH ₃ CO) ₂ O 2a	3la	96
24	1l	(CH ₃ CH ₂ CO) ₂ O 2b	3lb	95
25	HO(CH ₂) ₉ OH 1m	(CH ₃ CO) ₂ O 2a	3ma	72

Table 1 Reaction of substrate **1** with acid anhydride **2** catalyzed by carbon tetrabromide^a (Continued)

$\text{R}^1(\text{Ar})\text{XH} + (\text{R}^2\text{CO})_2\text{O} \xrightarrow[\text{solvent-free, 3-6 hours}]{\text{CBr}_4 (5 \text{ mol}\%)} \text{R}^1(\text{Ar})\text{XCOR}^2$				
Entry	Substrate 1	Acid anhydride	Product	Yield (%) ^b
X = O, S				
26	1m	(CH ₃ CH ₂ CO) ₂ O 2b	3mb	55
27	HO(CH ₂) ₆ OH 1n	(CH ₃ CO) ₂ O 2a	3na	79
28	1n	(CH ₃ CH ₂ CO) ₂ O 2b	3nb	82
29	CH ₃ (CH ₂) ₆ OH 1o	(CH ₃ CO) ₂ O 2a	3oa	92
30	1o	(CH ₃ CH ₂ CO) ₂ O 2b	3ob	99
31		(CH ₃ CO) ₂ O 2a	3pa	42
32	1p	(CH ₃ CH ₂ CO) ₂ O 2b	3pb	36
33		(CH ₃ CO) ₂ O 2a	3qa	89
34	1q	(CH ₃ CH ₂ CO) ₂ O 2b	3qb	47
35		(CH ₃ CO) ₂ O 2a	3ra	trace
36		(CH ₃ CO) ₂ O 2a	3sa	90
37	1s	(CH ₃ CH ₂ CO) ₂ O 2b	3sb	91
38		(CH ₃ CO) ₂ O 2a	3ta	83
39	1t	(CH ₃ CH ₂ CO) ₂ O 2b	3tb	90
40	EtSH 1u	(CH ₃ CO) ₂ O 2a	3ua	80
41	1u	(CH ₃ CH ₂ CO) ₂ O 2b	3ub	71
42	1b	(CH ₃ CH ₂ CH ₂ CO) ₂ O 2c	3bc	99
43	1b	[(CH ₃) ₂ CHCO] ₂ O 2d	3bd	98
44	1b	(PhCO) ₂ O 2e	3be	45

^a Reaction conditions: substrate **1** (0.50 mmol), acid anhydride (1.1 equiv.), carbon tetrabromide (5 mol%), solvent free, 60 °C.

^b Isolated yield based on substrate **1**.

results are summarized in Table 1. As shown in Table 1, this method is equally effective for phenols, alcohols and thiols. Complete conversion and good to excellent isolated yields were observed for most of substrates employed. Similar results were obtained with an electron-donating group or an electron-withdrawing group attached to the aromatic ring of phenol. Aliphatic alcohols were also suitable for this transformation under the standard conditions. For example, 96% yield of desired product **3ja** was obtained when benzylic alcohol **1j** reacted with acetic anhydride (Table 1, entry 19). Reaction of heptanol **1o** with propionic anhydride afforded the corresponding product **3ob** in almost quantitative yield (Table 1, entry 30). However, only moderate yields were generated when diphenylmethanol **1p** was employed as substrate in the reaction of acetic anhydride or propionic anhydride, which may be due to steric hinderance in the substrate (entries 31 and 32). For (1*R*,2*S*,5*R*)-2-isopropyl-5-methylcyclohexanol **1q**, 89% yield of product **3qa** could be obtained when the reaction was performed with acetic anhydride (entry 33). Under the same

conditions, only a trace of the desired product was detected when 2-methyl-1-phenylpropan-2-ol **1r** was used in the reaction (entry 35). Thiols also reacted smoothly with acid anhydrides to generate the desired products in good yields. For example, reaction of benzenethiol **1s** with acetic anhydride or propionic anhydride afforded the corresponding product in 90% or 91% yield, respectively (entries 36 and 37). Aliphatic thiols, such as ethanethiol **1u**, were also good substrates for this transformation. Employing 2-naphthalenol **1b** as substrate, the reaction of *n*-butyric anhydride or *i*-butyric anhydride both afforded the desired product in excellent yield (entries 42 and 43). However, the reaction of benzoic anhydride only gave the corresponding acylated product in 45% yield (entry 44). To establish the applicability of this method for larger scale processes, two reactions (20 mmol scale) were performed. The solid product **3ib** was easily isolated by crystallization from the crude product in 87% yield for the reaction of 1-(4-hydroxyphenyl)ethanone **1i** with propionic anhydride **2b**, and the liquid product **3oa** could be directly distilled from the crude reaction mixture (85% yield) in the reaction of 1-heptanol **1o** and acetic anhydride. These two examples also represented a cleaner workup procedure for this kind of transformation. Furthermore, it is noteworthy that, in some cases, the product obtained after the routine workup was of sufficient purity for spectra analysis and did not require further purification. For example, after completion of the reaction of compound **1a** with propionic anhydride **2b**, the reaction mixture was washed successively with 2% aqueous NaOH and saturated brine. After drying with Na₂SO₄ and concentrated under reduced pressure, the product obtained was pure enough (96% yield) after spectra analysis. The ¹³C NMR spectrum showed solely the product, and the signal of CBr₄ was not found.

Conclusions

In conclusion, we have described carbon tetrabromide as a useful and highly effective catalyst for the acylation of phenols, alcohols, and thiols under metal- and solvent-free conditions. This method not only provides an excellent complement to acylation reaction, but also avoids the use of hazardous acids or expensive Lewis acids and harsh reaction conditions.

Experimental

General procedure for CBr₄ catalyzed acylation reaction

A mixture of substrate **1** (0.5 mmol), acid anhydride **2** (0.55 mmol, 1.1 equiv.), and CBr₄ (5 mol%) under solvent-free conditions was stirred at 60 °C under air atmosphere. After completion of the reaction, as indicated by TLC, the reaction mixture was diluted with H₂O (2 mL) and extracted with Et₂O (2 × 3 mL). The organic phase was washed successively with 2% aqueous NaOH (3 mL) and saturated brine (3 mL). After drying with Na₂SO₄ and concentrating under reduced pressure, the crude product was separated and purified by flash chromatography column (silica gel) to afford the corresponding product (in some cases, the crude product was of sufficient purity and could be used for spectra analysis directly without further purification). (All the products are

known compounds. The characterizations of these compounds are identical with the literature reports.^{5–7} For details, please see ESI.†)

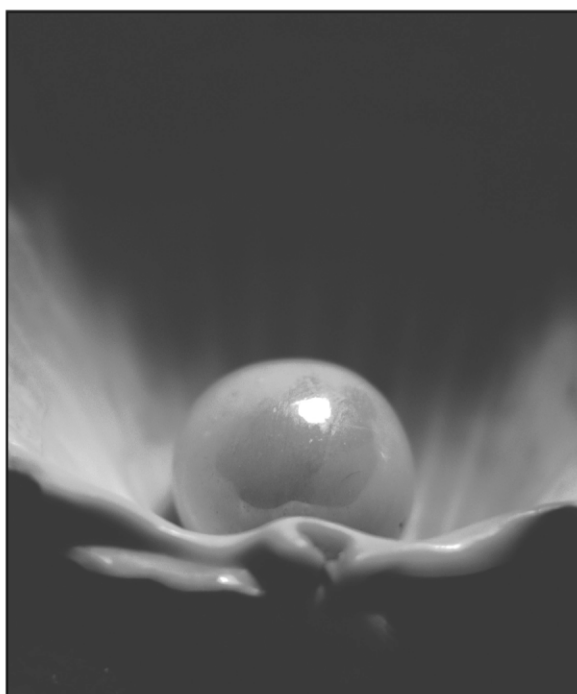
Acknowledgements

We thank Professors Xue-Long Hou and Zhen Yang for their invaluable advice during the course of this research. Financial support from National Natural Science Foundation of China (20502004, 20642006) and the Science & Technology Commission of Shanghai Municipality (05ZR14013) is gratefully acknowledged.

References

- P. I. Dalko and L. Moisan, *Angew. Chem., Int. Ed.*, 2004, **43**, 5138.
- (a) D. Basavaiah, A. J. Rao and T. Satyanarayana, *Chem. Rev.*, 2003, **103**, 811; (b) S.-K. Tian, R. Hong and L. Deng, *J. Am. Chem. Soc.*, 2003, **125**, 9900; (c) J. Wu, X. Sun and Y. Li, *Eur. J. Org. Chem.*, 2005, 4271; (d) J. Wu and H.-G. Xia, *Green Chem.*, 2005, **7**, 708.
- (a) J. Wu, W. Sun, X. Sun and H.-G. Xia, *Green Chem.*, 2006, **8**, 365; (b) J. S. Yadav, B. V. S. Reddy, K. Harikishan, C. Madan and A. V. Narsaiah, *Synthesis*, 2005, 2897; (c) A. S.-Y. Lee and F.-Y. Su, *Tetrahedron Lett.*, 2005, **46**, 6305; (d) M.-Y. Chen and A. S.-Y. Lee, *J. Chin. Chem. Soc.*, 2003, **50**, 103; (e) A. V. Reddy, V. L. N. Reddy, K. Ravinder and Y. Venkateswarlu, *Hetero. Commun.*, 2002, **8**, 459; (f) M.-Y. Chen, K.-C. Lu, A. S.-Y. Lee and C.-C. Lin, *Tetrahedron Lett.*, 2002, **43**, 2777; (g) M.-Y. Chen and A. S.-Y. Lee, *J. Org. Chem.*, 2002, **67**, 1384; (h) A. S.-Y. Lee, Y.-J. Hu and S.-F. Chu, *Tetrahedron*, 2001, **57**, 2121; (i) E. Abele, R. Abele and E. Lukevics, *J. Chem. Res. (S)*, 1999, 624; (j) A. S.-Y. Lee and C.-L. Cheng, *Tetrahedron*, 1997, **53**, 14255.
- For selected examples, see: (a) B. T. Cunningham, L. J. Guido and J. E. Baker, *Appl. Phys. Lett.*, 1989, **55**, 687; (b) T. J. de Lyon, N. I. Buchan, P. D. Kirchner, J. M. Woodall, G. J. Scilla and F. Cardone, *Appl. Phys. Lett.*, 1991, **58**, 517; (c) K. Tateno, Y. Kohama and C. Amano, *J. Cryst. Growth*, 1997, **172**, 5.
- T. W. Greene and P. G. M. Wuts, *Protecting Groups in Organic Synthesis*, John Wiley and Sons, New York, 3rd edn, 1999.
- (a) Nafion-H: R. Kumareswaran, K. Pachamuthu and Y. D. Vankar, *Synlett*, 2000, 1652; (b) Ytria-zirconia: P. Kumar, R. K. Pandey, M. S. Bodas and M. K. Dongare, *Synlett*, 2001, 206; (c) NBS: B. Karimi and H. Seradj, *Synlett*, 2001, 519; (d) LiClO₄·Y. Nakae, I. Kusaki and T. Sato, *Synlett*, 2001, 1581; (e) Ionic liquid: S. A. Forsyth, D. R. MacFarlane, R. J. Thompson and M. V. Itzstein, *Chem. Commun.*, 2002, 714; (f) Mg(ClO₄)₂: G. Bartoli, M. Bosco, R. Dalpozzo, E. Marcantoni, M. Massaccesi, S. Rinaldi and L. Sambri, *Synlett*, 2003, 39; (g) Zn(ClO₄)₂: G. Bartoli, M. Bosco, R. Dalpozzo, E. Marcantoni, M. Massaccesi and L. Sambri, *Eur. J. Org. Chem.*, 2003, 4611; (h) AlPW₁₂O₄₀: H. Firouzabadi, N. Iranpoor, F. Nowrouzi and K. Amani, *Chem. Commun.*, 2003, 764; (i) ZrOCl₂: R. Ghosh, S. Maiti and A. Chakraborty, *Tetrahedron Lett.*, 2004, **45**, 147; (j) BiOCl: R. Ghosh, S. Maiti and A. Chakraborty, *Tetrahedron Lett.*, 2004, **45**, 6775; (k) Al₂O₃: V. K. Yadav and K. G. Babu, *J. Org. Chem.*, 2004, **69**, 577; (l) MoOCl₂: C.-T. Chen, J.-H. Kuo, V. D. Pawar, Y. S. Munot, S.-S. Weng, C.-H. Ku and C.-Y. Liu, *J. Org. Chem.*, 2005, **70**, 1188; (m) Mn(haaccac)₂Cl: M. Salavati-Niasari, S. Hydrazadeh, A. Amiri and S. Salavati, *J. Mol. Catal. A: Chem.*, 2005, **231**, 191.
- (a) Cu(OTf)₂: K. L. Chandra, P. Saravanan, R. K. Singh and V. K. Singh, *Tetrahedron*, 2002, **58**, 1369; (b) In(OTf)₃: K. K. Chauhan, C. G. Frost, I. Love and D. Waite, *Synlett*, 1999, 1743; (c) Bi(OTf)₃: A. Orita, C. Tanahashi, A. Kakuda and J. Otera, *J. Org. Chem.*, 2001, **66**, 8926; (d) Ce(OTf)₃: R. Dalpozzo, A. De Nino, L. Maiuolo, A. Procopio, M. Nardi, G. Bartoli and R. Romeo, *Tetrahedron Lett.*, 2003, **44**, 5621; (e) LiOTf: B. Karimi and J. Maleki, *J. Org. Chem.*, 2003, **68**, 4951; (f) HClO₄·SiO₂: A. K. Chakraborty and R. Gulhane, *Chem. Commun.*, 2003, 1896; (g) BiOClO₄: A. K. Chakraborty, R. Gulhane and Shivani, *Synlett*, 2003, 1805; (h) Mg(ClO₄)₂: A. K. Chakraborty, L. Sharma,

- R. Gulhane and Shivani, *Tetrahedron*, 2003, **59**, 7661; (i) $\text{HBF}_4\text{-SiO}_2$: A. K. Chakraborti and R. Gulhane, *Tetrahedron Lett.*, 2003, **44**, 3521; (j) $\text{Cu}(\text{BF}_4)_2$: A. K. Chakraborti, R. Gulhane and Shivani, *Synthesis*, 2004, 111; (k) InCl_3 : A. K. Chakraborti and R. Gulhane, *Tetrahedron Lett.*, 2003, **44**, 6749; (l) ZrCl_4 : A. K. Chakraborti and R. Gulhane, *Synlett*, 2004, 627; (m) $\text{Zn}(\text{ClO}_4)_2\cdot 6\text{H}_2\text{O}$: Shivani, R. Gulhane and A. K. Chakraborti, *J. Mol. Catal. A: Chem.*, 2007, **264**, 208; (n) ErCl_3 : R. Dalpozzo, A. De Nino, L. Maiuolo, M. Oliverio, A. Procopio, B. Russo and A. Tocci, *Aust. J. Chem.*, 2007, **60**, 75; (o) $\text{Cu}(\text{ClO}_4)_2\cdot 6\text{H}_2\text{O}$: K. Jeyakumar and D. K. Chand, *Mol. Catal. A: Chem.*, 2006, **255**, 275; (p) Zeolite H β : K. V. V. K. Mohan, N. Narender and S. J. Kulkarni, *Green Chem.*, 2006, **8**, 368; (q) ZnO : S. M. Hosseini and H. Sharghi, *Tetrahedron*, 2005, **61**, 10903; (r) ZnO : F. Tamaddon, M. A. Amrollahi and L. Sharafat, *Tetrahedron Lett.*, 2005, **46**, 7841; (s) Bromodimethylsulfonium bromide: A. T. Khan, S. Islam, A. Majee, T. Chattopadhyay and S. Ghosh, *J. Mol. Catal. A: Chem.*, 2005, **239**, 158; (t) ATPB: A. T. Khan, L. H. Choudhury and S. Ghosh, *Eur. J. Org. Chem.*, 2005, **13**, 2782; (u) CsF-Celite: S. T. A. Shah, K. M. Khan, H. Hussain, M. U. Anwar, M. Fecker and W. Voelter, *Tetrahedron*, 2005, **61**, 6652; (v) Manganese(III) bis(2-hydroxy-anil)acetylacetonato: M. Salavati-Niasari, S. Hydarzadeh, A. Amiri and S. Salavati, *J. Mol. Catal. A: Chem.*, 2005, **231**, 191; (w) $\text{Er}(\text{OTf})_3$: A. Procopio, R. Dalpozzo, A. De Nino, L. Maiuolo, B. Russo and G. Sindona, *Adv. Synth. Catal.*, 2004, **346**, 1465; (x) $\text{H}_{14}[\text{NaP}_5\text{W}_{30}\text{O}_{110}]$: M. M. Heravi, F. K. Behbahani and F. F. Bamoharram, *J. Mol. Catal. A: Chem.*, 2006, **253**, 16; (y) $\text{Mg}(\text{NTf}_2)_2$: A. K. Chakraborti and Shivani, *J. Org. Chem.*, 2006, **71**, 5785.
- 8 D. P. Curran, *Pure Appl. Chem.*, 2000, **72**, 1649.
 9 W. Leitner, *Top. Curr. Chem.*, 1999, **206**, 107.
 10 T. Welton, *Chem. Rev.*, 1999, **99**, 2071.
 11 C.-J. Li and T.-H. Chan, *Organic Reactions in Aqueous Media*, John Wiley, New York, 1997.
 12 (a) F. Toda, *Acc. Chem. Res.*, 1995, **28**, 480; (b) J. O. Metzger, *Angew. Chem., Int. Ed.*, 1998, **37**, 2975; (c) K. Tanaka and F. Toda, *Chem. Rev.*, 2000, **100**, 1025.



Looking for that **special** chemical science research paper?

TRY this free news service:

Chemical Science

- highlights of newsworthy and significant advances in chemical science from across RSC journals
- free online access
- updated daily
- free access to the original research paper from every online article
- also available as a free print supplement in selected RSC journals.*

*A separately issued print subscription is also available.

Registered Charity Number: 207890

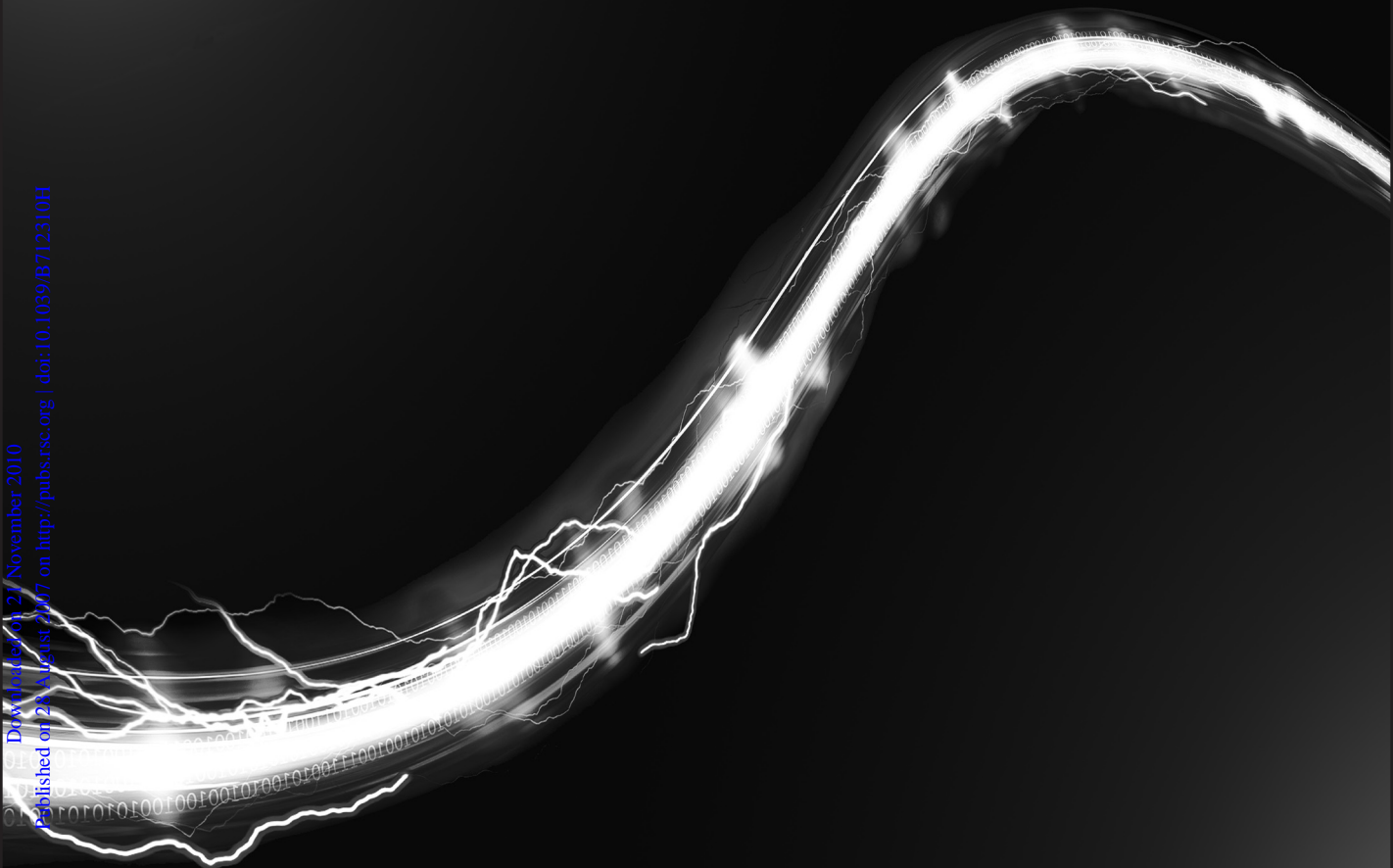
RSCPublishing

www.rsc.org/chemicalscience

RSC Journals Archive

Over 160 years of essential chemistry at your fingertips

Downloaded on 27 November 2010
Published on 23 August 2007 on <http://pubs.rsc.org> | doi:10.1039/B712310H



Featuring almost 1.4 million pages of ground-breaking chemical science in a single archive, the **RSC Journals Archive** gives you instant access to **over 238,000 original articles** published by the Royal Society of Chemistry (and its forerunner Societies) between 1841-2004.

The RSC Journals Archive gives a supreme history of top title journals including: *ChemComm*, *Dalton Transactions*, *Organic & Biomolecular Chemistry* and *PCCP (Physical Chemistry Chemical Physics)*.

As well as a complete set of journals with multi-access availability, the RSC Journals Archive comes in a variety of purchase options and available discounts.

For more information please contact sales@rsc.org

20060760

Environmental Science Books

Issues in Environmental Science & Technology

Series Editors:

R E Hester and R M Harrison

Format: **Hardback**

Price: **£45.00**

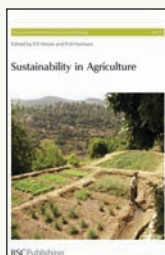
RSC Member Price: **£29.25**

Written by leading experts, this series presents a multidisciplinary approach to pollution and the environment. Focussing on the science and broader issues including economic, legal and political considerations.

Sustainability in Agriculture Vol. No. 21

Discusses the key factors impacting on global agricultural practices including fair trade, the use of pesticides, GM products and government policy.

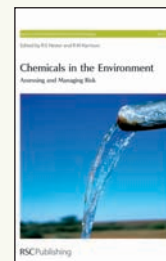
2005 | xiv+130 pages | ISBN-10: 0 85404 201 6
ISBN-13: 978 0 85404 201 2



Chemicals in the Environment Assessing and Managing Risk Vol. No. 22

Beginning with a review of the current legislation, the book goes on to discuss scientific and technical issues relating to chemicals in the environment and future developments.

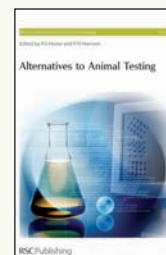
2006 | xvi+158 pages | ISBN-10: 0 85404 206 7
ISBN-13: 978 0 85404 206 7



Alternatives to Animal Testing Vol. No. 23

Provides an up-to-date discussion on the development of alternatives to animal testing including; international validation, safety evaluation, alternative tests and the regulatory framework.

2006 | xii+118 pages | ISBN-10: 0 85404 211 3
ISBN-13: 978 0 85404 211 1

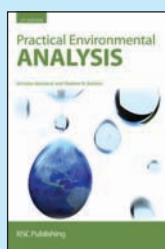


Practical Environmental Analysis 2nd Edition

By *M Radojevic and V N Bashkin*

A new edition textbook providing an up-to-date guide to practical environmental analysis. Ideal for students and technicians as well as lecturers wishing to teach the subject.

Hardback | 2006 | xxiv+458 pages | £39.95 | RSC member price £25.75 | ISBN-10: 0 85404 679 8 | ISBN-13: 978 0 85404 679 9



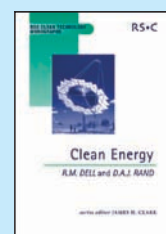
Clean Energy (RSC Clean Technology Monographs)

By *R M Dell and D A J Rand*

Series Editor *J H Clark*

Covering a broad spectrum of energy problems, this highly accessible book discusses in detail strategies for the world's future energy supply.

Hardback | 2004 | xxxvi+322 pages | £89.95 | RSC Member Price £58.25 | ISBN-10: 0 85404 546 5 | ISBN-13: 978 0 85404 546 4

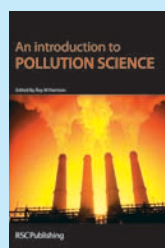


An Introduction to Pollution Science

By *R M Harrison*

A student textbook looking at pollution and its impact on human health and the environment. Covering a wide range of topics including pollution in the atmosphere, water and soil, and strategies for pollution management.

Hardback | 2006 | ca xii+322 pages | £24.95 | RSC Member Price £16.50 | ISBN-10: 0 85404 829 4 | ISBN-13: 978 0 85404 829 8

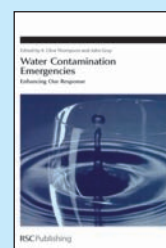


Water Contamination Emergencies Enhancing Our Response

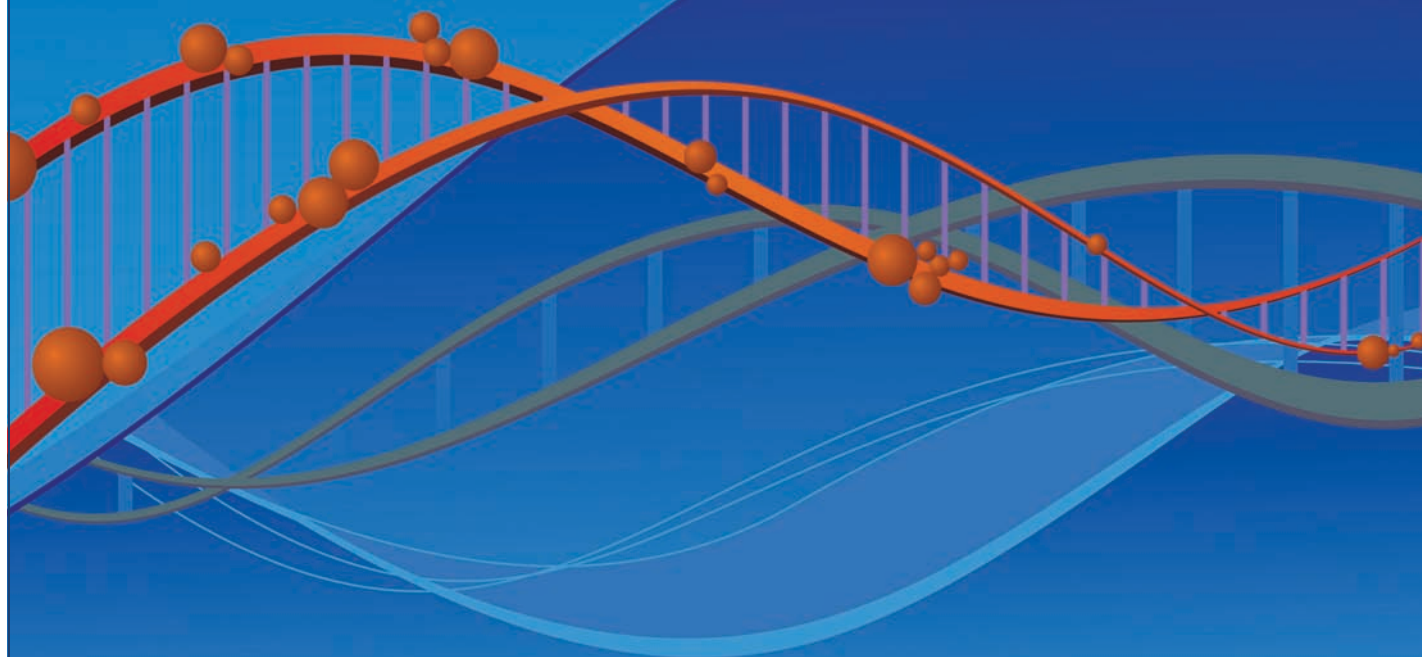
By *J Gray and K C Thompson*

A look at the impact and response of contaminated water supplies including the threat of chemical, biological, radiological and nuclear (CBRN) events.

Hardback | 2006 | x+372 pages | £99.95 | RSC Member Price £64.75 | ISBN-10: 0 85404 658 5 | ISBN-13: 978 0 85404 658 4



Methods in Organic Synthesis: Cover Competition



18060752

Are you creative?

Highly subscribed database *Methods in Organic Synthesis* is now holding a cover competition, for all those involved or interested in organic chemistry.

With a large readership and diverse array of abstracts in every issue, the winner of the competition can be sure that their cover will be seen by readers across the globe. The image will feature on the RSC website and on the front of *Methods in Organic Synthesis* throughout 2008, making it highly visible to our extensive international audience. In addition, the winner will receive a free subscription for one year (print and online).

Methods in Organic Synthesis highlights the most novel, current and topical research from the organic chemistry field, and as such the winning image should reflect these values. Can you bring organic chemistry to life visually?

Deadline for submissions: Monday 22nd October 2007

Go online and submit your image today

RSC Publishing

www.rsc.org/mos/covercomp

Registered Charity Number 207890